The polymorphic and pseudopolymorphic behaviour of gatifloxacin crystal modifications

Zak Perold

B.Pharm

Thesis submitted in partial fulfilment of the requirements for the degree Magister Scientiae in the Department of Pharmaceutics at the North-West University: Potchefstroom Campus.

Supervisor: Prof. W. Liebenberg

Co-supervisor: Mr. M. Brits

POTCHEFSTROOM

2006

Table of contents

Table of contents i

Abstract xi

Uittreksel xii

Aims and objectives xv

Chapter 1: Solid state properties of pharmaceuticals

Introduction to the crystal properties of active pharmaceutical ingredients (APIs) 1

1.1 Crystallisation, crystal growth and crystal stability 1

1.2 Crystal habit/morphology 4

1.3 What is polymorphism? 6

1.3.1 True polymorphs 7

1.3.2 Configurational and conformational polymorphs 8

1.3.3 Colour polymorphism/Polychromism 9

1.3.4 Dissapearing polymorphs 9

1.3.5 Polymorphic stability: A polymorphic relationship 10

1.4 Pseudopolymorphism 10

1.4.1 Hydrates 11

1.4.2 Solvates 12

1.4.3 The influence of water content on the status of hydration 14

1.4.4 Desolvated/dehydrated forms 14

1.4.5 Polymorphism among pseudopolymorphs 17

1.5 Amorphous solids 17
1.5.1 Glass transition temperature 18
1.5.2 Polymorphism among amorphous solids 19

1.6 The impact of polymorphism, crystal habit and the presence of amorphous forms on pharmaceutical manufacturing and product integrity 19
1.6.1 Polymorphism, pseudopolymorphism and the amorphous state 21
1.6.1.1 Solubility and bioavailability 22
1.6.1.2 Density and hardness 24
1.6.1.3 Water sorption 24
1.6.1.4 Stability 25
1.6.1.4.1 Physical stability 26
1.6.1.4.2 Chemical stability 27
1.6.1.5 Thermal behaviour 28
1.6.1.6 Electrical properties 30

1.7 Polymorphism and drug manufacture 31
1.7.1 Crystal size 31
1.7.1.1 Dissolution 31
1.7.1.2 Crystal habit 32
1.7.1.3 Flowability 33
1.7.1.3.1 Angle of repose 34
1.7.1.3.2 Carr's index and Hausner ratio 34
1.7.1.3.3 Powder flow properties of four solid forms of celecoxib 35
1.7.1.4 Granulation 35

1.7.2 Drying 36

1.7.3 Pressure 39
1.7.3.1 Milling 39
1.7.3.2 Tabletting/Compression 41
1.7.4 Lyophilisation 42
1.7.5 Spray drying 43
1.7.6 Mixing 43

Conclusion 43

Chapter 2: An overview of gatifloxacin

Introduction 45

2.1 Chemical properties 45
2.1.1 Structural formula and chemical name 45
2.1.2 Empirical formula 46
2.1.3 Molecular weight 46
2.1.4 Appearance 46
2.1.5 Solubility 46
2.1.6 Melting point 46
2.1.7 Chemical synthesis of gatifloxacin 46

2.2 Pharmacology 48
2.2.1 Indications 48
2.2.2 Mechanism of action 49
2.2.3 Resistance 49

2.3 Pharmacokinetics 50
2.3.1 Absorption 50
2.3.2 Distribution 51
2.3.3 Elimination 52

2.3.3.1 Excretion and metabolism 52
2.3.3.2 Inhibition or induction of cytochrome (CYP) enzymes 52
2.3.3.3 Effect of renal and hepatic impairment on excretion 52
2.3.4 Half-life 52

2.4 Special precautions 53
2.4.1 Interactions 53
2.4.1.1 Change in effectiveness 53
2.4.1.2 Drug interactions 53
2.4.1.3 Glucose homeostasis 54

2.5 Safety 54
2.5.1 Contra indications 54
2.5.2 Relative contra indications 54

2.6 Pharmaceutical preparations of gatifloxacin available in South Africa 55
2.6.1 Product 55
2.6.1.1 Tequin® 56
2.6.1.2 Tequin® injection 56
2.6.2 Dosage and administration 56
2.6.3 Regulations 56

2.7 Internationally available products 56
2.7.1 Tequin® 56
2.7.2 Zymar® 57
2.7.2.1 Product 57
2.7.2.2 Dosage and administration 57
2.7.3 Miscellaneous products 57
2.7.3.1 Tablets 57
2.7.3.2 Suspensions 58

2.8 Available literature on different gatifloxacin crystal forms 58

Conclusion 61

Chapter 3: Physico-chemical characterisation of APIs

Introduction 62

3.1 X-ray diffractometry 63
3.1.1 Single crystal diffractometry 63
3.1.2 The principal and application of x-ray powder diffraction (XRPD) 64
3.1.2.1 Bragg's law 64
3.1.2.2 Preffered orientation 65
3.1.3 Apparatus and conditions 66
3.1.3.1 X-ray powder diffraction (XRPD) 66
3.1.3.2 Variable temperature x-ray diffraction (VT-XRPD) 67

3.2 Infra-red (IR) spectrometry 67
3.2.1 Principal and applications 67
3.2.2 Apparatus and conditions 68

3.3 Thermal methods of analysis 69
3.3.1 Principal and applications 69
3.3.1.1 Differential Scanning Colorimetry (DSC) 69
3.3.1.2 Thermogravimetric analysis (TGA) 69
3.3.2 Apparatus and conditions 70
3.3.2.1 Differential Scanning Colorimetry (DSC) 70
3.3.2.2 Thermogravimetric analysis (TGA) 71

3.4 Microscopy 71
3.4.1 Principal and applications 71
3.4.1.1 Hot-stage microscopy (HSM) 71
3.4.1.2 Scanning electron microscopy (SEM) 72
3.4.2 Apparatus and conditions 73
3.4.2.1 Hot-stage microscopy (HSM) 73
3.4.2.2 Scanning electron microscopy (SEM) 73

3.5 Particle size uniformity 73

3.6 Karl Fischer analysis 73
3.6.1 Principal and applications 74
3.6.2 Apparatus and conditions 74

3.7 Methods used to prepare gatifloxacin crystal forms 74
3.7.1 Recrystallisation 75
3.7.2 Drying 76

3.8 Flowability 76

3.9 Ultra-violet spectrophotometry 76
3.9.1 Principal and applications 76
3.9.2 Apparatus and conditions 77

3.10 Dissolution and solubility testing 77
3.10.1 Principal and applications 78
3.10.1.1 Dissolution 78
3.10.1.2 Solubility 78
3.10.2 Apparatus, conditions and methods 78
3.10.2.1 Dissolution testing 78
3.10.2.2 Solubility testing 80

3.10.3 Medium preparation 82
3.10.3.1 0.01 M HCl 82
3.10.3.2 Acetate buffer pH 4.5 (U.S.P) 82
3.10.3.3 Milli-Q water 83
3.10.3.4 Phosphate buffer 6.8 (U.S.P) 83

Conclusion 83

Chapter 4: Gatifloxacin sesquihydrate raw material

Introduction 84

4.1 Gatifloxacin sesquihydrate 84

4.2 Anhydrous gatifloxacin 91

4.3 Comparison of gatifloxacin sesquihydrate and its anhydrous form 95

4.4 Dehydration behaviour of gatifloxacin sesquihydrate (H4) 100
4.4.1 Activation energy (E_a) needed for dehydration 100

Conclusion 103

Chapter 5: Gatifloxacin crystal modifications and the properties thereof

Introduction 104

5.1 Recrystallisations from alcohols 104
5.1.1 Recrystallisation of gatifloxacin using absolute ethanol (99-100%) 104
5.1.2 Recrystallisation of gatifloxacin using *n*-butanol as solvent 115

5.2 Recrystallisations from other organic solvents 129
5.2.1 Recrystallisation of gatifloxacin using THF as solvent 129
5.2.2 Recrystallisation of gatifloxacin using ethyl acetate as solvent 145
5.2.3 Recrystallisation of gatifloxacin using dichloromethane as solvent 157

5.3 Scanning electron microscopy 169

5.4 Flowability 174

5.5 Relative stability 175

Conclusion 178

Chapter 6: Solubility and dissolution behaviour of gatifloxacin crystal modifications

Introduction 181

6.1 Solubility testing 181
6.1.1 Solvated/hydrated forms of gatifloxacin 181
6.1.1.1 Gatifloxacin sesquihydrate (H4) 181
6.1.1.2 ZP0 182
6.1.1.3 Form ZP1 184
6.1.1.4 Form J 185
6.1.1.5 Form ZP2 186
6.1.1.6 Form ZP3 187

6.1.2 Desolvated/dehydrated forms of gatifloxacin 188
6.1.2.1 Anhydrous form from raw material 188
6.1.2.2 Isomorphic desolvate of form ZP0 189
6.1.2.3 Form Ω 190

6.1.2.4 Form I anhydrous 192
6.1.2.5 Form ZP4 193

6.2 Dissolution testing 194
6.2.1 Solvated/hydrated forms of gatifloxacin 194
6.2.1.1 Gatifloxacin sesquihydrate (H4) 194
6.2.1.2 ZP0 196
6.2.1.3 Form ZP1 197
6.2.1.4 Form J 198
6.2.1.5 Form ZP2 199
6.2.1.6 Form ZP3 200
6.2.2 Desolvated/dehydrated forms of gatifloxacin 201
6.2.2.1 Anhydrous gatifloxacin from raw material 201
6.2.2.2 Isomorphic desolvate of form ZP0 202
6.2.2.3 Form Ω 204
6.2.2.4 Form I anhydrous 206
6.2.2.5 Form ZP4 207

Conclusion 208

Chapter 7: Polymorphic behaviour of gatifloxacin crystal modifications

Introduction 213

7.1 Methods and materials 215

7.2 Recrystallisation study using absolute ethanol (99-100%) as solvent 217

7.3 Recrystallisation study using ethanol (95%) as solvent 217

7.4 Recrystallisation study using a mixture of 75% ethanol and 25% water as solvent 222

7.5 Recrystallisation study using a mixture of 50% ethanol and 50% water as solvent 224

7.6 Recrystallisation study using a mixture of 25% ethanol and 50% water as solvent 226

7.7 Discussion 227

Conclusion 233

Chapter 8: Summary and conclusion 236

Bibliography 245

Acknowledgements 254

Annexures 255

Poster presented at the 26th Annual conference of the Academy of Pharmaceutical Sciences, Port Elizabeth, 2005 256

Article in the process of submission 258

Abstract

The polymorphic and pseudopolymorphic behaviour of gatifloxacin crystal modifications

Objective: Gatifloxacin is a broad-spectrum fluoroquinolone antibacterial agent that exhibits polymorphism. There was however little information available regarding the physico-chemical properties of the different forms. This study was conducted to classify the gatifloxacin crystal modifications, to identify possible new forms and to investigate the physico-chemical properties thereof.

Methods: Various characterisation methods were used that included X-ray powder diffraction (XRPD), variable temperature X-ray powder diffraction (VT-XRPD), differential scanning calorimetry (DSC), thermogravimetric analysis (TGA), infrared spectrometry, hot-stage microscopy (HSM), scanning electron microscopy (SEM) and Karl-Fischer moisture determination (KF). Solubility and dissolution studies were also conducted.

Results: The results obtained made it possible to identify and characterise 5 possibly new forms of gatifloxacin: ZP0 (mono-ethanol solvate), ZP1 (sesqui-butanol solvate), ZP2 (hemi-ethyl acetate solvate), ZP3 (sesquihydrate) and ZP4 (anhydrous form). Previously described crystal forms (form J, form I anhydrous and form Ω) were identified and fully characterised in this study.

Isomorphism was identified for form ZP0. Contrary to the literature form J (from THF recrystallisation) did not produce a THF solvate, but rather a sesquihydrated form.

It was found that form Ω was the product from the desolvation/dehydration of either form ZP1 or ZP2. Since ZP1 and ZP2 are new forms, the drying of these forms poses new methods to produce form Ω

The dehydration behaviour of the commercial sesquihydrate (form H4) revealed that the dehydration activation energy (E_a) varied throughout the dehydration process.

Solubility testing of the various crystal forms revealed that some forms (ZP3, I, Ωand an anhydrous form from gatifloxacin sesquihydrate) were more soluble than the commercial sesquihydrated form. Dissolution testing revealed that ZP1, ZP3 and Ω have similar dissolution profiles to that of the commercial sesquihydrate.

Using different water:ethanol mixtures, it was possible to investigate the influence of water on the recrystallisation outcome using ethanol. It was observed that ethanol (99-100%) produced a mono-ethanol solvate, ethanol (95%) produced a mono-ethanol-hemihydrate, ethanol:water (75:25) produced a hemi-ethanol-sesquihydrate and ethanol in concentrations 50% v/v produced sesquihydrated forms. This made it possible to state that water content, however small, influences the product when present in so-called water-free solvents.

Conclusion: Gatifloxacin crystallises in a variety of crystal modifications that differ in physico-chemical properties. Five new forms were identified and characterised.

Uittreksel

Die polimorfiese en pseudopolimorfiese gedrag van gatifloksasien kristal modifikasies

Doelstellings: Gatifloksasien is 'n breë spektrum antimikrobiese middel wat polimorfisme openbaar. Daar was egter baie min fisies-chemiese inligting beskikbaar rakende die verskillende polimorfe. Met hierdie studie was dit gepoog om die verskillende kristalsoorte volledig te klassifiseer, nuwe vorme te identifiseer en om die fisies-chemiese eienskappe te ondersoek.

Metodes: Die karakteriseringsmetodes wat in die studie gebruik is, sluit die volgende in: X-straal poeier diffraktometrie (XRPD), variënde temperatuur X-straal poeier diffraktometrie (VT-XRPD), differensiële skanderingskalorimetrie (DSC), infrarooi spektrometrie (IR), termiese mikroskoop (HSM), skanderings elektron mikroskoop (SEM) en Karl Fischer waterbepaling (KF). Dissolusie en oplosbaarheid studies was ook uitgevoer.

Resultate: Vyf moontlike nuwe vorme is geindentifiseer en gekarakteriseer nl. ZP0 (mono-etanol solvaat), ZP1 (sesqui-butanol solvaat), ZP2 (hemi-etiel asetaat solvaat), ZP3 (sesquihidraat) en ZP4 ('n anhidriese vorm). Reeds bekende vorme (J, I en Ω) is ook vanuit die studie verkry en volledig geklassifiseer.

Isomorfiese gedrag was geidentifseer vir vorm ZP0. In teenstelling met die literatuur, is dit gevind dat vorm J (vanuit THF) nie 'n THF solvaat gevorm het nie, maar 'n sesquihidraat.

Die dehidrasie gedrag van vorm H4 het getoon dat die aktiverings energie (E_a) gevarieër het tydens die dehidrasie proses.

Die desolvering van ZP1 of ZP2 het tot die vorming van vorm Ωgelei. Aangesien ZP1 en ZP2 nuwe vorme is, is die bereiding van vorm Ω vanuit die vorme 'n nuwe bereidingsmetode om vorm Ωte berei.

Oplosbaarheid-studies van die verskillende kristalvorme het getoon dat sommige vorme (ZP3, I, Ω en 'n anhidriese vorm) beter oplosbaarheidsgedrag getoon het as die kommersieël beskikbare sesquihidraat vorm. Die dissolusie resultate het getoon dat vorme ZP1, ZP3 en Ω soortgelyke dissolusie profiele het as die kommersiële sesquihidraat vorm.

Om die invloed van water se teenwoordigheid in organiese oplosmiddels (wat gebruik word vir rekristalisasie) te ondersoek, is daar verskeie water:etanol mengsels berei en daarmee gerekristalliseer. Vanuit etanol (99-100%) is 'n mono-etanol solvaat berei, vanuit die etanol (95%) is 'n mono-etanol-hemi-hidraat berei, vanuit die etanol (75:25) mengsel is 'n hemi-etanol-sesquihidraat berei en in mengsels met etanol konsentrasies 50% v/v is daar sesquihidraat vorme opgelewer. Die resultate het bewys dat die teenwoordigheid van water in 'n sogenaamde water-vrye oplosmiddel, die final produk wat vorm, kan beïnvloed.

Gevolgtrekking: Gatifloksasien kristalliseer in verskeie kristalsoorte wat verskil in hul fisies-chemiese eienskappe. Vyf moontlike nuwe vorme vir gatifloksasien is geïdentifiseer.

Aims and objectives

Preparation, characterisation and investigation of various aspects of different gatifloxacin crystal modifications

Gatifloxacin is a highly effective fluoroquinolone anti-bacterial agent that is commonly used in the treatment of acute sinusitis; lower respiratory tract-, urinary tract- and various soft tissue infections (Chambers, 2001:797). Gatifloxacin acts as a bacterial inhibitor, as it inhibits bacterial replication (by inhibiting bacterial DNA gyrase) (Chambers, 2001:798). Gatifloxacin being a newer generation quinolone (compared to nalidixic acid and ciprofloxacin) has the advantage over the older generation that it is not significantly susceptible to resistance.

From the available literature on different gatifloxacin polymorphic forms, it was clear that gatifloxacin does exhibit polymorphism. The literature was found to be lacking in information regarding these crystal forms. Partly the scope of this study was to provide supplementary information regarding these previously described crystal forms. The supplementary data to be added to the available literature was focused on behavioural aspects, stability testing, dissolution and solubility testing, powder flow properties, the influence of drying and to investigate crystal morphology.

Seeing that gatifloxacin exhibits polymorphism, a further aim of this study was to investigate the possibility of new crystal forms.

To achieve these aims the following objectives were set and pursued:

1. Characterise the gatifloxacin sesquihydrate raw material.
2. Characterise the anhydrous form produced by the drying of gatifloxacin sesquihydrate.
3. Comparison between gatifloxacin sesquihydrate (H4) and its dried product.

4. To investigate the dehydration process of gatifloxacin sesquihydrate (H4) by means of activation energy determination.
5. Identify and characterise possible new crystal forms of gatifloxacin produced by recrystallising using absolute ethanol (99-100%), *n*-butanol, THF, ethyl acetate and dichloromethane respectively.
6. Provide supplementary data on previously described crystal forms.
7. Evaluate the influence of drying on the recrystallisation products from the various solvents.
8. Investigate the influence of temperature and relative humidity on an anhydrous form of gatifloxacin.
9. Evaluate possible differences in solubility and dissolution behaviour between the various crystal modifications.
10. Establish the influence of water content present in a recrystallisation solvent (using ethanol as an example).

This study was conducted to further the knowledge and understanding of the solid-state properties of gatifloxacin.

Comprehensive characterisation of the various crystal forms of polymorphic API's is essential to ensure the safety and efficacy of pharmaceutical products.

Chapter 1

Solid-state properties of pharmaceuticals

Introduction to the crystal properties of Active Pharmaceutical Ingredients (APIs)

Crystallisation is the process during which random molecules in solution, gas- or melt phase order themselves in reoccurring positions in a specific solid form. Thus, a crystal is a solid form of molecules (called unit cells) in a reoccurring order (Byrn *et al.*, 1999:5). The regular organisation of the crystal characterises the unique properties of the solid, therefore crystalline materials have a unique set of properties such as a definite melting point and a specific pattern in x-ray diffraction (Byrn *et al.*, 1999:5). Compounds without regular molecular arrangements are called amorphous solids (York, 2002:9).

Numerous APIs are used in the crystalline form (Byrn *et al.*, 1999:5). It is of great importance to focus extensively on the physico-chemical properties and behaviour of APIs during the pre-formulation phase of development to ensure the safety, efficacy and stability of pharmaceutical products.

1.1 Crystallisation, crystal growth and crystal stability

In order for crystallisation to take place, a solution must be in a super saturated state. In a super saturated solution the solute is at a concentration greater than the saturation value for the solute in that solvent, at specific temperature and pressure (Byrn *et al.*, 1999:16).

Apart from the fact that crystallisation depends on a super saturated state; it is also dependent on nucleation. Nucleation is the first step in the crystallisation process (Byrn *et al.*, 1999:16). The process of nucleation can be divided in two phases, primary- and secondary nucleation. Primary nucleation is the formation of stable molecular assemblies at a defect or impurity site (*nucleation site*) leading to

crystallisation (Byrn *et al.*, 1999:512). If further crystallisation takes place after initial crystals have been formed, it is referred to as secondary nucleation (Byrn *et al.*, 1999:17).

Nucleation can be initiated by various factors including: pre-existing nuclei on the equipment used; seeding of the solution with a desired form; defective surfaces; temperature irregularities or a change in concentration gradient (Byrn *et al.*, 1999:17).

It is important to note that when crystallisation begins, it induces /initiates a change in the immediate environment, making it an exhausting process to control. Nucleation is a very important factor in the determination of the crystal form that is to be crystallised, as it is the site on which further crystal growth will take place (Byrn *et al.*, 1999:18). It is therefore critical to control nucleation, when a desired crystal form is to be crystallised. Figures 1.1 and 1.2 illustrate how easy a mixture of two crystals may form.

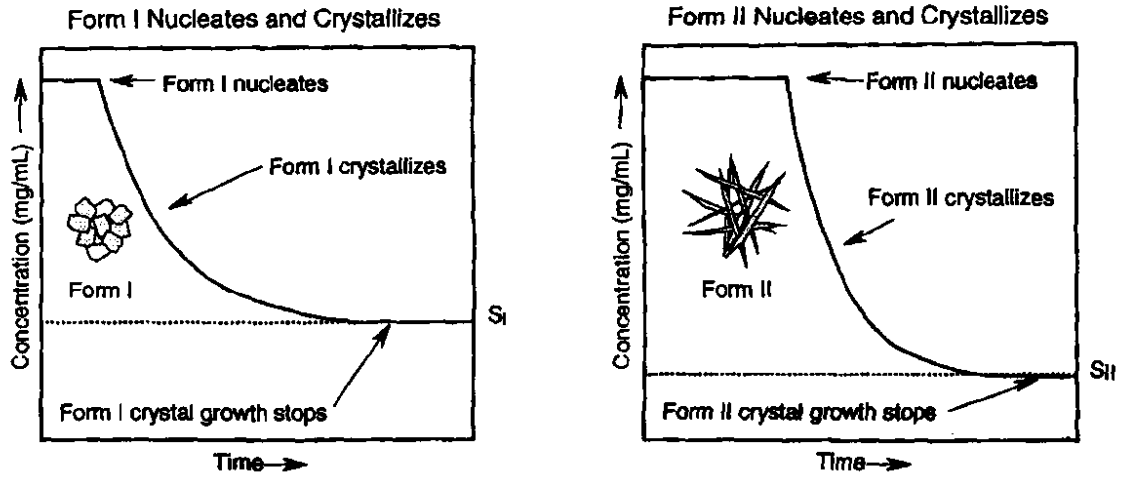

Figure 1.1 Example of Form I and Form II from a polymorphic system (Byrn *et al.*, 1999:18).

Figure 1.1 shows two different polymorphs existing for a specific compound. The lack of control on nucleation may result in the formation of a mixture of these two forms, as illustrated in figure 1.2.

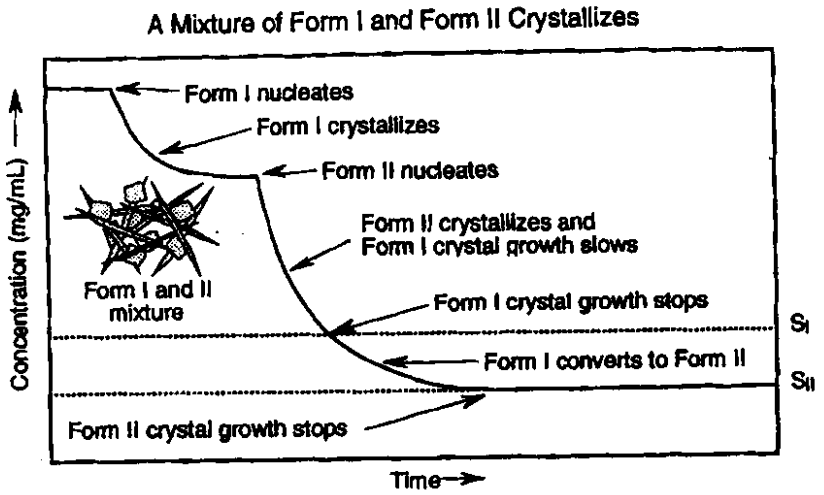

Figure 1.2 The influence of uncontrolled nucleation (Byrn *et al.*, 1999:18).

One method to control the outcome of crystallisation is to add the desired nuclei to the solution. This method is referred to as *seeding* and is often used in industrial crystallisation (Byrn *et al.*, 1999:18).

Specific forces are responsible for the unique structure of a crystal and the sustentation thereof. These forces are either non-covalent attraction forces or hydrogen bonds. Hydrogen bonding develops between a donor and acceptor molecule whereas non-covalent interactions functions on dipole moments and electrostatic distribution of the molecules (Byrn *et al.*, 1999:7).

The symmetry of molecules (or lack thereof) plays a role in the packing of the crystal. If the symmetry of the molecule allows close packing via close fitting, better crystals will be formed, compared to molecules that do not arrange easily (Byrn *et al.*, 1999:8).

The close packing theory states that the closer the molecules are packed together in the crystal structure (lattice), the smaller the free energy. With a decrease in free energy, an increase in heat of sublimation is expected. Therefore an increase in crystal density will lead to an increase in stability due to the increase in melting point (Byrn *et al.*, 1999:8). The thermodynamically stable crystal form should be the least soluble; because of the stronger forces enforcing the lattice, therefore metastable forms are considered to be more soluble (Lund, 1994:190).

1.2 Crystal habit/morphology

Crystal habit refers to the exterior shape, or morphology of the crystal (Byrn *et al.*, 1999:12). The crystal habit is divided in different faces. Faces do not grow at the same rate, thus resulting in a specific shape (needle, prismatic etc.) as shown in figure 1.3. The faces that grow most rapidly are those to which the molecules are bound more tightly (Buckton, 2002:148).

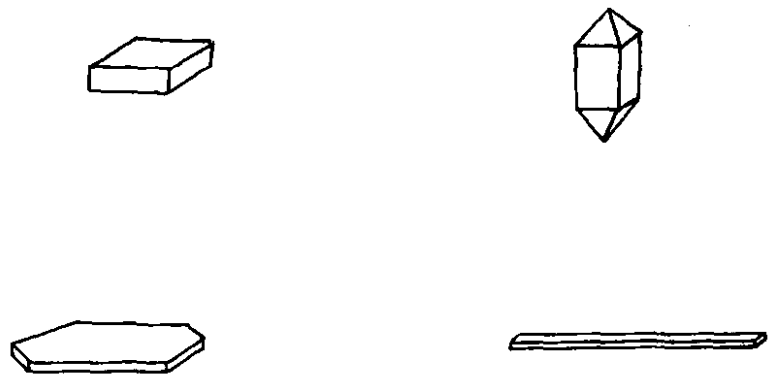

Figure 1.3 Different crystal habits (Byrn, 1982:6).

When a crystal grows, the largest crystal face is always the one that grows the slowest. This is because the face on which growth takes place becomes smaller, while the adjacent faces become larger (Buckton, 2002:148). Eventually the growing face will grow out of existence. This statement is illustrated in figure 1.4.

Crystal faces differ in the arrangement and exposure of functional groups. Differences in the affinity between the faces and the solvent molecules are therefore exhibited. The faces that are most likely to grow are the faces that have a high affinity for the solvent (Buckton, 2002:148).

As seen in figure 1.4, more than one crystal habit is possible for the same crystal origin.

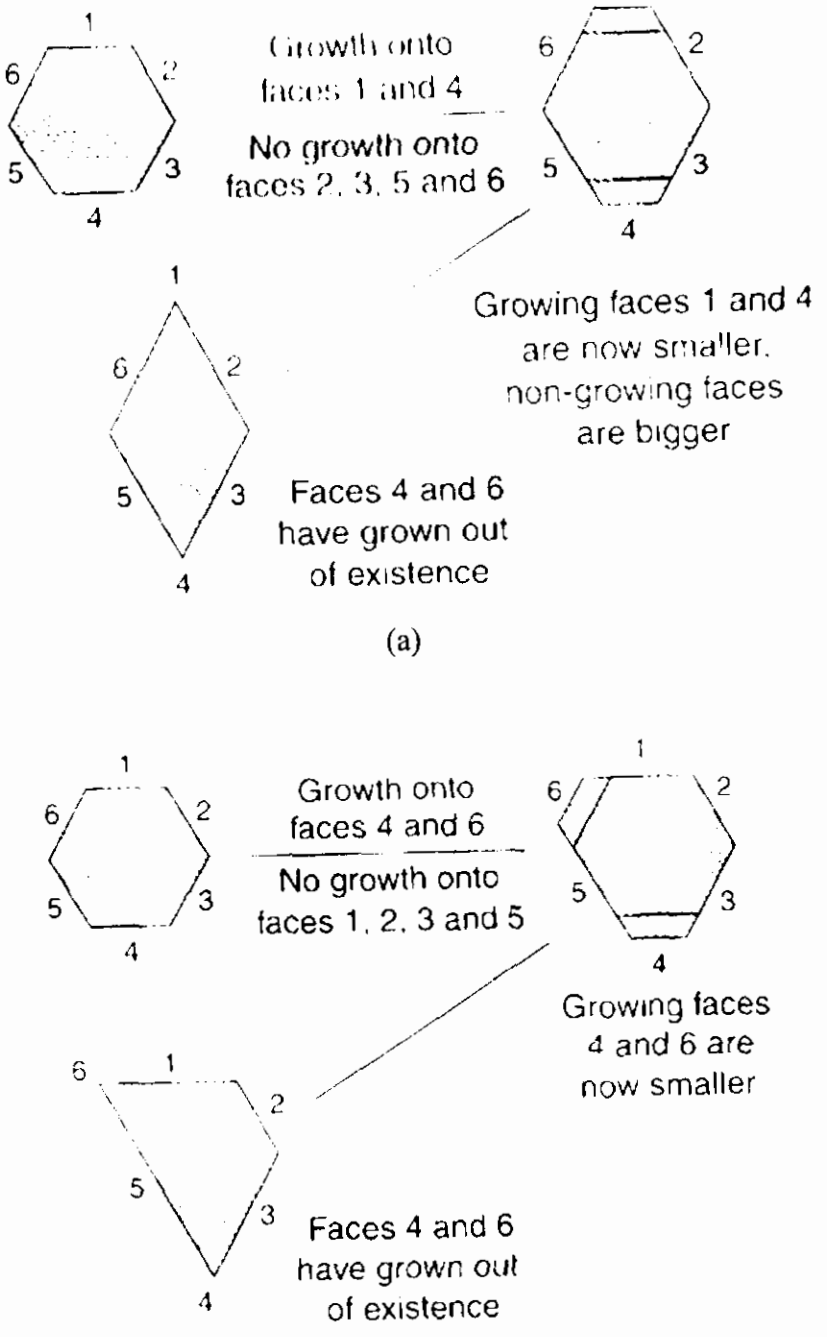

Figure 1.4 (a) Growth on faces 1 and 4 of a hexaganol crystal resulting in a diamond form. (b) Growth on faces 4 and 6 of a hexagonal crystal form resulting in a trapezoidal form (Buckton, 2002:148).

It should also be noted that crystal habit and crystal lattice are independent, therefore it is possible to change habit without inducing any changes in the lattice packing and vice versa, or both can change simultaneously (Lund, 1994:179). Aspirin is a well-known example where the same crystal packing exists as different crystal habits.

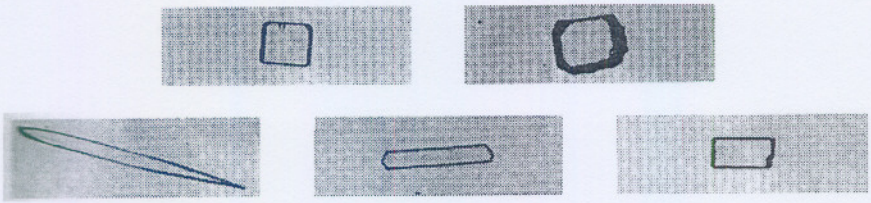

Figure 1.5 Different crystal habits of the same aspirin crystal form (Byrn *et al.*, 1999:13).

Investigating crystal habits may provide helpful information regarding the organisation of molecules in the lattice.

1.3 What is polymorphism?

Polymorphism is the phenomenon where a compound can exist in different solid forms due to the difference in crystal packing arrangement. Polymorphism and pseudopolymorphism are commonly exhibited in pharmaceuticals, particular in steroids and barbiturates. Different polymorphs of the same chemical entity may have different properties (such as solubility and stability) that might result in costly manufacturing/production problems. Extensive research of all possible polymorphic/pseudopolymorphic behaviour of solids can thus prevent formulation problems and ensure stable, active and adequately bio-available drug products (Byrn *et al.*, 1999:143).

Polymorphs, pseudopolymorphs and amorphous solids (discussed respectively in section 1.3, 1.4 and 1.5) may be the product of standard pharmaceutical processes such as crystallisation (CR), desolvation (DE), exposure to vapour (ESV), freeze drying (FD), exposure to heat (HE), melting (ME), milling (MI), precipitation (PR), quench cooling (QC), slurry conversion (SC), spray drying (SD), solid dispersion (SDSP) and wet granulation (WG) (Yu *et al.*, 1998:119). The schematic illustration in figure 1.6 indicates how these processes might give rise to various solid forms. Because of the close interrelationship between these processes, forms and conditions, it must be understood that polymorphic mixtures can easily be formed during phases and that care should be taken to distinguish between polymorphic mixtures and true/solvated/amorphous/isomorphic forms (Yu *et al.*, 1998:125).

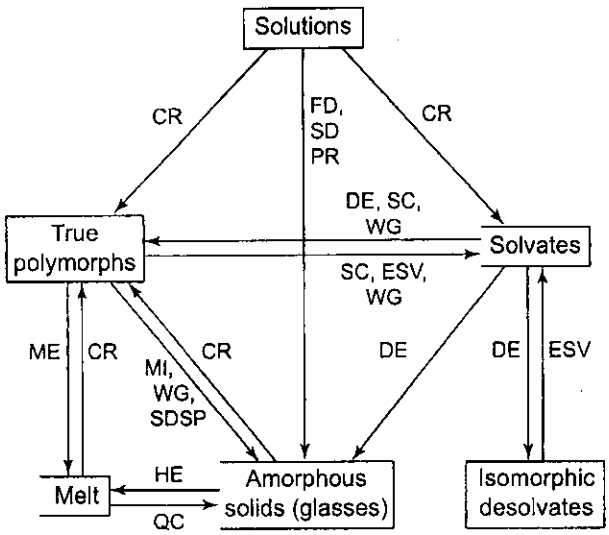

Figure 1.6 Types of solid forms that can be produced by various pharmaceutical processes (Yu *et al.*, 1998:119).

It is of utmost importance to control the crystal form of the APIs and excipients during and after the manufacturing process to ensure that the most suitable crystal form(s) is obtained in the final pharmaceutical product.

1.3.1 True polymorphs

Polymorphs are defined as different crystal forms of the same compound with different internal structure but the same chemical composition (Byrn *et al.*, 1999:13). Polymorphs give rise to different x-ray diffraction patterns (XRPD) and may have different physical and chemical properties. Polymorphic crystals may or may not have different crystal habits, as mentioned in section 1.2.

If the crystallisation conditions are changed during the recrystallisation process, crystals with different packing arrangements (polymorphs) may be formed. The most common causes are: different solvents being used, change in stirring conditions and the presence of impurities (Buckton, 2002:142). The conditions under which true polymorphs may form and their interrelationship with other forms are illustrated in figure 1.6. Figures 1.7 and 1.8 illustrate a schematic representation of polymorphism in a simplified manner.

Figure 1.7 The unit cell being used in the crystal packing of polymorph I and II (Buckton, 2002:142).

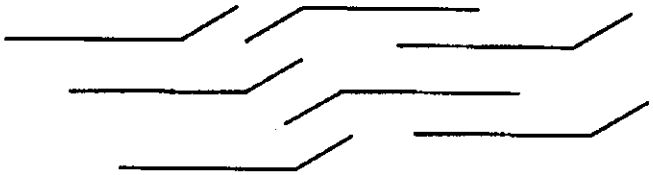

(a)

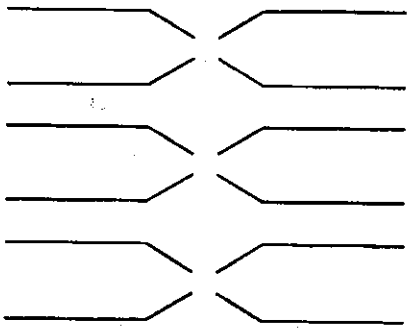

(b)

Figure 1.8 Polymorph I (a) and II (b) (Buckton, 2002:142).

1.3.2 Configurational and conformational polymorphism

Byrn *et al.* (1999:506) defined *configurational polymorphs* as: "a type of polymorphism in which one labile isomer of a compound (eg. a keto form) is present in one polymorph and another labile isomer (eg. an enol form) is present as another polymorph." A known example of a compound exhibiting configurational polymorphism is: ethyl 2-[(phenylmethyl)amino]-2-butenoate (Byrn *et al.*, 1999:150).

Byrn *et al.* (1999:506) defined *conformational polymorphism* as: "a type of polymorphism in which the conformation of the independent molecule in each polymorph is different". An example of a compound exhibiting conformational polymorphism is tri-α-naphtylboronamine (Byrn *et al.*, 1999:149).

1.3.3 Colour polymorphism/ Polychromism

When a compound crystallises in different colours it is referred to as *polychromism* or the compound is said to be *pleochroic* (Byrn *et al.*, 1999:156). Many researchers have reported colour polymorphism for dimethyl 3,6-dicloro-2,5-dihydroxyterephtalate which crystallises in white, yellow and light-yellow crystals due to differences in orientation of the carboxylate group with respect to the aromatic ring. Another example of colour polymorphism is that of 5-methyl-2-[4-methyl-2-nitrophenyl) amino]-3-thiophenecarbonitrile (He *et al.*, 2000:371). This compound crystallises in red, dark red, light red and orange crystals.

Polychromism is a very rare phenomenon, but despite the fact that they have different colours, they still have to be studied because they are still polymorphs, and therefore exhibit different physico-chemical properties (Byrn *et al.*, 1999:156).

1.3.4 Disappearing polymorphs

Sometimes the sudden appearance of a polymorphic form or the unexplained disappearance thereof is encountered, these forms are called *disappearing polymorphs* (Bladgen *et al.*, 1998:170). This can be explained due to the fact that some forms are very unstable (for example dehydration/hydration at ambient conditions) and are sometimes analysed during polymorphic transition. Other reasons for the existence of disappearing polymorphs include the presence of synthesis by-products, the presence of additives, or the percentage water content of so-called water-free organic solvents (as explained in section 1.4.3 and chapter 7) that influence the environmental conditions, that favour/inhibit the growth of a specific crystal form/s. An example of a pharmaceutical compound where a disappearing polymorph has been reported is that of sulphathiazole (Bladgen *et al.*, 1998:170).

1.3.5 Polymorphic stability: A polymorphic relationship

A relationship exists between the stability of a polymorphic form and its *Gibbs free energy* of the form at specific temperatures. To define this relationship the terms *monotropy* and *enantiotropy* are used. If only one stable- and a number of metastable crystals exist, irrespective of temperature and pressure, it is called monotropic polymorphism. In this case the metastable forms will transform into the stable form in time. Enantiotropic polymorphism is exhibited when different crystal forms are stable at different experimental conditions, such as change in temperature and pressure (Lund, 1994:179).

Burger and Ramberger (as referred to by Byrn *et al.,* 1999:85) have constructed two rules to enable one to distinguish between monotropically/enantiotropically related polymorphs. The two rules are *the heat of transition rule* and the *heat of fusion rule.*
For polymorphs to be enantiotropically related an endothermic transition between the two forms at some temperature must be observed (heat of transition rule) or the higher melting form must have the higher heat of fusion (heat of fusion rule).
For polymorphs to be monotropically related an exothermic transition must be observed between the two forms (heat of transition rule) or the higher melting form must have a lower heat of fusion (heat of fusion rule) (Byrn *et al.,* 1999:85).

1.4 Pseudopolymorphism

It is often found that during crystallisation the crystal entraps solvent in the lattice. This phenomenon is referred to as *solvation* and the crystals so produced are called *solvates* (or *hydrates* when the entrapped solvent is water) (Buckton, 2002:144). Solvates and hydrates of a compound are referred to as pseudopolymorphs (Yu *et al.,* 1998:118). Solvent inclusion into the lattice structure may stabilise the packing arrangement due to the fact that intermolecular bonding strength is increased (Byrn *et al.,* 1999:234).

1.4.1 Hydrates

Water molecules are small and have the capability to form hydrogen bonds with themselves and other functional groups of a compound, due to this ideal characteristic, hydrated crystal forms are plentiful (Byrn *et al.,* 1999:236).

Hydrates may form under various conditions and interconvert between other crystal forms, as shown in figure 1.6. The entrapment of solvent can be in stoichiometric or nonstoichiometric amounts (water:compound ratio). In table 1.1, a summary is given of these ratios with appropriate examples.

Table 1.1 Summary of some pharmaceutical hydrates

Nomenclature	**Ratio (Compound:H_2O)**	**Example**	**Reference**
Hemihydrate	1: ½	Estradiol	Park *et al.,* 2005:407.
Monohydrate	1:1	Niclosamide	Van Tonder *et al.,* 2004:417.
Sesquihydrate	1:1 ½	Pantoprazole	Zupancic *et al.,* 2005:59.
Dihydrate	1:2	Carbamazepine	Murphy *et al.,* 2002:121.
Trihydrate	1:3	Ampicillin	Han *et al.,* 1998:63.
Tetrahydrate	1:4	LY 333531 (C_β proteienkinase inhibitor)	Engel *et al.,* 2000:239.
Pentahydrate	1:5	Gatifloxacin	Raghavan *et al.,* 2002:5.
Hexahydrate	1:6	α cyclodextrine	Maggi *et al.,* 1998:211.
Octahydrate	1:8	Nedocromil	Zhu *et al.,* 2002:23.

1.4.2 Solvates

Solvates are formed under the same conditions as hydrates, also being pseudopolymorphs, and have the same interrelationship with other solid forms (as shown in figure 1.6). Many organic solvents have been used to form solvated crystal forms. Table 1.2 lists solvents that have been reported to produce solvated forms of drug compounds.

Table 1.2 Solvents that form solvates with drugs and organic compounds (Byrn *et al.*, 1999:236)

Water
Methanol, ethanol, 1-propanol, isopropanol, 1-butanol, isobutanol
Acetone, methyl ethyl ketone
Acetonitrile
Diethyl ether, tetrahydrofuran, dioxane
Acetic acid, butyric acid, phosphoric acids
Hexane, cyclohexane
Benzene, toluene, xylene
Ethyl acetate
Ethylene glycol
Dichloromethane, chloroform, carbon tetrachloride, 1,2-dicloroethane
N- methylformamide and *N, N*-dimethylformamide, *N*-methylacetamide
Pyridine
Dimethylsulfoxide

Solvate incorporation may also be in stoichiometric or nonstoichiometric amounts (see table 1.1).

An example of a solvated API is the anti-histaminic drug, terfenadine. Sheikh Salem *et al.* (1996:258) crystallised terfenadine using methanol, propylene glycol, ethanol, isopropanol, propanol, butanol, isobutanol, pentanol and 2-pentanol. Interestingly solvates were formed from crystallisation from ethanol, methanol, isopropanol, isobutanol, and 2-pentanol, but not from propylene glycol, propanol, butanol, or pentanol. It seemed that solvation status was favoured by the use of the iso-alcohols while the *n*-alcohols produce true polymorphs of terfenadine.

Thermo gravimetric analysis (TGA) of the methanol solvate of terfenadine revealed a weight loss of 0.312 mg from the initial weight of 3.132 mg. Therefore a

$$\frac{0.312}{3.132} \times 100\% = 9.96\%$$

weight loss was due to methanol loss from the crystal structure (as shown in figure 1.9).

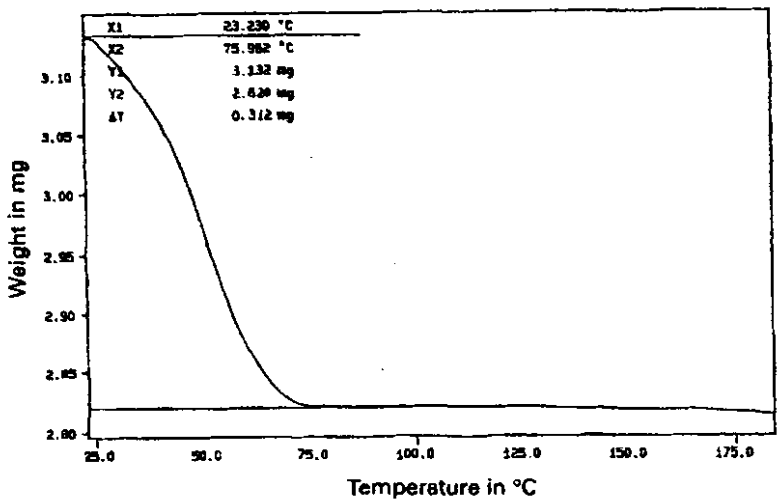

Figure 1.9 TGA of the methanol solvate of terfenadine (Hakanen & Laine, 1995:225).

Differential scanning colorimetry (DSC) analysis of the methanol solvate of terfenadine revealed a desolvation peak maximum at ±80°C (endotherm ↑) as shown in figure 1.10.

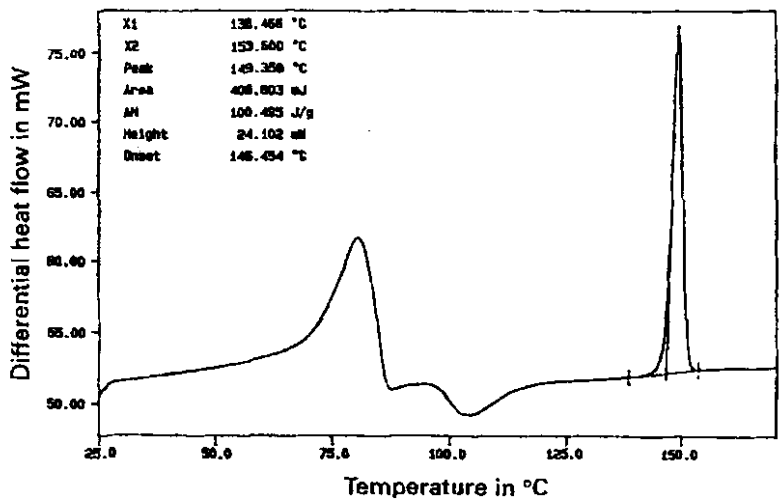

Figure 1.10 DSC thermogram of the methanol solvate of terfenadine (Hakanen & Laine, 1995:224).

1.4.3 The influence of water content on status of hydration

When organic solvents are to be used during polymorphic screening, the water content of these solvents should be taken into account. Byrn *et al.* (1999:241) have reported that when a drug substance is known to form multiple hydrated pseudopolymorphs, a small difference of water content can easily produce different hydrated crystals from the recrystallisation. As seen in figure 1.11, small differences in the water content of ethyl acetate (ranging from 0-3.2%) resulted in three different hydrated pseudopolymorphs. The importance to control moisture (water) content of solvents that are used during recrystallisation processes should therefore be stressed.

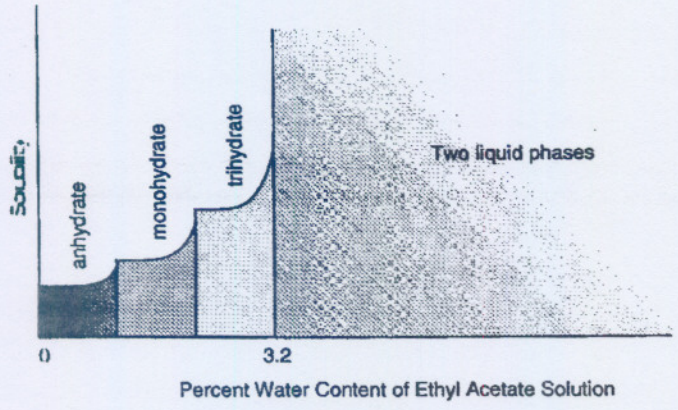

Figure 1.11 Crystallisation of hydrated crystals forms from so-called water-free solvents (Byrn *et al.*, 1999:241).

1.4.4 Desolvated/dehydrated forms

As mentioned earlier, polymorphs have different XRPD patterns. It is also true for pseudopolymorphs. It is known that solvent or water molecules could play an important role in the stabilisation of the crystal lattice. If the solvent is part of the force holding the crystal together it will possibly result in crystal collapse when removed from the lattice. Crystal collapse will give rise to formation of a different crystal or polymorph. In figure 1.10, an exothermic peak is observed just after the desolvation endothermic peak, indicating that when the methanol is removed from the

crystal lattice, the lattice becomes unstable and has to rearrange in a crystal form with a melting endotherm at ±148°C (Hakanen & Laine, 1995:224).

An X-ray powder diffraction (XRPD) pattern was taken of the methanol solvate before and after desolvation. The XRPD patterns differed, proving the fact that the crystal forms do indeed differ from each other. The XRPD patterns of these samples are illustrated in figure 1.12 (Hakanen & Laine, 1995:224).

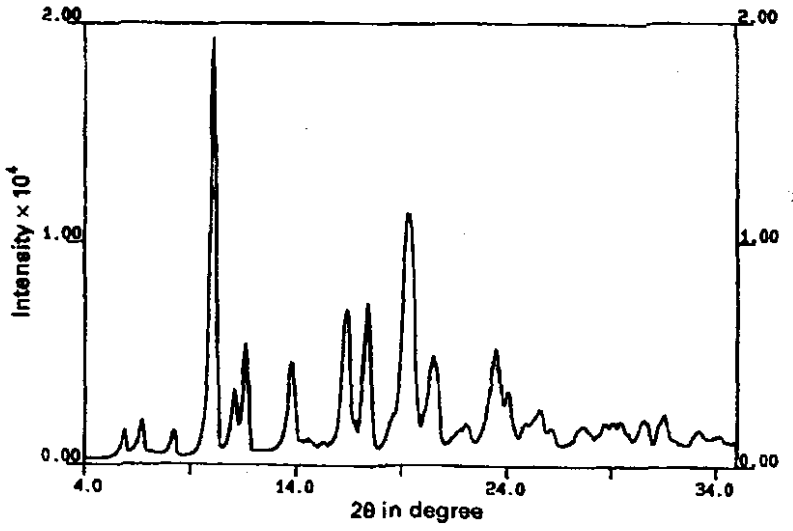

(a)

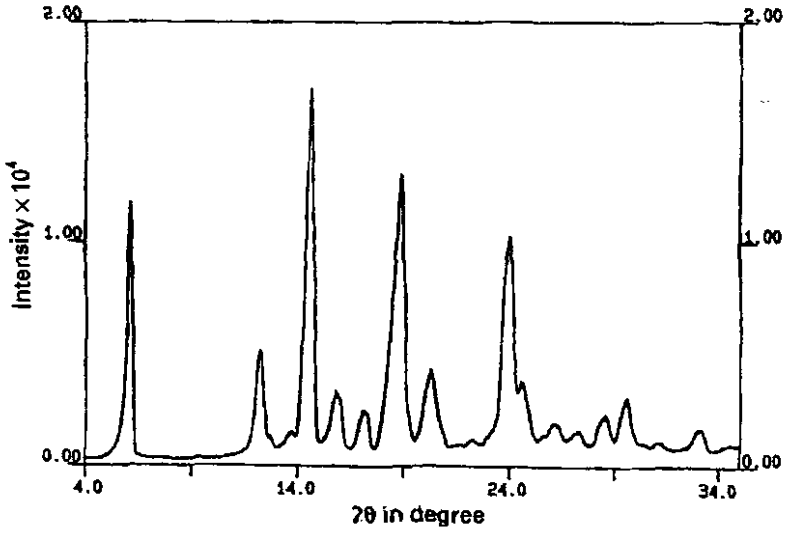

(b)

Figure 1.12 (a) XRPD pattern of the methanol solvate and (b) desolvated product (Hakanen & Laine, 1995:224).

If the crystal lattice does not collapse during desolvation, the solvent does not play a significant role in the stabilisation of the lattice and the original crystal form stays the same (*desolvated solvate*) (Byrn, 1982: 7). A *desolvated solvate* is also referred to as an *isomorphic desolvate* (Yu *et al.*, 1998:119). These desolvated solvates are less dense than their fully solvated forms (Yu *et al.*, 1998:119) as illustrated in figure 1.13. It should be noted that isomorphic forms have only slightly different XRPD's than their parent solvated compound (Yu *et al.*, 1998:124, Byrn *et al.*, 1995:951). Examples of such API's include erythromycin A, cefachlor and cephalexin (Stephenson *et al.*, 1998:536).

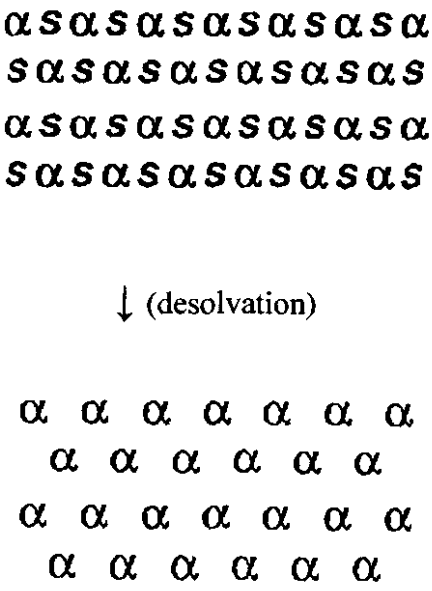

Figure 1.13 A simple demonstration of pseudopolymorphism and isomorphic desolvation. The ∝ symbol resembles a drug molecule, whereas the *s* resembles a solvent/water molecule (Yu *et al.*, 1998:119).

The solvent molecules may be hard to lose, or it may be lost with great ease. In the latter case, solvated crystal forms may be overlooked, as there are pseudopolymorphs that lose solvent very fast, even at ambient conditions (Byrn *et al.*, 1999:236).

1.4.5 Polymorphism among pseudopolymorphs

As with polymorphs where at least two crystal forms exist for the same compound (the same molecular entities), polymorphism among pseudopolymorphs are also possible where the compound has the same solvated/hydrated status (stoichiometry) for two or more crystal forms of the pseudopolymorph. An example of this phenomenon is that of niclosamide that have two monohydrates (Van Tonder *et al.*, 2004:417). The term *polymorphic pseudopolymorphism* is commonly used for these instances, the forms either being polymorphic hydrates or polymorphic solvates.

1.5 Amorphous solids

It is known that a crystal contains some disordered regions (Byrn *et al.*, 1999:249). When a solid exist as molecules in random order, it is called an *amorphous solid* (Buckton, 2002:145). Amorphous solids have few characteristics. They present a broad (halo-shaped) or no x-ray powder diffraction and/or NMR patterns (Byrn *et al.*, 1999:249) and have no definite melting point (Buckton, 2002:145). It should also be noted that amorphous solids can either be anhydrous, solvated or hydrated.

Amorphous solids can be demonstrated by figure 1.14.

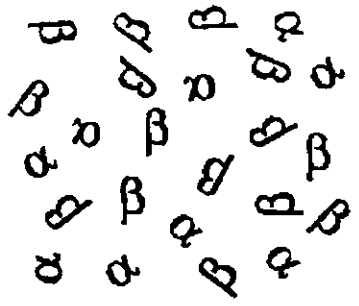

Figure 1.14 A simple illustration explaining the amorphous state. Where the ∝ symbol resembles the drug molecule in one possible conformation and the β symbol another possible conformation (Yu *et al.*, 1998:119).

1.5.1 Glass transition temperature

Amorphous solids have a specific temperature where major changes in properties are exhibited; this temperature is called the *transition temperature* (Tg). When the amorphous solid is stored below the Tg temperature, it is in the so-called *glassy state.* Above the Tg, the amorphous solid is characterised as a *rubber* (Buckton, 2002:146). Pharmaceuticals that form glasses (above and below ambient conditions) are listed in table 1.3 with their corresponding Tg values, melting points (Tm) and Tg/Tm.

Table 1.3 Pharmaceuticals forming glasses above and below ambient conditions (Fukuoka *et al.*, 1989:1047)

Pharmaceutical	Tg (K)	Tm (K)	Tg/Tm
Cholecalciferol	296	352	0.84
Sulfisoxazole	306	460	0.67
Stilbestrol	308	439	0.70
Phenobarbitol	321	443	0.72
Quinidine	326	445	0.73
Salicin	333	466	0.71
Sulfathiazole	334	471	0.71
Sulfadimethoxine	339	465	0.73
17β-Estradiol	348	445	0.80
Aspirin	243	408	0.59
Antipyrine	256	380	0.67
Methyltestosterone	270	421	0.64
Phenylbutazone	277	377	0.73
Atropine	281	379	0.74
Ergocalciferol	290	376	0.77

From table 1.3 it can be seen that the Tg/Tm ratio varies between ±0.60 and ±0.84. The Tg/Tm ratio may be used to calculate the range in which the Tg value of an API lies, when a Tm value (in K) is known (Byrn *et al.*, 1999:251). Therefore the lower range of the Tg value can be calculated using equation 1 and the higher range using equation 2:

$$Tg_{(L\ RANGE)} = 0.6 \times Tm \qquad \text{(Equation 1.1)}$$

$$Tg_{(H\ RANGE)} = 0.85 \times Tm \qquad \text{(Equation 1.2)}$$

$$\text{Therefore } Tg_{(L\ RANGE)} \leq Tg \leq Tg_{(H\ RANGE)}$$

1.5.2 Polymorphism among amorphous solids

As mentioned earlier, whenever solids have different structures and share the same molecular entities, it is referred to as polymorphism. This is also the case for amorphous solids, and is known as *poly-amorphism*. Poly-amorphism for various compounds has been reported (Hancock *et al.*, 2002:1152 and Kieffer, 2002:644). If *poly-amorphism* is suspected, it should be extensively studied, as it sometimes happen that an amorphous form exhibit different properties from time to time. This variation in physico-chemical properties may result in falsely identifying a second amorphous form (Kivelson & Tarjus, 2002:630).

1.6 The impact of polymorphism, crystal habit and the presence of amorphous forms on pharmaceutical manufacturing and product integrity

It has been stressed throughout this chapter, that the different solid forms of a pharmaceutical substance should be taken into account because of the differences in behaviour. Now one may ask: "Where does polymorphism fit in the drug development process?" The answer is simple. Although polymorphic behaviour must be taken into account from the start of drug manufacture to when the dosage form is used, polymorphic screening should be performed during the synthesis and pre-formulation (as indicated in figure 1.15) to anticipate possible polymorphic transitions and to identify areas that need to be controlled throughout the manufacturing process (Byrn *et al.*, 1999:15).

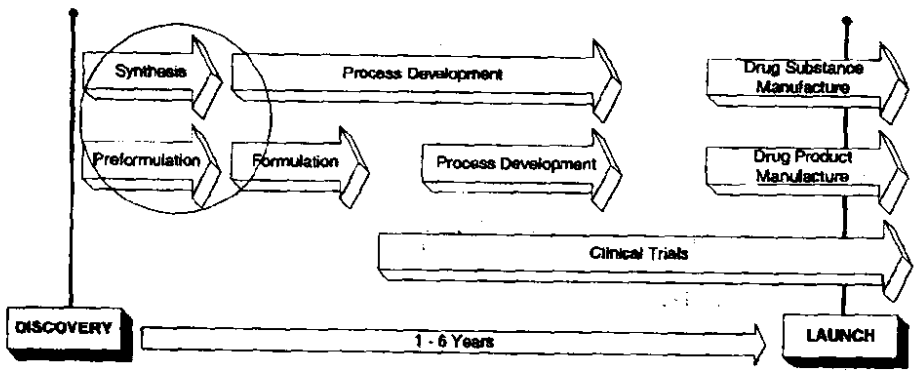

Figure 1.15 The drug development process (Newman & Stahly, 2002:2).

The specifications regarding polymorphic screening have been documented by the International Committee on Harmonization (ICH) to standardise and guide this process (Dotzel, 2000:83056). A simple flow chart (shown in figure 1.16) can be followed to guide and help decide the fate of the drug.

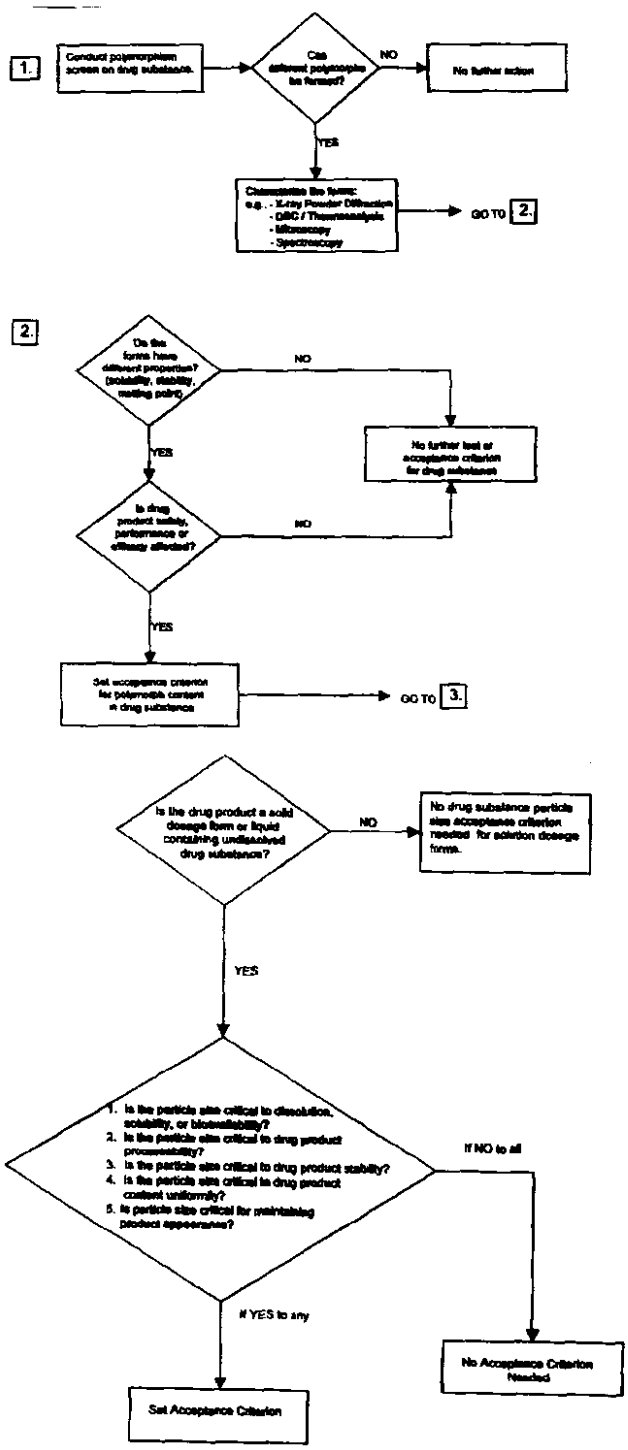

Figure 1.16 Flow chart 4 from the ICH Q6A document (Dotzel, 2000:83056-83057).

The Food and Drug Administration (FDA) requires this process and its specifications to be followed before a New Drug Application (NDA) is to be released.

Now that it is understood why polymorphism (and related subjects) is important and how it should be studied, one must be wary of the effect thereof on pharmaceutical manufacturing, product stability and efficacy. Illustrated in figure 1.17 is a flow chart of processes commonly used during solid dosage form design that may be influenced by the presence of polymorphism or vice versa (Zhang *et al.*, 2004:379).

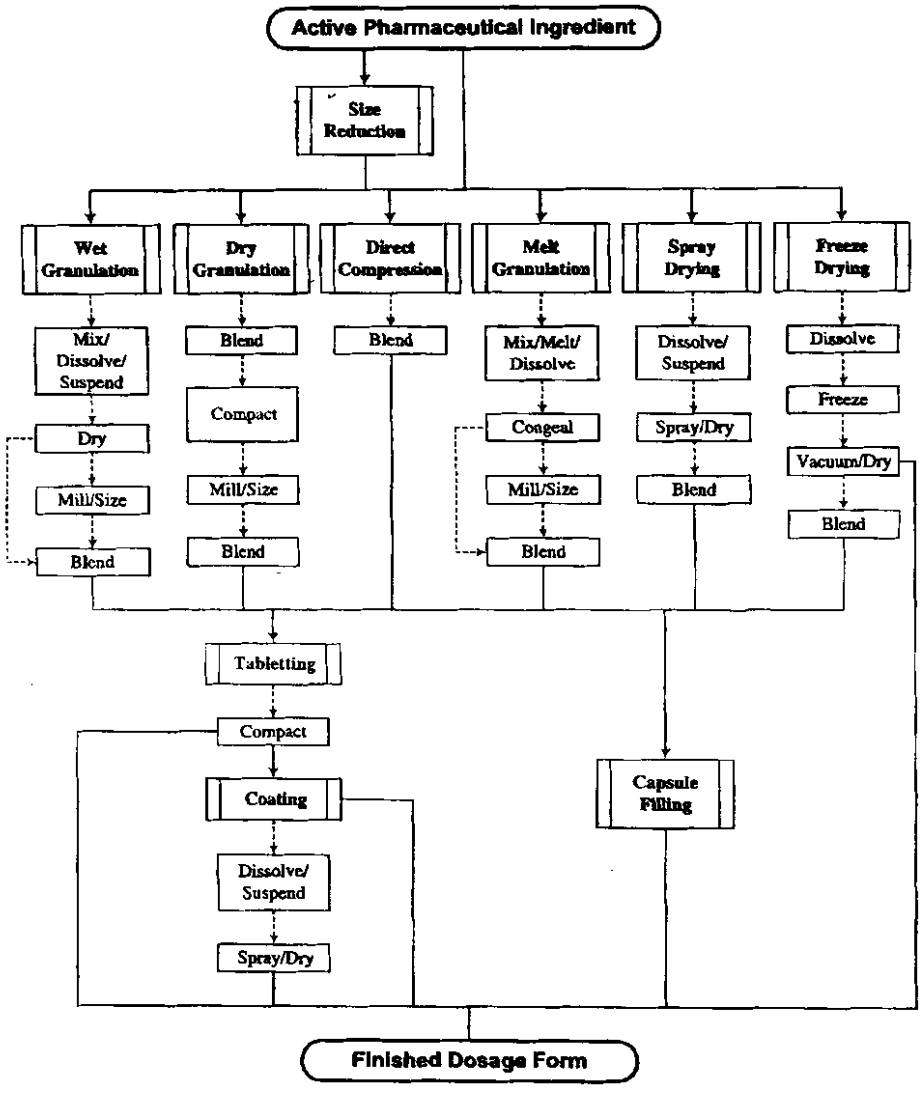

Figure 1.17 Common processes used for preparing solid dosage forms (Zhang *et al.*, 2004:379).

In this section some practical examples will be referred to, to explain and clarify the implication of different processes influencing polymorphism. It should be noted that many of these factors are interlinked (especially to stability), and should not be treated separately.

1.6.1 Polymorphism, pseudopolymorphism and the amorphous state

Byrn *et al.* (1999:15) stated that the properties listed in table 1.4 depend on the structure of solids. These properties of polymorphs may differ from each other, since it is clear that polymorphs have different internal structures.

Table 1.4 Properties of a compound that depend on structure differences (Byrn *et al.*, 1999:15)

Density	Water uptake	Solid-state reactivity
Hardness	Optical properties	Physical Stability
Cleavage	Electrical properties	Chemical stability
Solubility	Thermo-analytical behaviour	

1.6.1.1 Solubility and bioavailability

It has already been mentioned in section 1.1 that the most stable crystal form possesses the highest melting point (in most cases). Melting point and solubility are related through heat of fusion. Heat of fusion is the amount of energy created during melting/fusion. Crystals with strong lattices have a high melting point, and thus have a greater heat of fusion than crystals that have weaker lattices (Wells, 2002:127).

Because solubility requires the disruption of the crystal lattice, it is also dependant on the strength of the crystal lattice - which is why different polymorphs may exhibit differences in solubility. In most of the cases it can be assumed that solubility is indirectly proportional to polymorph stability, meaning that the weaker the lattice the better the solubility. Buckton (2002:144) stated the following simple relationship between melting point, lattice strength and dissolution: the higher the melting point of a solid, the stronger is its lattice. Strong lattices are not easily loosened and therefore gives rise to slower dissolution rates. Figure 1.18 plots the relationship between

solubility and stability for the three polymorphs of riboflavin stating that the higher the melting point, the lower the solubility.

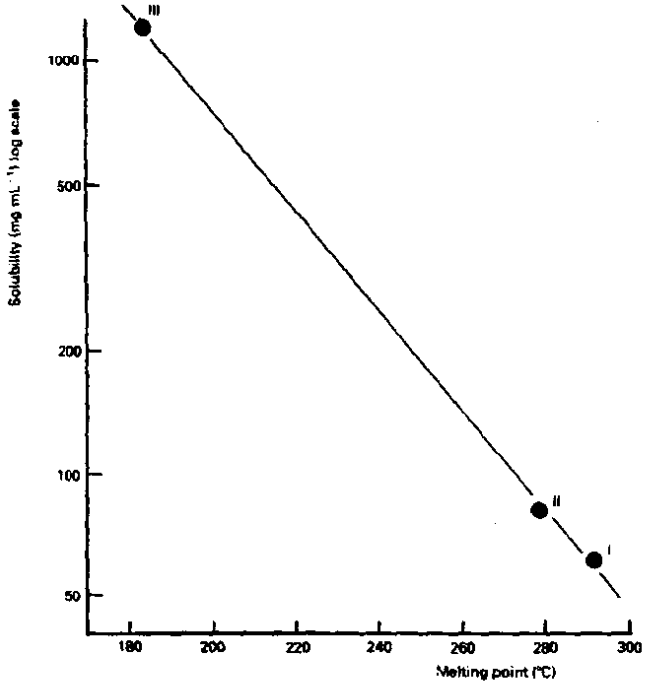

Figure 1.18 The relationship between solubility and thermal stability of riboflavin polymorph I, II and III (Wells, 2002:127).

Of importance to the pharmaceutical product is the possibility that the metastable (less stable forms) might give rise to higher solubility than the saturated solubility (Buckton, 2002:142). These supersaturated solutions will eventually return to equilibrium as the stable form precipitates. If a drug is used as a metastable form, and a supersaturated solution is created for a sufficient period of time before equilibrium is reached, it will cause an increase in bioavailability due to the higher concentration of drug substance available for absorption (Buckton, 2002:143). This characteristic may be dangerous if the API reaches toxic plasma concentrations, but can also be advantageous in the case of APIs that are known to have poor bioavailability.

Solubility differences of polymorphs should be taken into account, not only to ensure that adequate plasma a concentration of the drug is achieved, but also that it is safe for use.

1.6.1.2 Density and hardness

From figure 1.8, it is easy to comprehend that polymorphs have different densities. Density can be defined as the mass of substance that has a distinct volume. When comparing polymorph I and II from figure 1.8, it can be seen that polymorph I is denser than polymorph II (Buckton, 2002:143). This is because the lattice structure of I allows a denser packing of the unit cell to that of form II.

Figure 1.8 can be used to discuss why polymorphs differ in hardness and breakability. It can be seen that polymorph II have definite lines (vertically or horizontally) that can be seen as "weak spots". Polymorph I have more interwoven unit cells, which show no "weak points". Thus it can be derived that polymorph I will be harder to break/mill than polymorph II (Buckton, 2002:143).

Because of the difference in density and hardness, polymorphs have different milling and tabletting properties. These differences should therefore be studied prior to drug manufacture, to predict and aid in possible formulation difficulties. Milling, mixing and tabletting are further discussed in section 1.7.3.

1.6.1.3 Water sorption

Because polymorphs differ in crystal packing, it is understood that the volume of each may differ (Byrn *et al.*, 1995:951), creating different volumes of solvent that the crystal may entrap (if it has a tendency to do so).

To illustrate the difference in water sorption capability between different crystal forms (that have different volumes), an antibiotic, cephaloridine is used as example (Byrn *et al.*, 1995:951). Three different solvated/hydrated crystal forms were prepared and thereafter desolvated/dehydrated. These desolvated/dehydrated crystal forms were then exposed to the same experimental conditions of relative humidity. From this study it was observed that the desolvated di-methanol solvate took up two waters of hydration, the desolvated mono-methanol solvate took up one water molecule and the dehydrated hydrate took up 3/4 of a water molecule.

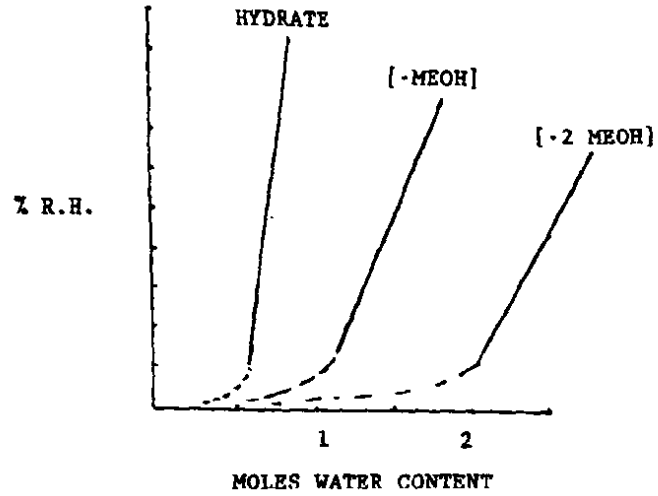

Figure 1.19 Water sorption behaviour of three desolvated crystal forms of cephaloridine (Byrn *et al.*, 1995: 952).

From this example is can be seen that the same compound (as different crystal forms) may vary in solvation/hydration ability. This is an important factor to consider during product development and manufacture, as tabletting processes may include wet granulation (Byrn *et al.*, 1995:951). The most common cause for impaired powder reconstitution is that powder cohesion develops, and this is most frequently due to moisture sorption (Carstensen, 1990:369).

Water sorption can clearly influence drug stability if the drug is prone to hydrolysis, thereby decreasing the shelf life of the product; or it may have serious effect on product integrity (brittle tablets) that will limit transport; or cause polymorph interconversion.

1.6.1.4 Stability

At this point it is clear that polymorphs exist as different forms of the same compound that vary in stability. Stability, both physical and chemical, is intertwined with many factors, especially temperature humidity and pressure, therefore stability can be characterised by those factors.

1.6.1.4.1 Physical stability

Physical stability can be explained as the existence of different forms, with different tendencies to convert to one another, therefore with respect to physical transformations (polymorphic interconversion) of the compound.

As mentioned earlier, solids in the amorphous state are in the most cases the least stable forms in the range of polymorphs existing for the compound. These forms may interconvert to other forms (mainly crystalline forms) in a very short span of time, and physical stability is therefore explained by the example of the interconversion of indomethacin from an amorphous form to the most stable crystalline form thereof. The interconversion of amorphous indomethacin is depicted in the x-ray powder diffraction (XRPD) pattern in figure 1.20. As mentioned in section 1.5, amorphous forms have a broad or no XRPD pattern; thus it can be seen that the amorphous indomethacin converts to a more crystalline state as a function of time.

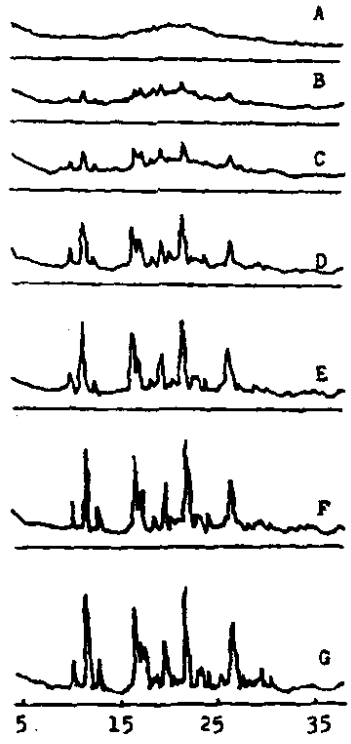

Figure 1.20 The conversion of amorphous indomethacin as a function of time. A: at start, B: 24h, C: 48h, D: 7days, E: 14days, F: 30days, G: 67days (Fukuoka *et al.*, 1989:1048).

The conversion of the amorphous form may result in a decrease in solubility as more crystalline solids have stronger lattices.

Physical stability does not only include the phase change from amorphous to more crystalline forms, but also the phase change between true polymorphs, solvated to desolvates and hydrates to dehydrated forms which are influenced by various factors (as discussed in this chapter).

1.6.1.4.2 Chemical stability

Different solid forms have different chemical reactivity (solid-state reactivity). For example the peptide DL-Ala-Met that is more prone to oxidation in the amorphous state compared to the crystalline state a seen in figure 1.21 (Byrn *et al.*, 2001:120).

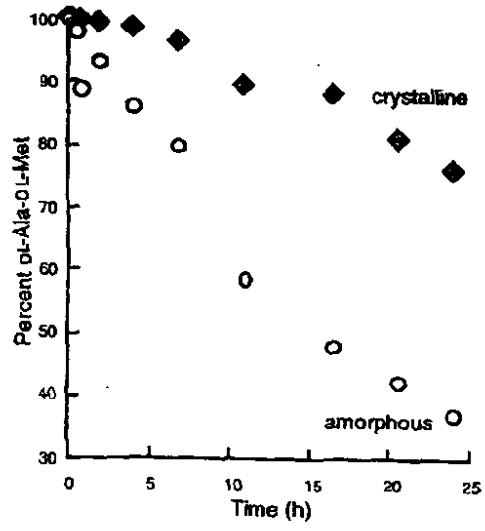

Figure 1.21 Difference in oxidation behaviour of crystalline and amorphous DL-Ala-Met at ambient conditions (Byrn *et al.*, 2001:120).

It was also found that UV degradation between these forms also varied. The crystalline solid was much less prone to UV degradation compared to the amorphous counterpart as illustrated in figure 1.22 (Byrn *et al.*, 2001:120).

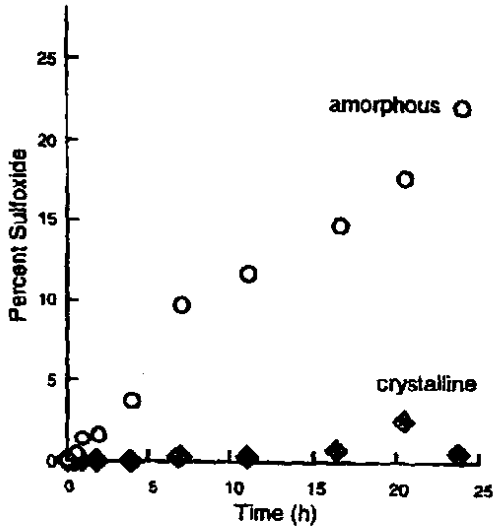

Figure 1.22 UV degradation behaviour of crystalline and amorphous DL-Ala-Met at ambient conditions (Byrn *et al.*, 2001:120).

It is now clear that chemical stability, such as hydrolysis; UV degradation and oxidation may vary between polymorphs.

Thus to conclude: stability, both physical and chemical, is therefore surely one of the most important factors to consider as it may have a serious impact on product safety and efficacy.

1.6.1.5 Thermal behaviour

It has been mentioned in section 1.6.1.2 that polymorphs have different crystal densities and different forces stabilising the lattice and different free energies. These differences have been explained to correspond with thermal behaviour such as the melting point. It is also known that some forces such as Van der Waals forces are more easily overcome than hydrogen bonding. Thus it is easily understood that depending on the type of forces present and the density of the lattice, that polymorphs will exhibit different melting points; different thermally induced interconversion and different desolvation and/or dehydration behaviour.

Figure 1.23 shows three differential scanning colorimetry (DSC) thermograms of three polymorphs of the antihelminthic drug, mebendazole (Form A, B and C). Each of these polymorphs exhibits different thermal behaviour (De Villiers *et al.*, 2005:2).

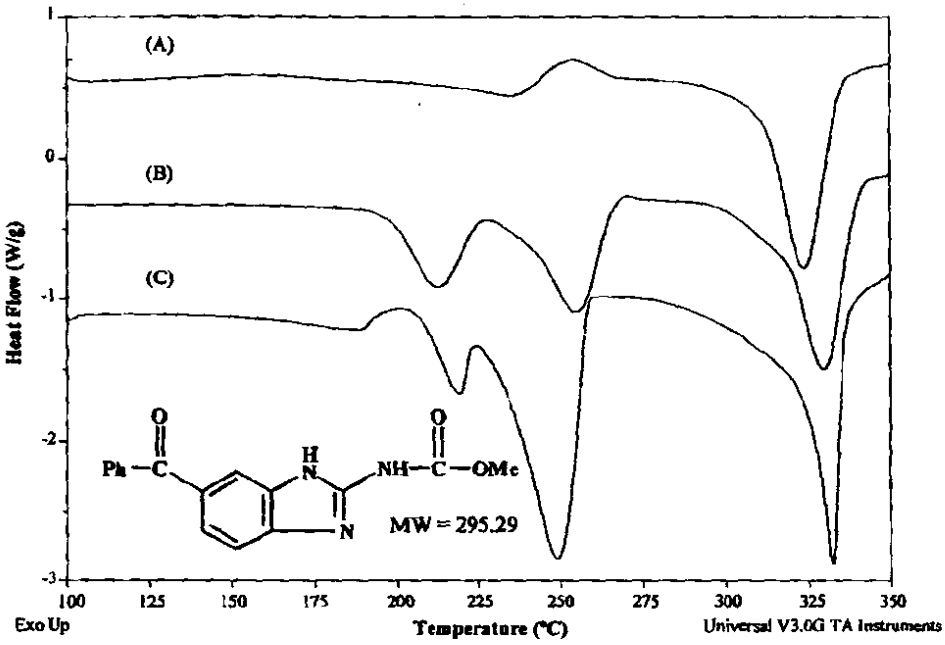

Figure 1.23 The DSC thermograms of form A, B and C of mebendazole (De Villiers *et al.*, 2005:2).

A polymorph can also change during heating either converting to a mixture of polymorphs (change is not instantaneous) or eventually to another crystal form. The thermal behaviour of mebendazole polymorphs can be seen in figure 1.23. From figure 1.24 it was observed that the XRPD at 25°C represents polymorph C that converts into a mixture of polymorphs A and C (202°C). At 221°C it was observed that polymorphs A and C converted into polymorph A as seen in the XRPD pattern at 221°C (de Villiers *et al.*, 2005:3).

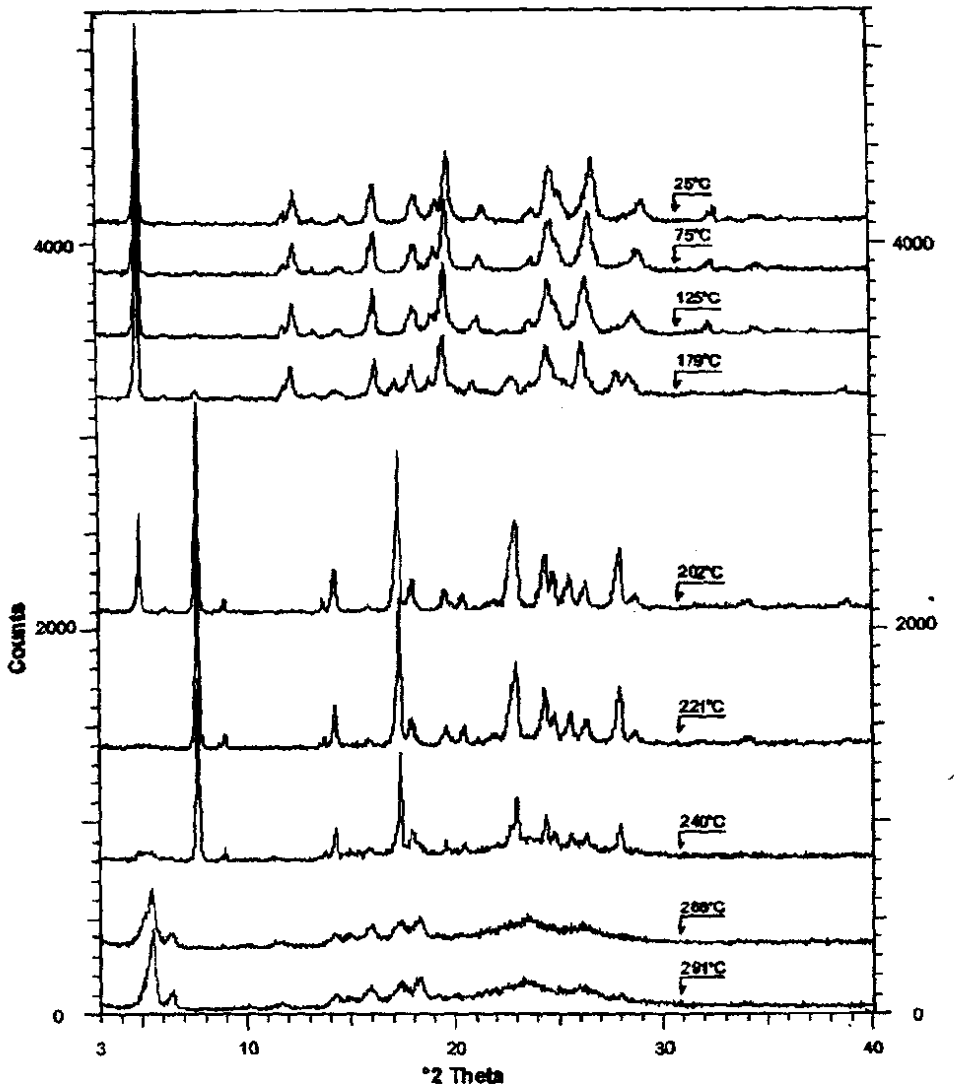

Figure 1.24 Variable temperature XRPD (VT-XRPD) patterns of mebendazole form C taken at different temperatures, characterising specific crystal changes (de Villiers *et al.*, 2005:3).

1.6.1.6 Electrical properties

Electrical properties (such as conductivity) are closely related to the solubility of the compound (Garcia *et al.*, 1999:1360). The higher the solubility the higher the conductivity will be. To prove and explain this property among polymorphs, see sections 1.7.1.1 and 1.7.1.2.

1.7. Polymorphism and drug manufacture

It is now clear that different polymorphs exhibit different physico-chemical properties. It is therefore not only important to be able to choose the most suitable form for the manufacture of pharmaceuticals, but to make sure that the desired form is not affected by or does not influence the various areas of drug manufacture. Byrn *et al.* (1999:15) gave the following summary of actions/factors that have to be controlled/supervised that are known to cause problems during the manufacturing process (table 1.5).

Table 1.5 Control areas for solid forms (Byrn *et al.*, 1999:15)

Yield	Milling	Dissolution
Filtration	Mixing	Suspension formulations
Washing	Tabletting	Lyophilisation
Drying	Flowability	

It should be noted that many of these control areas are influenced by each other or the same factors. Therefore many of these areas can be discussed in conjunction to each other.

The control areas have therefore been paired together due to overlapping similarities of the factors that are interrelated but does not implicate that these head groups and their subgroups are fully detached from the other groups.

1.7.1 Crystal size

1.7.1.1 Dissolution

Garcia *et al.* (1999:1360) reported that a pharmaceutical compound (not named because of confidentiality) converted form a monoclinic form A to a triclinic form B during dissolution. The conductivity and solubility of both these forms were determined. The conductivity of the solution in pure water was determined from the start to the finish of the dissolution of form A. It was found that both the conductivity and solubility decreased throughout the dissolution, indicating the conversion of form

A to form B. In figure 1.25 the conversion is plotted; conductivity as a function of time.

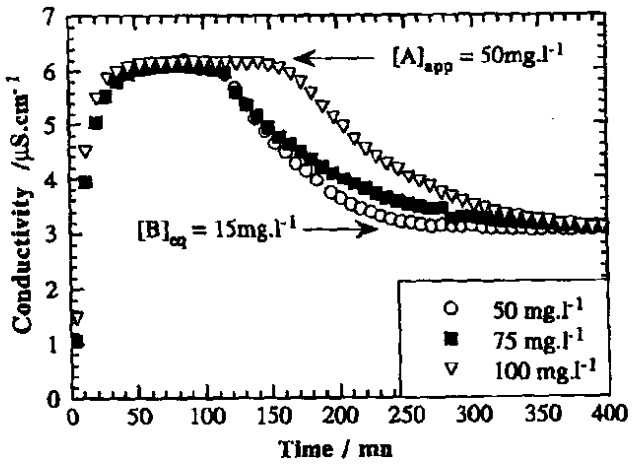

Figure 1.25 Variation of conductivity vs. time due to the solution mediated phase transformation of form A into form B for concentrations ranging form 50 to 100 mg/l at 40°C in pure water. [A]app being the apparent solubility of form A and [B]eq the solubility of form B (Garcia *et al.*, 1999:363).

1.7.1.2 Crystal habit

In many cases a polymorph does not exist in only one crystal habit. Such is the case of the pharmaceutical compound mentioned under 1.7.1.1. Garcia *et al.* (1999:1363) found that polymorph A of this compound exists as an acicular or tabular crystal habit.

Because different crystal habits give rise to different crystal sizes, it is understood that different crystal habits may probably give rise to different solubility and dissolution results. This can be clarified due to the difference in surface area (Buckton, 2002:148). Dissolution rate is directly proportional to surface area (Buckton, 2002:148). As seen in figure 1.26, three different crystal forms and their relative surface areas, giving rise to different exposed surface area leading to difference in dissolution ability.

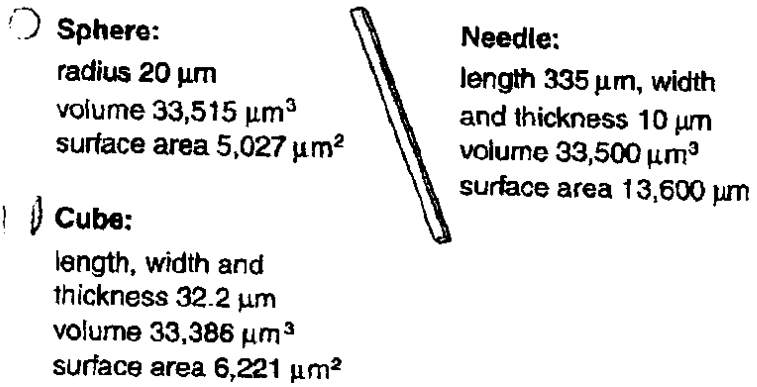

Figure 1.26 The relative surface areas of a sphere, a cube and a needle that each have similar volumes of material (Buckton, 2002:148).

It can be seen in figure 1.27 that the conductivity (measuring solubility) is definitely different between the two possible crystal habits of Form A. Bear in mind the conversion of Form A to polymorph B explained in 1.7.1.1 (applicable for both crystal habits of Form A).

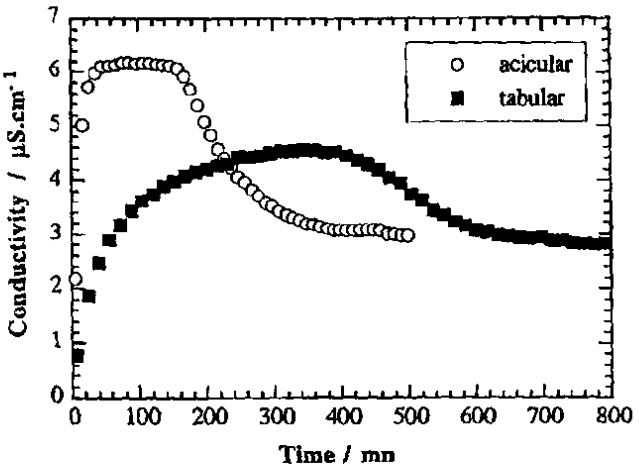

Figure 1.27 Variation of conductivity vs. time for acicular and tabular crystal habits of polymorph A using the same concentrations at 40°C in pure water (Garcia *et al.*, 1999: 1364).

1.7.1.3 Flowability

Examining figure 1.3, it is easy to see that the different crystal habits will differ in flowability. A simple rule to remember is that the smaller and rounder the shape the better the flowability (Lund, 1994:184). Bear in mind that flowability is also

influenced by the tendency of cleavage and that good particle flow is necessary for good uniformity (Buckton, 2002:148).

Flowability is characterised by either one of the following: angle of repose, Carr's index or the Hausner ratio (Lund, 1994:184).

1.7.1.3.1 Angle of repose

The angle of repose is a method in which powder (specific amount) is allowed to fall under the influence of gravity for a specific instant of time. The angle of incline of the formed cone is then assessed. The smaller the angle, the better the powder flows. Good powder flow is depicted by an angle of repose of less than 30° (Lund, 1994:184).

1.7.1.3.2 Carr's index & the Hausner ratio

Carr's index is given by equation 1.3 and the Hausner ratio is given by equation 1.4.

$$\text{Carr's index} = \left(\frac{Td - Pd}{Td}\right) \times 100\% \qquad \text{(Equation 1.3)}$$

$$\text{Haussner ratio} = \frac{Td}{Pd} \qquad \text{(Equation 1.4)}$$

Whereas:

Poured density (Pd) is the volume occupied by a certain mass of material when poured into a measuring cylinder.

Tapped density (Td) is the volume occupied by a certain mass of material when poured into a measuring cylinder and then lightly tapped.

Good powder flow is depicted by a Carr index of less than 15% or a Hausner ratio that is closer to 1 (Lund, 1994:184).

1.7.1.3.3 Powder flow properties of four solid forms of Celecoxib

In table 1.6, the results of Chawla *et al.* (2003:316) are summarised and indicate the differences in the powder flow properties of different celecoxib crystal forms.

Table 1.6 Density and other parameters of different solid-state forms of celecoxib (Chawla *et al.*, 2003:316)

Form	Poured density (g/ml)	Tap density (g/ml)	Carr's Index (%)	Hausner ratio
Celecoxib	0.362± 0.04	0.517 ± 0.01	29.961 ± 1	1.428 ± 0.1
CEL-DMA	0.564± 0.03	0.729 ± 0.03	22.542 ± 1	1.291 ± 0.1
CEL-DMF	0.445± 0.04	0.645 ± 0.02	31.049 ± 1	1.450 ± 0.1
CEL- amorph	0.475 ± 0.02	0.698 ± 0.02	31.964 ± 2	1.470 ± 0.1

From these results, it can be seen that form CEL-DMA (Celecoxib DMA solvate) has the best flow properties when comparing the Carr's indexes and Hausner ratios of the forms.

Using Carr's index/Hausner ratio it is possible to analyse powder flow during pre-formulation on a small scale providing valuable information during formulation, as these results can be anticipated by the formulating pharmacist (Lund, 1994:184).

1.7.1.4 Granulation

Granulation is a process in which small uneven shaped particles are adjusted to ensure uniformity of the particles and the product of which it will be composed. Wet granulation is a process in which a solvent, mostly water, is used together with binding material to ensure the preferred shape and size of the material. Therefore it is possible for polymorphs (that have a tendency to do so) to form hydrated forms if a wet granulation process is needed during drug manufacture of the polymorph (Morris *et al.*, 2001:107).

The wet granulated product is thereafter dried (will be further discussed in section 1.7.2) which can further lead to a chain of events that is of importance in polymorphism as shown in figure 1.28.

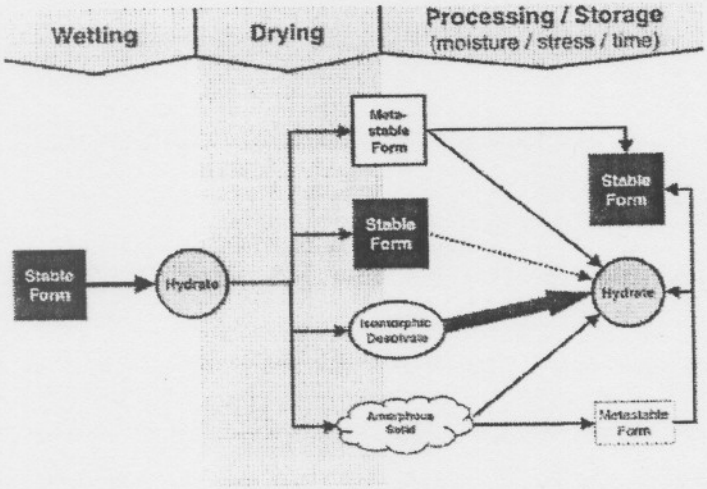

Figure 1.28 Possible transformations during wet granulation when hydrate formation is involved (Morris *et al.*, 2001:107).

1.7.2 Drying

As anticipated, drying can have various effects on polymorphs and pseudopolymorphs. Polymorphic interconversion, dehydration/desolvation and isomorphic products are commonly found upon drying. Drying is an undeniable process during pharmaceutical manufacturing and should definitely be controlled and the effects thereof studied on the pharmaceutical compound that is prepared for manufacture (Morris *et al.*, 2001:107).

Airaksinen *et al.* (2004:132) investigated the influence of two drying methods used to dry theophylline monohydrate (that formed from the stable anhydrous form during wet granulation). A multi-chamber micro scale fluid bed dryer (MMFD) was used with 0.5 g/m^3 or 7.6 g/m^3 inlet air respectively. At temperatures of 30, 50, 70, 90°C samples were taken from the dryer and analysed using XRPD. These XRPD patterns revealed mixtures of three forms of theophylline, form I, I* and form II (being a

stable anhydrous form, a metastable anhydrous form and a monohydrate respectively) as shown in figure 1.29.

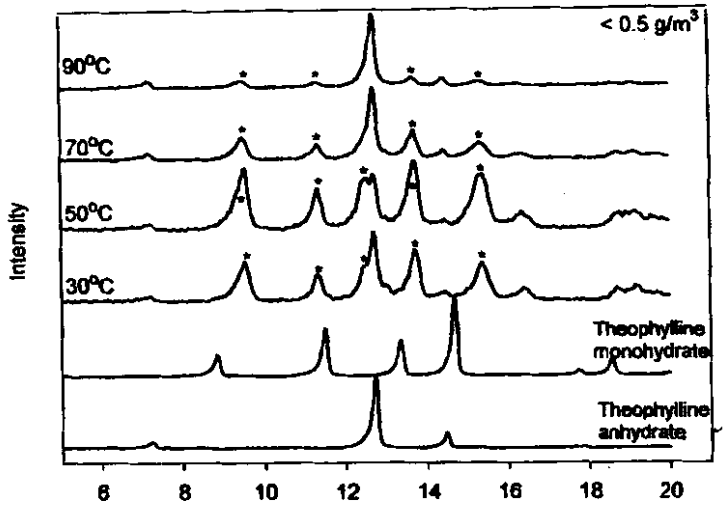

(a)

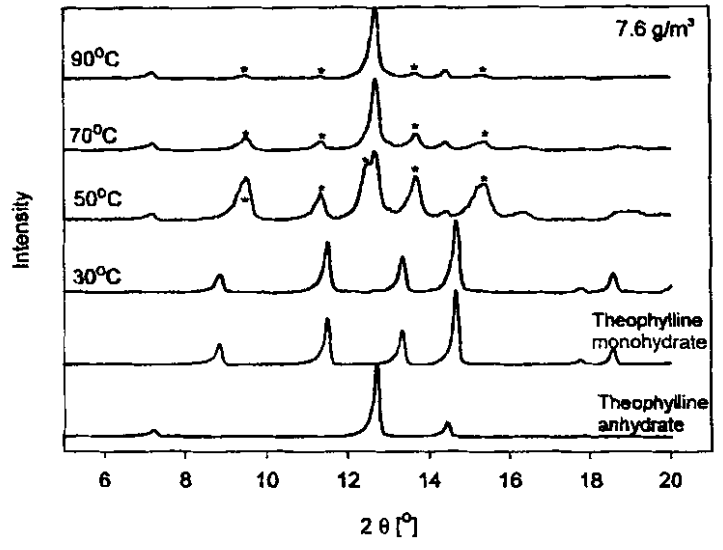

(b)

Figure 1.29 (a) XRPD from the MMFD using ≤ 0.5 g/m^3 and (b) XRPD from the MMFD using 7.6 g/m^3 inlet air (Airaksinen *et al.*, 2004:133).

The percentages of each form present in the mixtures were evaluated at 30, 50, 70, 90°C. The results are shown in figure 1.30 together with the percentage moisture content values of the granules at these temperatures.

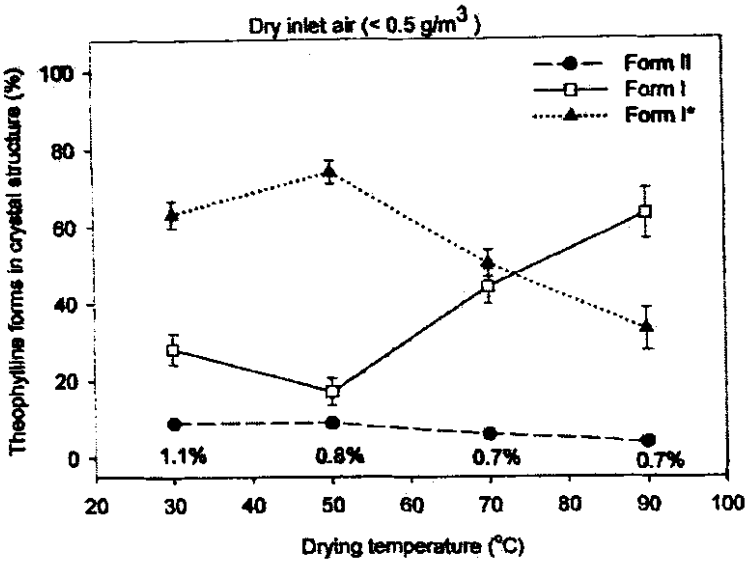

(a)

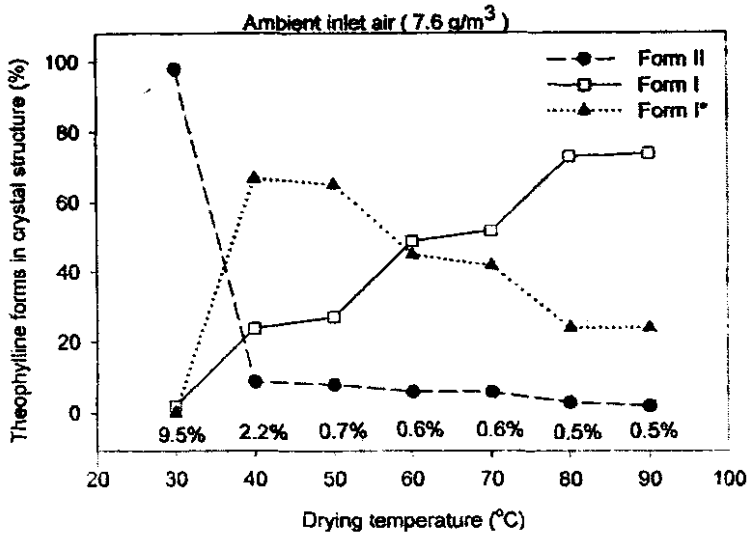

(b)

Figure 1.30 Relative amounts of theophylline forms I, I* and II at 30, 50, 70, 90°C for (a) and (b) (Airaksinen *et al.*, 2004:134).

From these results it is clear that not only drying temperatures may have a significant influence on polymorphic transition, but also the different drying conditions.

In the case of theophylline the presence of its monohydrated form will result in a decrease in solubility and dissolution rates (as reported by De Smidt *et al.*, 1986:497).

Therefore different conditions and drying temperatures should be studied to be able to find the most suitable drying method (and conditions) if drying is necessary, or that this data can be used to assist in alternative formulation processes.

1.7.3 Pressure

Milling and tabletting was grouped together due to their overlapping factor of pressure. Milling and tabletting may alter crystal habit and/or induce polymorphic interconversion. It should be noted however that pressure gives rise to friction (and therefore heat) and could cause changes due to increased temperatures.

1.7.3.1 Milling

Bartolomei *et al.* (1999:299) reported that the β-blocker, propranolol exist in two polymorphs (I and II). The effect of grinding on these two polymorphic forms was evaluated and it was found after vigorous grinding (after 15 minutes) an amorphous form was produced.

Brits (2003:152) studied the effect of grinding on the pseudopolymorphic form $H_{\alpha\beta}$, of venlafaxine. It was found that after grinding, form $H_{\alpha\beta}$ produced a mixture of form $H_{\alpha\beta}$ and form H_{β}. Figure 1.31 shows the disappearance of a characteristic °2θ peak of form Hαβ at 10.3 °2θ.

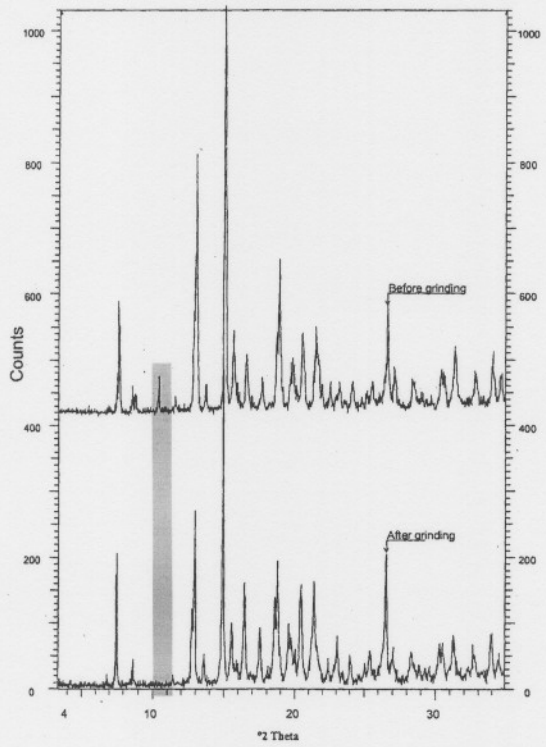

Figure 1.31 XRPD patterns of form Hαβ before and after grinding (Brits, 2003:153).

DSC analysis confirmed the phase transformation due to a disappearing endothermic melting peak at 208°C and an increase in intensity of the 220°C endothermic melting peak of the higher melting form (H_β) (Brits, 2003:152).

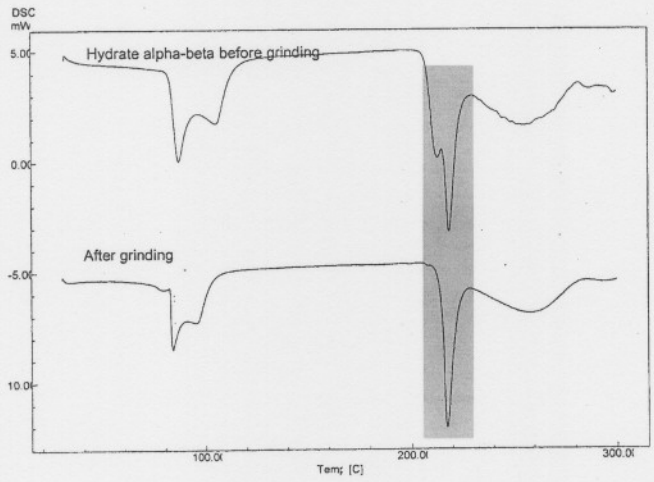

Figure 1.32 The effect of grinding on the DSC thermograms of form $H_{\alpha\beta}$ before and after grinding (Brits, 2003:152).

1.7.3.2 Tabletting/Compression

It should be noted that polymorphs (or mixtures thereof) differ in compressibility. Martino *et al.* (2001:209) conducted a study to find a means to improve compressibility of acetazolamide. Two polymorphic forms and a mixture thereof were prepared by different crystallisation methods (figure 1.33). The mixture of forms I and II was prepared by spray drying technique.

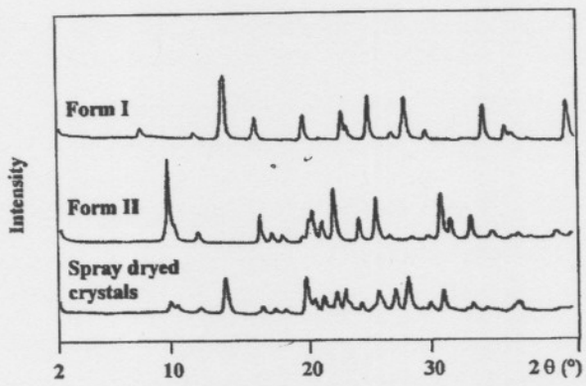

Figure 1.33 XRPD patterns of form I, II and sprayed dried crystals of acetazolamide (Martino *et al.*, 2001:217).

It was found that polymorph I and II was irregularly shaped after slight grinding while the mixture of the two gave rise to spherical particles after slight grinding. The crystals also varied in diameter: form II < mixture < form I (Martino *et al.*, 2001:17).

After the single compression cycle of form I and II, very few tablets were produced and all these tablets had a tendency to cap. The capping of the tablets was explained by the immediate elastic recovery that was higher for these forms. Compression of the spray-dried crystals produced well-formed tablets that did not have a tendency to cap. This phenomenon was studied, and was explained by the fact that the mixture's immediate elastic recovery was lower to that of the two forms alone, and the particle size was also more favourable for compression, compared to that of the two forms alone (Martino *et al.*, 2001:219).

1.7.4 Lyophilisation

Lyophilisation and sublimation are common processes used to produce amorphous powders (such is the case of many suspension formulations). Although an amorphous form is expected as product, it may happen that a solid crystallises during such treatment or during storage. This will in most cases result in a difference in solubility and dissolution (Byrn *et al.*, 1995:25).

Freeze drying of pentamidine isethionate, resulted in either form A or form B which which was determined by the concentration of the solution and the rate of freeze drying. It was found that higher concentrations (10%) of the mother solution (to be freeze dried) and a lower rate of freeze-drying resulted in the formation of form B, while the same solution resulted in form A when the rate of the process was increased. It was also found that form A can be formed upon freeze-drying of a solution of ≤ 4% (Chongprasert *et al.,* 1998:1155). This process is illustrated in figure 1.34.

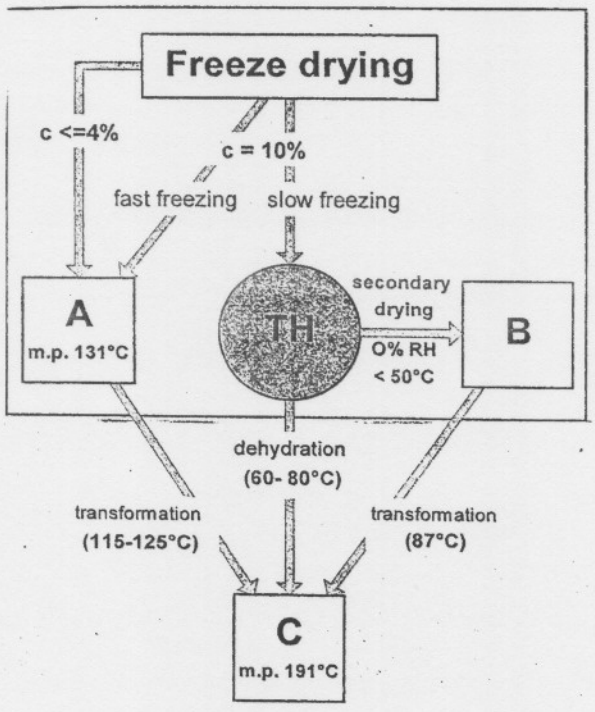

Figure 1.34 Phase transitions during freeze drying of pentamidine isethionate (Chongprasert *et al.,* 1998:1160).

1.7.5 Spray drying

As mentioned in section 1.7.3.2, it was noted that a mixture of polymorph I and II of acetazolamide was produced through spray drying. Therefore spray-drying techniques should also be controlled, as spray drying may influence polymorphic behaviour. This information can then be used to anticipate or overcome possible polymorphic interconversion (Martino *et al.*, 2001:220).

1.7.6 Mixing

Also using the example of acetazolamide (section 1.7.3.2), it was seen that a polymorphic mixture had different characteristics compared to that of the polymorphs alone. Therefore mixtures of polymorphs may be used advantageous (as in the case of acetazolamide) or it may have unfavourable, depending on the situation (Martino *et al.*, 2001:217).

Conclusion

When choosing a specific polymorphic (or pseudopolymorphic) form of an API, the pros and cons of each form should be evaluated (table 1.1).

Once a specific form has been chosen, it is necessary to control certain processes during preformulation and production, as mentioned in table 1.2 (bearing in mind the product manufacturing pathway as illustrated in figure 1.16), to ensure that the final product still contains the desired form.

Such decision-making is only possible if polymorphic screening has been conducted, and sufficient information regarding the behaviour and properties of the various forms of the API is available.

In this study polymorphic screening was done on gatifloxacin crystal modifications that was crystallised from various organic solvents.

Background literature on gatifloxacin is discussed in chapter 2. Methods and apparatus that were used during this study are discussed in chapter 3. The results from this study are reported from chapter 4 onwards.

Chapter 2

An overview of gatifloxacin

Introduction

Gatifloxacin can be classified as a flouroquinolone anti-bacterial agent, which belongs to the DNA gyrase inhibitor family along with ciprofloxacin for example. Gatifloxacin is a synthetically derived analogue of nalidixic acid and is active against various gram-positive and gram-negative bacteria. This flouroquinolone antibiotic is a drug of choice for the treatment of acute sinusitis, lower respiratory tract-, urinary tract- and various soft tissue infections (Chambers, 2001:797).

2.1 Chemical properties

2.1.1 Structural formula and chemical name

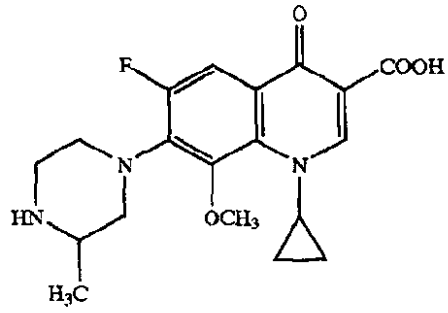

Figure 2.1 Structural formula of gatifloxacin, (±)-1-cyclopropyl-6-fluoro-1-4-dihydro-8-methoxy-7-(3-methyl-1-piperazinyl)-4-oxo-3-quinolinecarboxylic acid (Niddam-Hildeshcim *et al.*, 2005:2).

Gatifloxacin is also identified as chemical substance AM 1155 (ChemIndustry.com, 2005).

2.1.2 Empirical formula

$C_{19}H_{22}FN_3O_4$

2.1.3 Molecular weight

Molecular weight ($C_{19}H_{22}FN_3O_4$) = 375.40 g/mol

2.1.4 Appearance

Gatifloxacin is a white to cream coloured crystalline powder (ChemicalLAND21, 2005).

2.1.5 Solubility

Gatifloxacin in the sesquihydrated crystal form displays a pH dependant solubility profile that reaches maximum aqueous solubility in a pH range of 2-5 (Bristol-Meyers Squibb, 2004).

2.1.6 Melting point

181-185°C (ChemicalLAND21, 2005).

2.1.7 Chemical synthesis of gatifloxacin

Niddam-Hildesheim *et al.* (2005:1) invented a method for the chemical synthesis of gatifloxacin in high purity. According to the mentioned inventors there are various methods of synthesis for gatifloxacin (US patent, no. 4,980,470; US patent no. 4,997,943 and US patent no. 5,157,117). Niddam-Hildesheim *et al.* (2005:2) claimed to produce gatifloxacin that is of higher purity and in a greater yield, compared to other patents. The synthesis described by these inventors will be briefly discussed.

The chemical compounds that are used in the synthesis of gatifloxacin (3) can be seen in figure 2.2, whereas (1) is 1-cyclopropyl-6,7-difluoro-1,4-dihydro-8-methoxy-4-

oxo-3 quinoline carboxylic acid and (2) is 2-methylpiperaxine. During this synthesis a number of impurities are produced as by-products. The by-products are: desmythyl gatifloxacin or DesMe-GTF (6); hydroxy gatifloxacin or OH-GTF (5); dimethyl gatifloxacin or DiMe-GTF (8), anti-gatifloxacin (Anti-GTF) (7) and 2-methyl piperazine gatifloxacin or 2-Me-GTF (4). A schematic representation of the synthesis is illustrated in figure 2.2.

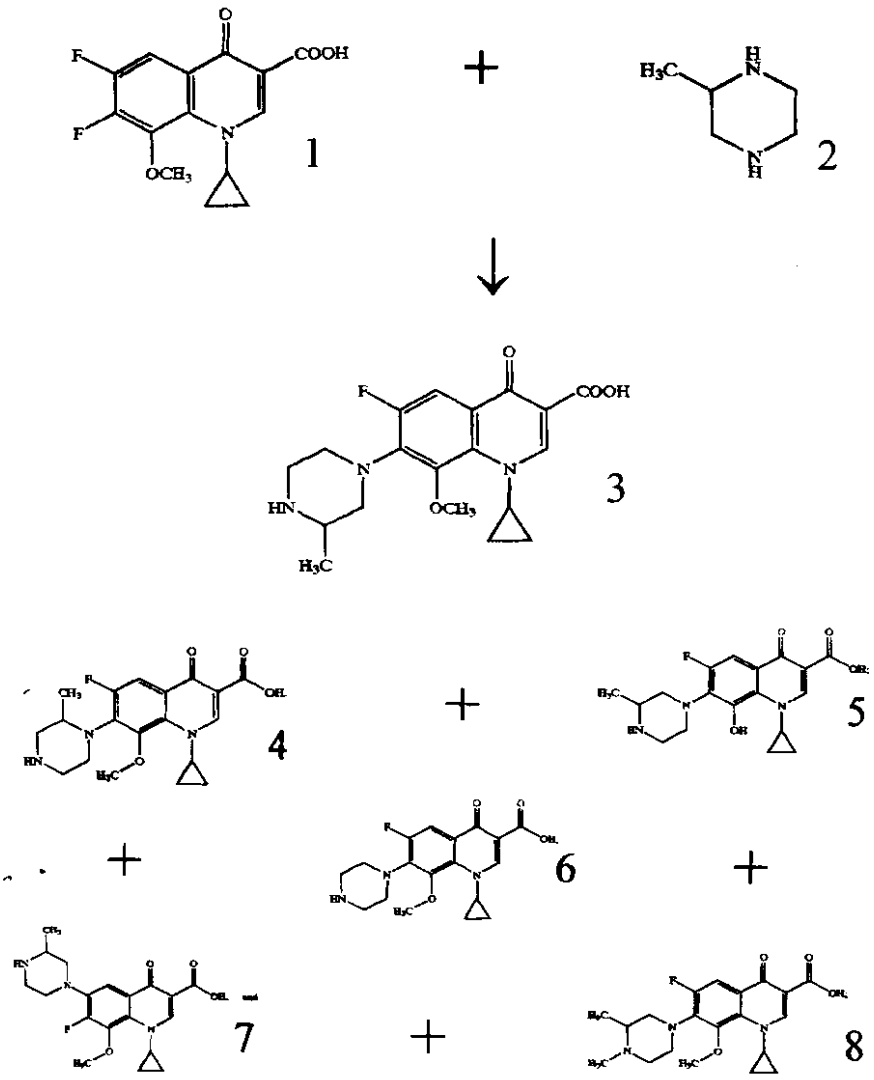

Figure 2.2 The reagents, product and impurities in the synthesis of gatifloxacin. Structures 1-3 are the structures that are used or formed in the highest concentrations compared to structures 4-8.

It should be noted that there are three methods of preparation described in the patent, only the suggested synthesis method will be discussed (Niddam-Hildesheim *et al.*, 2005:1-3).

The first step is to heat the reaction mixture of (1) and (2) in DMSO to 40-70°C in an inert gas atmosphere for 12 hours. Thereafter a co-solvent (water, toluene, benzene or dimethylcarbonate) is added to the reaction mixture at a holding temperature of preferably 25°C (but not more than 40°C) until there is no further increase of suspended solids for half an hour. When this state is achieved the suspended solid can be isolated by any filtering technique (the solid being gatifloxacin).

Using this synthesis technique various impurities are formed. As seen in table 2.1, the impurities are present in very low percentages.

Table 2.1 The five known impurities in the synthesis of gatifloxacin as determined by HPLC

Impurity	% Impurity
DesMe-GTF	0.08
OH-GTF	0.24
DiMe-GTF	Not detected
Anti-GTF	0.02
2-Me-GTF	0.19

2.2 Pharmacology

2.2.1 Indications

Gatifloxacin can be used for:

Acute sinusitis caused by *Streptococcus Pneumoniae* or *Heamophilus Influenza;* urinary tract infections caused by *Escherichia Coli, Klebsiella Pneumoniae or Proteus Mirabilis;* pyelonephritis due to *Escherichia Coli;* uncomplicated skin and skin structure infections due to *Staphyllococcus Aureus* and *Streptococcus Pyogenes*

and uncomplicated urethral and cervical gonorrhoea due to *Neisseria Gonorrhoeae*. Gatifloxacin is also effective against Multi Drug Resistant *Streptococcus Pneumoniae* (MDRSP) (Bristol-Meyers Squibb, 2004).

Gatifloxacin is also effective against *Staphylococcus Epidermidis* and lesser-known bacteria such as *Listeria Monocytogenes*, *Neisseria Meningitides*, *Proteus Mirabilis* and some mycobacteria according to *in vitro* research (Allergan, 2005:1).

2.2.2 Mechanism of action

Flouroquinolones target and inhibit DNA gyrase (bacterial enzyme). DNA gyrase is responsible to maintain the coiled structure of DNA that is required for normal transcription and replication inside the bacterial cell. Inhibiting DNA gyrase effectively prevents DNA synthesis and thereby inhibits bacterial growth (Chambers, 2001:798).

Gatifloxacin sesquihydrate is administered as a racemate, where the R- and S enantiomers show little to no change in activity and disposition (Bristol-Meyers Squibb, 2004).

2.2.3 Resistance

Resistance to quinolone treatment have been reported. This quinolone resistance is due to mutation of the target enzyme or change in intracellular availability of the drug (Chambers, 2001:798). This mutation of the target enzyme (DNA-gyrase) causes a decrease in affinity for the receptor, thereby reducing the drug-binding properties and reducing the effectiveness (Behta *et al.*, 2005). The cause of the decreased intracellular availability is due to the enhancement of the bacterial efflux system, which is responsible for the disposal of harmful substances that accumulate within the bacterial cell (Behta *et al.*, 2005). Gatifloxacin being a newer generation quinolone (compared to nalidixic acid and ciprofloxacin) has the advantage over the older generation that it is not significantly susceptible to resistance.

2.3 Pharmacokinetics

Pharmacokinetic properties of gatifloxacin as an anhydrous form were not available during the duration of this study. Being the commercially available form, gatifloxacin sesquihydrate had extensive pharmacokinetic properties available. Therefore the pharmacokinetic properties of the sesquihydrate form will be discussed and referred to as gatifloxacin in this discussion.

2.3.1 Absorption

Gatifloxacin shows excellent absorption from the oral route of administration. Gatifloxacin is 96% bio-available and peak plasma concentration is obtained between 1 and 2 hours after oral administration (Bristol-Meyers Squibb, 2004). The oral route exhibits very similar behaviour to that of the intravenous route, as illustrated in figure 2.3.

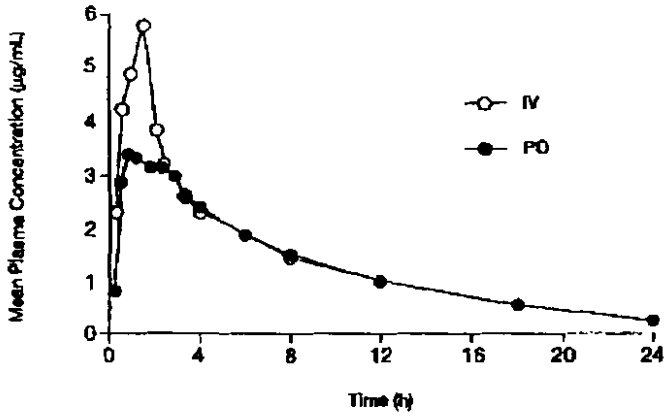

Figure 2.3 Mean plasma concentration-time profiles of gatifloxacin following intravenous (IV) and oral (PO) administration of a single dose of 400 mg to healthy subjects (Bristol-Meyers Squibb, 2004).

When a dose of 400 mg was taken orally on a daily basis it produced a peak plasma concentration of 4.2 µg/ml and a trough plasma concentration of 0.4 µg/ml at steady state. A peak plasma concentration of 4.6 µg/ml and a trough plasma concentration of 0.4 µg/ml were obtained at steady state when a dose of 400 mg was administered

intravenously (Bristol-Meyers Squibb, 2004). Therefore the route of administration is considered to be equal and interchangeable.

Absorption of gatifloxacin is impaired by the presence of aluminium and magnesium in the gastro-intestinal tract (Bristol-Meyers Squibb, 2004).

2.3.2 Distribution

The tendency of gatifloxacin to bind to serum protein is very low. Protein binding is approximately 20% and is independent of concentration (Bristol-Meyers Squibb, 2004). At steady state, the volume of distribution ranges from 1.5 – 2.0 l/kg.

As shown in table 2.2, gatifloxacin is widely distributed throughout body tissues and fluids.

Table 2.2 The distribution of gatifloxacin and the corresponding tissue (or fluid)/ serum ratio (Bristol-Meyers Squibb, 2004)

Fluid or tissue	Tissue (or fluid):Serum
Respiratory	
Alveolar macrophages	26.5:1
Bronchial mucosa	1.65:1
Lung epithelial lining fluid	1.67:1
Lung parenchyma	4.09:1
Sinus mucosa	1.78:1
Sputum	1.28:1
Skin	
Skin blister fluid	1.00:1
Reproductive	
Ejaculate & Seminal fluid	1.07:1 & 1.01:1
Cervix	1.45:1
Vagina	1.22:1

Due to gatifloxacin's minimal protein binding it is possible to achieve rapid and advantageous distribution to target areas (Chambers, 2003:798).

2.3.3 Elimination

2.3.3.1 Excretion and metabolism

Gatifloxacin is primary excreted (unchanged) by the kidneys (Chambers, 2003:799). More than 70% of the unchanged drug is recovered in the urine 48 hours after administration. Gatifloxacin undergoes both glomerular filtration and tubular secretion (Bristol-Meyers Squibb, 2004).

5% of the unchanged drug is excreted via faeces and less than 1% is excreted as ethylenediamine and methylethylenediamine metabolites by the kidneys (Bristol-Meyers Squibb, 2004).

2.3.3.2 Inhibition or induction of cytochrome (CYP) enzymes

In vitro studies with cytochrome P450 enzymes (CYP) revealed that gatifloxacin does not inhibit CYP enzymes (that are mainly responsible for drug elimination). *In vivo* studies demonstrated that gatifloxacin is not responsible for inducing enzymes (Bristol-Meyers Squibb, 2004).

2.3.3.3 Effect of renal and hepatic impairment on excretion

Moderate renal impairment showed a decrease of 57% in gatifloxacin clearance and severe renal impairment resulted in a 77% decrease in clearance (Bristol-Meyers Squibb, 2004).
Moderate hepatic impairment had little to no effect on the clearance of gatifloxacin, however there are no knowledge regarding the effect on drug clearance in patients with severe hepatic impairment (Bristol-Meyers Squibb, 2004).

2.3.4 Half-life

Gatifloxacin has a half-life of 8 hours in patients not suffering from any renal or hepatic impairment (Chambers, 2003:799).

2.4 Special precautions

As with any drug, there are always possible risks and precautionary information to consider prior the administration thereof. The risks and precautions of gatifloxacin are discussed in this section.

2.4.1 Interactions

2.4.1.1 Change in effectiveness

Probenicid is an inhibitor of tubular secretion and – absorption, therefore concomitant administration will result in greater plasma concentration. Concomitant administration of gatifloxacin and probenicid revealed a 44% increase in the half-life of gatifloxacin (Bristol-Meyers Squibb, 2004).

As mentioned (section 2.3.1), gatifloxacin's absorption is decreased in the presence of aluminium and magnesium due to the formation of insoluble gatifloxacin compounds, resulting in a lower plasma concentration (Chambers, 2003:799). Antacids containing aluminium and magnesium should therefore be taken 4 hours before or after the administration of gatifloxacin (Bristol-Meyers Squibb, 2004).

2.4.1.2 Drug interactions

Gatifloxacin is neither an inducer nor inhibitor of major CYP450 enzymes (section 2.3.3.2). Therefore inhibition or inducing of drug metabolism is minimal (Bristol-Meyers Squibb, 2004).

Concomitant use of gatifloxacin and digoxin revealed a slight increase in digoxin plasma concentrations in 8 out of 11 patients, and a significant increase in the rest of the patients. Monitoring of digoxin plasma concentrations is essential to determine whether dosage adjustment should be considered. If necessary, alternate treatment should be considered (Bristol-Meyers Squibb, 2004).

2.4.1.3 Glucose Homeostasis

Gatifloxacin has little to no effect on the pharmacokinetics of anti-diabetic drugs such as glyburide, however it does cause disturbances in blood glucose. Symptomatic hyper- and hypoglycaemia have been reported, and it is therefore of great importance to monitor blood glucose levels in diabetic patients (Bristol-Meyers Squibb, 2004). Dosage adjustment may be necessary or alternate therapy should be considered.

2.5 Safety

2.5.1 Contra indications

Patients with known hypersensitivity to any quinolone such as ciprofloxacin should avoid taking gatifloxacin (Gibbon, 2003:281).

Gatifloxacin should not be used by patients receiving treatment for arrhythmia due to the lack of data describing its potential risks on QTc (Bristol-Meyers Squibb, 2004).

Porphyric patients should not be treated with gatifloxacin; alternate therapy is advised (Gibbon, 2003:25).

As explained in section 2.3.3.3, moderate to severe renal impairment, causes an increase in plasma concentration. Patients with a creatinine clearance of less than 40 ml/min should not use gatifloxacin in a dosage of 400 mg/day (Bristol-Meyers Squibb, 2004). Alternate treatment is thus advised for patients with a creatinine clearance of less than 40 ml/min (Gibbon, 2003:280).

2.5.2 Relative contra indications

The safety of gatifloxacin in patients under the age of 18 years has not yet been established (Gibbon, 2003:280), alternate therapy is therefore advised.

Pregnant or lactating woman should not take gatifloxacin, because the safety during pregnancy has not yet been established (Gibbon, 2003:280).

Insufficient information regarding the safety of gatifloxacin in patients with a history of central nervous system disorders exists (at the time of this study); therefore special consideration must be taken in such cases.

As mentioned in section 2.4.1.3 gatifloxacin causes symptomatic hyper- and hypoglycaemia. Intolerability in diabetic patients should be taken into account.

Gatifloxacin has a very low potential of producing photosensitivity even at doses of 400 mg QD, but being a quinolone, it may present erythematous symptoms (Bristol-Meyers Squibb, 2004). Patients with a history of photosensitivity should be advised of the possible risks.

2.6 Pharmaceutical preparations of gatifloxacin available in South Africa

2.6.1 Product

Gatifloxacin is marketed under Tequin® as the sesquihydrate crystal form thereof. Tequin® is manufactured by Bristol-Myers Squibb in two dosage forms, tablet and injection. The product is illustrated in figure 2.4.

Figure 2.4 Tequin® 400 mg tablet packaging.

2.6.1.1 Tequin® tablets

The white, film-coated, almond-shaped tablets contain 200 mg or 400 mg of active gatifloxacin sesquihydrate (Gibbon, 2003:281) and are printed with "BMS" on one side and "Tequin" on the other side. The tablets are packed in blister packs of 7's (Bristol-Meyers Squibb, 2004).

2.6.1.2 Tequin® injection

Tequin® preparation for injection is available in two concentrations of 200 mg/20 ml or 400 mg/40 ml (Gibbon, 2003:281) both of which is intended for dilution in 5% dextrose (or 0.9% NaCl) to a final concentration of 2 mg/ml; with a final pH ranging from 3.5-5.5 (Bristol-Meyers Squibb, 2004).

2.6.2 Dosage and administration

The adult dose is 400 mg daily for 7-14 days (Gibbon, 2003:281) depending on the severity of the infection, or as a single 400 mg dose for uncomplicated urinary tract infections and uncomplicated gonorrhoea (Bristol-Meyers Squibb, 2004).

2.6.3 Regulations

Tequin® is a class 4 scheduled pharmaceutical product and may only be dispensed in the R.S.A when prescribed by a medical doctor.

2.7 Internationally available products

2.7.1 Tequin ®

Tequin® as described in section 2.6, is also available outside of the R.S.A.

2.7.2 Zymar®

2.7.2.1 Product

Zymar® is an ophthalmic solution containing gatifloxacin sesquihydrate in a concentration of 0.3% (3 mg/ml) and is supplied by Allergan pharmaceuticals. Zymar® is supplied as a sterile, clear pale-yellow isotonic solution that has an osmolality of 260-330 mOsm/kg. It is packed in a white low-density-poly-ethylene (LDPE) bottle with controlled dropper with a tan coloured cap (Allergan, 2005). The product logo of Zymar® can be seen in figure 2.5.

Figure 2.5 Zymar® ophthalmic solution (Allergan, 2005).

2.7.2.2 Dosage and administration

One drop every 2 hours in the infected eye(s) while awake, for the first two days. Instil one drop every 4 hours while awake, for the next five days (Allergan, 2005:1).

2.7.3 Miscellaneous products

2.7.3.1 Tablets

Literature searches for commercially available gatifloxacin products revealed a number of brand names such as Gatiquin® (Cipla), G-flox® (INTAS), Gatizone-

400® and Tymer® (Jamjoom Pharma) that are available as tablets. Product information regarding these brand names was limited at the time of this study.

2.7.3.2 Suspensions

Suspension formulations of gatifloxacin were prepared by Bristol-Meyers Squibb to compare oral bioavailability between a tablet and suspension dosage administration (Bristol-Meyers Squibb, 2004). However the oral suspension was not formulated to be marketed and distributed, and at the time of this study, there were no oral suspension marketed by any pharmaceutical company, in spite the fact that research have been done on oral suspensions.

Further studies on the product integrity and stability of gatifloxacin in suspension form (or powder for suspension) may possibly lead to a different dosage form being designed that may be of value to patients that have difficulty in swallowing tablets.

2.8 Available literature on different gatifloxacin crystal forms

Various companies and individuals have already patented many different crystal forms of gatifloxacin. In this section all patents available at the time of this study will be mentioned. If a crystal form from table 2.3 is referred to in forthcoming chapters, that crystal form will be focused on in more detail in that specific section from that chapter.

Table 2.3 Various gatifloxacin crystal forms described in the literature

Patent number	Inventor (references)	Describing form(s):	Data available:
US 2004/0038988 or WO 03/105851.	Niddam-Hildesheim *et al.*, 2004b:1-6.	O and V.	O: classified as a trihydrate or mixture of forms; XRPD, DSC, TG. V: classified as a mixture of forms; XRPD, KF, TG.
US 6,413,969 or WO 02/22126.	Raghavan *et al.*, 2002:1-18.	H5 (see also H5 sesquihydrate form - WO 2004/087688). TE, RP, T1RP, T2RP, T1H5, T2H5, H6, TH6, Ω and E.	H5 classified as a pentahydrate; XRPD, DSC, TG, KF. The interrelationship between TE, RP, T1RP, T2RP, T1H5, T2H5, H6, TH6, Ω and E. XRPD.
US 2004/0171621 or WO 2004/054583.	Amir *et al.*, 2004:1-26.	CW, CX, CY, CZ, W, X, Y, Z, CH1, CH2, RH, HX1, HX2.	CW classified as a DMSO solvate; XRPD, DSC, TGA. CX (DMSO solvate), CY (not classified) and CZ (DMSO solvate) are all related to form CW by the corresponding of CW most influential peaks. W not classified; XRPD, DSC, TGA. Y classified as a hemi-hydrate; XRPD, DSC, TGA, KF. Z classified as a di-acetonitrile, dihydrated form; XRPD, KF, TGA, DSC, TG. CH1, CH2, RH are all not classified; XRPD. HX1, HX2 are not classified (wet samples analysed); XRPD, KF.

Table 2.3 continued...

Patent number	Inventor (references)	Describing form(s):	Data available:
US 2004/0009989 or WO 03/094919.	Niddam-Hildesheim *et al.*, 2004a:1-55.	A, B, C, D, E1, F, G, H, I, J.	A, C, D, F and G are all not classified; XRPD, TGA, DSC. B was classified as a butanol solvate; XRPD, DSC, TGA. I **(note: I the letter - not roman numbering. See roman I, patent WO 03/086402)** was classified as a butanol solvate; XRPD, DSC, TGA. E1 classified as a mono-acetonitrile solvate or a dihydrate; XRPD, TGA, KF, DSC. H classified as a toluene solvate; XRPD, DSC, TG. J classified as a variable hydrated-solvate form depending on the solvent used, but still have the same XRPD. Form J can be prepared using iso-propanol, 1-buthanol, acetone, THF and methyl ethyl acetate. All of these solvated forms contain a water content varying between 2.79-4.84% together with the corresponding solvent. XRPD, TG, KF. Alternate preparation methods of previously described forms (application in progress) forms Ω and T2RP. Form Ω being an anhydrous form and T2RP a hemihydrate.

Table 2.3 continued...

Patent number	Inventor (references)	Describing form(s):	Data available:
WO 2004/087688.	Reddy *et al.*, 2004b:1-26.	H1, H2, H3, H4, H5.	H1,H4 and H5 classified as sesquihydrates; XRPD. H2, H3 not classified; XRPD.
WO 2004/101547.	Reddy *et al.*, 2004a:1-13.	H6.	H6 classified as a hemihydrate; XRPD. **Note: This data presented is not sufficient for a classification, though it is classified as such.**
WO 2004/101527.	Vakil *et al.*, 2004:1-18.	Ω.	Ω_2 classified as an anhydrous form, XRPD comparable to Ω from patent US 6,413,969 with the exception of a peak at 23.59 °2θ which is absent.
WO 03/086402.	Reddy *et al.*, 2003:1-25.	I **(note: number not letter)** and II.	Both I and II are classified as anhydrous forms. XRPD, DSC, TG and IR.
US 2004/0192700 or WO 2004/012739.	Niddam-Hildesheim *et al.*, 2004c:1-8.	L, M, P, Q, S and T1.	All these forms were not classified; XRPD.

It should be noted that most of these patents are cryptic and lack significant data needed for characterisation and identification purposes.

Conclusion

From this chapter, it is clear that gatifloxacin is a highly useful anti-bacterial drug, effective and relatively safe. It also poses a daunting task during polymorphic screening, as there was little information available regarding the forms described in the patents. Gatifloxacin is also a complicated structure that possesses highly intricate crystal structure possibilities.

Physico-chemical properties of gatifloxacin crystal modifications will be discussed from chapter 4 onwards.

Chapter 3

Physico-chemical characterisation of APIs

Introduction

In this chapter methods for the analysis of different solid forms are briefly discussed together with the apparatus and conditions used in this study. These methods enable one to identify and characterise different solid forms and to investigate various aspects of these different crystal modifications.

The most commonly used techniques during polymorphic screening (Yu *et al.*, 1998:124) are given in table 3.1. This table explains why these methods are used. Many of these techniques have been encountered in chapter 1 where specific examples have been discussed.

Table 3.1 Information obtained from different physical techniques for solid forms (Yu *et al.*, 1998:124)

Type	XRPD	IR	Thermal methods (such as DSC and TGA)	Microscopy
True polymorphs	Unique diffraction peaks.	Characteristic spectra. Sensitive to H bonding.	Unique melting points, heat of fusion and transition.	Color, crystal habit.
Pseudopoly-morphs	Same as for true polymorphs.	Unique solvent bands. Shifted spectra bands. Sensitive to H-bonding.	Dehydration/desolvation peaks. Weight loss. Unique melting point and recrystallisation.	Same as true polymorphs. Desolvation or dehydration by hot-stage microscopy (in presence of silicon oil).
Isomorphic forms	Slightly different pattern to that of parent pseudo-polymorphs.	Solvent band disappear compared to parent pseudopolymorph. Spectra band shifted.	Disappearance of dehydration/desolvation peaks, same melting point as parent pseudopolymorph.	Possible visible cracks and fissure after parent desolvation.
Amorphous solids	No diffraction peaks/ Broad/Halo shaped.	Broadened spectra.	Glass transition, often followed by recrystallisation.	Irregular shaped particles.
Mixture of crystal forms	Composite pattern of crystalline components.	Composite spectra of all components.	Mixture of composite components.	Composite of mixture.

The aim of this chapter was to provide insight into the principals and applications of the various techniques and apparatus that were used during this study.

3.1 X-ray diffractometry

3.1.1 Single crystal diffractometry

When one wishes to analyse a single crystal, a good quality single crystal is to be used. Using the diffraction angles and intensities obtained from such an x-ray analysis, it is possible to elucidate the positions of the molecules within the unit cell of the crystal. The unit cell parameters given as *a, b, c* as well as their corresponding angles α, β, γ, are also determined, making it possible to stack these unit cell parameters into a three-dimensional display of the lattice. With this three-dimensional model lattice answers to the differences in physico-chemical properties can be found (such as stability and solvation/hydration status tendencies). The most commonly observed unit cells among pharmaceutical solids are triclinic, monoclinic and orthorhombic from the possible seven classes of unit cells (the others being tetragonal, hexagonal, rhombohedral and cubic) (Newman & Stahly, 2002:7).

In table 3.2, the relationship between *a, b, c* and their angles α, β and γ are given for the most commonly found pharmaceutical unit cells.

Table 3.2 Relationship between the type of unit cell, its parameters and corresponding angles

Unit cell	Relationship
Triclinic	$a \neq b \neq c$, $\alpha \neq \beta \neq \gamma \neq 90°$
Monoclinic	$a \neq b \neq c$, $\alpha \neq \gamma \neq 90°$ with $\beta = 90°$
Orthorhombic	$a \neq b \neq c$ with $\alpha = \beta = \gamma = 90°$

3.1.2 The principal and applications of x-ray powder diffraction (XRPD)

As mentioned, a good quality single crystal is necessary to generate single-crystal x-ray diffraction data. Because the growth of such single crystals is a fine art that is mastered by few, x-ray powder diffraction is used as a good alternative. XRPD is a useful tool when comparing powdered samples (Newman & Stahly, 2002:7).

As mentioned, crystals are the product of ordered packing of molecules. XRPD is used in polymorphic characterisation because crystals have unique diffraction patterns due to the fact that it acts as a three-dimensional grating system for x-rays that have wavelengths comparable to that of the inter-atomic distances (Byrn *et al.*, 1999:48).

3.1.2.1 Bragg's law

Bragg first interpreted the diffraction pattern in 1913 with his equation:

$$n\lambda = 2d\ sin\theta \qquad \text{(Equation 3.1)}$$

which states that "a multiple (n) of the wavelength (λ) must equal twice the distance (d) between planes multiplied by the sine of the angle of incidence" (Byrn *et al.*, 1999:54).

XRPD patterns in this study were produced by a 2θ powder diffractometer. A schematic representation thereof is illustrated in figure 3.1.

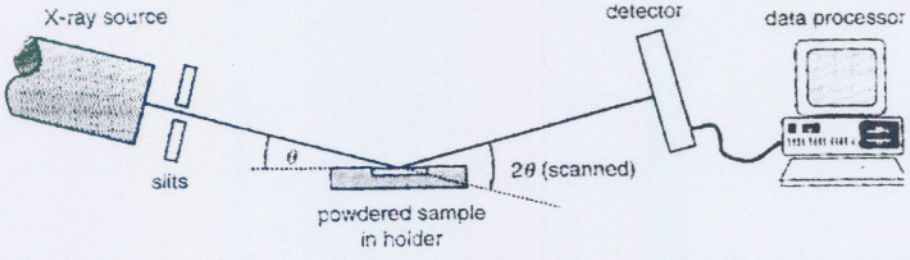

Figure 3.1 Schematic presentation of a modern 2θ x-ray diffractometer (Byrn *et al.*, 1999:54).

The XRPD pattern of the powder is generated by the data processor as diffraction peaks at their corresponding °2θ values (as shown in figure 3.1) with varying intensitities. The diffraction peak intensities are expressed as the ratio between the peak at the specific 2θ value; compared to the peak maximum and is commonly known as the I/I_{max} value. The d value (also known as d-spacing) as illustrated in figure 3.2, can be calculated using Braggs's law when the x-ray wavelength and the diffraction angle are known (equation 3.1).

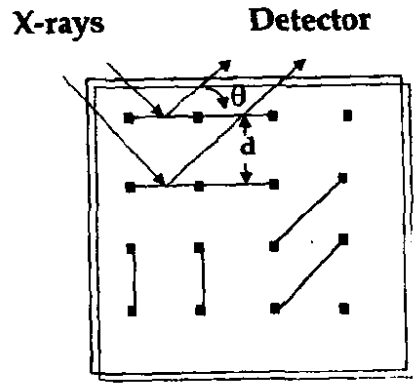

Figure 3.2: A schematic representation of x-ray diffraction (Newman & Stahly, 2002:6).

3.1.2.2 Preferred orientation

Preferred orientation is the tendency of crystals to pack against each other with some degree of order, which can influence peak intensity but not peak position in XRPD patterns (Newman & Stahly, 2002:8). The effect of preferred orientation is important because it is often magnified when the sample bed is smoothed out to the surface of the sample holder. To ensure that preferred orientation is kept to a minimum, the sample should be lightly ground (carefully not to induce possible phase transformation), as reduction in particle size is proven to lessen the effect of preferred orientation. The effect of preferred orientation is illustrated in figure 3.3.

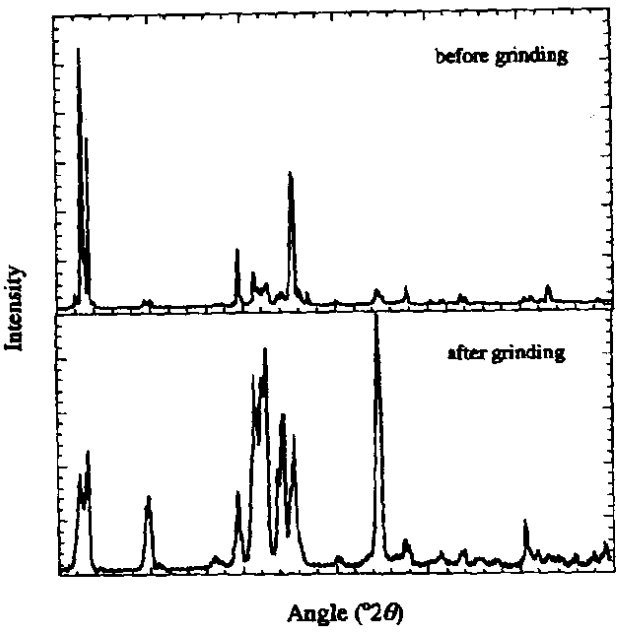

Figure 3.3 The resulting XRPD patterns before and after grinding of a sample that had not undergone phase transformation (Newman & Stahly, 2002:8).

For the purpose of this study, XRPD was used as x-ray diffraction method.

3.1.3 Apparatus and conditions

3.1.3.1 X-ray Powder Diffraction (XRPD)

A Bruker D8 Advanced diffractometer (Bruker, Germany) was used to obtain XRPD and Variable Temperature X-ray Powder Diffraction (VT-XRPD) patterns. A sufficient amount of sample was lightly ground to decrease preferred orientation using a pestle and mortar. The ground sample was transferred into an aluminium sample holder.

The sample was then exposed to the following measurement conditions: target, Cu; voltage, 40 kV; current, 30 mA; divergence slit, 2 mm; anti-scatter slit, 0.6 mm, detector slit, 0.2 mm; monochromator; scanning speed, 2°/min with a step size of 0.025° and a step time of 1.0 sec.

3.1.3.2 Variable temperature X-ray Powder Diffraction (VT-XRPD)

VT-XRPD was used to study the change in XRPD pattern as a function of temperature. A heat-stage was used to heat the sample to the desired temperature. This temperature was then maintained for the duration of the analysis (3-40°2θ). Samples were analysed at temperatures ranging from 25-180°C.

The same measuring conditions as mentioned under section 3.1.3.1 were used in conjunction with an Anton Paar TTK 450 low temperature camera (Anton Paar, Austria) with a heating rate of 0.1°C/sec.

3.2 Infra-red (IR) spectroscopy

3.2.1 Principal and applications

IR spectroscopy is based on the conversion of IR radiation to molecular vibrations and can be used in qualitative and quantitative analysis (Newman & Stahly, 2002:10). The IR beam undergoes absorption, reflection and diffraction by the powder sample but only the diffuse reflectance contains the absorbtivity information about the sample (Bugay & Findlay, 2002:511). A schematic representation of diffuse reflectance sample accessory is illustrated in figure 3.4.

IR spectrometry is an easy and sensitive way to analyse the structure and conformation of an organic compound. IR spectroscopy has been proven to be a powerful tool in the characterisation of polymorphic solids (Byrn *et al.*, 1999:111).

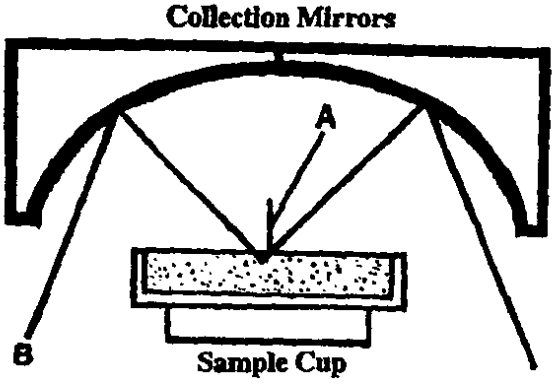

Figure 3.4 Schematic representation of the diffuse reflectance sampling accessory. Where A is the blocker device to eliminate specular reflectance; B is the path of the IR beam (Bugay & Findlay, 2002:511).

The diffuse reflectance sampling technique is a very popular technique used during polymorphic screening, due to the minimal sample manipulation and preparation (to lessen the chances of possible induction of phase transformation) (Newman & Stahly, 2002:10).

In some cases the IR spectra of different crystal forms are very alike. There are two possible reasons for this phenomenon. One reason is that the crystal packing arrangements and conformations bears little difference. The second is that the molecule possesses too many stretching and rotational vibrations that overwhelm the vibrational differences of the samples (Byrn *et al.*, 1999:112).

3.2.2 Apparatus and conditions

For the recording of DRIFT-IR spectra a Nicolet Nexus 470-DRIFT-IR spectrometer (Nicolet instrument corporation, USA) was used at wave numbers ranging from 400-4000 cm^{-1}. Diffuse Reflectance Infrared Fourier Transform spectroscopy (DRIFTS) was used to record the IR spectrum of the sample. The samples were dispersed in powdered KBr (background) and transferred into the reflectance cell prior to analysis.

3.3 Thermal methods of analysis

Differential Scanning Colorimetry (DSC) and thermogravimetric analysis (TGA) were used to evaluate the various crystal forms. The TGA was used to verify thermal events (desolvation/dehydration) in the DSC thermograms, which may indicate pseudopolymorphic behaviour.

3.3.1 Principal and applications

3.3.1.1 Differential Scanning Calorimetry (DSC)

With DSC one observes the change in energy during the heating of the sample, compared to an empty reference pan. A thermal event involving absorption of heat-energy is called endothermic, while an event involving the release of heat-energy is called an exothermic event. The amount of heat-energy released or absorbed is directly proportional to the area under the peak (Newman & Stahly, 2002:9). DSC can be used to:

1. determine characteristic temperatures (melting points, dehydration/desolvation, glass transition),
2. distinguish between polymorphs and to
3. determine compatibility between API's and excipients etc.

3.3.1.2 Thermal Gravimetric Analysis (TGA)

TGA measures the total weight loss of a sample as a function of temperature (Newman & Stahly, 2002:9). When binary mixtures of solvents (for example, ethanol and water) are incorporated into a crystal lattice, TGA will not necessarily be able to distinguish between the various solvation molecules (water and ethanol) present in the solvated crystal forms. Karl-Fischer analysis can be used to identify the water content present in hydrated and binary solvated crystal forms (section 3.6).

The theoretical weight loss for solvated gatifloxacin samples were calculated using equation 3.2 and are given in table 3.3.

$$\% \text{ Weight loss} = \frac{Mw_{(s)}}{[Mw_{(s)} + Mw_{(g)}]} \times 100\% \qquad \text{(Equation 3.2)}$$

Whereas:
$Mw_{(s)}$ is the molecular weight of solvent and
$Mw_{(g)}$ is the molecular weight of anhydrous gatifloxacin (375.39g/mol)

Table 3.3 Relationship between solvation status and % weight loss for gatifloxacin

Solvent properties		**Relationship between solvation status and % weight loss**					
Solvent name	$Mw_{(s)}$	**1**	**1.5**	**2**	**2.5**	**3**	**4**
Acetone	58.05	13.399	20.098	26.798	33.497	40.197	53.595
Ethanol	46.07	10.931	16.396	21.862	27.328	32.793	43.724
n-Butanol	74.12	16.489	24.734	32.978	41.223	49.467	65.956
Water	18.02	4.580	6.869	9.159	11.449	13.780	18.318
THF	72.11	16.114	24.170	32.228	40.285	48.342	64.459
Ethyl acetate	88.1	23.407	35.110	46.813	58.516	70.220	93.626
Benzene	78.11	17.224	25.836	34.448	43.060	51.671	68.895
Dichloromethane	84.93	18.451	27.676	36.901	41.127	49.445	65.927
Acetic Acid	60.05	13.791	20.686	27.581	34.476	41.204	55.163

3.3.2 Apparatus and conditions

3.3.2.1 Differential Scanning Calorimetry (DSC)

An appropriate amount of sample (ranging from 2-3 mg) was weighed into an aluminium sample pan. The sample pan was fitted with a lid and lightly crimped. The lids were pierced to ensure that solvent vapours would be able to escape readily from the crimped pans. Pressure build-up in a crimped sample pan may alter the course of desolvation and

may produce inaccurate DSC thermograms. DSC samples pans were analysed by either a Shimadzu DSC-50 (Shimadzu, Kyoto, Japan) or a Perkin Elmer Pyris-1 DSC (Perkin Elmer, USA). Both these apparatus heated the samples at a heating rate of 10°C/minute to a maximum of 200°C. The only difference in the conditions between these two instruments was that the nitrogen flow rate of the Shimadzu DSC-50 (Shimadzu, Kyoto, Japan) was set to 35 ml/min whereas the Perkin Elmer Pyris-1 DSC (Perkin Elmer, USA) was set to 20 ml/min.

3.3.2.2 Thermogravimetric Analysis (TGA)

Samples ranging between 5-15 mg were weighed into an open platinum sample pan. TGA analysis was performed using a Shimadzu TGA-50 (Shimadzu, Kyoto, Japan). Samples were heated at a heating rate of 10°C/min, under a nitrogen purge of 35 ml/min to a maximum temperature of 160°C.

3.4 Microscopy

Microscopy is applied during polymorphic screening to analyse melting point, desolvation, phase transformation and crystal habit to name but a few. This section deals with two techniques of microscopy: hot-stage and SEM microscopy.

3.4.1 Principal and applications

3.4.1.1 Hot-stage microscopy (HSM)

HSM is used to provide visual evidence to supplement DSC and TGA observations. HSM is a technique in which the visual effects of heating can be observed (Newman & Stahly, 2002:10). HSM is very common yet highly useful in the investigation of pharmaceutical solids (Kuhnert-Brandstatter, 1971:1).

Table 3.4 Events that can be observed with HSM (Newman & Stahly, 2002:10)

Event	Observation
Dehydration/desolvation.	Darkening of the crystal or bubble formation in presence of silicon oil; crystal fissures and cracks.
Solid state transitions/Phase transformation.	Recrystallisation from the melt or internal rearrangement. Change in outward appearance or transparency. Sublimation.
Melting behaviour.	Melting.
Possible changes in crystal structure.	Change in birefringence without melting.

3.4.1.2 Scanning Electron Microscopy (SEM)

With SEM electron beams are used (instead of light) to analyse the surface characteristics of a solid. With SEM it is possible to achieve high quality photographic enlargements of the sample, which is why SEM is most commonly used during polymorphic screening to characterise crystal surface/morphology (Byrn *et al.,* 1999:77). The relevance of SEM in crystallography is a known reality; where it plays a vital role in the study of polymorphism in pharmaceutical solids (figure 3.5).

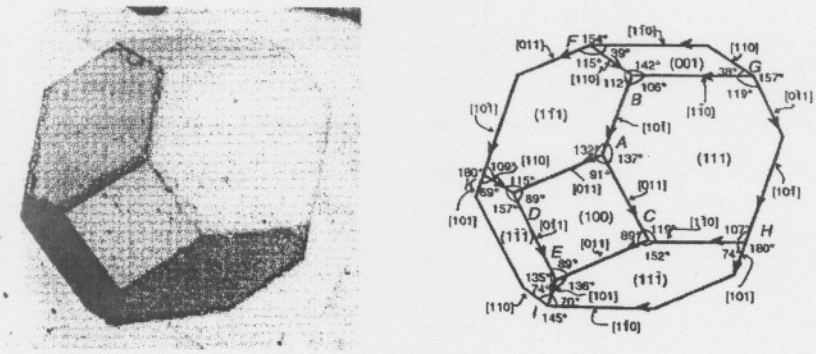

Figure 3.5 SEM view of potassium hexafluorotitanate crystal at a 690x magnification and the interfacial angles calculated from the photomicrograph (Strom, 1976 as referred to by Byrn *et al.,* 1999:73).

3.4.2 Apparatus and conditions

3.4.2.1 Hot-stage microscopy (HSM)

A small amount of sample was placed on an object plate either in a drop of silicon oil or as is, and covered with a cover plate. A Nikon Eclipse E400 (Nikon, Japan) thermo-microscope was used in conjunction with a Metratherm 1200d-heating unit. Events were captured with a Nikon Coolpix 5400 digital camera (Nikon, Japan) that was affixed to the microscope.

3.4.2.2 Scanning electron microscopy (SEM)

A small amount of sample was used to cover the carbon tape that was affixed to the pin. The sample was then covered with gold-palladium film (Eiko engineering ion coater IB-2) inside a vacuum. The sample was then affixed to the microscope sample holder and analysed using a FEI Quanta 200 ESEM & Oxford INCA 400 EDS system (FEI, USA).

3.5 Particle size uniformity

All powder samples used were sieved using a 250 μm and a 106 um sieve. The fraction between 106-250 μm was used in all the experiments. Sieving was performed to ensure uniformity of particle size, as different particle sizes may influence solubility (and dissolution), it was necessary to keep the particle size uniform throughout the study.

3.6 Karl-Fischer analysis

Karl-Fischer (KF) analysis was done to evaluate the total moisture content of the samples. The KF value in conjunction with the TGA value was used to determine the stoichiometry of the incorporated solvents.

3.6.1 Principal and applications

Karl-Fischer titration is a very popular method for quantifying water content (EMD Chemicals Inc, 2005). The principal of KF titration is based on the Bunsen reaction between sulphur dioxide and iodine in an aqueous medium. Karl Fischer developed a method for the water determination of samples. KF titration is based on the following reaction:

$$ROH + SO_2 + R'N \rightarrow [R'NH]SO_3R + H_2O + I_2 + 2R'NH \rightarrow 2[R'NH]I + [R'NH]SO_4R$$

The alcohol reacts with suphur dioxide and base to produce an intermediate alkylsulfite salt, which is then oxidized by iodine to an alkylsulfate salt. The oxidation reaction consumes water. Therefore the extent of oxidation is restricted by the amount of water present. Water and iodine are consumed in a ratio of 1:1. Therefore when all the water has been consumed, the excess iodine is voltametrically determined by the titrator electrode. The excess iodine detected, reflects the endpoint of the reaction. The water content is then determined when the amount of KF reagent and concentration iodine consumed are known (EMD Chemicals Inc, 2005).

3.6.2 Apparatus and conditions

A Metro-ohm (Metro-Ω) KF Titrino (Metro-Ω, Switzerland) was used in the determination of water content in samples. The apparatus was calibrated using distilled water and sodium tartrate dihydrate.

3.7 Methods used to prepare gatifloxacin crystal forms

Various crystal forms of gatifloxacin were prepared using several analytical solvents in recrystallisation studies.

3.7.1 Recrystallisation

Supersaturated solutions of gatifloxacin were prepared using various organic solvents as listed in table 3.5. Weighed gatifloxacin sesquihydrate raw material was transferred into an appropriate recrystallisation container. Supersaturated solutions were prepared by dissolving the gatifloxacin sesquihydrate raw material in the appropriate solvent, whilst the heat of the solution was kept at the boiling point of the solvent. These solutions were prepared under constant magnetic stirring. The containers were then covered with either a cap or in the case of beakers with laboratory parafilm. The solutions were then left at ambient conditions until the crystal yield was sufficient for analysis.

Table 3.5 Solvents and their properties used during this study

Solvent	Supplier	Boiling point (°C)	Molecular weight (g/mol)
Acetone	Saarchem UnivAR®	56.50	58.05
Ethanol	99.7-100% AnalR BDH	78.50	46.07
n-Butanol	Saarchem UnivAR®	117.50	74.12
THF	Merck ProAnalyst	66.00	72.11
Ethyl acetate	Merck ProAnalyst	77.00	88.10
Benzene	Merck ProAnalyst	80.10	78.11
Dichloromethane	Saarchem UnivAR®	39.80	84.93
Water	----------	100.00	18.02

The recrystallisation method's yield of crystals was low (comparing to the amount of raw material used). Average solubility of gatifloxacin in the organic solvents used was poor, and therefore the volume of solvent needed in the recrystallisation process was fairly large.

3.7.2 Drying

Samples were dried using an Ecotherm drying oven or a vacuum oven equipped with Vacuubrand (Vacuubrand, Germany) vacuum controllers both of which was supplied by Labotec (Labotec, South Africa). The specific drying conditions (duration, temperature, vacuum conditions) varied, the specific drying conditions will be discussed in chapter 4 and 5.

3.8 Flowability

As explained in chapter 1 section 1.7.1.4, flowability can be expressed by three methods:

1. Angle of repose
2. Carr's index (CI) and
3. Haussner ratio (HR).

Large amounts of sample are needed for angle of repose determination, it was therefore decided that Carr's index and Haussner ratio would be appropriate methods to express flowability (seeing that smaller sample sizes are required).

A sufficient amount of sample was weighed into a small measuring cylinder. The mass (g) and the volume (ml) were recorded. The cylinder was then tapped for 30 seconds and the volume was recorded. The initial volume (Pd) and the final volume (Td) were determined. The CI and HR value were determined using equations 1.3 and 1.4.

3.9 Ultraviolet-visible spectrophotometry

3.9.1 Principal and applications

Most pharmaceutical compounds absorb I.R radiation between 200-800 nm in the electromagnetic spectrum. UV spectrophotometry is therefore often employed in qualitative and quantitative analysis of active pharmaceutical ingredients. UV

spectrophotometry is based on the ability of substances with Π electrons or atoms possessing unshared electron pairs to absorb electromagnetic radiation (Miyawa & Schulman, 2002:187).

The Lambert-Beer relationship is the principal on which quantitative analysis is based on. The Lambert-Beer relationship states that the concentration of the analyte is directly proportional to that of the intensity of light absorbed (Miyawa & Schulman, 2002:187). The Lambert-Beer relationship is expressed in equation 3.3.

$$A = \varepsilon C d \qquad \text{(Equation 3.3)}$$

Whereas:
A is the absorbance
ε is the molar absorbtivity (L mole/cm)
c is the concentration (mole/l)
d is the path length (cm)

3.9.2 Apparatus and conditions

A Beckman DU-610 spectrophotometer (Beckman, USA) was set to the absorbance maximum of gatifloxacin (293 nm) using the sipper-sampler assembly.

3.10 Dissolution and solubility testing

It has been explained in chapter 1 that polymorphs may exhibit differences in solubility that may therefore influence their bio-availability. In this study the solubility and dissolution behaviour of all the prepared crystal forms were tested.

3.10.1 Principal and applications

3.10.1.1 Dissolution

Dissolution is the experimental method used to observe the rate at which a sample dissolves in a specific dissolution medium. A general powder dissolution method described by Lötter *et al.* (1983:59-66) was used for the dissolution testing of the different crystal forms produced by recrystallisations using different solvents. The results obtained were compared to the dissolution profile of the commercially available gatifloxacin sesquihydrate form.

3.10.1.2 Solubility

Swanepoel *et al.* (2003:345-349) emphasised the importance to evaluate the solubility of polymorphs in multiple solvents to identify a discriminating solvent for polymorph identification.

The human body has different physiological environments that differ in pH, therefore it is applicable to test the solubility of the different crystal forms in a pH ranging from 2-7 (physiological pH ranges) to enable the prediction of drug distribution throughout the human body (for efficacy and toxicological reasons).

3.10.2 Apparatus, conditions and methods

3.10.2.1 Dissolution testing

Dissolution testing was performed on a VanKel Vanderkamp 600 or a VanKel 7000 (VanKel industries, Chatham, USA) dissolution system.

The dissolution apparatus was set to paddles (U.S.P 2005:2413) and rotated at 50 rpm. 450 ml dissolution medium (0.01 M HCl) was accurately transferred into each vessel and allowed to equilibrate at 37.0±0.2°C prior to analysis.

200 mg of the sieved sample and 100 mg glass beads were accurately weighed into a test tube. 50 ml of dissolution medium (that has equilibrated at 37.0±0.2°C) was withdrawn from each vessel with a pipette and transferred into individual beakers. 5 ml of dissolution medium was withdrawn from each beaker and transferred to its corresponding sample test tube. The samples were then vortexed for 2 minutes and directly transferred into the corresponding vessel. The remainder of the dissolution medium from the beaker was used to rinse out the test tube, which was then transferred into the corresponding vessel. 10 ml was withdrawn from each vessel (through 0.45 µm microfilters) on time intervals of 7.5, 15 and 30 minutes (respectively for each vessel).

The withdrawn sample was allowed to cool to ambient temperature. 3 ml of the withdrawn sample was then diluted to 200 ml with dissolution medium.

A standard solution was prepared by accurately weighing 44.44 mg of the sample into a weighing boat and transferring it into a 100 ml volumetric flask. 20 ml methanol was then added to the volumetric flask that was sonicated for 10 minutes. The solution was allowed to cool and then diluted to 100 ml with dissolution medium. This solution was diluted to a final concentration of 6.666 µg/ml.

The UV-absorbance of the samples and standard were read at 293 nm using dissolution medium as blank.

The UV-absorbance of the samples were read 5 times at 293 nm on a Beckman DU – 650i spectrophotometer (Beckman, USA). The average of these readings was used in the calculation (equation 3.4). The % CV was also determined to ensure reliable results.

The percentage sample dissolved was calculated using equation 3.4.

$$\%Dissolved = \frac{(A_{std} \times C_{std} \times DV \times 100\% \times 200)}{(A_{sample} \times M_{sample} \times 3)} \qquad \text{(Equation 3.4)}$$

Whereas:

A_{std} is the average UV-absorbance of the standard

C_{std} is the concentration of the standard (g/ml)

DV is the dissolution medium volume (ml)

200 and 3 are the dilution factors

A_{sample} is the average UV-absorbance of the sample

M_{sample} is the sample weight of the crystals dissoluted (g)

3.10.2.2 Solubility testing

Solubility testing was done using a water bath equipped with a Julabo EM/4 thermostat (Julabo, Germany) that maintained the temperature at 37±2°C. A Heidolph RZR-2000 rotator (Heidolph, Germany) was used to rotate the test tubes at 65 rpm inside a thermally controlled water bath.

The solubility of the various crystal forms were determined in 4 different media i.e., 0.01 M HCl, acetate buffer (pH 4.5), milli-Q water and phosphate buffer (pH 6.8). 5 ml of the medium was transferred to each test tube (that contained 25 mg of sample) and sealed with parafilm and a cap. Each experiment was performed in 5 fold.

After 24 hours the test tubes were removed from the apparatus and allowed to cool, and then suitably diluted. The amount gatifloxacin dissolved in the media were spectrophotometrically determined at 293 nm.

To acquire a standard graph/regression line the following procedure was followed:
47.62 mg gatifloxacin sesquihydrate (raw material) was accurately weighed to obtain an anhydrous mass of 47.62×0.93 (fraction of gatifloxacin present in gatifloxacin sesquihydrate) = 44.42 mg of anhydrous gatifloxacin.

The 44.42 mg gatifloxacin was then dissolved in 20 ml methanol and diluted to 100 ml with 0.01 M HCl (Mother solution =M). Further dilutions were made as described in table 3.6 and the UV-absorbance of the samples were read at 293 nm on the UV-spectrophotometer.

Table 3.6 Regression line sample preparation

Sample	Concentration (µg/ml)	Average absorbance
Mother solution (M)	444.42	3.0180
A	6.67	0.6245
B	3.33	0.3123
C	1.67	0.1565
D	0.83	0.0792
E	0.42	0.0398
F	0.21	0.0201
G	13.32	1.2460
H	26.65	2.3910

The absorbance vs. concentration graph for the various standard solutions obeyed Lambert-Beer's as illustrated in figure 3.6.

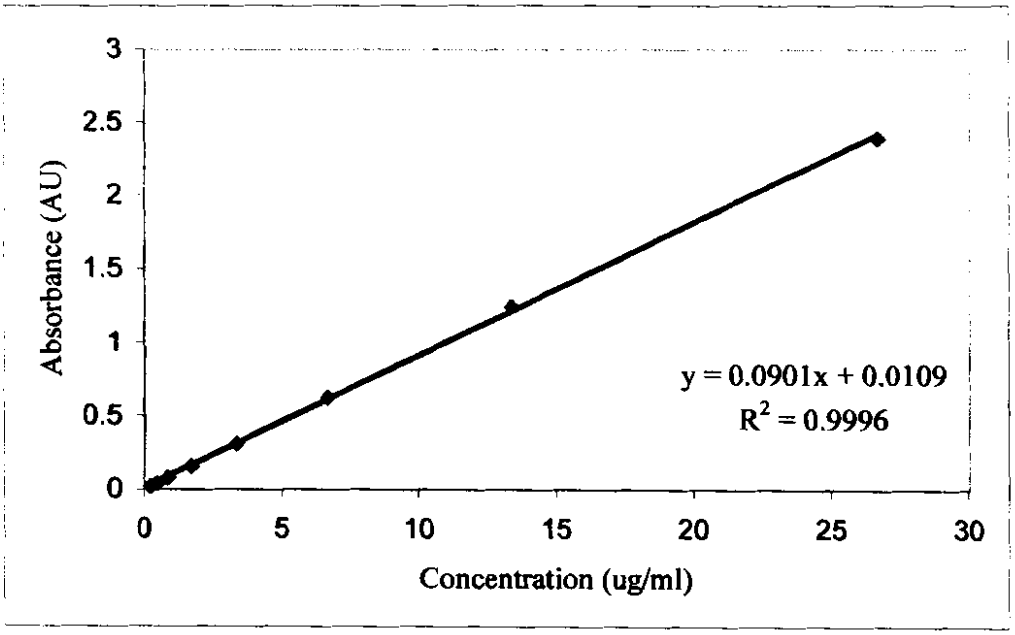

Figure 3.6 Standard regression line for gatifloxacin.

The equation y = 0.0901x + 0.0109 was then used to calculate the unknown concentration of the samples from solubility testing.

3.10.3 Medium preparation

Some studies (Behta *et al.*, 2005; Bristol-Meyers Squibb, 2004) proved the formation of gatifloxacin chelates (which decreases solubility – for example with tetracycline antibiotics), therefore the use of distilled water was not advisable.

All the media used during solubility and dissolution testing were prepared using milli-Q water from a Milli-Q academic water system (Millipore, France).

3.10.3.1 0.01 M HCl

0.01 M HCl was prepared using a dilution of 1 ml 32% HCl (UnivAR®, Merck, Saarchem) in 1liter milli-Q water.

10 liters of 0.01 M HCl were prepared.

3.10.3.2 Acetate buffer pH 4.5 (U.S.P.)

Acetate buffer pH 4.5 was prepared as follows:
11.4 ml glacial acetic acid (Unilab®, Merck, Saarchem) was dissolved in 100 ml milli-Q water. From this acetic acid solution 14 ml were dissolved together with 2.99 g $NaC_2H_3O_2.3H_2O$ (Unilab®, Merck, Saarchem) in 900 ml milli-Q water. The pH was then adjusted (if necessary) to the accepted pH ranges of 4.5±0.05. The solution was then diluted to the final volume of 1 liter.

2 liters of this medium were prepared.

3.10.3.3 Water

Milli-Q water was used as is.

3.10.3.4 Phosphate buffer pH 6.8 (U.S.P.)

Phosphate buffer (pH 6.8) was prepared as follows:
6.805 g KH_2PO_4 (UnivAR®, Merck, Saarchem) and 0.896 g NaOH pellets (UnivAR®, Merck, Saarchem) were dissolved in 800 ml milli-Q water. The pH was then adjusted (if necessary) to the accepted pH ranges of 6.8±0.05. Then this final solution was diluted to 1 liter.

2 liters of this medium were prepared.

Conclusion

All the instruments that were used in this study were calibrated/validated using acknowledged methods and techniques and were well maintained to ensure true and reliable results. Statistical equations and the repetition of sampling were also implemented to further the accuracy of data.

Chapter 4

Gatifloxacin sesquihydrate raw material

Introduction

Hydrates are crystal forms that have incorporated water molecules inside their lattices, which can be in stoichiometric or non-stoichiometric amounts. Gatifloxacin sesquihydrate is a pseudopolymorph of gatifloxacin that has 1½ molecules water per molecule gatifloxacin (1½:1) or 3 molecules water per 2 molecules gatifloxacin (3:2). A schematic representation of a sesquihydrated crystal unit cell is given in figure 4.1.

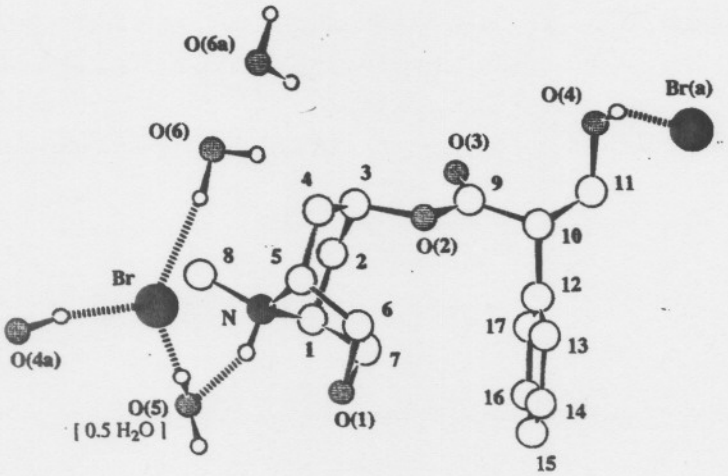

Figure 4.1 A schematic representation of a unit cell for scopolamine hydrobromide sesquihydrate (Michel *et al.*, 1994:509).

In this chapter the physico-chemical properties of the commercially preferred gatifloxacin sesquihydrate and its dehydrated crystal form will be discussed.

4.1 Gatifloxacin sesquihydrate

Gatifloxacin sesquihydrate raw material (batch number 20031110) was obtained from XIAMEN MCHEM PHARMA (GROUP) LTD situated in China. The raw material was manufactured in November 2003 (expiration date: November 2006). In table 4.1 the certificate of analysis of this raw material is displayed.

Table 4.1 Certificate of analysis (CoA) for gatifloxacin sesquihydrate raw material (XIAMEN MCHEM PHARMA (GROUP) LTD, CoA)

Item	**Specification**	**Test result**
Visual	White or yellowish crystalline powder	White or yellowish crystalline powder
Assay by HPLC	≥98.50%	99.75%
Impurities determined by HLPC	≤1.00%	0.25%
Total water content	4.00-8.00%	6.71%
Residue on ignition	≤0.20%	0.05%
Heavy metals	≤20 ppm	≤20 ppm
Conclusion: The raw material complied with above-mentioned specifications and conformed to corporation standard.		

A XRPD diffractogram of the raw material is illustrated in figure 4.2.

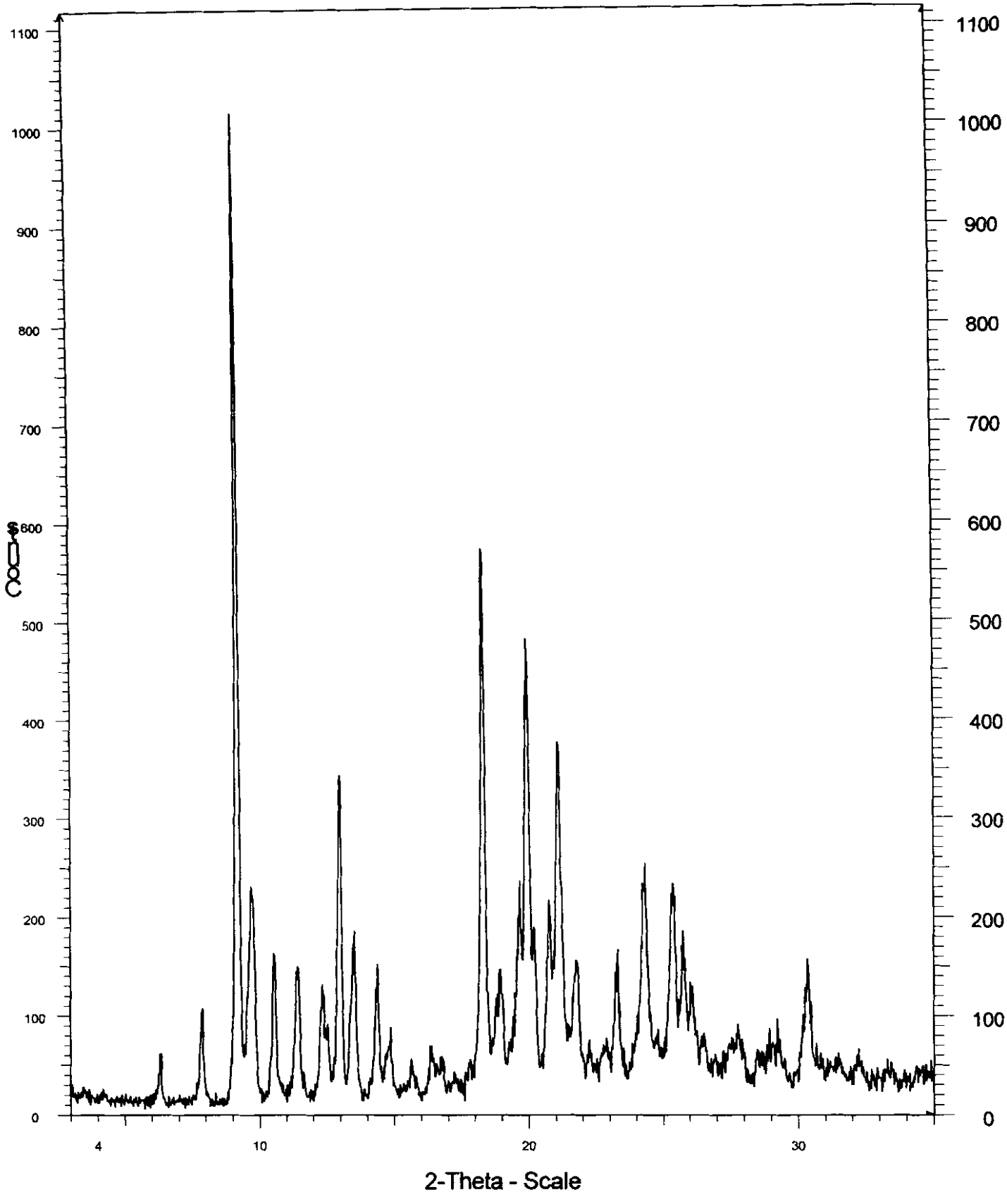

Figure 4.2 XRPD pattern of gatifloxacin sesquihydrate.

As mentioned in chapter 2 (table 2.3), gatifloxacin sesquihydrate exhibits *polymorphic pseudopolymorphism.* The XRPD pattern of the raw material was compared to all the known sesquihydrated forms and it was found to resemble form H4. The XRPD pattern of H4 is illustrated in figure 4.3.

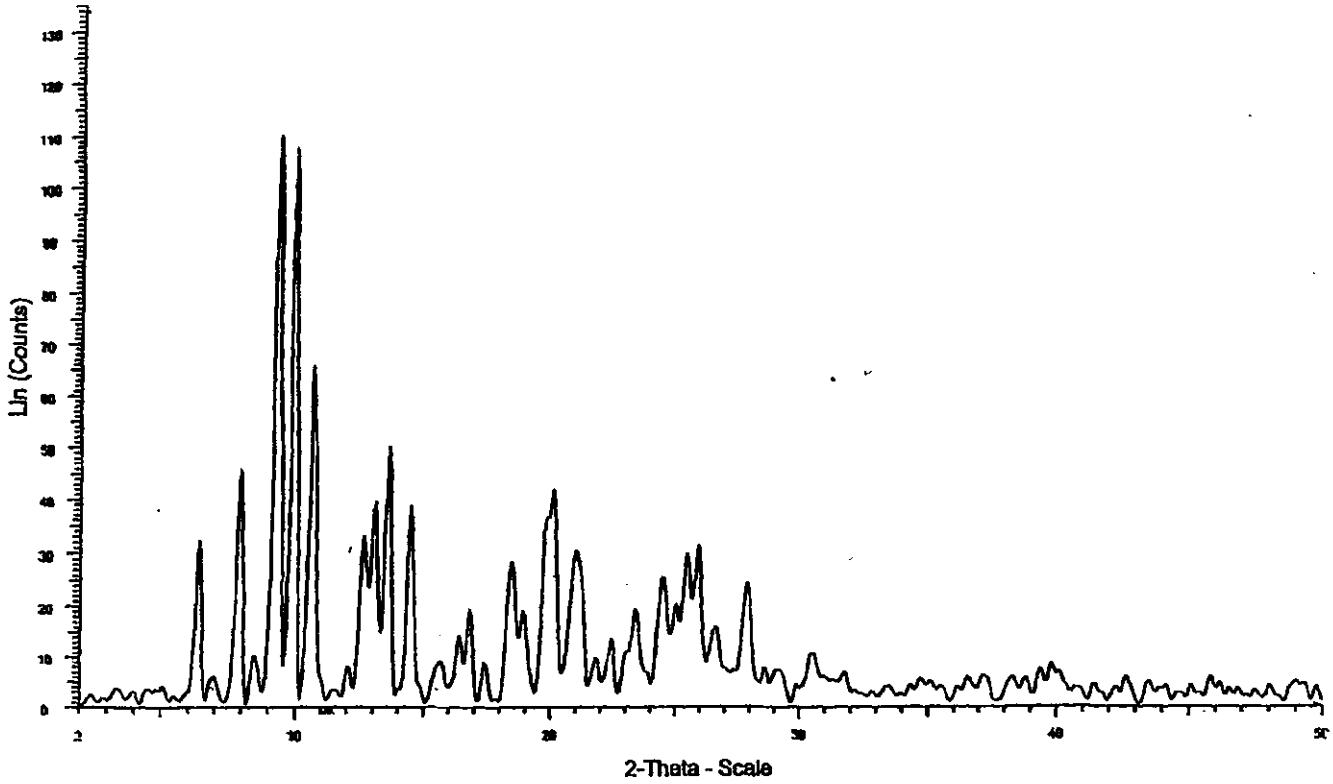

Figure 4.3 XRPD pattern of gatifloxacin sesquihydrate form H4 (Reddy *et al.,* 2004b:26).

There were peaks of low intensity present at 6.9 and 8.3°2θ in the diffractogram of the patented H4 (figure 4.3), but there were no peaks present at these positions in the diffractogram of the raw material (figure 4.2). A possible reason for this may be that the peak intensities of the raw material XRPD (figure 4.2) are significantly higher compared to that of figure 4.3. Thus the presence of smaller peaks may not be as visible in more crystalline samples (figure 4.2).

The DSC thermogram of the raw material revealed a broad dehydration endotherm with a peak maximum at 97.21°C, a small melting endothermic peak at 165.30°C and a final sharp melting endothermic peak at 189.68°C. TG analysis confirmed a total water content of 6.09% while KF analysis revealed a total moisture content of 6.34%. The values of both the TGA and KF resembled that of the theoretical water content of

a sesquihydrated crystal form of gatifloxacin (6.87%). The DSC and TGA thermograms are illustrated in figure 4.4.

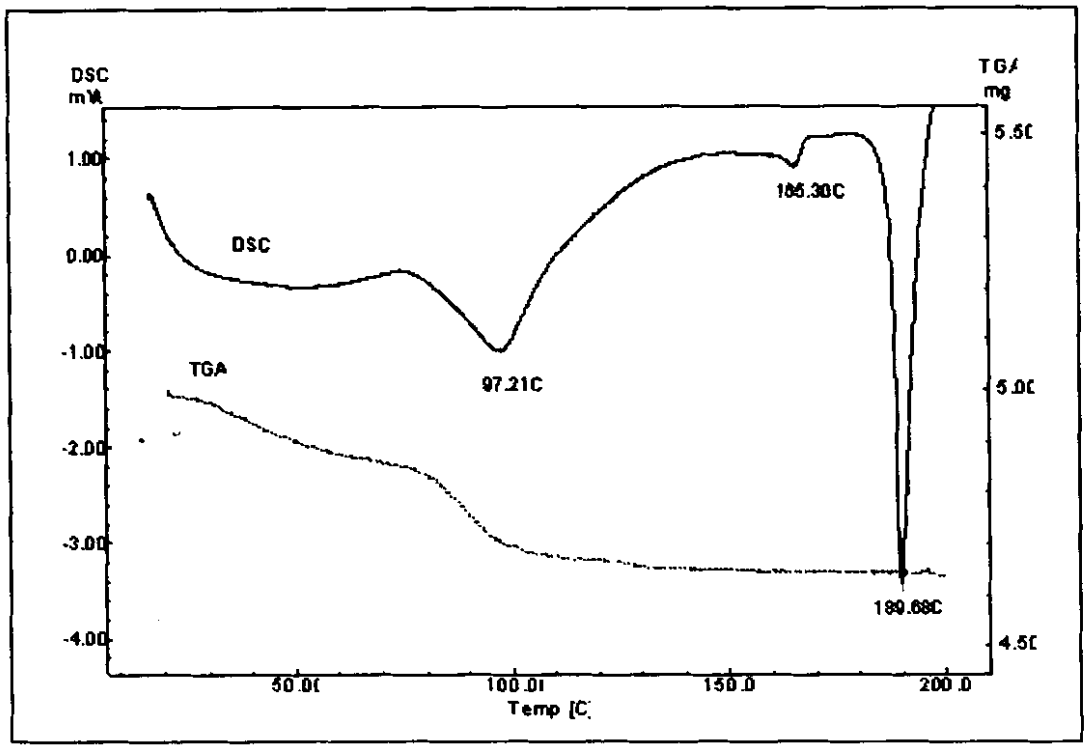

Figure 4.4 The DSC and TGA thermograms of gatifloxacin sesquihydrate form H4.

The dehydration step in the TGA thermogram and the dehydration endotherm (97.21°C) in the DSC thermogram reflected the dehydration of the sesquihydrate at the vaporisation temperature of water (100.00°C).

Hot-stage microscopy was used to confirm the thermal events as seen in figure 4.4. These HSM observations are discussed in table 4.2.

Table 4.2 Photomicrographs of the HSM events observed for gatifloxacin sesquihydrate form H4

Photomicrograph	Observation	Temperature (°C)
Sample emerged in silicon oil		
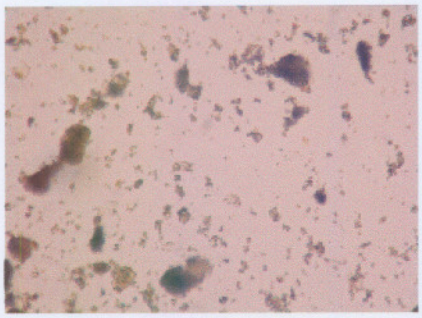	Initial.	25
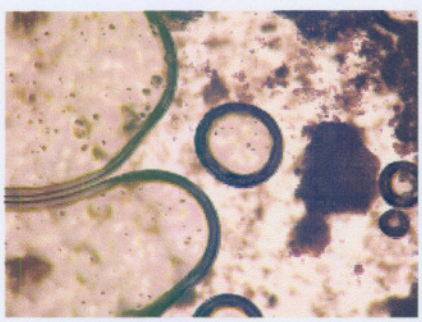	Dehydration (bubble evolution in silicon oil) of the hydrated crystal form occurred at 100°C.	100
Sample without silicon oil		
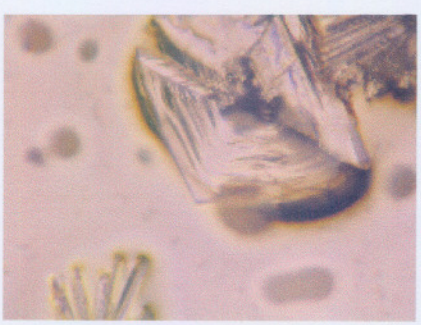	Melting started at 161°C followed by instantaneous recrystallisation at 162°C. The recrystallised product is illustrated.	165
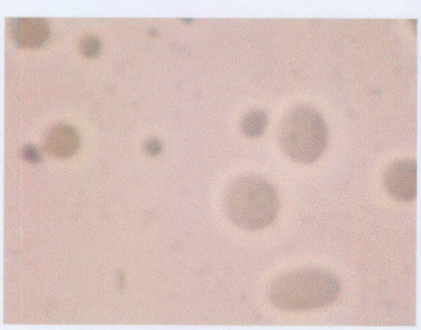	Melting of the recrystallised product commenced at 182°C and was completed at 189°C.	182

To investigate the influence of dehydration (drying) on gatifloxacin sesquihydrate (H4), a VT-XRPD study was conducted. The VT-XRPD patterns of the raw material can be seen in figure 4.5.

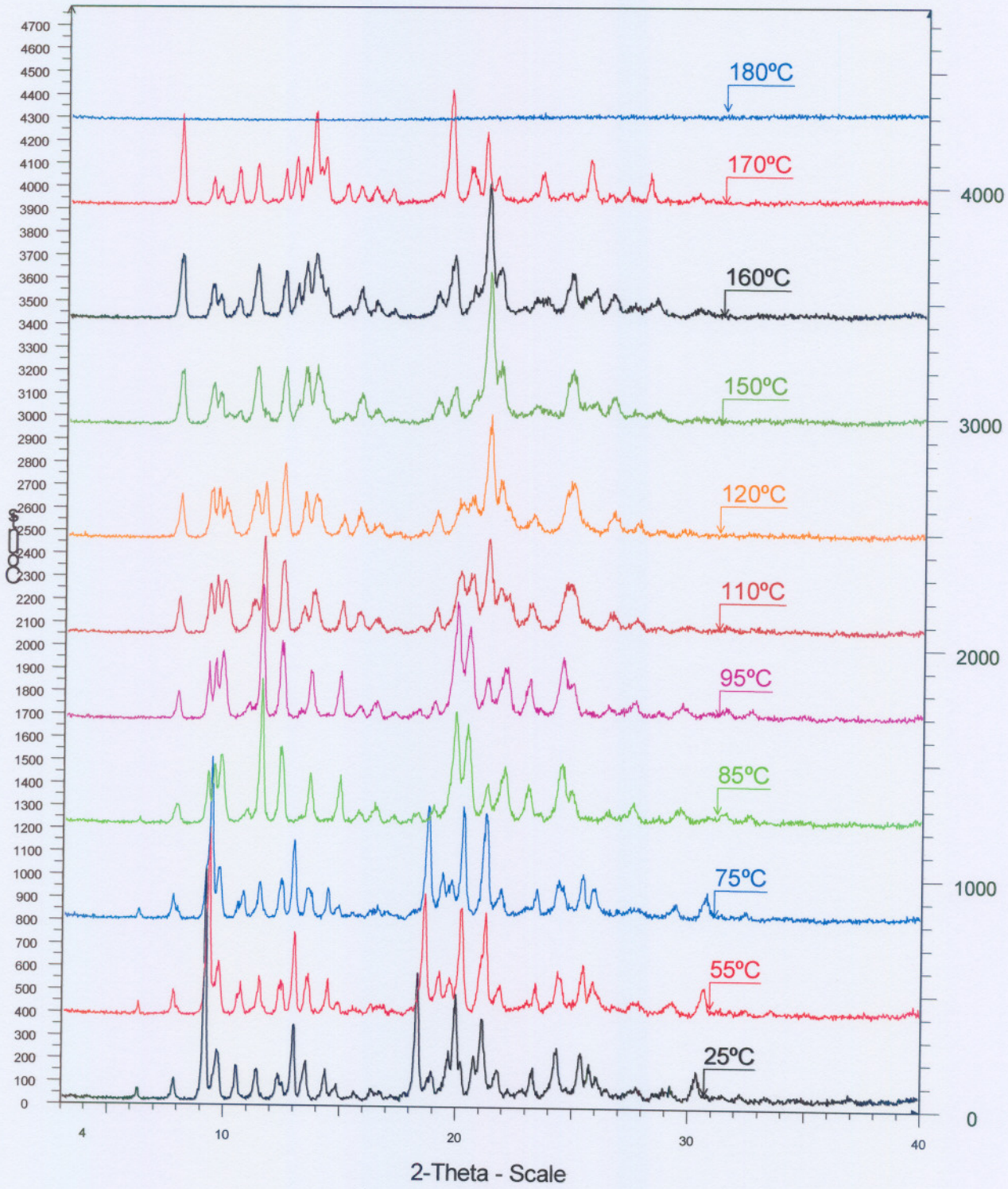

Figure 4.5 Overlay of the VT-XRPD patterns of gatifloxacin sesquihydrate form H4 at temperatures ranging from 25-180°C.

No significant differences in the XRPD pattern were observed at temperatures ranging from 25-75°C. However, the XRPD pattern at 85°C differed significant from the XRPD pattern at 75°C. These differences include the decrease in the relative intensity of peaks at 6.2°2θ and the disappearance of peaks at 10.5, 12.9, 14.3, 18.3, 19.6, 23.3, 25.4, 25.8 and 30.4 °2θ. A few peaks appeared at 15.7, 23.5 and 24.9 °2θ. Peaks at 11.4, 12.3, 14.8, 16.3, 21.9 and 24.4 °2θ increased in their relative intensities. The only noticeable difference between the XRPD patterns at 85°C and 95°C was the disappearance of the peak at 6.2°2θ. Between 95 and 110°C the peaks at 13.2 and 18.9°2θ showed an increase in their intensities while the peaks at 14.9, 19.9 and 20.4°2θ revealed a decrease in their intensities. Comparing the XRPD patterns at 110 and 120°C it was observed that the peaks at 11.5, 20.0 and 20.5°2θ decreased in their relative intensities. Between 120°C and 160°C the peaks at 9.8 and 11.5°2θ decreased in their relative intensity while the peaks at 6.7 and 20.0°2θ increased in their relative intensities. Between 160°C and 170°C no significant differences in the XRPD patterns were observed. The amorphous XRPD pattern at 180°C represented the melting of the sample. Throughout the analysis slight shifting in the °2θ peak positions was observed. This may be attributed to a possible change in powder bed height due to recrystallisation caused by the prolonged exposure to increased temperatures.

The desolvation process between 75°C (onset) and 130°C (endset) can be held accountable for the changes observed in the XRPD patterns between 75°C-130°C. The differences in the XRPD patterns observed between 150-170°C may be attributed to the thermal events visible at 160°C in the DSC thermogram (as seen in figure 4.4 and table 4.2).

4.2 Anhydrous gatifloxacin

Gatifloxacin sesquihydrate was dried at 140°C for 4 hours in a vacuum oven (Labotec, South Africa) set at 15 mBar.

The XRPD pattern of the dried sample is displayed in figure 4.6.

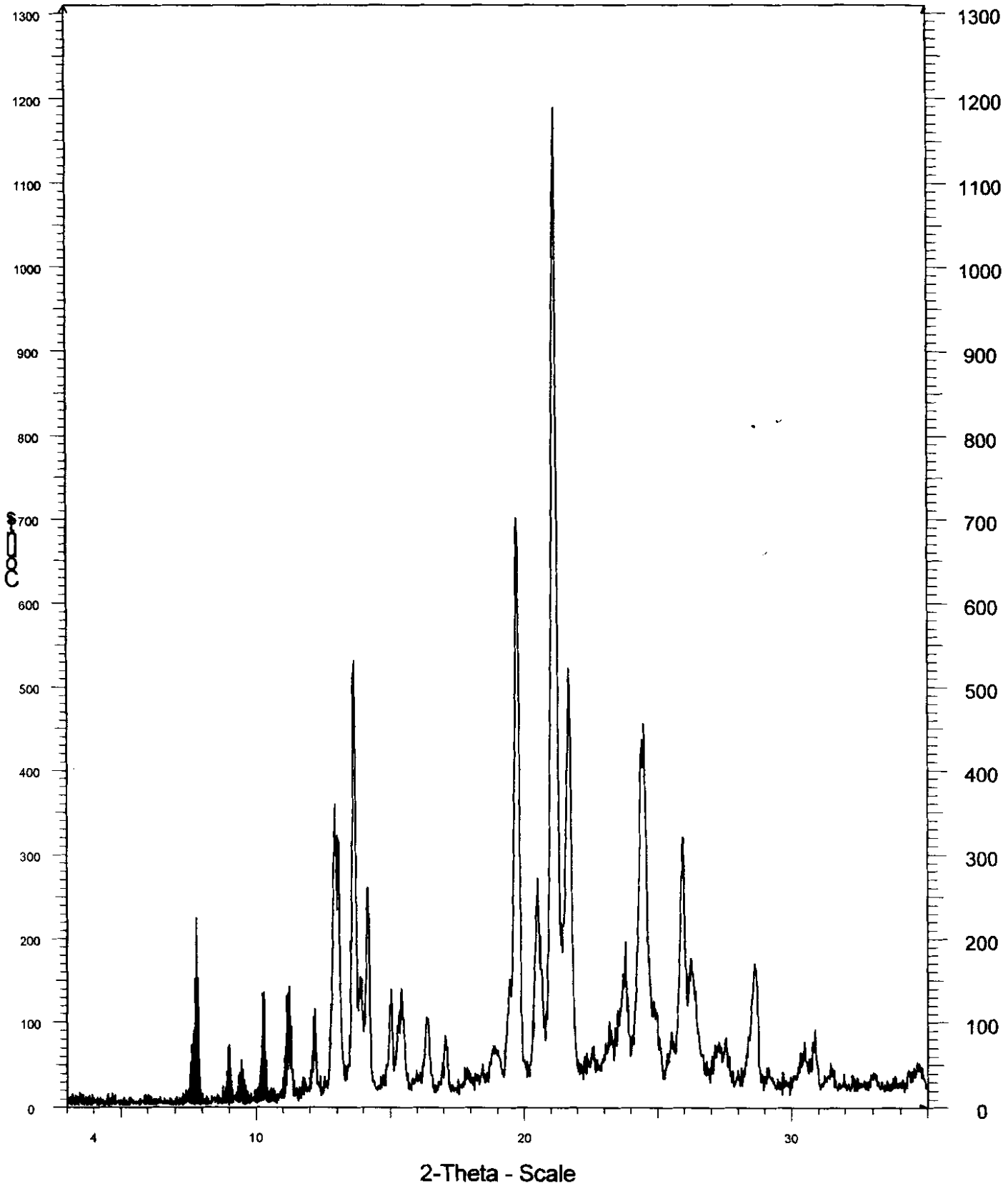

Figure 4.6 XRPD pattern for gatifloxacin sesquihydrate dried for 4 hours at 140°C and 15 mBar (anhydrous gatifloxacin).

The XRPD pattern obtained was compared to the XRPD patterns at the various temperatures of the VT-XRPD study of the raw material (figure 4.5). No exact match was found but it seemed as if the XRPD pattern of the dried sample could be fitted between the VT-XRPD patterns analysed at 160-170°C.

The DSC thermogram (figure 4.7) of the dried sample did not reveal any desolvation endotherms, as expected. A small melting endotherm at 160.72°C and a small recrystallisation exotherm at 166.20°C followed by a final melting endothermic peak at 185.29°C were observed. The TGA thermogram revealed a total mass loss of 0.98%, which compared well to the total moisture content of 1.11% determined by KF analysis. This total moisture content can be considered insignificant and therefore classified this dried sample to be an anhydrous form of gatifloxacin. The DSC and TGA thermograms are illustrated in figure 4.7.

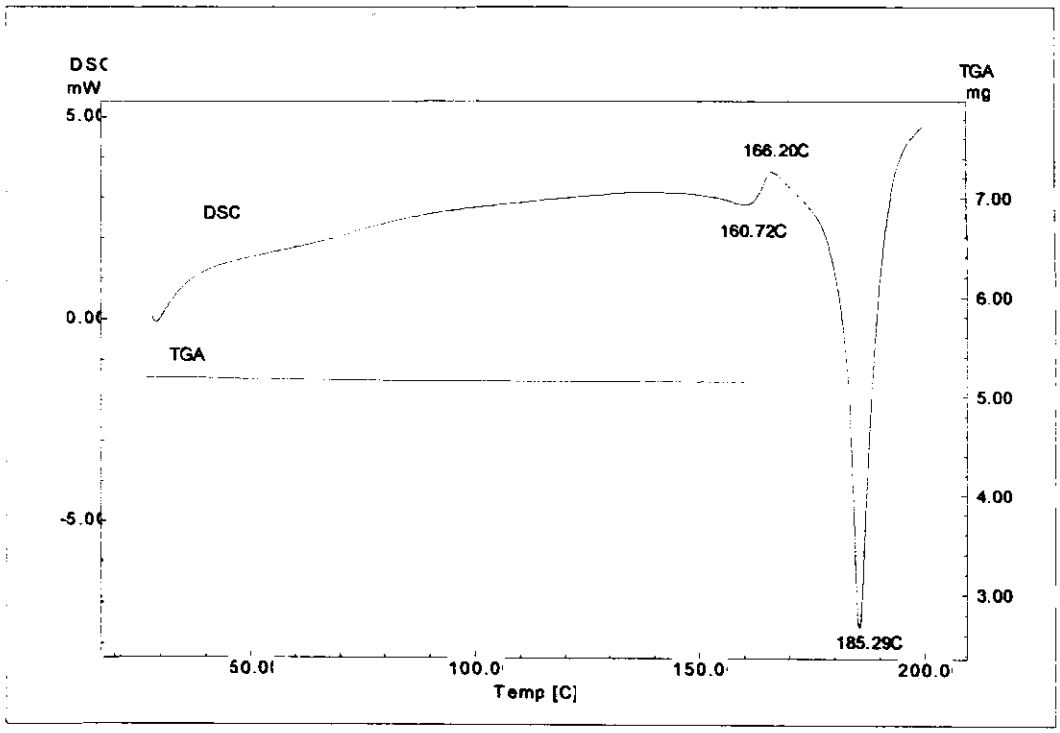

Figure 4.7 The DSC and TGA thermograms of anhydrous gatifloxacin.

HSM observations of the anhydrous form correlated well with the thermal events as displayed in figure 4.7. These observations are discussed in table 4.3.

Table 4.3 Photomicrographs of the HSM events observed for the anhydrous gatifloxacin

Observation	Event	Temperature (°C)
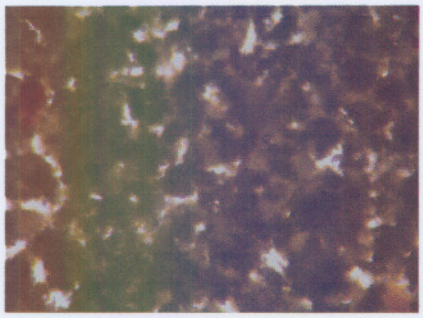	Initial.	25
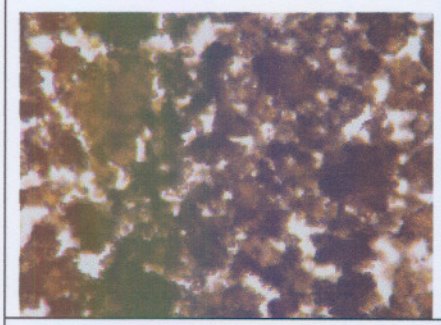	Sample melted rapidly at 160°C followed by an immediate recrystallisation at 165°C.	165
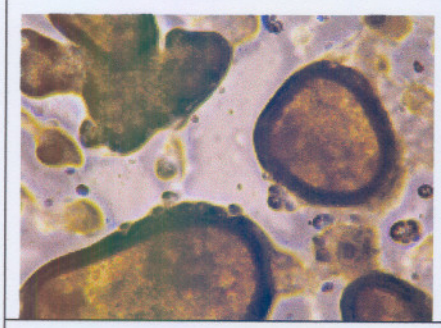	Melting of the recrystallised product started at 182°C.	182
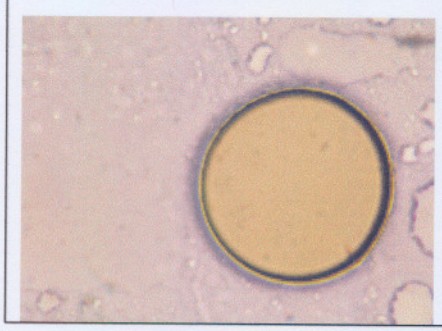	Melting process completed at 187°C.	187

4.3 Comparison between gatifloxacin sesquihydrate and its anhydrous form

To distinguish between these two forms it is suggested that the following methods of analyses be utilised: XRPD (table 4.4), thermal behaviour (table 4.5) and IR spectrometry (table 4.6 and figure 4.8).

Table 4.4 XRPD peak position (°2θ) and relative peak intensities of gatifloxacin sesquihydrate and its anhydrous form

Gatifloxacin sesquihydrate		Anhydrous form	
Position (°2θ)	Intensity (I/I_0)	Position (°2θ)	Intensity (I/I_0)
6.25	5.8	-------	-------
7.79	10.0	7.75	18.7
-------	-------	8.93	6.0
9.14	100.0	-------	-------
-------	-------	9.37	4.5
9.67	22.6	-------	-------
-------	-------	10.21	11.1
10.49	16.0	-------	-------
-------	-------	11.16	11.8
11.36	14.6	-------	-------
-------	-------	11.74	2.7
-------	-------	12.12	9.6
12.29	12.7	-------	-------
12.96	33.8	12.92	30.1
13.47	18.1	-------	-------
-------	-------	13.62	44.6
-------	-------	14.15	21.8
14.33	14.8	-------	-------
14.78	6.9	-------	-------
-------	-------	14.99	11.5
-------	-------	15.39	11.6
15.62	5.3	-------	-------
16.34	6.6	16.35	8.7
16.73	5.5	-------	-------
-------	-------	17.04	6.9
17.80	5.2	17.83	3.7
18.31	56.5	-------	-------
18.94	14.3	18.86	5.9
19.65	23.2	19.73	58.9
19.95	47.4	-------	-------
20.23	18.5	-------	-------
-------	-------	20.48	22.7
20.77	21.2	-------	-------
21.10	37.0	21.15	100.0
21.77	15.2	21.68	43.8
22.24	7.2	-------	-------
22.85	6.6	-------	-------
23.28	15.1	-------	-------

Table 4.4 continued…

Gatifloxacin sesquihydrate		Anhydrous form	
Position (°2θ)	Intensity (I/I_0)	Position (°2θ)	Intensity (I/I_0)
-------	-------	23.24	7.5
-------	-------	23.77	16.4
24.31	22.7	24.45	36.6
-------	-------	24.91	9.6
25.36	22.9	-------	-------
-------	-------	25.55	7.3
25.76	18.1	-------	-------
26.05	13.0	25.94	26.8
-------	-------	26.24	14.7
26.50	7.9	-------	-------
-------	-------	27.29	6.3
-------	-------	27.53	6.6
27.78	8.8	-------	-------
-------	-------	28.65	14.2
29.04	7.0	-------	-------
29.28	9.4	29.17	3.8
30.37	15.4	-------	-------
-------	-------	30.50	6.3
-------	-------	30.88	7.6
-------	-------	31.51	3.7
32.26	6.3	-------	-------
-------	-------	33.08	3.3
-------	-------	34.71	4.3

Table 4.5 Thermal behaviour of gatifloxacin sesquihydrate and its anhydrous form

Event	Gatifloxacin sesquihydrate	Anhydrous form
Dehydration endotherm	Present at 97.21°C	Absent
Melting point	189.68°C	185.29°C
Total moisture content (TGA)	6.09%	Insignificant (0.98%)

Table 4.6 The main absorptions in the IR spectra of gatifloxacin sesquihydrate and its anhydrous form

Gatifloxacin sesquihydrate raw material	Anhydrous form
Wavenumber (cm^{-1})	Wavenumber (cm^{-1})
-------	3490
3340	3329
2975	-------
-------	2944
2842	-------
-------	2813
-------	1719
1635	1648
-------	1616
1551	1542
1448	1448
1394	1396
1359	1351
1322	1319
1283	1277
-------	1242
-------	1217
1209	1185
1179	-------
1143	1153
1118	1114
1095	1094
1070	-------
-------	1058
1025	-------
997	1000
940	941
912	911
890	887
-------	870
847	847
822	834
-------	821
-------	805
773	782
738	735
689	686
664	661
647	648
599	594
-------	573
542	546
514	523
-------	503
490	485
-------	472
450	451
-------	438

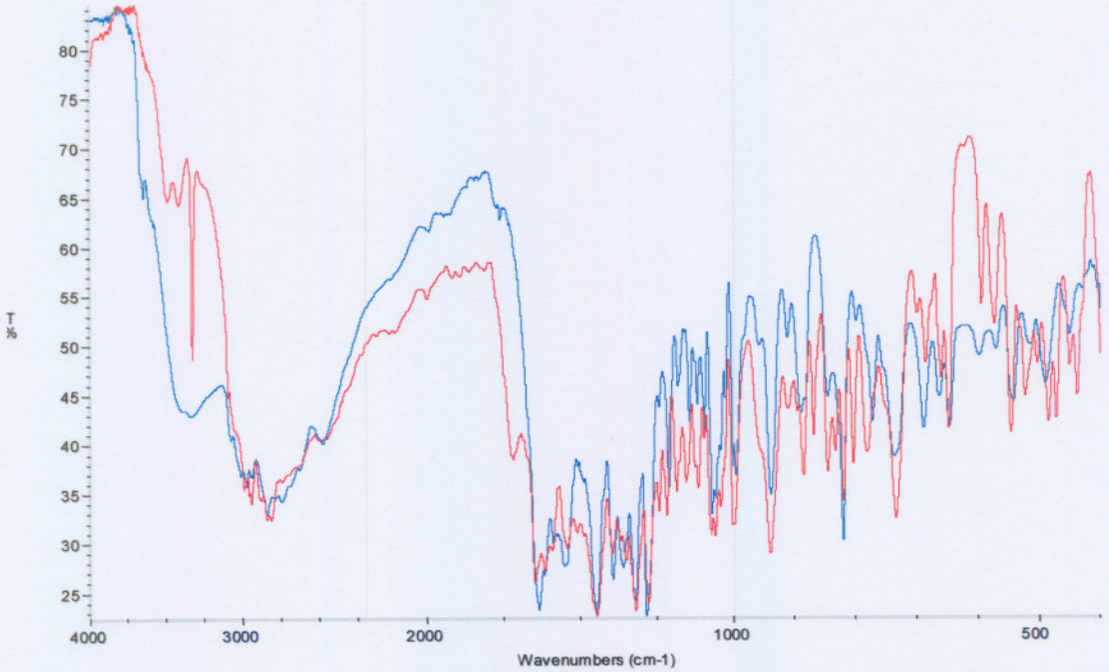

Figure 4.8 Superimposed IR spectra of gatifloxacin sesquihydrate raw material and its anhydrous form.

To obtain insight regarding the powder flow properties of these two forms the Carrs index (CI) and Haussner ratio (HR) of the samples were calculated. The analysis of each sample was performed in three fold as discussed in chapter 3. The averages of the results are given in table 4.7. Flow properties are classified as follows (by Staniforth, 2002:208):

- excellent (5<CI<15)
- good (12<CI<16)
- poor (23<CI<35)
- extremely poor (CI>40)

Table 4.7 Flowability properties of gatifloxacin sesquihydrate raw material and its anhydrous form

Crystal form	Average CI	Average HR	Flow properties
Gatifloxacin sesquihydrate	44.33	1.80	Extremely poor
Anhydrous gatifloxacin	42.96	1.75	Extremely poor

SEM photomicrography was used to study the morphology of gatifloxacin sesquihydrate and its anhydrous product (table 4.8).

Table 4.8 SEM photomicrographs of the gatifloxacin sesquihydrate and the anhydrous product thereof

Crystal form	Photomicrograph	Brief description
Sesquihydrate (H4)	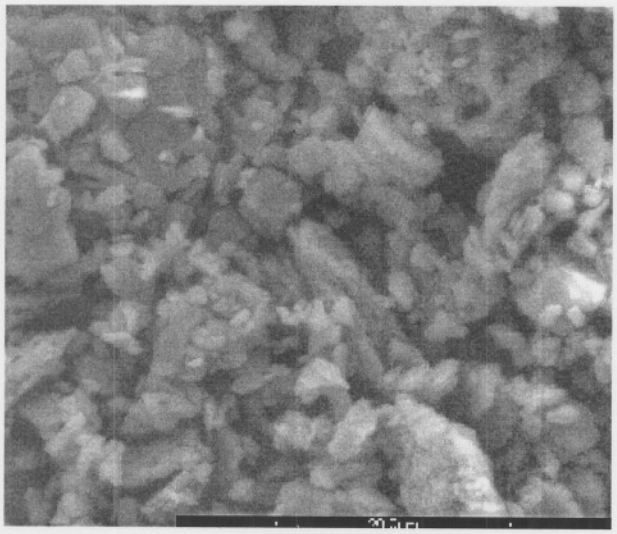	Shapeless particles that revealed a tendency to agglomerate.
Anhydrous gatifloxacin	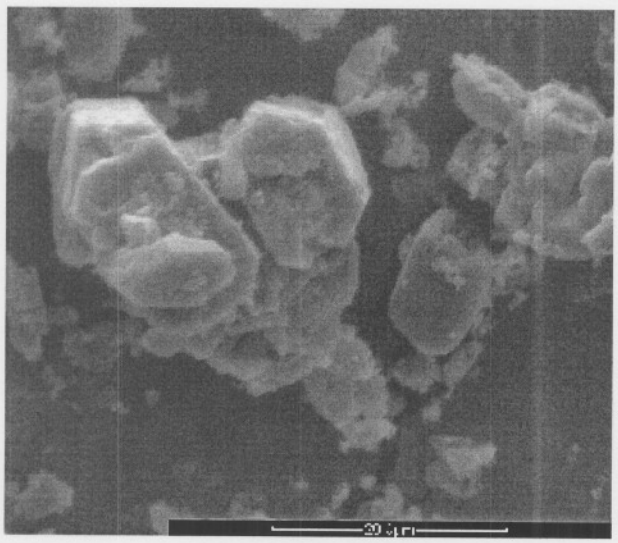	The anhydrous form revealed photomicrographs of particles that were shapeless and tended to agglomerate.

The extremely poor flow properties (table 4.7) can be attributed to the agglomerating behaviour and the non-spherical shape of these crystal forms as observed in the SEM results (table 4.8).

4.4 Dehydration behaviour of gatifloxacin sesquihydrate (H4)

This section discusses the dehydration behaviour of gatifloxacin sesquihydrate (H4).

4.4.1 Activation energy (E_a) needed for dehydration

To calculate the dehydration activation energy for gatifloxacin sesquihydrate, the method described by Flynn & Wall (1966:323-328) was used. This method involved the heating of samples at different heating rates (3, 5, 7 °C/min) by means of TGA to a final temperature of 160°C. The TGA thermograms obtained with the three different heating rates are illustrated in figure 4.9.

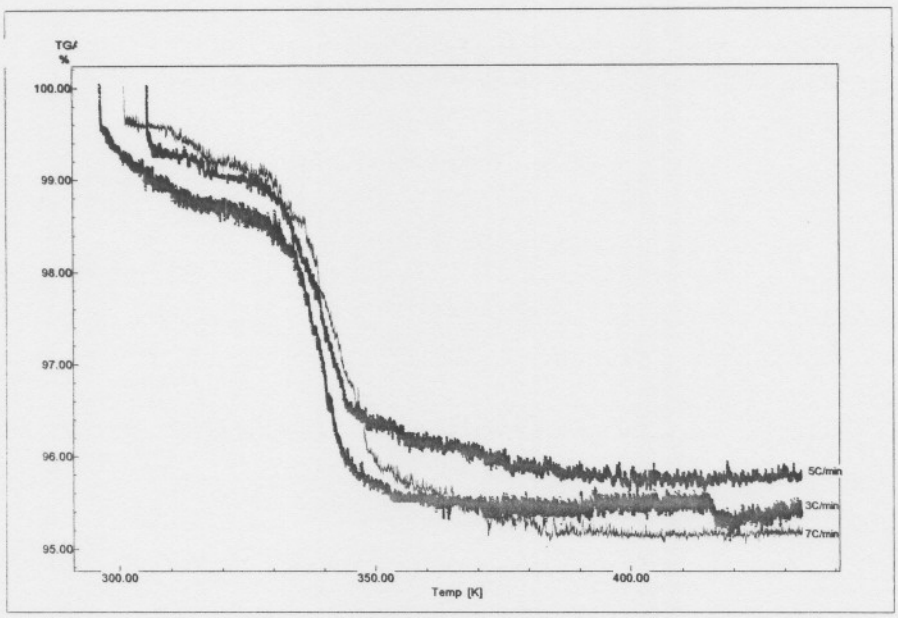

Figure 4.9 TGA thermograms of gatifloxacin sesquihydrate (H4) at 3 °C/min, 5 °C/min and 7 °C/min.

The temperatures (in K) at which 1, 1½, 2, 2½, 3, 3½ and 4% of weight loss occurred, were determined for each sample at each heating rate (3, 5 and 7°C/min). According to Flynn & Wall (1966:323-328), the activation energy (E_a) can be calculated by equation 4.1 when the slope of $-\log(\beta)$ vs. $1/T$ is known (whereas β is the heating rate in °C/sec and T is the temperature (K) at which a specific weight loss had occurred).

$$E_a \approx 4.35 \text{ d log } \beta/\text{d } 1/T \qquad \text{(Equation 4.1)}$$

Whereas:

E_a is the activation energy in cal/mole

d log β/d 1/T = slope of the curve

The results obtained are tabulated in tables 4.9 and 4.10 and illustrated in figure 4.10.

Table 4.9 Temperatures (in Kelvin) at specific weight loss from TGA analysis at 3, 5 and 7°C/min heating rates

Heating rate (°C/sec)	Temperature (K) at the specific weight loss					
	1%	1½%	2%	2½ %	3%	3½ %
0.0500	300.7	310.8	331.5	335.9	337.4	339.8
0.0833	306.6	329.9	337.6	340.0	342.5	346.8
0.1166	315.9	336.3	338.7	340.9	343.3	355.2

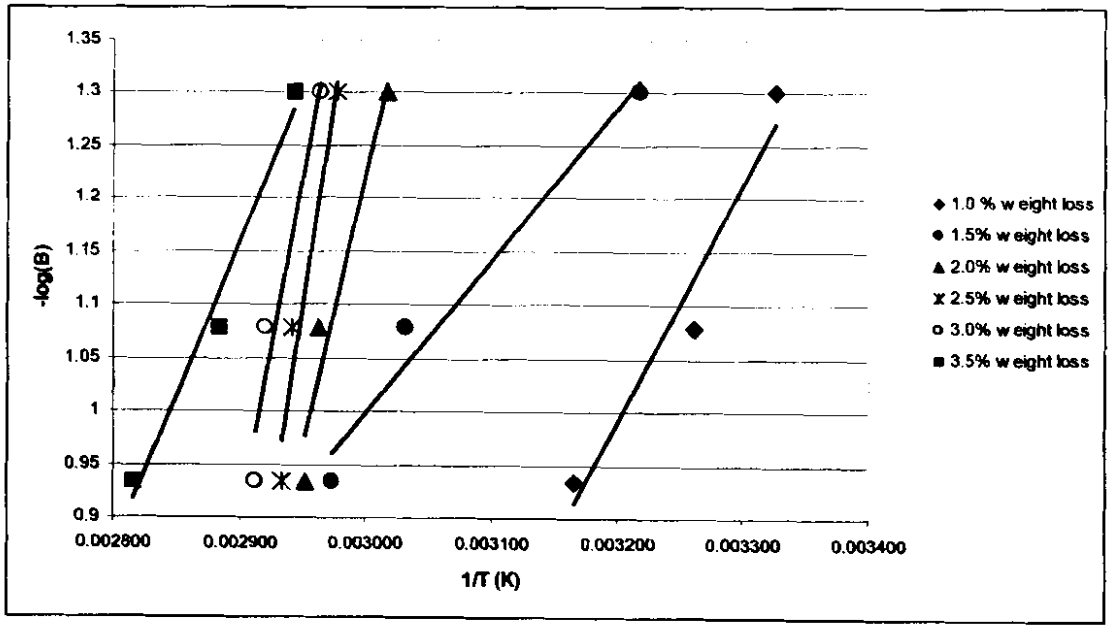

Figure 4.10 The linear relation between –log (β) and 1/T for the various % weight losses.

Table 4.10 Slope determinations from plots of –log(β) vs. 1/T and corresponding calculated activation energy

Plot of – log(β) vs. 1/T of:	**Slope obtained from regression line (trend line)**	**Calculated activation energy (cal/mole) using equation 8.1**
1%	2236.6	9729.2
1½ %	1429.6	6218.8
2%	5166.9	22476.0
2½ %	7725.9	33607.7
3%	6432.0	27979.2
3½ %	2863.9	12458.0
4%	1345.3	5852.1

From figure 4.10 and table 4.10 it is clear that the activation energy for the dehydration of gatifloxacin sesquihydrate (H4) did not remain constant throughout the dehydration process (as the slope varied between each plot – figure 4.10). This behaviour may be attributed to the following:

1. The TGA thermograms indicated that the dehydration process took place in two distinguishable steps. The mechanism of dehydration during these steps might differ that could lead to changes in the activation energy needed during the dehydration process. Similar behaviour was reported by Zhou *et al.* (2003:1367) for nedocromil sodium trihydrate.
2. Dehydration is normally an endothermic reaction and recrystallisation an exothermic reaction. During the dehydration process, dehydration and recrystallisation occurred simultaneously (as illustrated in figure 4.5), that might have influenced the resultant observed activation energy.

Conclusion

This preliminary study on the commercially available gatifloxacin sesquihydrate proved to be useful, as its physico-chemical properties are not fully described in the literature. This chapter revealed significant differences in the physico-chemical properties of the sesquihydrate and its dehydration product. The investigation of the dehydration process of form H4 led to the understanding that the activation energy (Ea) varies throughout the dehydration process.

Since this sesquihydrated form was the raw material used in the recrystallisations, this study serves as the point of reference for the chapters to follow. The pharmaceutical relevance (difference in solubility and dissolution behaviour) of gatifloxacin sesquihydrate and its modifications will be discussed in chapters 5 and 6.

Chapter 5

Gatifloxacin crystal modifications and the properties thereof

Introduction

The recrystallisation method described in chapter 3 was used to prepare various gatifloxacin crystal forms. The effect of drying on these recrystallised products was also evaluated. The aim of this chapter is to provide a comprehensive overview of the physico-chemical properties of the prepared crystal forms, to identify possible new polymorphs and to supply supplementary information regarding crystal forms already described in the literature (prior-art forms).

The solvents that were used during the recrystallisation studies were divided into two parts (alcohols and other organic solvents). The results obtained from the alcohols are discussed in section 5.1 and the results from other organic solvents are discussed in section 5.2.

5.1 Recrystallisation products from alcohols

Gatifloxacin recrystallisations were performed using absolute ethanol and *n*-butanol as solvents.

5.1.1. Recrystallisation of gatifloxacin using absolute ethanol (99-100%)

The recrystallisation product from absolute ethanol was removed from the mother liquor (i.e. absolute ethanol) and dried on filter paper for 1½ hours at ambient conditions prior to analysis.

VT-XRPD revealed an initial XRPD pattern (25°C) that is characteristic of a crystalline powder (i.e. relatively strong diffraction peaks), as seen in figure 5.1. During the analysis there were no significant changes in the XRPD pattern between 25°C and 160°C. No significant changes in the crystal lattice were observed during

desolvation, thus implying isomorphism. Isomorphism is a phenomenon where the desolvated crystal form reveals a similar XRPD pattern to it parent solvated form. Isomorphism is an uncommon phenomenon, but has been reported by many researchers like Stephenson *et al.* (1998:536) for erythromycin A, cefachlor and cephalexin.

A slight shifting in the °2θ peak positions was observed for the XRPD patterns from 25-160°C. These slight changes can be attributed to a possible change in powder bed height due to the prolonged exposure to increased temperatures (crystal expansion and relaxation). Significant changes in the XRPD patterns were observed between 160°C and 180°C. The pattern at 170°C revealed few peaks in the range of 5-15°2θ with low intensities. At 180°C the XRPD pattern revealed amorphic behaviour due to the melting of the sample.

XRPD, TGA, KF and DSC results were used to compare this crystal form to previously described crystal forms (see table 2.3). Form E, produced form recrystallisation using 90-95% ethanol, was described as a six-sided platelet ethanol solvate that has gigantic solvent channels (patent number US 6,413,969). The gigantic solvent channels caused this crystal form to be very unstable when removed form the mother liquor (Raghavan *et al.*, 2002:1-18). The ethanol solvate (as prepared in this study) was found to be fairly stable at ambient conditions (i.e. desolvation did not occur) and the VT-XRPD studies indicated that desolvation did not cause significant changes in the crystal lattice. The ethanol solvate prepared in this study can thus be considered to be a novel pseudopolymorph of gatifloxacin and was dubbed ZP0.

Further investigations into the behaviour of ethanol recrystallisations are discussed in chapter 7.

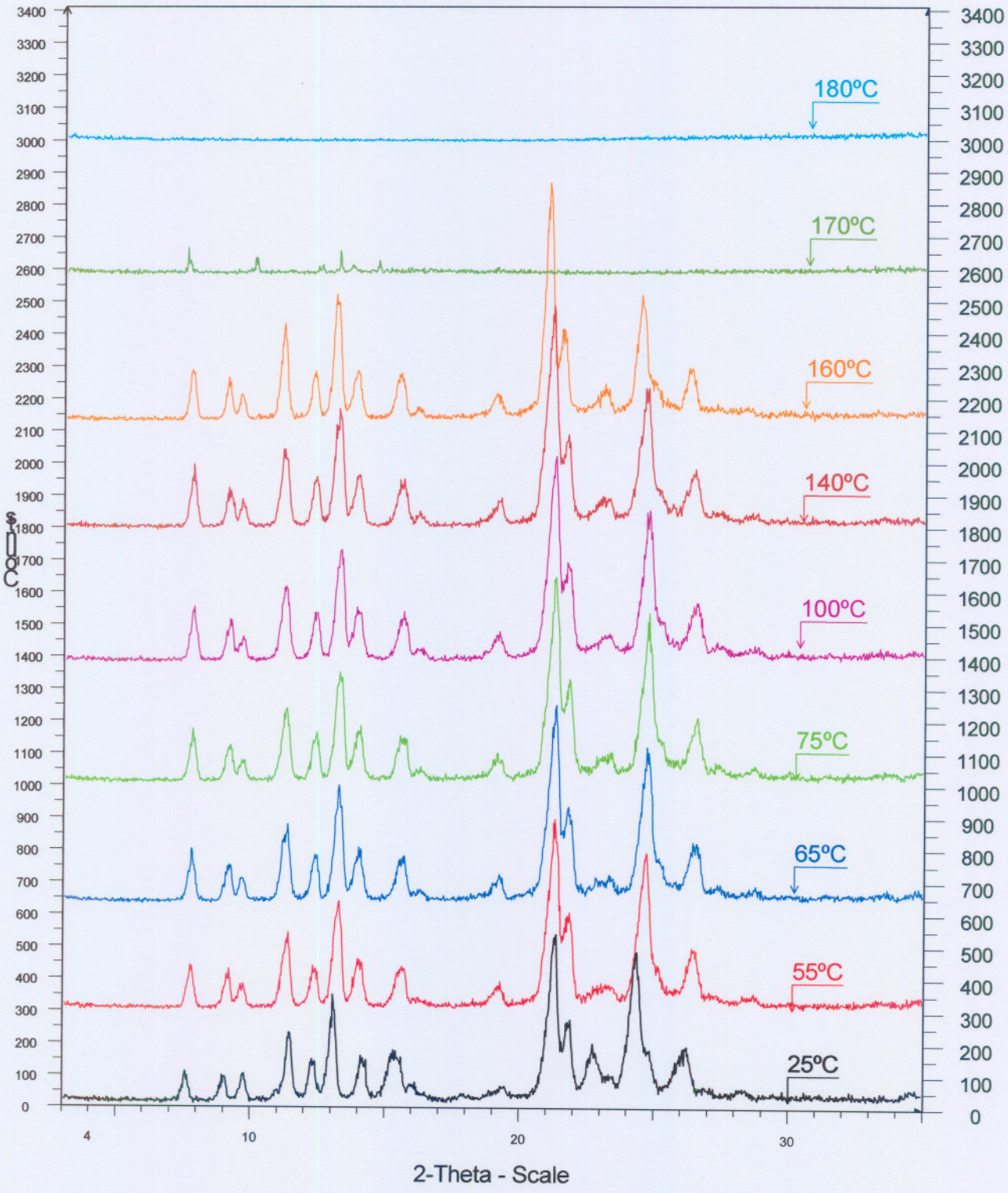

Figure 5.1 Overlay of the VT-XRPD patterns of ZP0 at temperatures ranging from 25-180°C.

The DSC thermogram (figure 5.2) of ZP0 revealed a desolvation endothermic peak (69.97°C), another endothermic peak (166.70°C) followed by a sharp exothermic peak (170.04°C) and a final melting endotherm at (190.13°C). The desolvation peak temperature was comparable to the boiling point of ethanol (78.50°C).

TGA revealed a mass loss (12.82%) that commenced at 43.83°C and ended at 88.52°C, which correlated to the mass loss associated with ethanol desolvation. Karl-Fischer (KF) determination revealed a total moisture content of 1.76%, which can be considered as surface moisture. The TGA curve is superimposed with the DSC thermogram in figure 5.2. TGA and KF confirmed that the solvent incorporated into the crystal lattice was indeed ethanol; ZP0 can thus be classified as a mono-ethanol solvated crystal form of gatifloxacin.

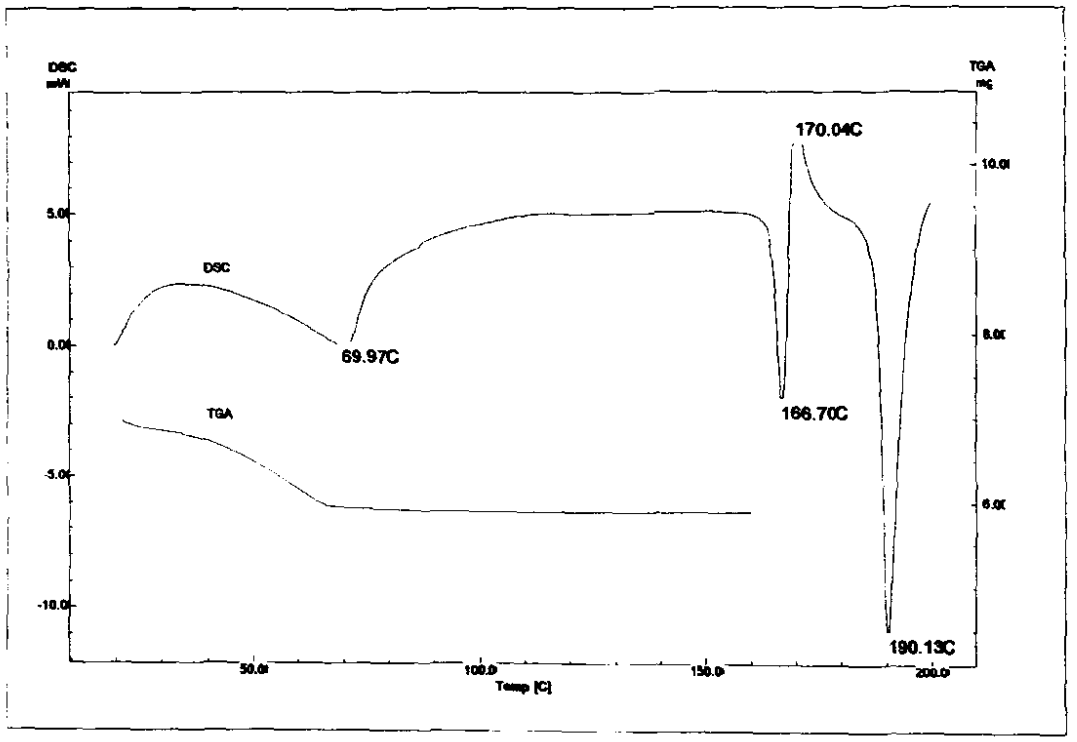

Figure 5.2 Superimposed DSC and TGA thermograms of ZP0.

With HSM a slight darkening of the crystals was observed at 101°C. The darkening of crystals confirmed the desolvation process. The slight difference in the desolvation peak maximum temperature of the DSC thermogram and the temperature at which the darkening was observed might be due to a higher heating rate of the HSM heat stage. HSM confirmed the endotherm at 166.70°C to be indicative of melting. The

endothermic peak present at 170.04°C indicated the formation of a recrystallisation product from the melt, and the final endotherm present at 190.13°C indicated the melting point of the recrystallised product. HSM in conjunction with the DSC thermogram supported the phase changes observed in the XRPD patterns between 160°C and 180°C. The typical amorphous XRPD pattern at 180°C indicated the melting of the recrystallised product. The slight differences between the temperatures of the DSC thermogram and that of the VT-XPRD may be imputed to the fact that the VT-XRPD sample was exposed for a longer period to increased temperatures compared to the DSC sample heating rate of 10°C/min. The HSM events are illustrated in table 5.1.

Table 5.1 Photomicrographs of the HSM events observed for ZP0

Photomicrograph	Observation	Temperature (°C)
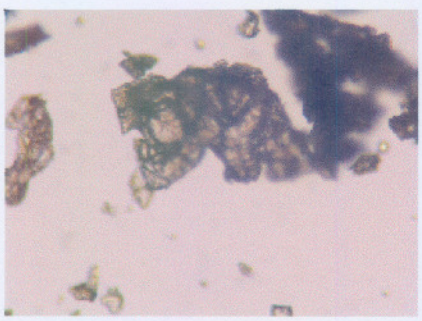	Initial.	25
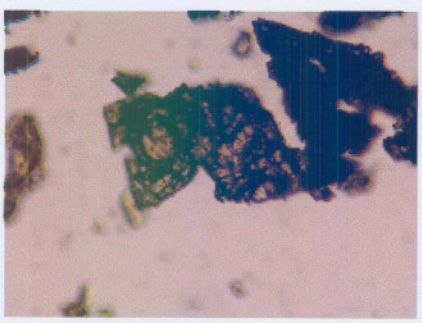	Darkening of crystals indicated desolvation.	101

Table 5.1 continued…

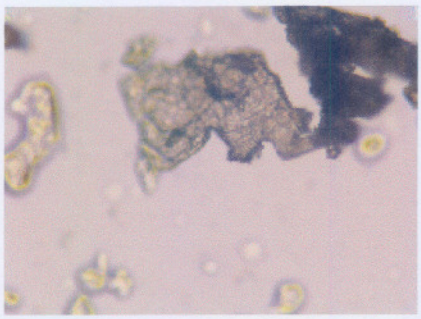	Melting began at 166°C.	166
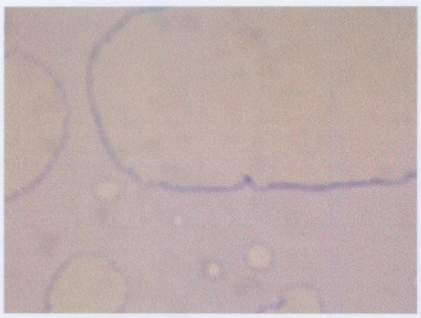	Melting completed at 169°C.	169
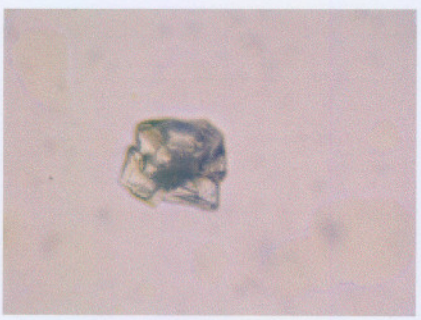	Recrystallisation product from the melt.	171
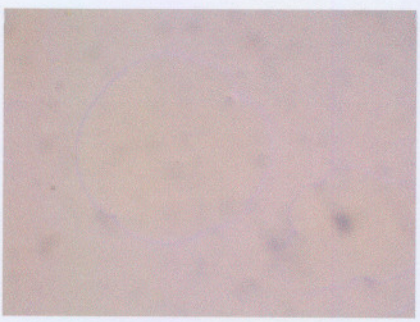	Melting of the recrystallised product completed.	192

ZP0 was then dried for 12 hours at 90°C. As anticipated, there were no significant changes in the XRPD patterns (peak positions) or peak intensities compared to the solvated ZP0 and its desolvated form (figure 5.3), thus implying that the incorporated solvent molecules (ethanol) didn't play an important role in stabilising the solvated crystal lattice. The drying process thus produced an *isomorphic* desolvated form of ZP0.

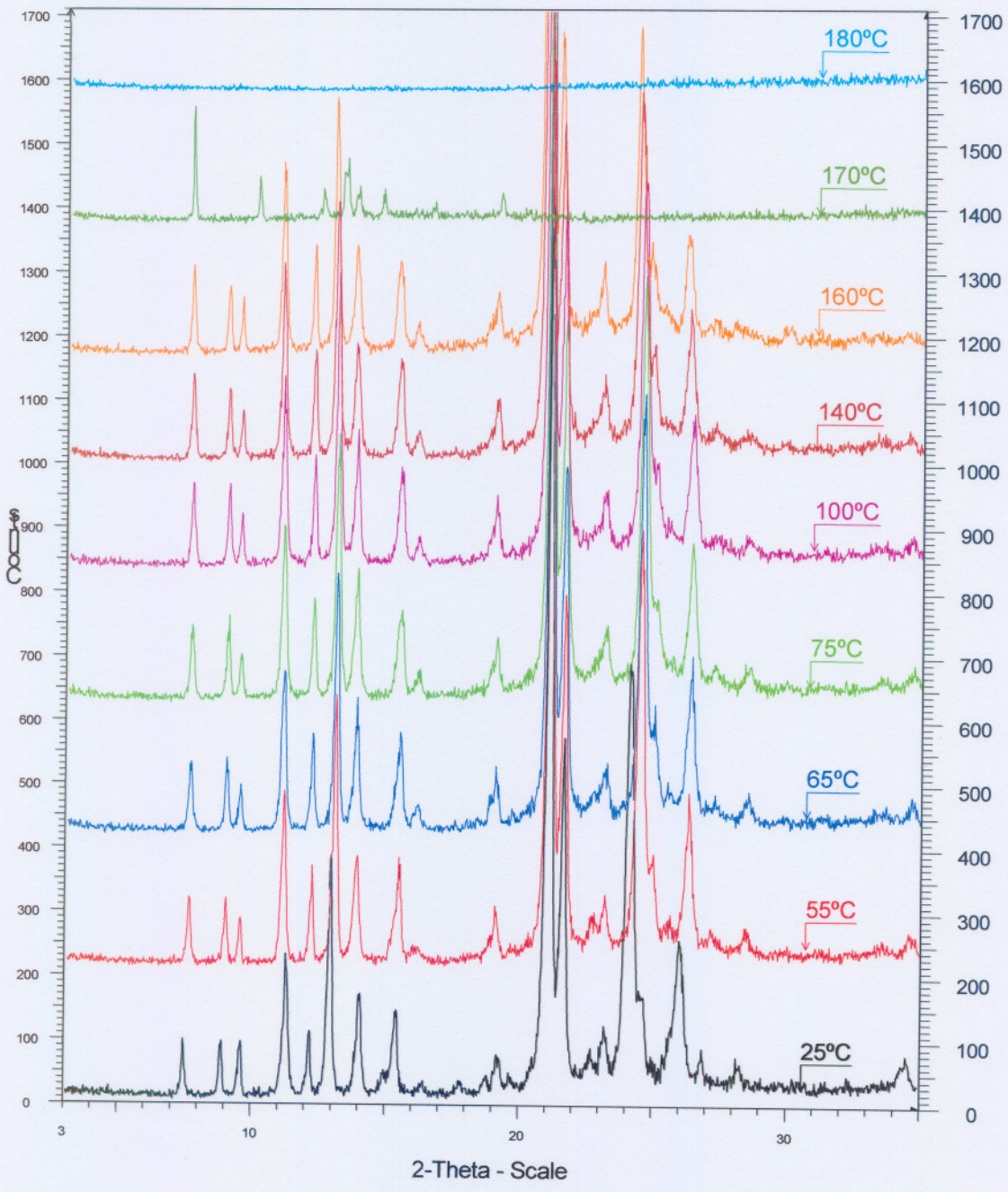

Figure 5.3 Overlay of the VT-XRPD patterns of the isomorphic desolvated ZP0 at temperatures ranging from 25-180°C.

The XRPD pattern of the isomorphic desolvated form was comparable to that of the solvated ZP0 (as ethanol solvate) however the thermal properties of the desolvated form differed significantly from the solvated form. The isomorphic desolvate form is characterised by the absence of a desolvation endotherm in the DSC thermogram and revealed a TGA mass loss of 1.70% (which may be considered as surface moisture). An overlay of the DSC thermogram and TGA is shown in figure 5.4. Thermal events for the isomorphic desolvate (figure 5.4) e.g. the endotherms at 166.81°C and 190.18°C and the exotherm at 170.18°C were similar to the thermal events observed in the temperature of 150-200°C for the solvated form (figure 5.2) As for the solvated form, these thermal events correlated well with the phase changes observed in the XRPD patterns from 160°C to 180°C.

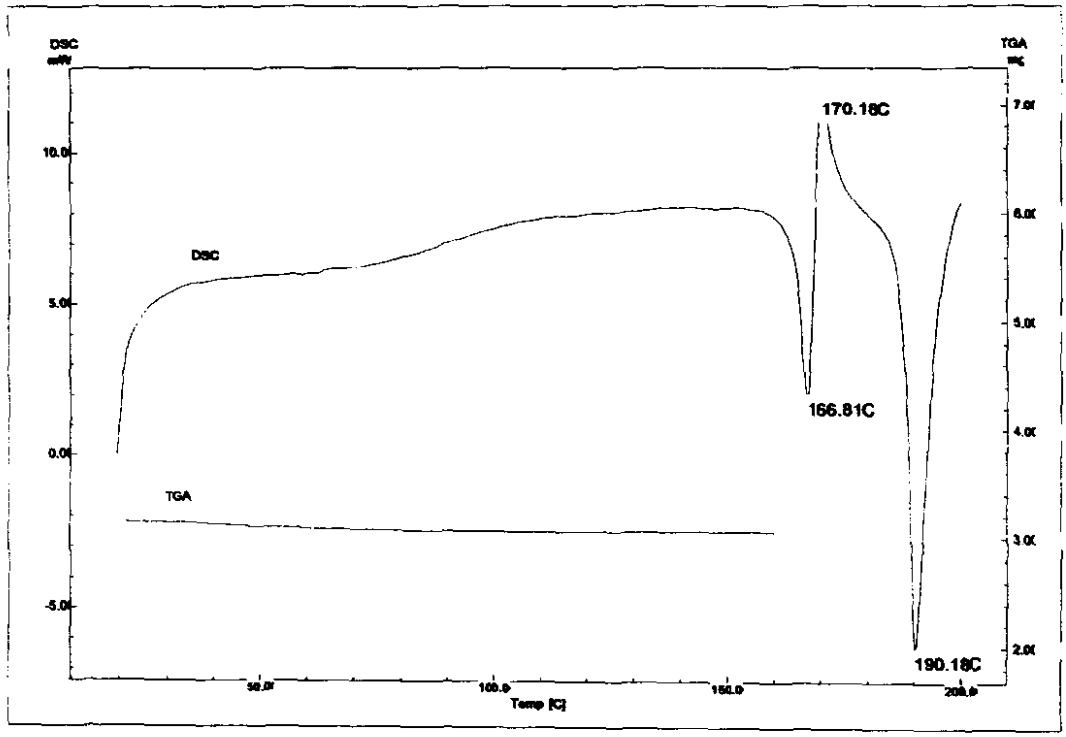

Figure 5.4 Superimposed DSC and TGA thermograms of isomorphic desolvate form.

It should be noted that slight changes were observed between the solvated and dried sample, but as reported by Yu *et al.* (1998:124) and Byrn *et al.* (1995:951), the XRPD of an isomorphic desolvate will differ slightly from the XRPD pattern of its parent solvate. Due to the fact that ZP0 revealed isomorphism, XRPD analysis does not provide significant differences in the XRPD patterns to distinguish between the

solvated and desolvated form (as seen in table 5.2). As a result discriminating methods should be considered.

Table 5.2 XRPD peak position (°2θ) and relative peak intensities of ZP0 and its isomorphic desolvated product

ZP0		Isomorphic desolvate	
Position (°2θ)	**Intensity (I/I_0)**	**Position (°2θ)**	**Intensity (I/I_0)**
7.54	19.9	7.38	6.9
8.97	16.9	8.80	6.7
9.69	18.6	9.52	6.7
11.41	42.8	11.23	16.4
12.29	27.3	12.11	7.9
13.05	65.3	12.89	27.3
14.16	28.2	13.99	12.1
15.25	30.7	15.34	10.3
16.03	12.3	16.35	2.1
19.40	11.2	19.20	5.1
21.29	100.0	21.01	100.0
21.83	49.8	21.61	40.7
22.77	37.1	22.65	6.2
23.46	18.0	23.19	8.7
24.34	90.5	24.11	49.1
24.83	33.0	24.56	12.2
25.93	27.8	25.99	18.2
26.03	30.7	26.84	6.2
26.24	35.6	——	——

The thermal properties (table 5.3) may be used to distinguish between these two forms. As with the XRPD patterns, the IR spectra (table 5.4 and figure 5.5) revealed no significant differences and should preferably not be used to distinguish between these two forms. The XRPD peak at 26.24°2θ and the slight difference in the IR spectra (±3500 cm^{-1}) may be attributed to the presence of ethanol in the parent solvate which is absent in the isomorphic desolvate.

Table 5.3 Thermal behaviour of ZP0 (ethanol solvate) and its isomorphic desolvate

Event	ZP0	Isomorphic desolvate
Desolvation peak	69.97°C	Absent
TGA mass loss	12.82%	Insignificant (1.7%)

Table 5.4 The main absorptions in the IR spectra of ZP0 (ethanol solvate) and its isomorphic desolvate

ZP0 (ethanol solvate)	ZP0 (desolvate)
Wavenumber (cm^{-1})	Wavenumber (cm^{-1})
3481	3485
2987	2987
2836	2833
1743	1746
1645	1648
1590	1591
1545	1542
1446	1448
1458	1452
1395	1397
1322	1319
1280	1279
1215	1215
1177	1176
1144	1145
1110	1110
1094	1094
1053	1054
1036	1037
1001	1002
940	940
913	914
886	887
843	844
821	821
786	786
734	734
686	686
647	647
594	660
574	647
549	549
519	520
486	487
451	451

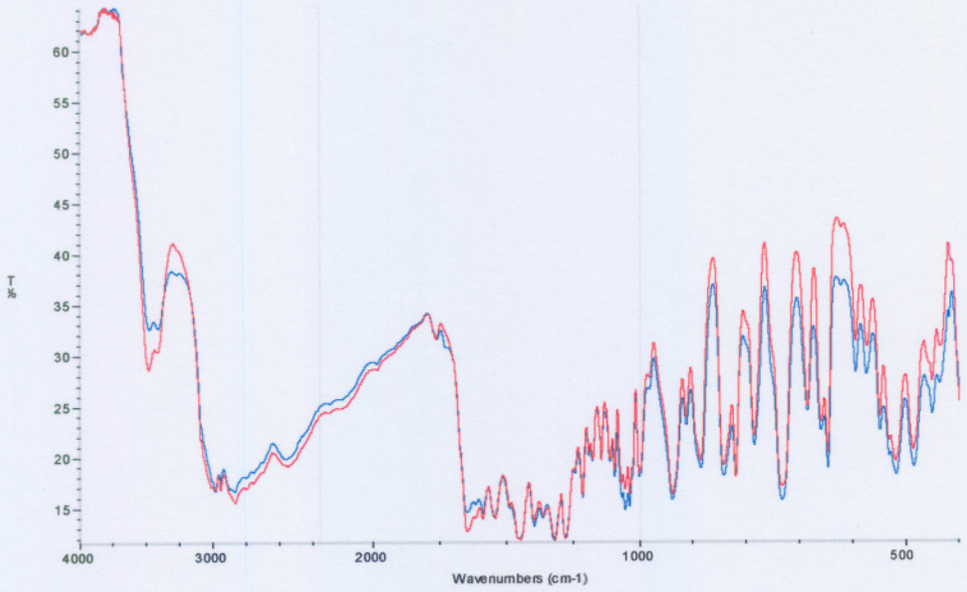

Figure 5.5 Superimposed IR spectra of ZP0 (ethanol solvate) and the isomorphic desolvate.

HSM observations of the isomorphic desolvated form confirmed the thermal events of the corresponding DSC thermogram. The HSM events are discussed in table 5.5.

Table 5.5 Photomicrographs of the HSM events observed for the isomorphic desolvate

Photomicrograph	Observation	Temperature (°C)
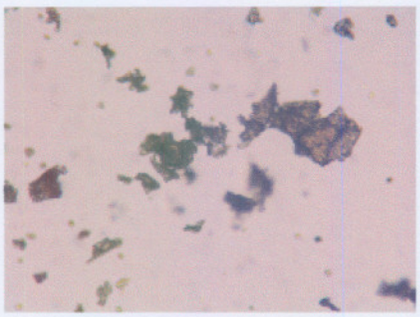	Initial.	25
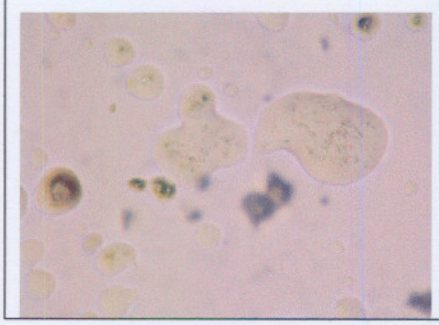	Melting of sample.	167

Table 5.5 continued…

Photomicrograph	Observation	Temperature (°C)
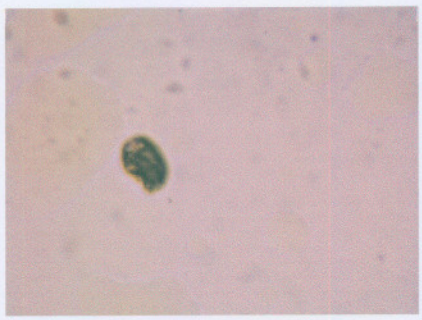	Recrystallisation from melt.	169
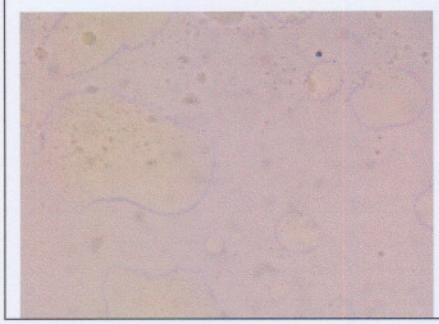	Melting of recrystallised sample completed.	187

5.1.2 Recrystallisation of gatifloxacin using *n*-butanol as solvent

The recrystallisation product obtained when using *n*-butanol as solvent, was removed from the solvent and dried on filter paper for 2 hours at ambient conditions prior to analysis.

The XRPD, TGA, KF and DSC results obtained from the analysis of this recrystallisation product were used to compare this crystal form to previously described crystal forms (see table 2.3). None of the physico-chemical properties of the previously described forms were found to be comparable to that of the recrystallisation product from *n*-butanol. In the literature it was mentioned that gatifloxacin might exist in different butanol solvated crystal forms (forms I, J and B). It can thus be stated that the various butanol solvates of gatifloxacin exist as polymorphic pseudopolymorphs. From the results obtained in this study, it was possible to add this new butanol solvated form to the list of polymorphic pseudopolymorphs of gatifloxacin. This new butanol solvate was dubbed ZP1.

ZP1 revealed significant changes in the XRPD patterns at the various temperature intervals during the VT-XRPD analysis that suggested that desolvation of the sample occurred (figure 5.6).

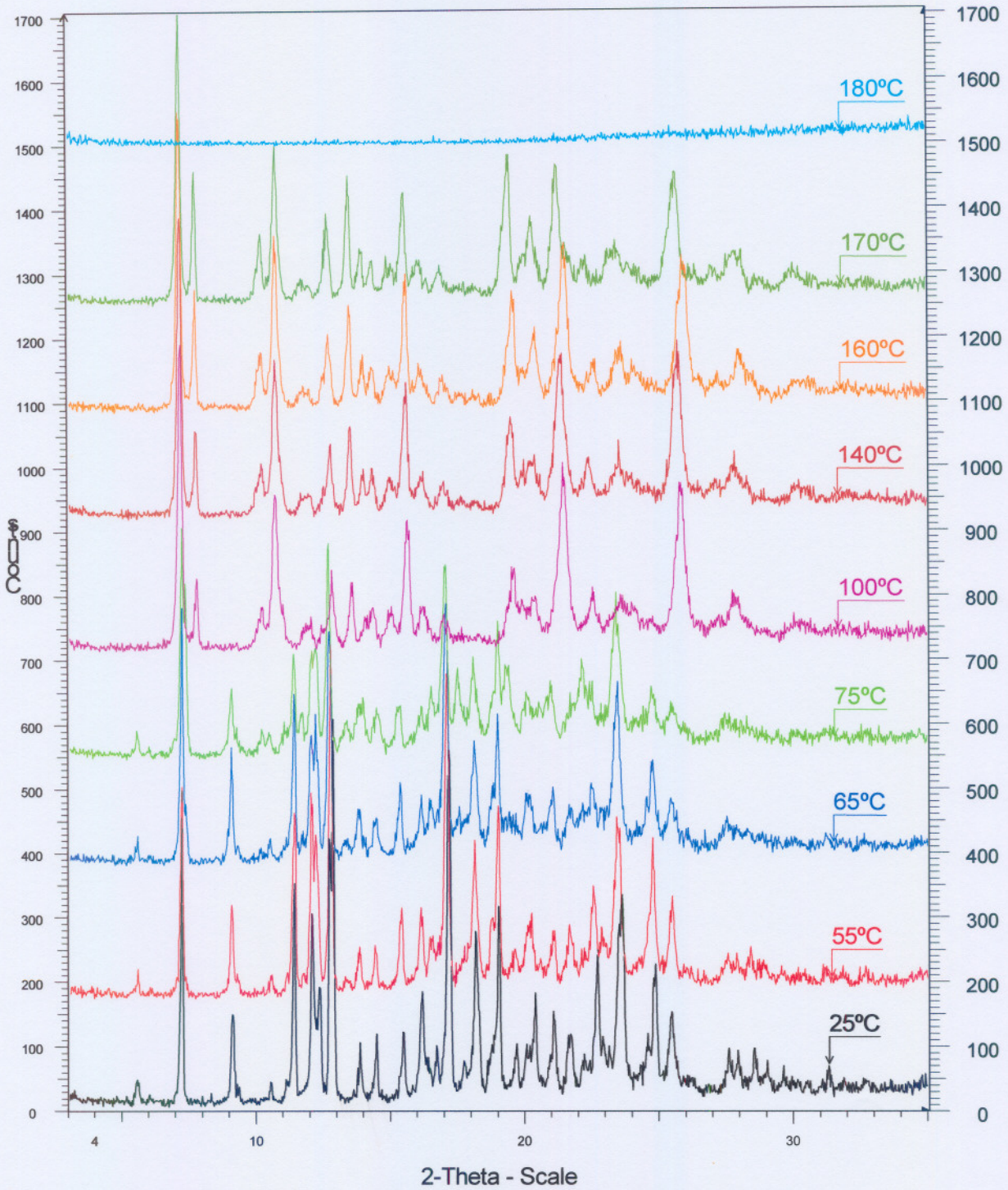

Figure 5.6 Overlay of the VT-XRPD patterns of ZP1 at temperatures ranging from 25-180°C.

In figure 5.6 it can be observed that the crystal lattice seemed to remain unaffected from 25°C to 65°C. Various differences were observed between the XRPD pattern of 75°C and 100°C. Some of the most significant differences include the disappearances of peaks at 5.51-5.93, 9.01, 17.49, 19.34 °2θ and the appearance of peaks at 7.17, 7.74, 10.65, 15.62 and 21.48 °2θ. The crystal lattice seemed to remain unchanged up to 170°C. Between 140°C and 170°C the only difference observed was that of the slight peak shifting in the °2θ peak positions. This can be explained by the change in powder bed height due to the prolonged exposure to increased temperatures that could have caused crystal expansion and relaxation.

The changes in the XRPD patterns between 65°C and 100°C could be attributed to the desolvation process as seen in figure 5.7 and figure 5.8. The onset and endset temperatures of the desolvation process (85-119°C) of the TGA and DSC thermograms are comparable to the boiling point of *n*-butanol. The last endothermic peak at 189.95°C suggested that the amorphic XRPD pattern at 180°C was representative of the melting process of the sample.

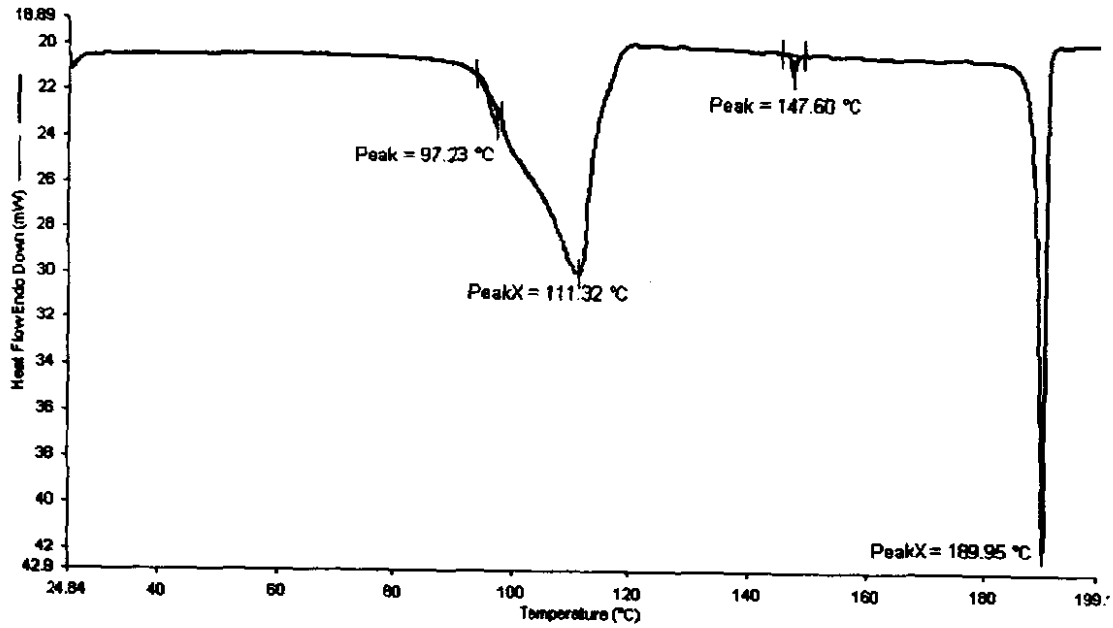

Figure 5.7 DSC thermogram of ZP1.

The total mass loss from TGA was found to be 22.08%. The moisture content determined by KF was 0.64% (which can be considered as surface moisture). It is therefore suggested that ZP1 is a 1½:1 butanol solvate. The TGA thermogram is illustrated in figure 5.8.

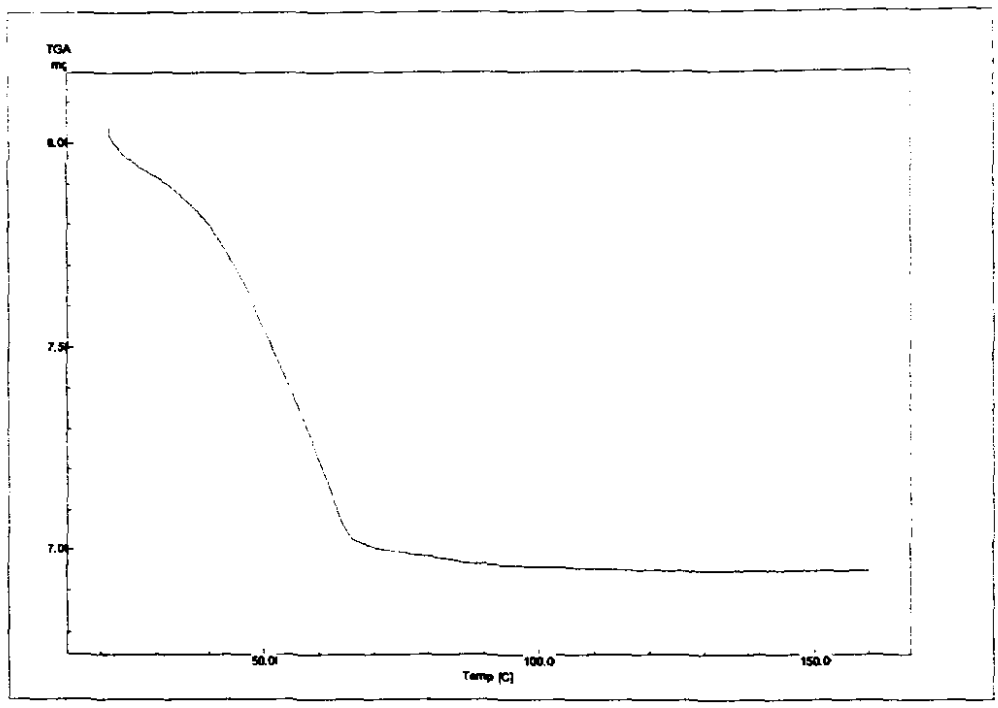

Figure 5.8 TGA thermogram of ZP1.

A twin endothermic peak (desolvation peak) was observed in the DSC thermogram (figure 5.7), which suggested that the desolvation process might have occurred in two steps, the TGA however did not clearly reveal a two-step desolvation process.

HSM observations (table 5.6) confirmed the desolvation process. HSM also indicated the melting process of smaller crystals at 147°C and the melting of all the crystals at 188°C. The melting process at 147°C however does not implicate that ZP1 is a mixture of two forms, but rather that the smaller crystals melt at a lower temperature than the larger crystals due to the fact that the smaller crystals have a smaller heat capacity compared to the larger crystals. HSM observations are discussed in table 5.6.

Table 5.6 Photomicrographs of the HSM events observed for ZP1

Photomicrographs	Observation	Temperature (°C)
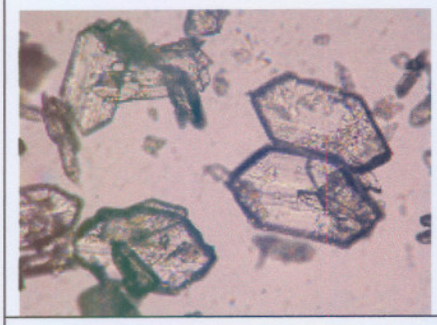	Initial.	25
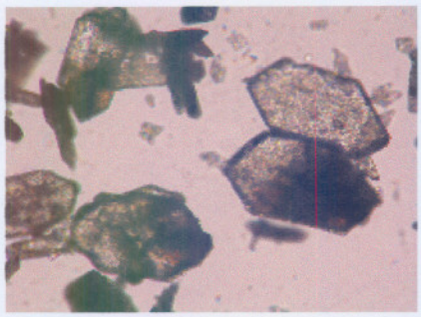	Darkening of crystals commenced at 85°C, which indicated desolvation of the crystals.	85
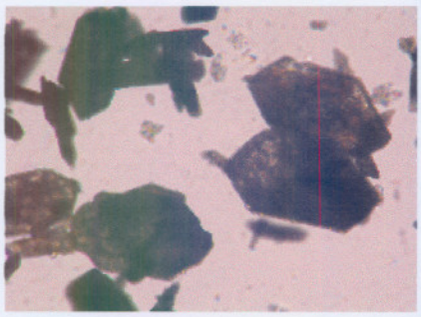	Darkening of crystals ended at 103°C.	103
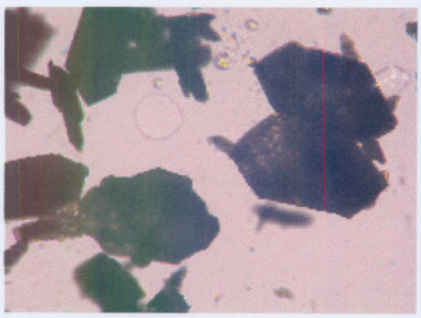	Small crystals melted at 147°C.	147

Table 5.6 continued…

Photomicrographs	Observation	Temperature (°C)
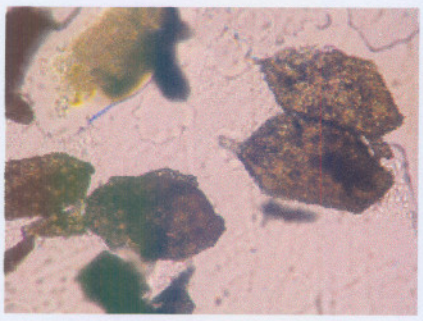	Melting of larger crystals commenced at 182°C.	182
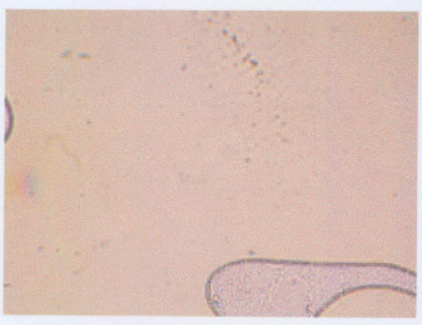	Melting process of all crystals completed at 188°C.	188

ZP1 was thereafter dried at 120°C for 12 hours. It should be noted that the XRPD pattern obtained for the dried sample did not compare to that of the anticipated desolvated form (140°C) obtained from the solvated ZP1 (figure 5.6). This phenomenon can be attributed to the possible stabilisation of the desolvated product to a more thermodynamically stable crystal form due to the prolonged exposure to the increased temperature (140°C). This statement suggested that the desolvation product as observed at 140°C from the VT-XRPD of ZP1 (figure 5.6) is in fact a metastable form that will eventually convert to the crystal form similar to the dried product from ZP1. The VT-XRPD behaviour of the dried sample from ZP1 is illustrated in figure 5.9.

XRPD, TGA, KF and DSC results obtained from the analysis of this dried product were used to compare this crystal form to previously described crystal forms (see table 2.3). It was found that this dried form resembled form Ω. Form Ω as described by Vakil *et al.* (2004:1-18) in patent WO 2004/101527 revealed diffraction peaks at °2θ values as seen in table 5.7. Various XRPD patterns of

mentioned patent. Form Ω (as found in this study) resembled at least one of these XRPD patterns.

Table 5.7 XRPD peak listing of form Ω described by Vakil *et al.* (2004:10)

Form Ω	
Position (°2θ)	**Intensity (I/I_0)**
7.76	45.0
10.23	26.0
12.85	37.0
13.61	70.0
14.12	30.0
14.97	17.0
16.37	14.0
17.03	12.0
19.74	100.0
20.51	37.0
21.46	12.0
23.79	25.0
24.46	12.0
25.94	42.0
27.58	11.0
28.65	24.0
30.44	11.0
30.89	11.0
31.48	7.0

The water content as determined by the inventors of form Ω was insignificant, and thereby proved form Ω to be an anhydrous form of gatifloxacin.

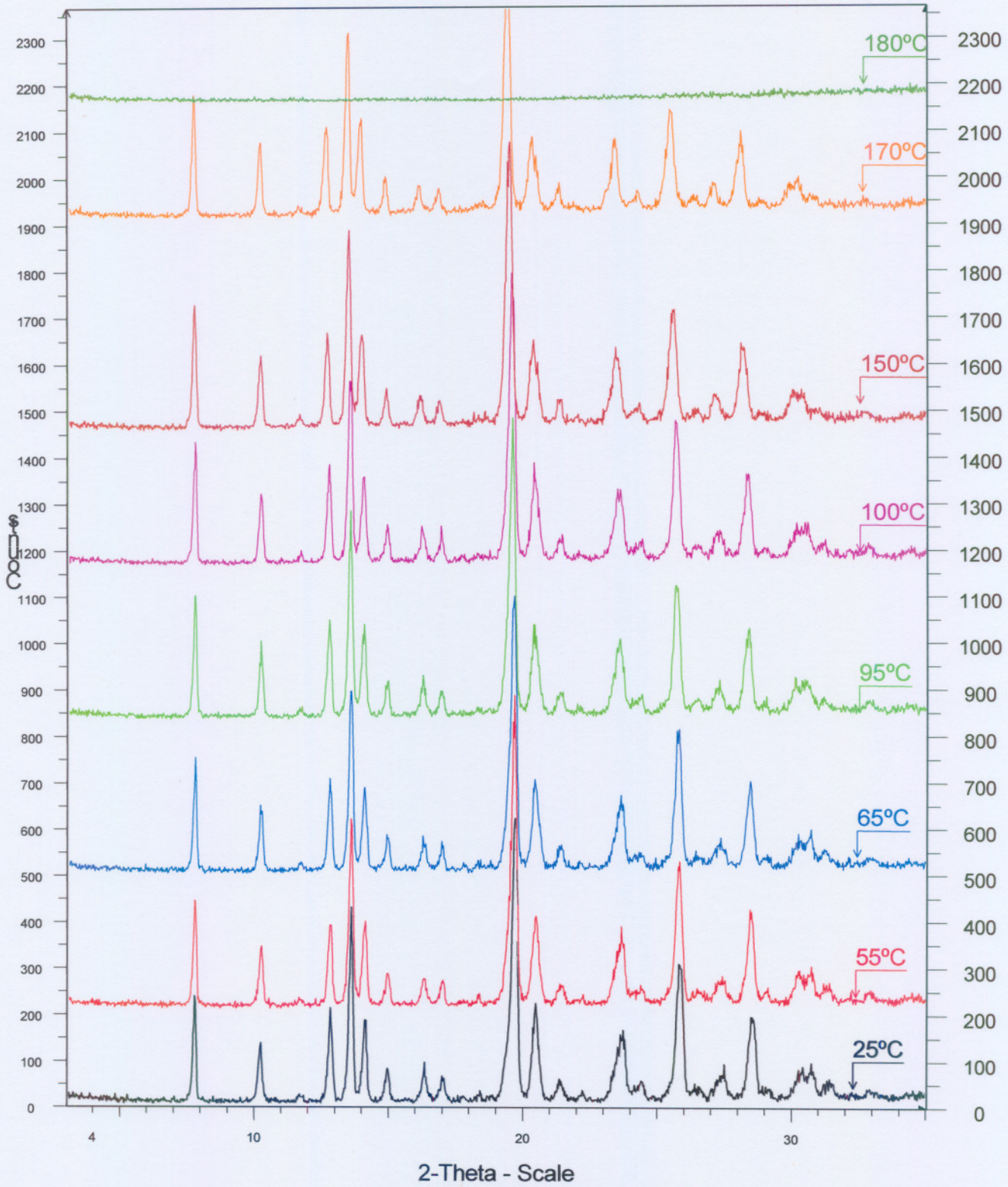

Figure 5.9 Overlay of the VT-XRPD patterns of form Ω at temperatures ranging from 25-180°C.

In figure 5.9 slight peak shifting was observed. The expansion and relaxation of the lattice or changes in the powder bed height can be explanatory to this occurrence. No significant changes were observed over the temperature range 25-170°C, supporting the hypothesis that this crystal lattice is a thermodynamically stable lattice.

The DSC thermogram revealed only one endothermic peak at 190.06°C, which indicated the melting process. The absence of strong diffraction peaks at 180°C in the XRPD pattern (figure 5.9) can therefore be attributed to the melting of the sample. The DSC thermogram of form Ω is illustrated in figure 5.10.

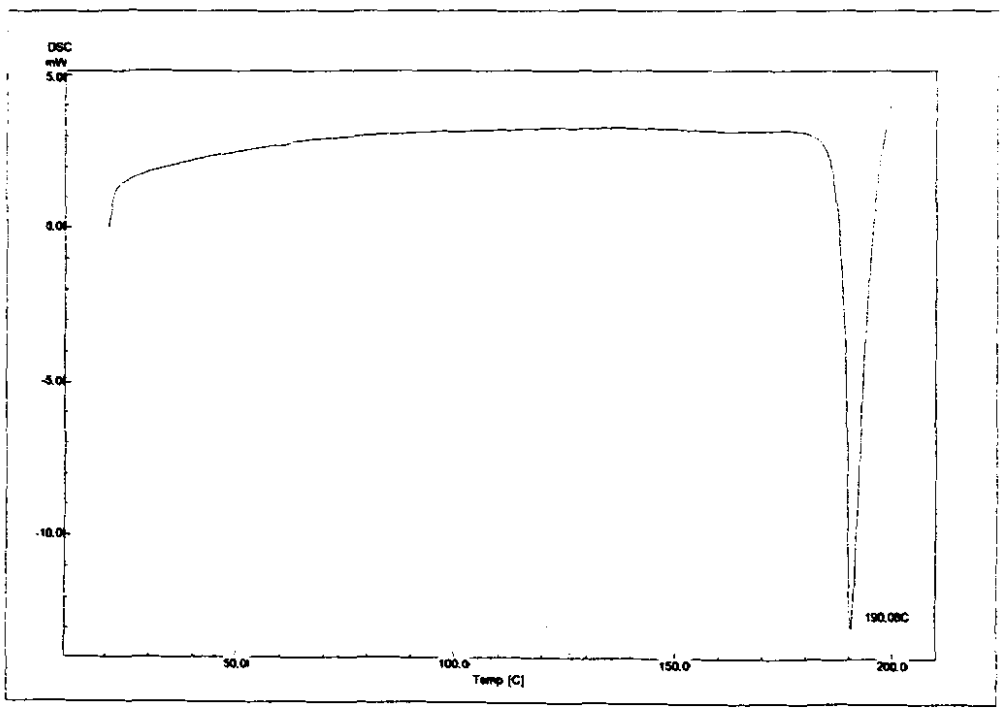

Figure 5.10 DSC thermogram of form Ω.

TGA and KF revealed values of 0.19% and 0.40% respectively. The absence of a desolvation peak concurred with these results. The TGA thermogram is illustrated in figure 5.11.

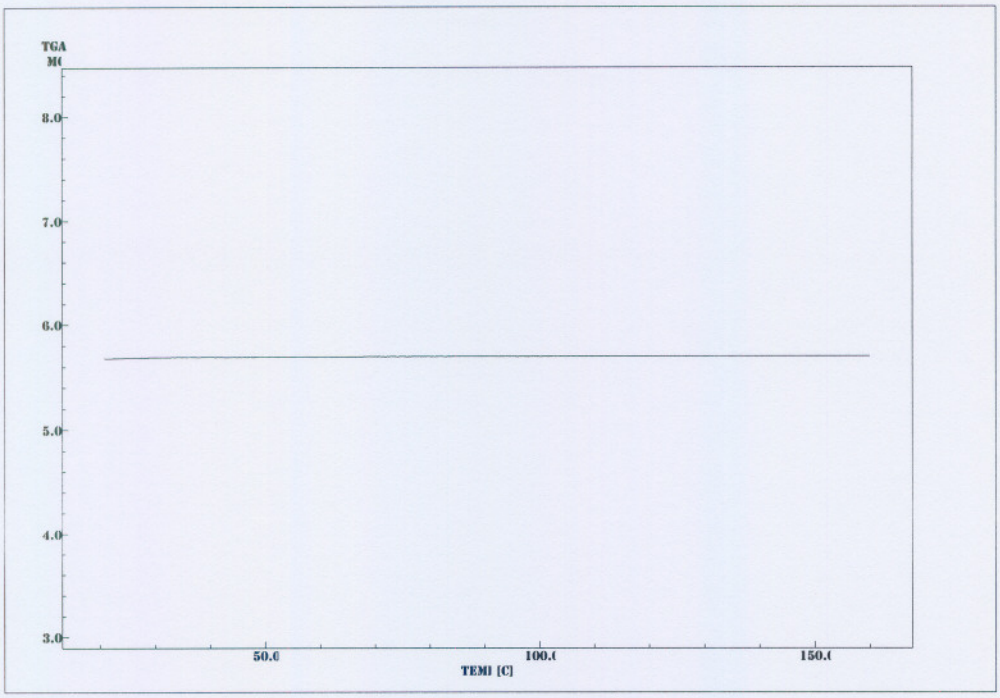

Figure 5.11 TGA thermogram of form Ω.

To distinguish between ZP1 and Ω one may use the XRPD data (table 5.8), thermal behavioural differences (table 5.9) and IR spectral differences (table 5.10 and figure 5.12). It is advised to use XRPD in conjunction with at least 2 other methods of analysis for polymorphic identification.

Table 5.8 XRPD peak position (°2θ) and relative peak intensities of form ZP1 and form Ω

ZP1		Form Ω	
Position (°2θ)	**Intensity (I/I_0)**	**Position (°2θ)**	**Intensity (I/I_0)**
5.53	8.1	-------	-------
7.19	88.7	-------	-------
-------	-------	7.73	37.9
9.08	26.2	-------	-------
-------	-------	10.19	21.8
10.52	7.5	-------	-------
11.37	62.7	-------	-------
-------	-------	11.69	2.7
12.05	54.3	12.07	1.9
12.31	33.7	-------	-------
12.81	98.6	12.813	33.9
-------	-------	13.58	69.0
13.83	18.5	-------	-------
-------	-------	14.08	29.7
14.44	20.8	-------	-------
-------	-------	14.95	12.9

Table 5.8 continued…

ZP1		Form Ω	
Position (°2θ)	**Intensity (I/I_0)**	**Position (°2θ)**	**Intensity (I/I_0)**
15.47	21.3	-------	-------
16.16	32.4	-------	-------
-------	-------	16.31	15.0
16.70	17.6	-------	-------
17.16	100.0	17.024	9.5
17.74	13.3	17.76	3.2
18.18	49.3	-------	-------
-------	-------	18.40	5.2
19.04	56.3	-------	-------
19.69	18.1	19.68	100.0
20.10	17.9	-------	-------
20.38	32.1	20.46	35.6
21.11	27.1	-------	-------
-------	-------	21.39	9.4
21.71	20.6	-------	-------
22.21	15.2	22.24	5.3
22.70	44.1	-------	-------
23.62	59.5	23.72	26.5
-------	-------	24.44	8.7
24.63	21.0	-------	-------
24.87	40.1	-------	-------
25.49	26.9	-------	-------
-------	-------	25.87	48.7
26.22	8.4	-------	-------
27.64	16.8	27.51	14.7
27.97	16.1	-------	-------
28.60	16.8	28.58	31.0
29.04	13.4	-------	-------
29.69	12	-------	-------
30.57	7.9	30.46	13.9
-------	-------	30.78	15.0
31.37	12	-------	-------
-------	-------	31.53	8.2
32.77	7.9	-------	-------

Table 5.9 Thermal behaviour of ZP1 and form Ω

Event	ZP1	Form Ω
Desolvation peak	111.32°C	Absent
% mass loss (TGA)	22.08%	Insignificant (0.19%)

Table 5.10 The main absorptions in the IR spectra of ZP1 and form Ω

ZP1	Form Ω
Wavenumber (cm^{-1})	Wavenumber (cm^{-1})
-------	3737
3676	-------
-------	3329
3292	-------
-------	3061
-------	2960
-------	2891
2866	-------
	2813
2461	-------
1758	-------
-------	1720
-------	1618
1581	-------
-------	1556
-------	1509
1459	1462
-------	1439
-------	1391
1360	1350
1321	1326
-------	1302
1280	1277
-------	1242
1223	-------
1183	1185
1145	1154
1114	1115
1093	-------
-------	1075
1057	1059
-------	1044
-------	1030
999	999
937	942
897	908
-------	886
-------	870
846	848
-------	834
822	821
800	806
773	779
733	735
-------	701
-------	675
667	667
652	650
592	594
574	573
538	545
-------	524
512	-------

Table 5.10 continued…

ZP1	Form Ω
Wavenumber (cm^{-1})	Wavenumber (cm^{-1})
-------	503
487	485
-------	472
453	451
-------	438
424	-------

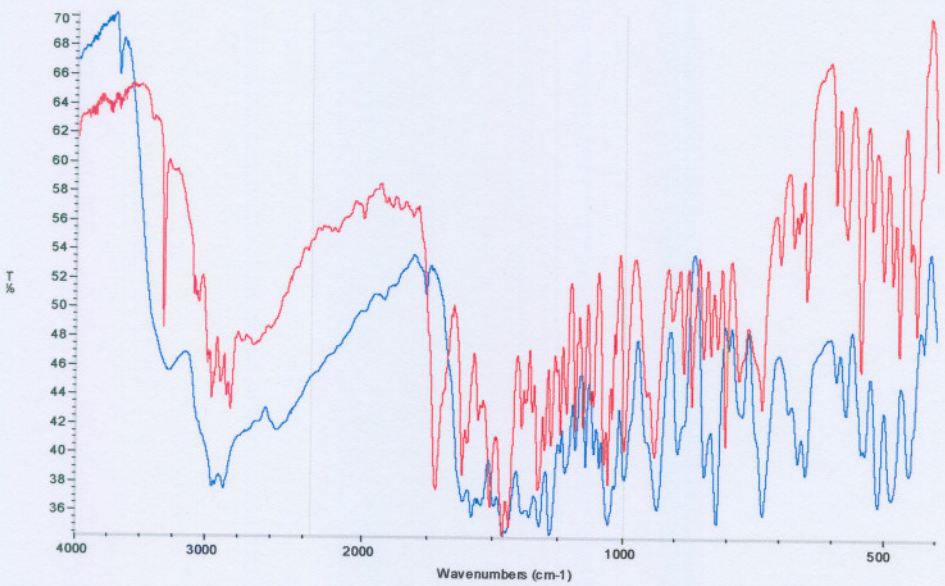

Figure 5.12 Superimposed IR spectra of ZP1 and form Ω.

From these discriminating results, it is clear that form ZP1 differed significantly from its dried product. The thermal event (melting) of form Ω as seen in the DSC thermogram (figure 5.10) was confirmed by HSM. Hexagonal plate-like crystal can be seen in table 5.11.

Table 5.11 Photomicrographs of the HSM events observed for form Ω

Photomicrograph	Observation	Temperature (°C)
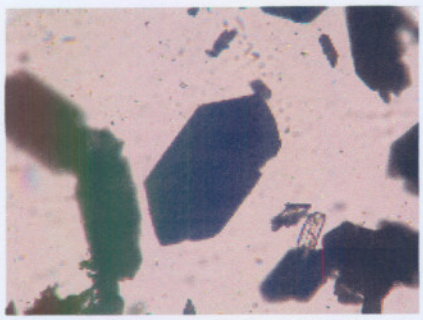	Initial.	25
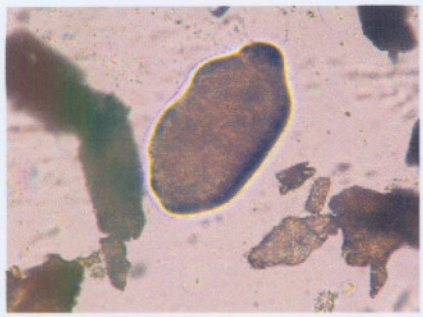	Melting started.	182
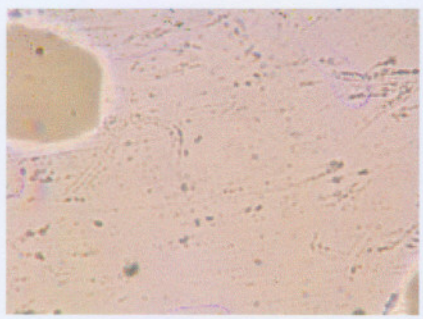	Melting process of crystals complete.	186

5.2 Recrystallisation products from other organic solvents

In this section the physico-chemical properties and behaviour of gatifloxacin crystals recrystallised from THF, ethyl acetate and dichloromethane as solvents will be discussed.

5.2.1 Recrystallisation of gatifloxacin using THF as solvent

The recrystallisation product from THF was removed from the mother solution (THF) and dried on filter paper for 2½ hours at ambient conditions prior to analysis.

XRPD, TGA, KF and DSC results were used to compare this crystal form to previously described crystal forms. According to Niddam-Hildesheim *et al.* (2004a:1-55) form J is formed by recrystallisation using iso-propanol, 1-buthanol, acetone, THF or methyl ethyl acetate as solvent. The XRPD pattern of the THF recrystallisation product in this study reflected diffraction peaks comparable to that in literature for form J (6.7, 11.3, 13.8 and 16.4 ±0.2 °2θ). The innovators of form J claimed that this form was obtained from THF recrystallisation as a THF solvate. There was however little information regarding the physico-chemical properties of form J. The results obtained in this study differed to those of the available data on form J (except for the XRPD pattern), but the obtained form was nevertheless considered to be form J.

VT-XRPD patterns of the crystals obtained revealed significant changes throughout the analysis (25-180°C). The XRPD pattern at 25°C revealed peaks with low intensities except for one prominent peak at 16.45 °2θ. This crystal lattice seemed to remain stable from 25°C to 85°C, except for the increase in the intensity of the peak present at 6.31 °2θ. Between 85°C and 95°C significant differences were observed. The peak at 6.31 °2θ disappeared, peaks at 7.72, 10.20, 12.75-14.92 and 20.4-24.38 °2θ appeared and the intensities of the peaks between 26-28 °2θ increased. The 100% peak (peak of maximum intensity) at 16.45 °2θ also diminished to one of the smaller peaks at 95°C. No significant changes were observed from 95-170°C. The absence of an XRPD pattern obtained at

180°C was anticipated to represent that of the sample during the melting process. The VT-XRPD of form J is illustrated in figure 5.13.

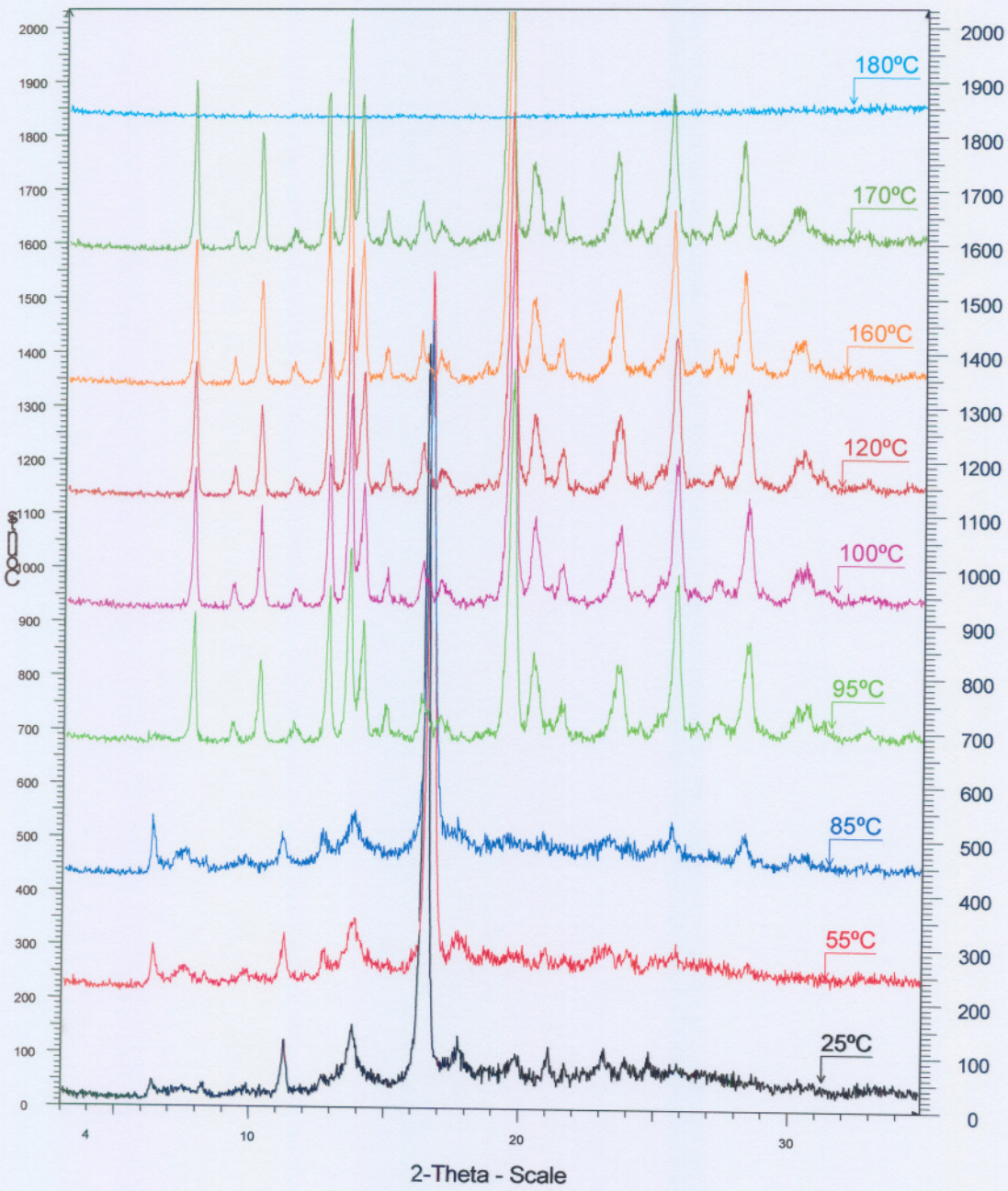

Figure 5.13 Overlay of the VT-XRPD patterns of form J at temperatures ranging from 25-180°C.

The DSC thermogram (figure 5.14) revealed a desolvation endotherm at 100.43°C followed by a recrystallisation exotherm at 102.77°C. These two peaks (indicative of desolvation) confirmed the changes observed in the XRPD patterns at 85-95°C. The small difference in temperature (VT-XRPD vs. DSC observations) may be attributed to the sample being exposed to the prolonged increase in temperature during the VT-XPRD analysis. The DSC thermogram also revealed a final melting point of 188.21°C, which concurred with the XRPD observations at 180°C.

HSM observations of form J confirmed all the thermal events present in the DSC thermogram (fig. 5.14). An interesting observation was made at 101°C. The endotherm at 100.43°C seemed to be two overlapping events (desolvation and melting). HSM also revealed that the small endotherm at 177.57°C and the small exotherm at 179.07°C represented melting followed by a rapid recrystallisation (also seen in the DSC thermogram). This behaviour was found to be similar to that of ZP0 (section 5.1.1). The HSM events of form J can be seen in table 5.12.

Table 5.12 Photomicrographs of the HSM events observed for form J

Photomicrograph	Observation	Temperature (°C)
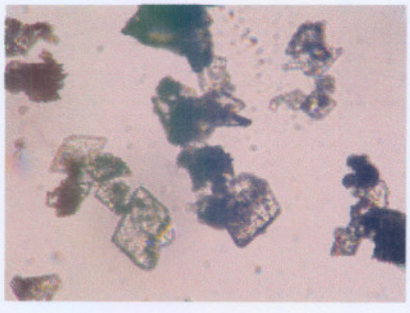	Initial.	25

Table 5.12 **continued...**

Photomicrograph	Observation	Temperature (°C)
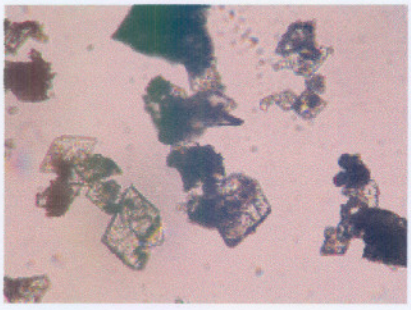	Darkening of crystals occurred.	90
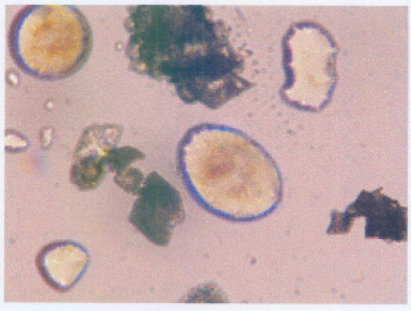	Desolvated crystals melted at 101°C.	101
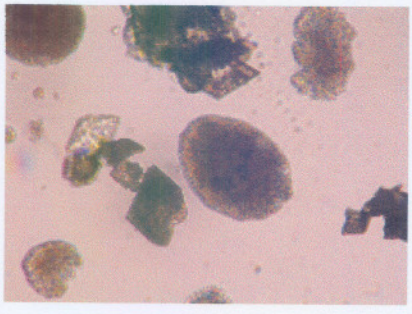	Recrystallisation of the melt occurred at 111°C to form a recrystallisation product (A).	111

Table 5.12 continued…

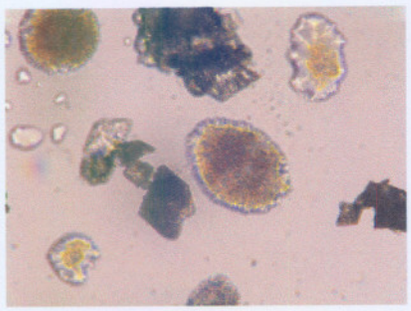	Melting of recrystallised product (A).	160
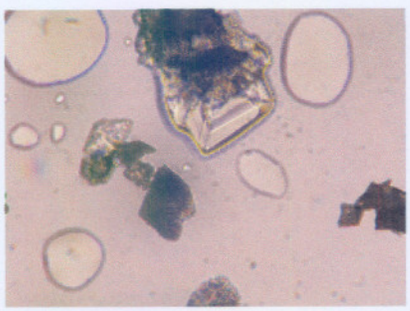	Melt from product A recrystallised at 164°C to form recrystallisation product B.	164
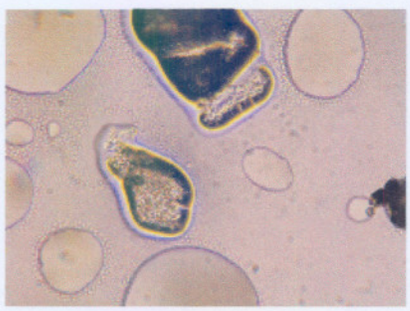	Melting of recrystallised product B.	183
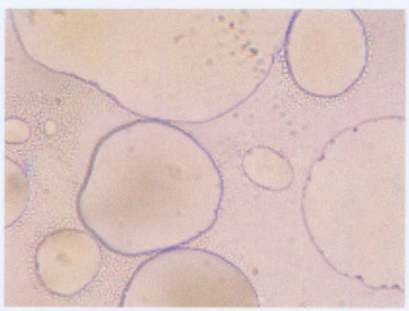	Melting of recrystallision product B completed.	188

The TGA revealed a total mass loss of 10.10% in two steps of 4.10% and 6.00% respectively, KF revealed a total moisture content of 6.28%. The DSC and TGA thermograms are illustrated in figure 5.14 and 5.15 respectively.

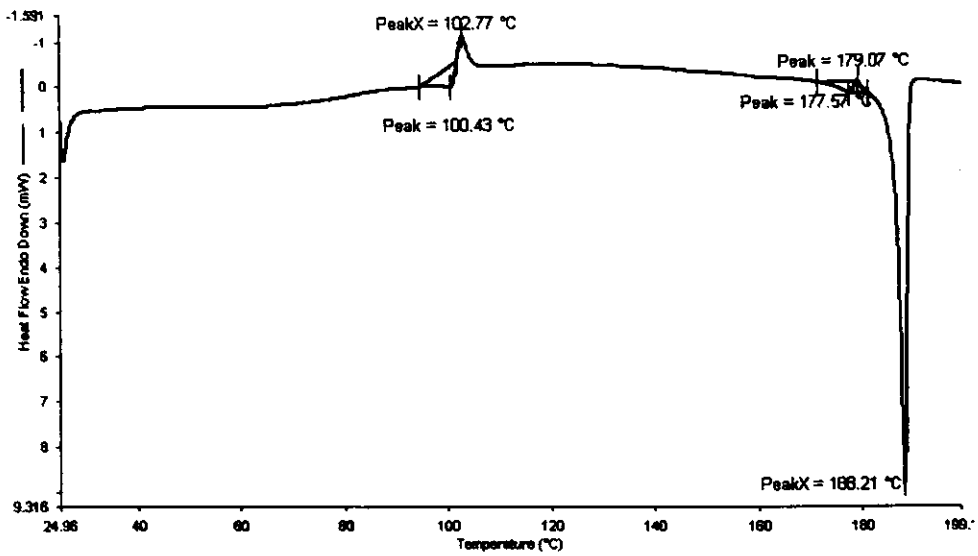

Figure 5.14 DSC thermogram of form J.

The first step in the TGA suggested the desolvation of THF while the second step suggested the dehydration process. The boiling point of THF being 66.0°C supported the first step to be the loss of THF, while the boiling point of water (100.0°C) supported the second step to be dehydration. It can thus be concluded that form J might be a *solvated hydrate*.

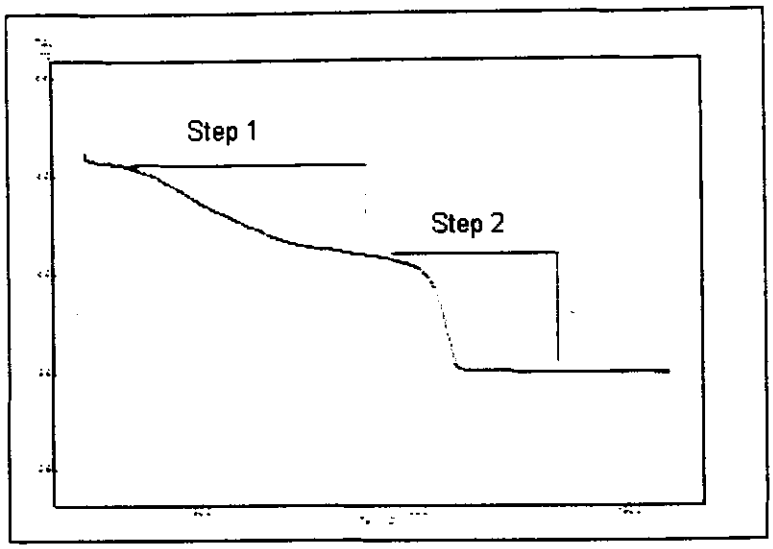

Figure 5.15 TGA thermogram of form J.

Dahl *et al.* (1989:605) reported similar behaviour for triamterene, which incorporated DMF and water in its crystal lattice. The crystal lattice of the triamterene·DMF·H_2O solvated hydrate is illustrated in figure 5.16.

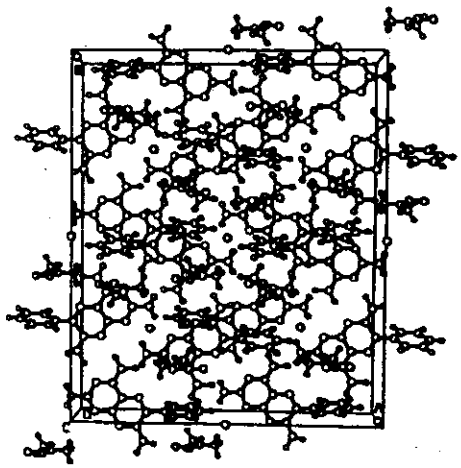

Figure 5.16 Crystal lattice of the triamterene·DMF·H_2O solvated hydrate (Dahl *et al.*, 1989:605).

The calculated TGA weight loss for THF for a mono-THF solvated form of gatifloxacin is 16.11%. No HSM observations were made between 20-90°C (the temperature range of step 1- THF desolvation), indicating that form J is more likely to be a hydrated form with

some surface THF. However the exact status (adsorbed on the surface or incorporated into the lattice) is not known, but might be clarified by means of single x-ray crystallography. The water content of 6.28% and the second step in the TGA suggested that form J might be a sesquihydrated form of gatifloxacin possessing some surface THF.

Form J was thereafter dried at 110°C for 12 hours. The dried form obtained revealed the anticipated XRPD pattern of the dehydrated form of form J. A slight shift in the °2θ positions of the main peaks were observed. This shift might have been due to the possible differences in powder bed height. The 180°C XRPD pattern represented the melting process of the sample. The VT-XRPD patterns are shown in figure 5.18.

According to Niddam-Hildesheim *et al.* (2004a:1-55) form J transforms into form Ω when heated between 90-170°C (preferably at 120°C). The results obtained for the dried form J (in this study) revealed similarities to that of form Ω, but more resemblances to anhydrous form I, and was thus considered as form I. Form I was invented by Reddy *et al.* (2003:1-21) and described in patent WO 03/086402 which provided comprehensive data (XRPD, DSC, TGA, KF, IR) on form I. The XRPD diffraction peak values can be seen in table 5.13.

Table 5.13 XRPD peak listing of form I anhydrous as described by Reddy *et al.* (2003:1-25)

Form I anhydrous	
Position (°2θ)	**Intensity (I/I_0)**
7.76	100.0
10.20	26.8
12.85	71.7
13.62	89.3
14.11	29.3
14.93	9.8
16.33	12.2
17.01	7.2
19.72	100.0
20.49	35.2

Table 5.13 **continued...**

Form I anhydrous	
Position (°2θ)	**Intensity (I/I_0)**
21.46	9.7
23.59	15.1
23.77	14.9
24.44	3.7
25.93	71.9
27.56	10.9
28.65	40.9
30.50	8.4
30.87	6.7
31.48	5.6

The moisture content determined by KF of form I was 0.4%, the total weight loss was 0.6% by TGA and the melting point was 188.35°C (DSC). The IR spectrum of form I anhydrous is displayed in figure 5.17 (Reddy *et al.*, 2003:1-21).

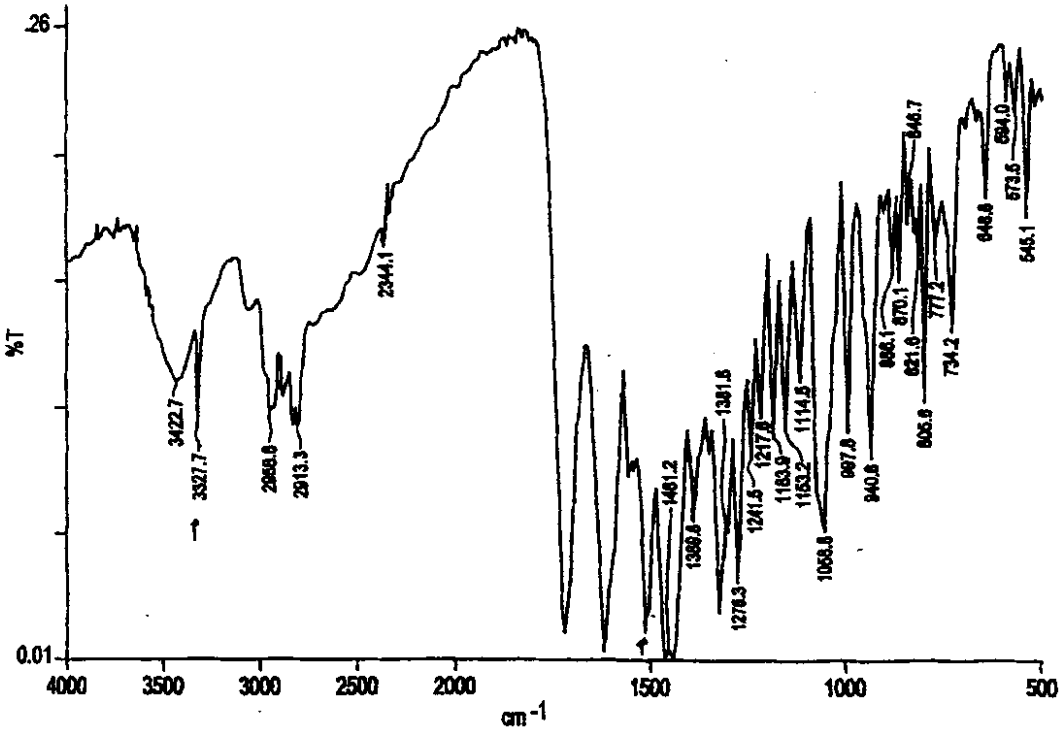

Figure 5.17 IR spectrum of form I anhydrous Reddy *et al.* (2003:3).

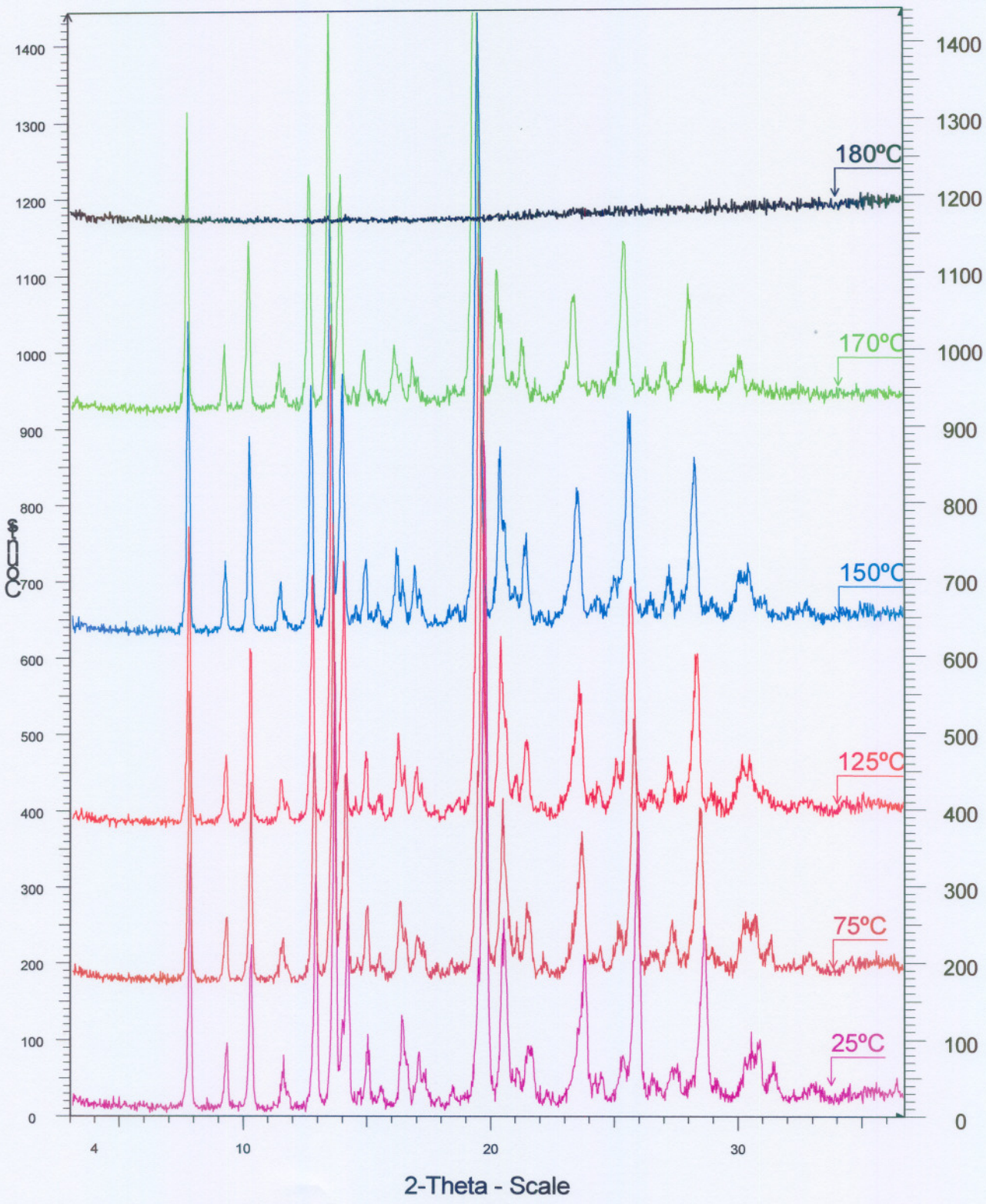

Figure 5.18 Overlay of the VT-XRPD patterns of form I at temperatures ranging from 25-180°C.

The DSC thermogram of form I anhydrous (figure 5.19) revealed a sharp meting endotherm at 188.26°C. The anticipated melting endotherm (at 177.57°C) and recrystallisation exotherm (at 179.56°C) as seen in the DSC thermogram of form J were not observed in the DSC thermogram of form I anhydrous. A possible reason for this phenomenon is that the desolvated form J transformed to a more thermodynamically stable form due to the prolonged exposure to heat (drying procedure). The sharp endotherm at 188.26°C confirmed the absence of peaks in the XRPD diffractogram at 180°C to be indicative of the melting of the sample.

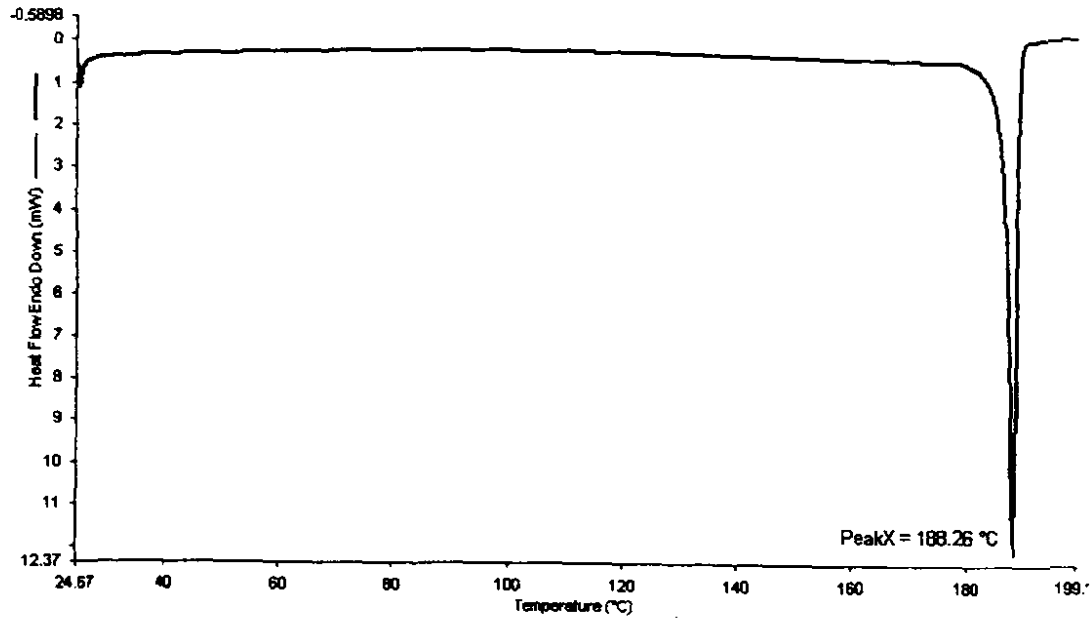

Figure 5.19 DSC thermogram of form I anhydrous.

TGA revealed a total mass loss of 0.368% and the KF revealed a moisture content of 0.271%. Both of these values can be considered as insignificant. The TGA thermogram can be seen in figure 5.20.

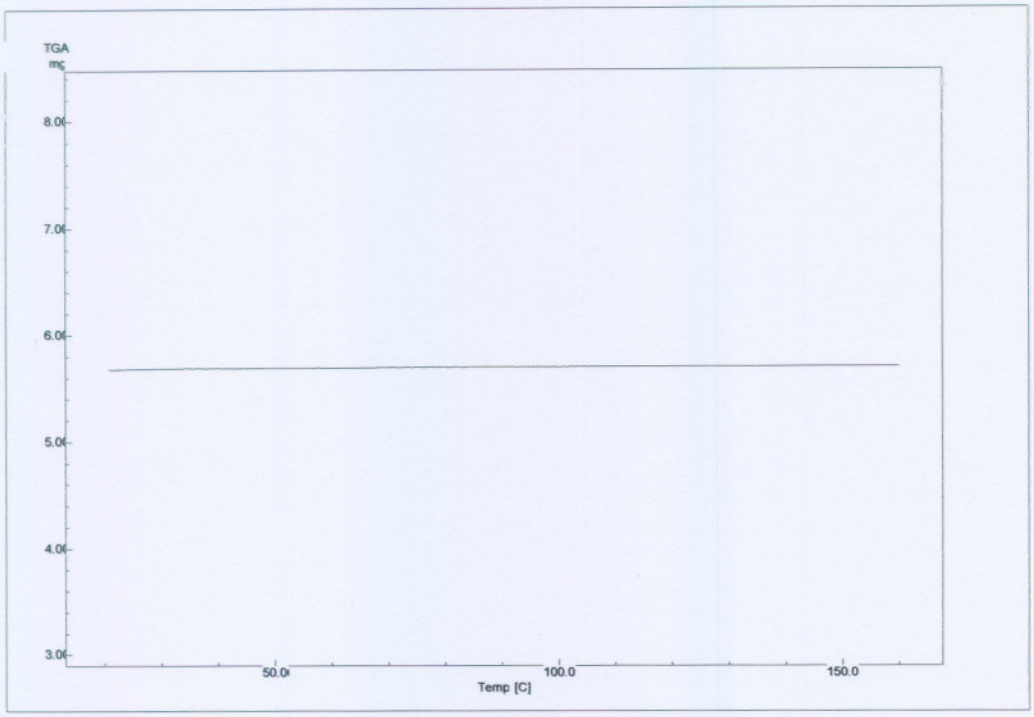

Figure 5.20 TGA thermogram of form I anhydrous.

HSM event observation concurred with the thermal behaviour of form I. These events are discussed in table 5.14.

Table 5.14 Photomicrographs of the HSM events observed for form I anhydrous

Photomicrograph	Observation	Temperature (°C)
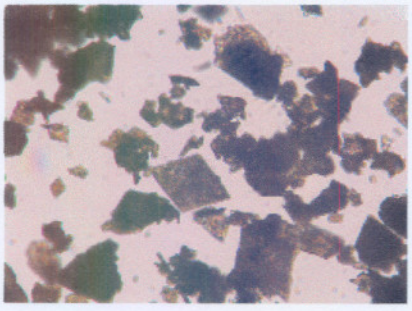	Initial.	25

Table 5.14 continued…

Photomicrograph	Observation	Temperature (°C)
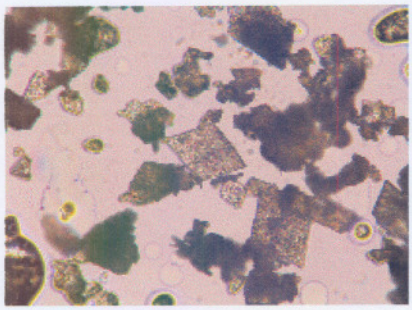	Melting started.	180
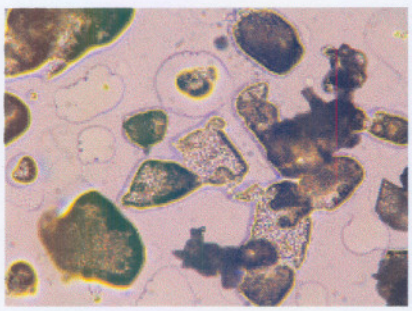	Melting.	186
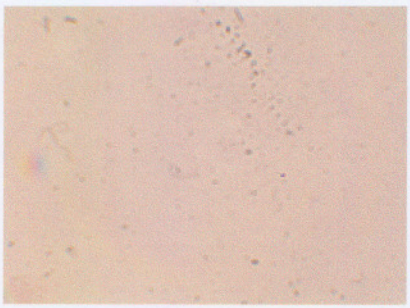	Melting completed.	189

To distinguish between the hydrated form J and the dehydrated form (form I) one may use XRPD (table 5.15), DSC, TGA (table 5.16) and IR (table 5.17 and figure 5.21).

Table 5.15 XRPD peak position (°2θ) and relative peak intensities of J and form I

Form J		Form I anhydrous	
Position (°2θ)	Intensity (I/I_0)	Position (°2θ)	Intensity (I/I_0)
6.31	3.2	-------	
-------		7.76	38.9
8.19	2.8	-------	
-------		9.25	10.5
-------		10.22	25.1
11.25	8.5	-------	
-------		11.54	8.7
12.66	4.0	-------	
-------		12.87	35.6
13.76	10.7	13.63	67.1
-------		14.15	30.2
-------		14.63	3.3
-------		14.97	11.8
-------		15.51	4.2
16.45	100.0	16.40	13.9
-------		17.04	9.2
-------		17.28	6.0
17.72	9.3	17.83	2.6
-------		18.41	4.3
19.86	7.0	19.75	100.0
-------		20.50	29.0
21.08	8.0	21.07	6.8
-------		21.50	10.1
21.73	5.9	-------	
-------		22.26	3.6
23.16	7.9	-------	
-------		23.78	23.6
24.00	6.8	-------	
-------		24.47	6.2
24.86	7.5	-------	
-------		25.34	8.7
-------		25.94	42.1
-------		26.58	5.4
-------		27.36	7.0
-------		27.51	6.3
28.26	4.6	-------	
-------		28.64	27.9
-------		30.38	7.5
-------		30.54	12.2
-------		30.88	11.1
-------		31.45	7.8
32.58	3.4	-------	

Table 5.16 Thermal behaviour of form J and form I (anhydrous)

Event	Form J	Form I (anhydrous)
Dehydration and melting overlapping endotherm	100.27°C	Absent
Recrystallisation exotherm	102.60°C	Absent
Melting endotherm	177.57°C	Absent
Recrystallisation exotherm	179.56°C	Absent
Total mass loss (TGA)	10.1% (two steps)	Insignificant (0.368%)

Table 5.17 The main absorptions in the IR spectra of form J and form I anhydrous

Form J	Form I
Wavenumber (cm^{-1})	Wavenumber (cm^{-1})
3676	-------
3408	-------
-------	3329
-------	3273
-------	3098
-------	3082
-------	2960
-------	2893
2875	-------
-------	2813
-------	1999
-------	1720
1617	1617
--------	1509
-------	1489
1449	-------
1392	1391
1319	1327
1277	1277
-------	1242
1208	1218
1181	1185
1144	1154
1115	1115
-------	1060
1094	-------
1056	------
996	997
940	941
887	909
-------	886

Table 5.17 continued…

Form J Wavenumber (cm^{-1})	Form I Wavenumber (cm^{-1})
-------	870
844	848
-------	834
822	821
-------	805
773	779
734	734
-------	701
-------	675
-------	661
-------	650
-------	594
-------	574
545	546
513	524
487	503
-------	485
-------	472
449	438
429	-------

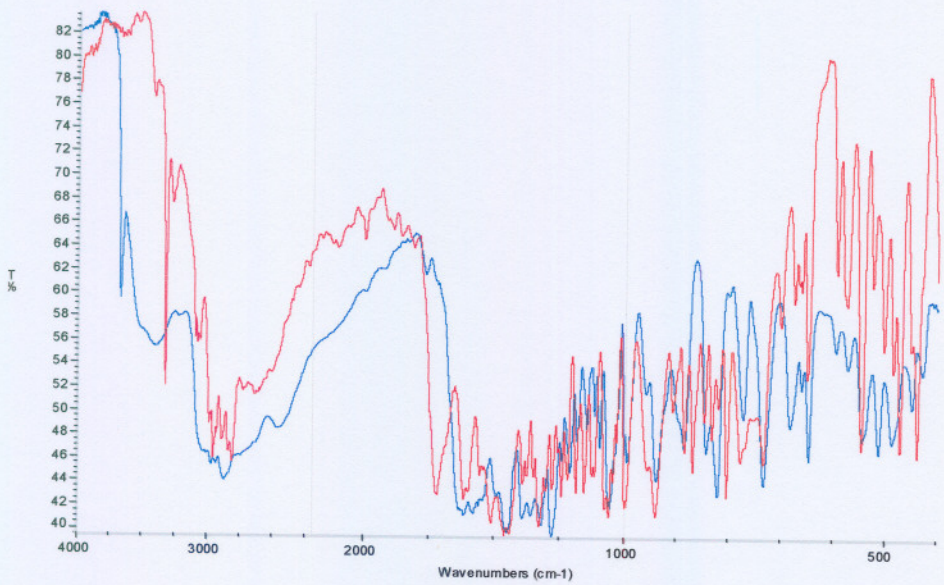

Figure 5.21 Superimposed IR spectra of form J and form I anhydrous.

5.2.2 Recrystallisation of gatifloxacin using ethyl acetate as solvent

The recrystallisation product from ethyl acetate was removed from the solvent and dried on filter paper for 1 hour at ambient conditions prior to analysis.

The results obtained from this recrystallisation product did not resemble any previously described forms. Therefore this recrystallisation product was dubbed ZP2.

A VT-XRPD study ranging from 25-180°C was conducted and the results are illustrated in figure 5.22.

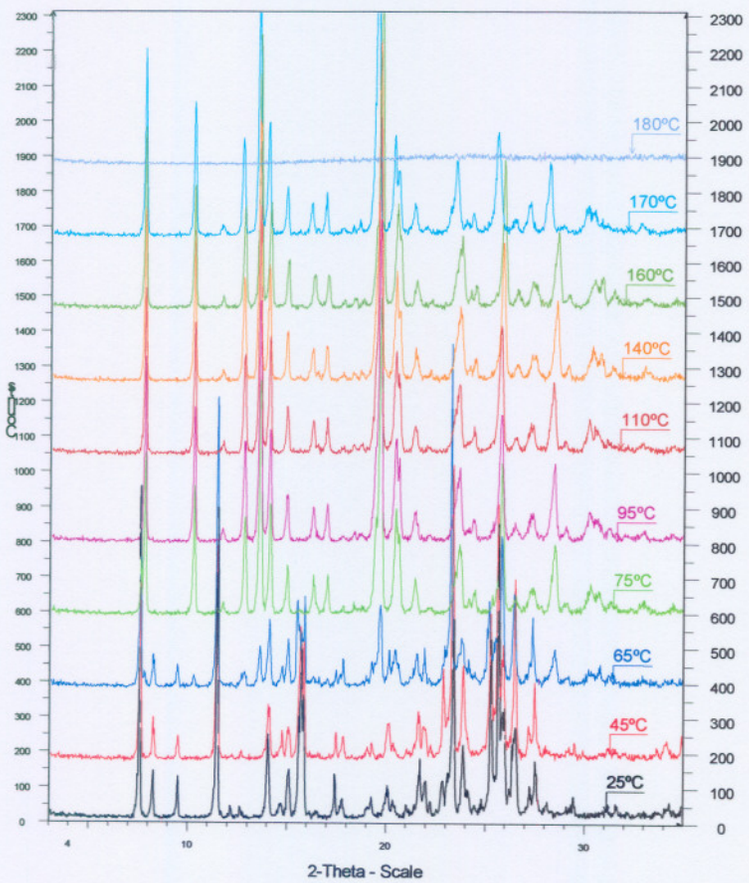

Figure 5.22 Overlay of the VT-XRPD patterns of form ZP2 at temperatures ranging from 25-180°C.

The XRPD pattern at 25°C revealed various high intensity diffraction peaks, which are characteristic of crystalline powders. No significant differences were observed in the XRPD patterns from 25 to 45°C. Significant differences were observed between the XRPD patterns obtained at 45°C and 65°C, i.e. the appearance of peaks at 10.19, 13.54, 15.78, 19.63 and 28.46 °2θ, and the increased intensity of peaks at 12.61 and 23.38°2θ. The peak at 23.90°2θ decreased in intensity. More differences were observed between the XRPD patterns obtained at 65°C and 75°C. These differences included the disappearance of peaks at 8.15, 9.37, 11.36, 14.67, 15.47, 15.78, 21.88 and 23.79 °2θ, the appearance of peaks at 16.23 and 16.93 °2θ. Peaks at 10.20, 12.76, 13.53, 14.05, 19.62 and 28.46 °2θ indicated an increase in the relative intensity count thereof. The remainder of the VT-XRPD analysis (75-170°C) revealed no significant differences. The absence of peaks in the XRPD recording at 180°C indicated the melting of this form.

The DSC thermogram of ZP2 (figure 5.23) revealed an endotherm with a peak maximum at 85.91°C and a sharp endotherm at 190.30°C. The total mass loss revealed by the TGA thermogram was 10.08%. The onset and endset temperatures of the desolvation process illustrated in the TGA thermogram were 79.40°C and 89.65°C respectively. The desolvation temperature compared to the boiling point of ethyl acetate (77.0°C) and the desolvation endotherm observed at 85.91°C. The endotherm observed at 190.30°C indicated the melting of the crystals and supported the observation in the XRPD pattern at 180°C. The superimposed DSC and TGA thermograms are illustrated in figure 5.23.

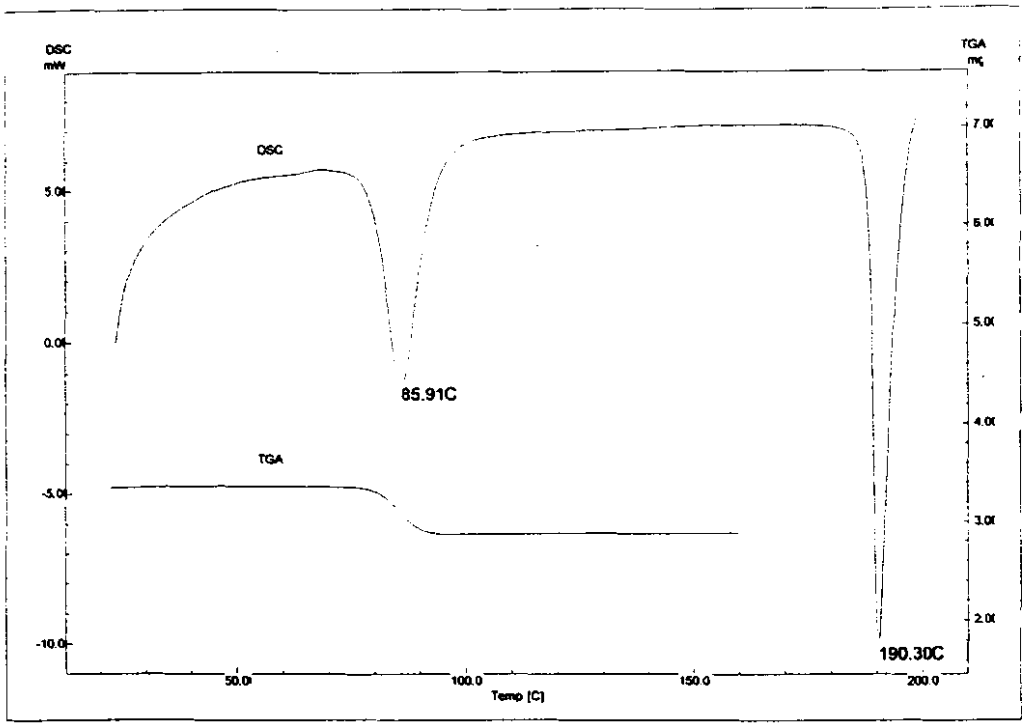

Figure 5.23 Superimposed DSC and TGA thermograms of ZP2.

KF analysis revealed a total moisture content of 0.52%. The total mass loss of 10.08% observed in the TGA thermogram can therefore be attributed to the desolvation of the ethyl-acetate which was incorporated into the lattice. The theoretical ethyl acetate content for a mono-ethyl acetate solvate is 23.41%, ZP2 may therefore be classified as a hemi-ethyl-acetate solvate of gatifloxacin.

The desolvation process and final melting point were also confirmed by HSM analysis (table 5.18).

Table 5.18 Photomicrographs of the HSM events observed for ZP2

Photomicrograph	Observation	Temperature (°C)
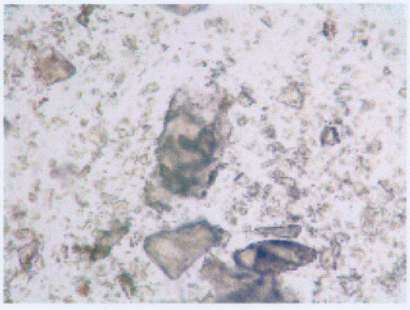	Initial.	25
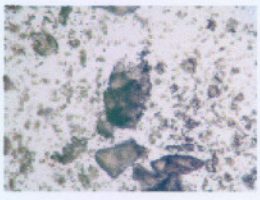	Darkening of crystals, which indicated the onset of the desolvation process.	88
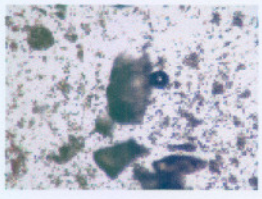	Bubble evolution started at 95°C and continued until ±101°C which indicated the desolvation process.	95
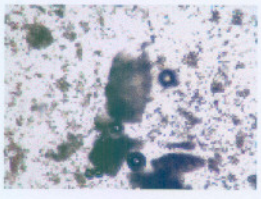		98
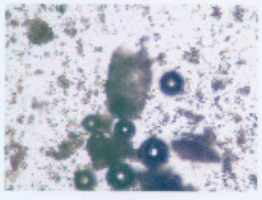		101

Table 5.18 continued…

Photomicrograph	Observation	Temperature (°C)
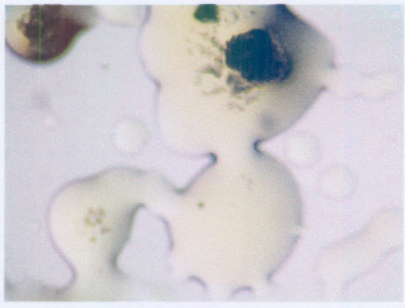	Melting of the sample was observed at 186°C.	186
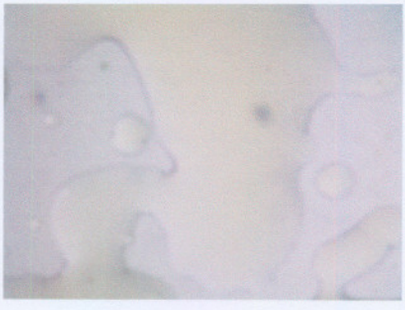	The melting of the sample was completed at 190°C.	190

ZP2 was thereafter dried at 100°C for 12 hours. The VT-XRPD patterns for the dried sample are illustrated in figure 5.24 and were similar to that of form Ω (dried product of ZP1). By drying form ZP1 or ZP2, form Ω can be prepared.

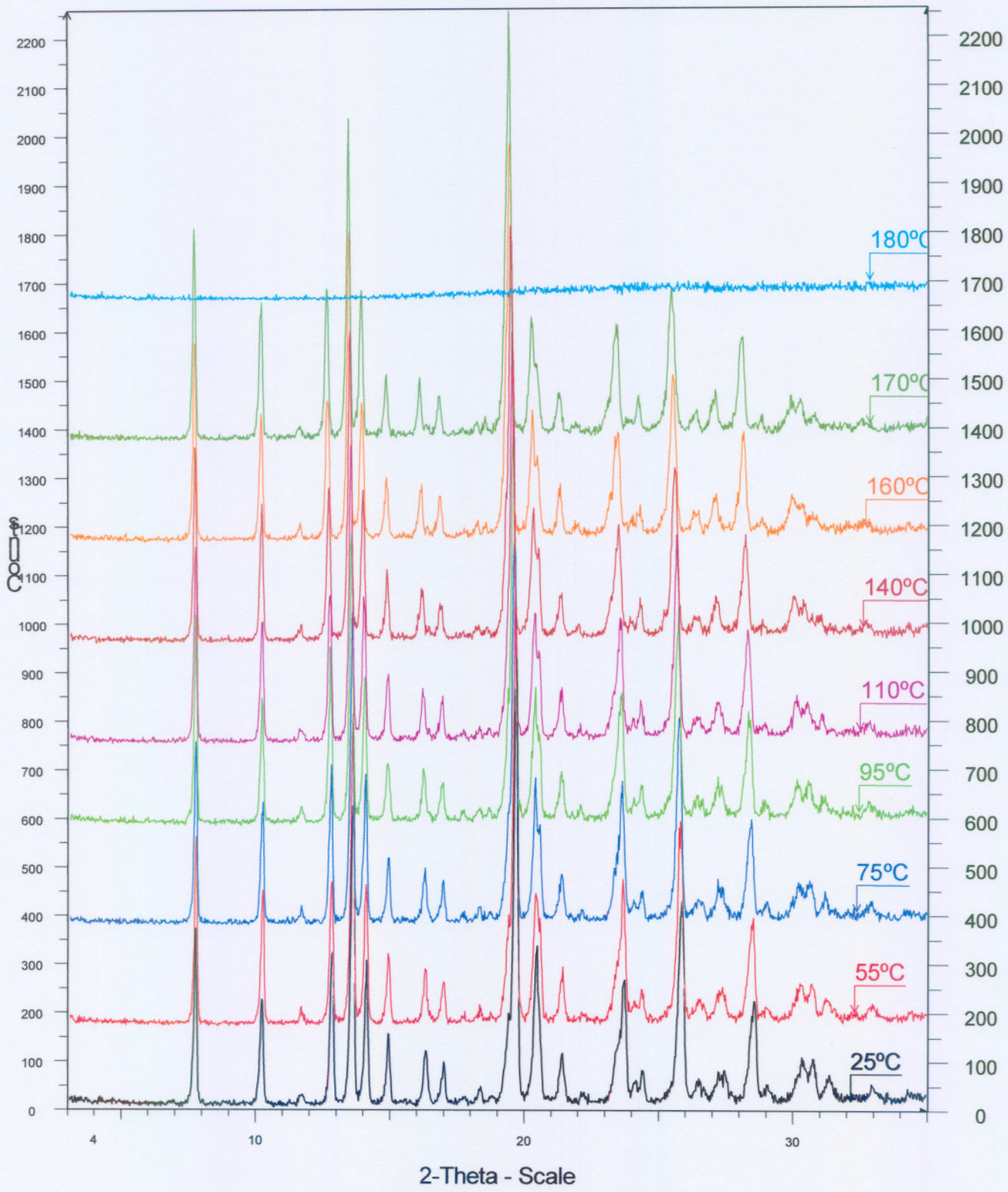

Figure 5.24 Overlay of the VT-XRPD patterns of form Ω (from ZP2) at temperatures ranging from 25-180°C.

From figure 5.24 it was observed that the XRPD patterns between 25°C and 170°C remained unchanged. The XRPD pattern of form Ω (from ZP2) was also compared to that of form Ω (dried product from ZP1). These two XRPD patterns were found to be comparable (figure 5.25).

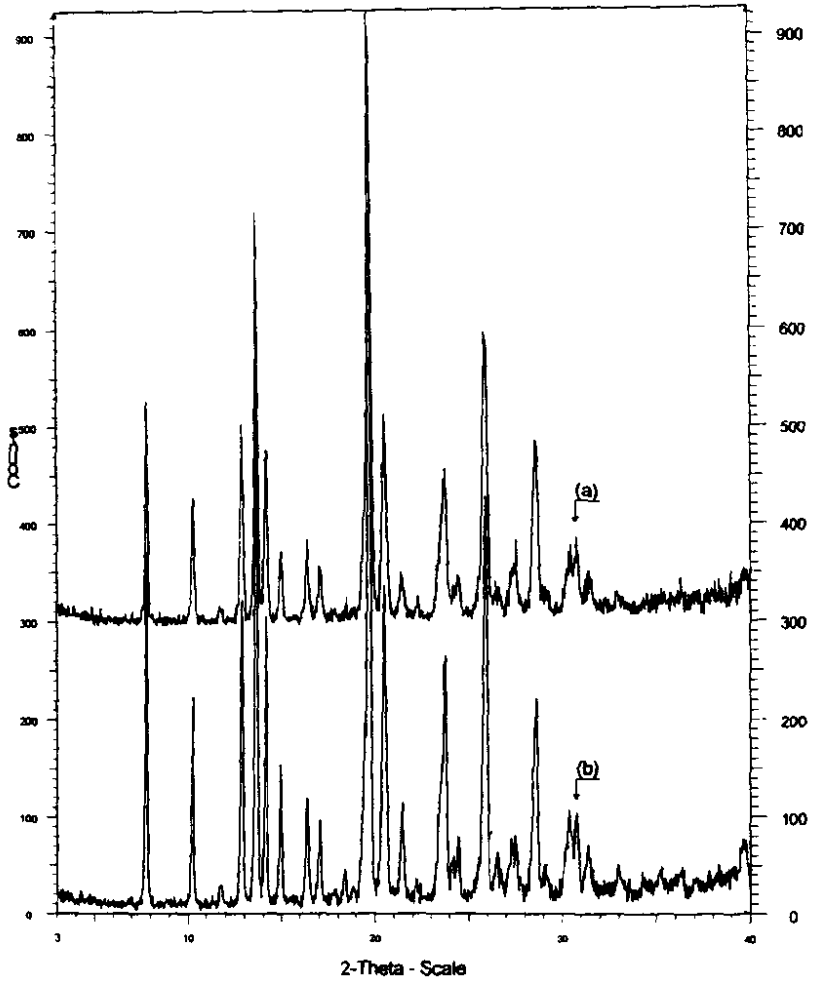

Figure 5.25 Superimposed XRPD patterns of form Ω from ZP1 (a) and form Ω from ZP2 (b).

The DSC thermogram revealed only one sharp endotherm at 190.51°C, which was comparable to the melting point of form Ω (from ZP1) (190.06°C). This indicated that the XRPD pattern at 180°C of form Ω (from ZP2) to be representative of the melting process of the sample.

The total mass loss observed from the TGA thermogram was 0.115% and the KF analysis revealed a moisture content of 0.56%. Both these values might be considered as insignificant and confirmed form Ω (from ZP2) to be free from any solvent or water. An overlay of the DSC and thermograms of Ω (from ZP2) is illustrated in figure 5.26.

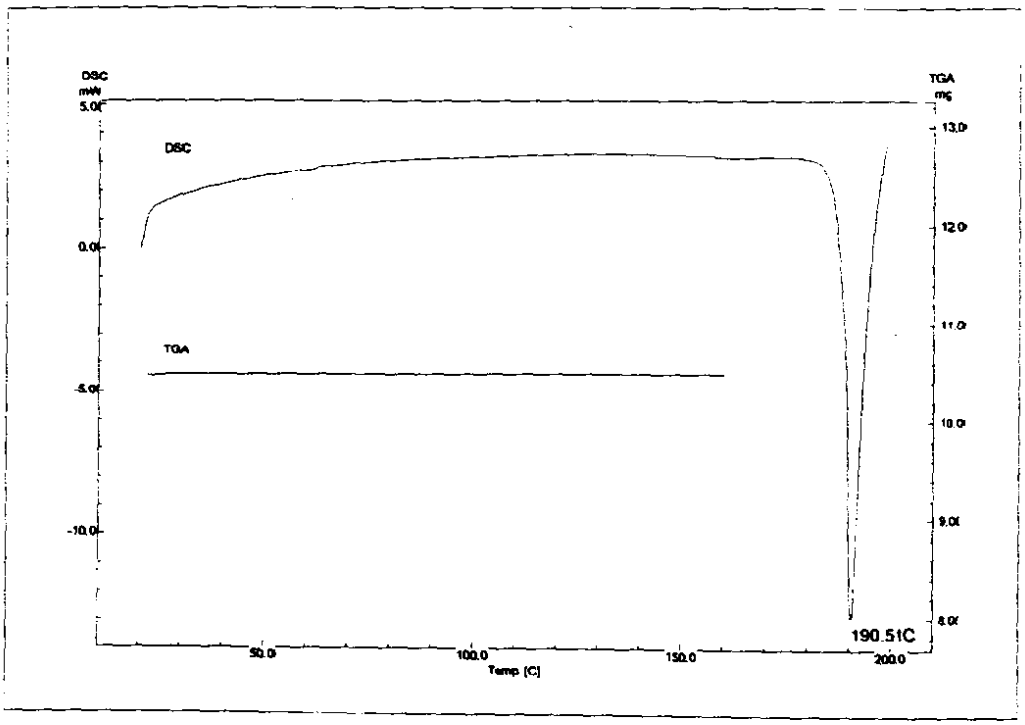

Figure 5.26 Superimposed DSC and TGA thermograms of form Ω (from ZP2).

The HSM events observed confirmed the thermal behaviour of form Ω (from ZP2) as observed in the DSC thermogram. These events are tabulated in table 5.19.

Table 5.19 Photomicrographs of the HSM events observed for form Ω (from ZP2)

Photomicrograph	Observation	Temperature (°C)
	Initial.	25
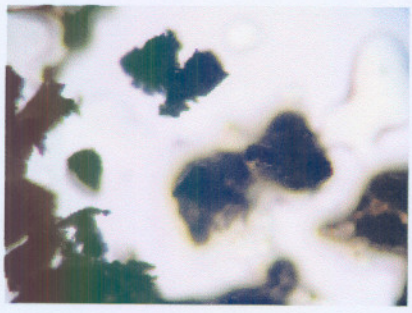	Melting process of the sample started.	185
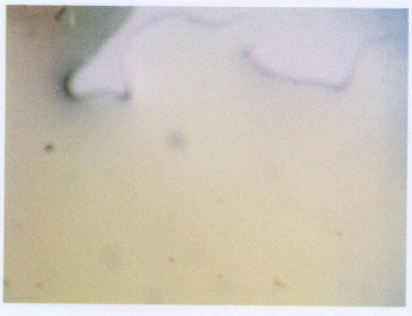	Melting completed.	189

To be able to distinguish between ZP2 and form Ω (from ZP2) a combination of the following techniques may be used: XRPD (table 5.20), thermal behaviour (table 5.21) and IR (table 5.22 and figure 5.27).

Table 5.20 XRPD peak position (°2θ) and relative peak intensities of form ZP2 and form Ω (from ZP2)

ZP2		Form Ω (from ZP2)	
Position (°2θ)	**Intensity (I/I_0)**	**Position (°2θ)**	**Intensity (I/I_0)**
-------	-------	6.78	1.5
-------	-------	7.69	40.0
7.53	100.0	-------	-------
8.17	14.8	-------	-------
9.45	13.1	-------	-------
-------	-------	10.17	24.1
11.44	93.7	-------	-------
-------	-------	11.66	2.8
12.12	4.5	-------	-------
12.61	4.2	-------	-------
-------	-------	12.80	34.7
-------	-------	13.57	67.3
14.01	25.8	14.10	32.8
14.65	5.3	-------	-------
15.04	15.4	14.92	16.5
15.69	51.3	-------	-------
-------	-------	16.31	12.7
16.47	2.8	-------	-------
-------	-------	16.97	10.3
17.39	14.0	-------	-------
17.76	6.8	17.77	2.6
-------	-------	18.35	4.8
-------	-------	18.80	2.8
19.10	4.4	-------	-------
19.25	7.3	19.35	18.1
-------	-------	19.67	100.0
20.06	10.7	-------	-------
20.35	6.5	20.45	36.1
21.04	5.1	-------	-------
-------	-------	21.39	12.2
21.69	18.7	-------	-------
21.95	11.6	-------	-------
22.21	6.1	22.17	3.1
22.82	12.1	-------	-------
23.38	60.5	23.45	13.5
-------	-------	23.72	28.5
23.90	22.8	-------	-------
24.15	9.3	24.13	5.8
-------	-------	24.43	8.4
24.83	7.0	-------	-------
25.29	54.4	-------	-------
25.68	89.0	-------	-------
25.90	32.9	25.86	46.0
26.52	28.1	26.52	6.7
27.25	10.8	27.28	8.2
27.55	18.1	27.50	8.5
28.13	6.2	-------	-------

Table 5.20 continued…

ZP2		form Ω (from ZP2)	
Position (°2θ)	Intensity (I/I_0)	Position (°2θ)	Intensity (I/I_0)
-------	-------	28.59	23.9
-------	-------	29.10	5.4
29.47	7.6	-------	-------
-------	-------	30.40	11.4
-------	-------	30.79	11.0
31.17	4.1	-------	-------
-------	-------	31.39	7.6
31.63	5.7	-------	-------
-------	-------	33.01	5.0
-------	-------	33.57	3.8
-------	-------	34.38	3.5

Table 5.21 Thermal behaviour of ZP2 and form Ω (from ZP2)

Event	ZP2	Form Ω (from ZP2)
Desolvation endotherm	Present at 85.91°C	Absent
Total mass loss (TGA)	10.08%	Insignificant (0.12%)

Table 5.22 The main absorptions in the IR spectra of ZP2 and form Ω (from ZP2)

ZP2	Form Ω (from ZP2)
Wavenumber (cm^{-1})	Wavenumber (cm^{-1})
-------	3737
3340	3330
3060	3061
2968	2960
2937	-------
-------	2891
2817	2813
1998	-------
1930	-------
1890	-------
1735	-------
-------	1720
1618	1618
1542	1556
1509	1510
1458	1462
-------	1439
1390	1391
1374	-------
-------	1350
1324	1326
1302	1302
1276	1277

Table 5.22 continued…

ZP2	Form Ω (from ZP2)
Wavenumber (cm^{-1})	Wavenumber (cm^{-1})
1243	1242
1222	1218
1187	1185
1152	1154
1123	1115
1070	1075
1053	1059
-------	1044
1024	1030
1001	999
970	-------
940	942
915	909
885	886
874	870
-------	848
830	834
817	821
807	806
776	779
731	735
704	701
675	675
667	667
648	650
634	-------
607	-------
589	594
574	573
548	545
524	524
501	503
486	485
469	472
453	451
437	438

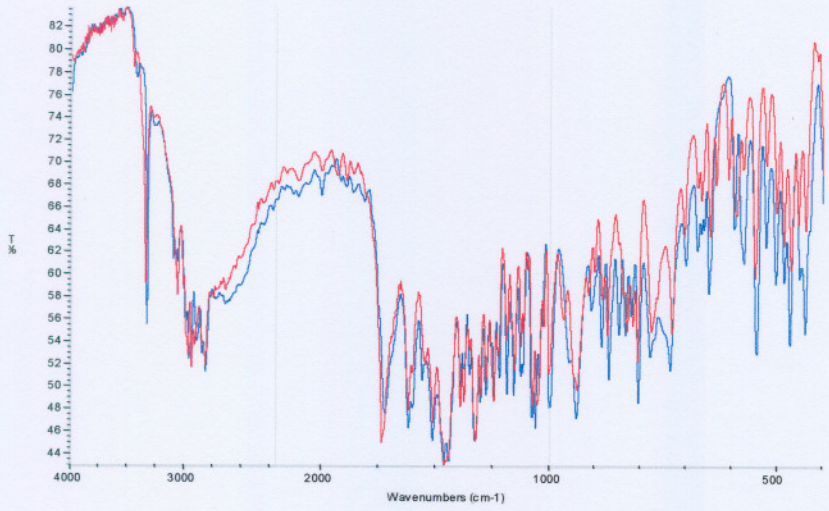

Figure 5.27 Superimposed IR spectra of ZP2 and form Ω (from ZP2).

5.2.3 Recrystallisation of gatifloxacin using dichloromethane as solvent

The gatifloxacin recrystallisation product from dichloromethane was removed from the solvent and dried on filter paper for 1½ hours at ambient conditions prior to analysis.

The results obtained for this recrystallisation product did not resemble any forms described in the literature and was dubbed ZP3.

An overlay of the VT-XRPD patterns for ZP3 is illustrated in figure 5.28.

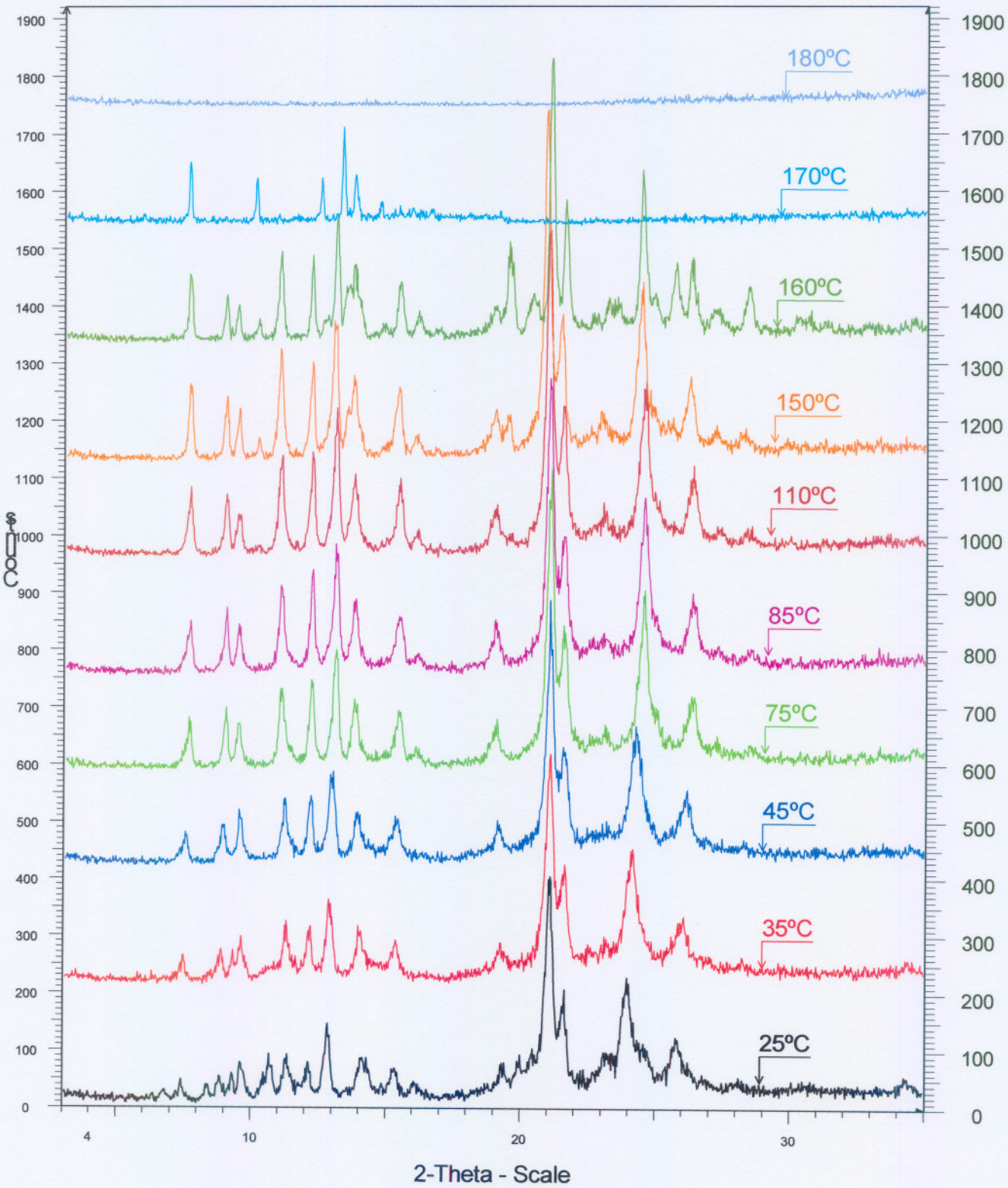

Figure 5.28 Overlay of the VT-XRPD patterns of ZP3 at temperatures ranging from 25-180°C.

Various significant differences were observed in the VT-XRPD patterns illustrated in figure 5.28. Between 25°C and 35°C two slight differences were observed at 10.67 and 16.01 2°θ (disappearance of peaks). From 30°C to 110°C peaks at 7.37 and 25.80 °2θ showed an increase in their intensities. Between 110°C and 150°C two peaks appeared at 10.13- and 19.49 °2θ. From 150°C to 160°C the increase in the intensities of two peaks at 21.05 and 28.42°2θ were observed. Only 6 relative weak peaks were observed for the XRPD pattern at 170°C. This XRPD pattern differed significantly from the XRPD pattern at 160°C. The XRPD pattern at 180°C represented the melting of the sample.

The DSC thermogram (figure 5.29) revealed a broad endotherm with a peak maximum at 65.86°C. Byrn *et al.* (1999:234) stated that it is not necessary that desolvation/dehydration correlate with the boiling point of the solvent. This statement made it possible to identify the broad endotherm (65.86°C) as desolvation/dehydration. An endotherm and exotherm were observed at 164.92°C and 167.91°C respectively. A final endotherm was observed at 187.71°C.

TGA analysis revealed a total weight loss of 6.74% that commenced at 30.00°C and terminated at 110.00°C, which verified the broad desolvation endotherm (56.86°C). This long desolvation process explains the changes observed in the XRPD patterns between 25°C and 110°C. KF moisture determination revealed a cumulative moisture content of 7.77%. The slight difference between the TGA and KF values may be regarded as insignificant, and therefore confirmed that ZP3 is a sesquihydrated form of gatifloxacin. The DSC and TGA thermograms are illustrated in figure 5.29.

HSM confirmed the observations from the DSC thermogram. The differences in XRPD patterns from 150°C-180°C might be attributed to these thermal events. The final endotherm at 187.71°C confirmed the XRPD pattern at 180°C which represented the melting of the recrystallised product.

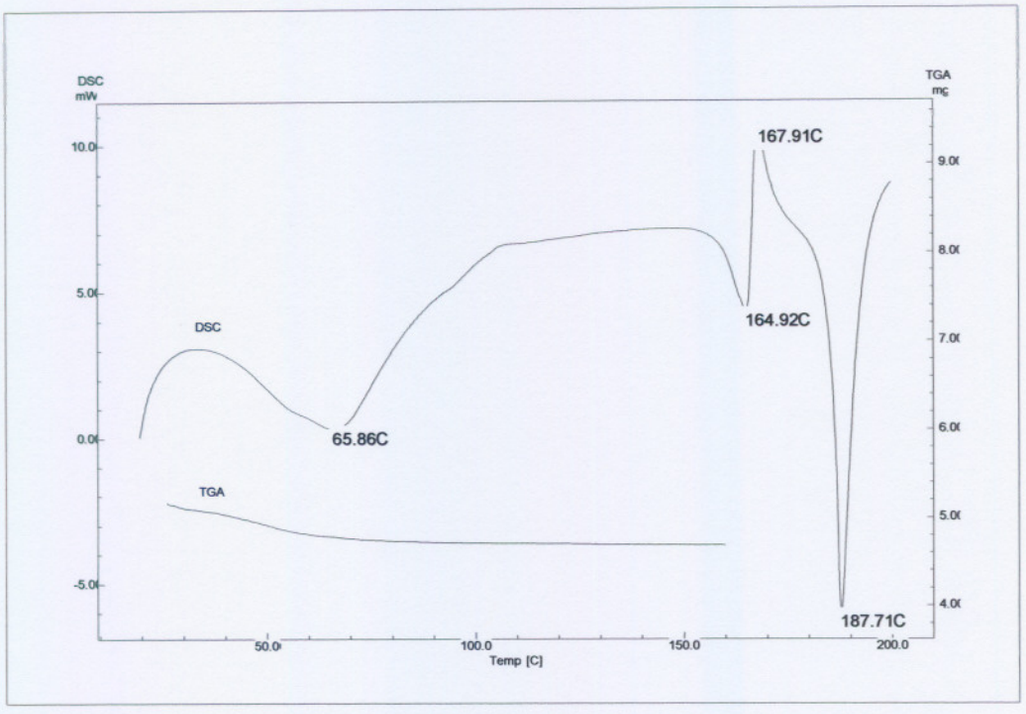

Figure 5.29 The DSC and TGA thermograms of ZP3.

HSM events of ZP3 concurred with the DSC and TGA thermograms. HSM events are illustrated in table 5.23.

Table 5.23 Photomicrographs of the HSM events observed for ZP3

Photomicrograph	Observation	Temperature (°C)
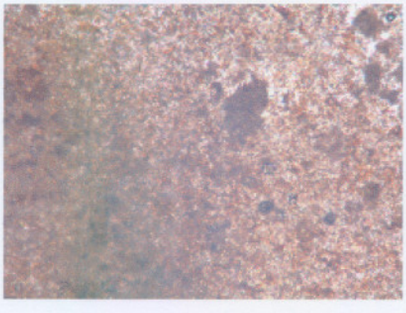	Initial.	25

Table 5.23 continued…

Photomicrograph	Observation	Temperature (°C)
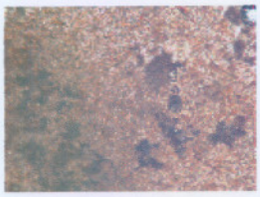	Darkening of crystals and bubble evolution confirmed the dehydration process.	61
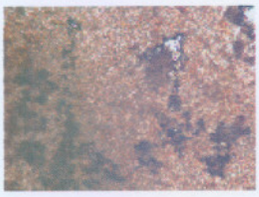		100
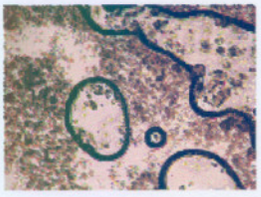		107
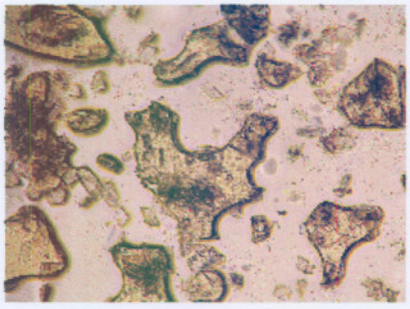	Melting of the sample occurred at 169°C.	169
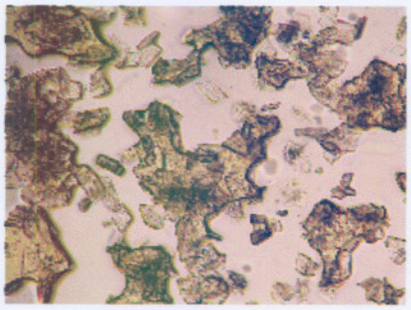	Recrystallisation from melt occurred at 172-175°C.	172-175

Table 5.23 continued…

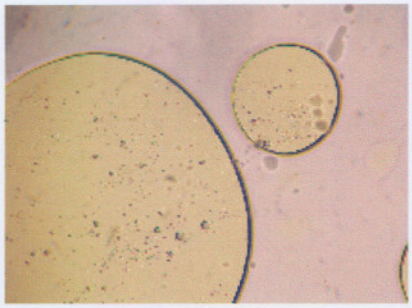	The recrystallised product melted at 184-189°C.	184-189

The slight differences in the temperatures for the various thermal events (i.e. desolvation, melting, recrystallisation etc.) observed in the DSC thermogram and the HSM photomicrographs can be attributed to the fact that the environmental conditions of these two techniques differed.

ZP3 was then dried for 12 hours at 110°C.

The XRPD pattern of the dried product of ZP3 resembled some characteristic XRPD peaks of previously described forms. It was however decided that none of these forms entirely matched the XRPD profile of the dried form of ZP3, therefore it was named ZP4.

The VT-XRPD patterns of the ZP4 can be seen in figure 5.30.

The initial XRPD pattern at 25°C (figure 5.30) revealed a XRPD pattern comparable to that of the pattern at 160°C from the VT-XRPD pattern of ZP3 (figure 5.30).

A slight difference in the XRPD patterns at 25 and 140°C was observed. The change observed was the disappearance and appearance of overlapping peaks in the range of 7.4-7.7°2θ. The XRPD pattern at 150°C could be attributed to melting. No change in the XRPD pattern was observed from 150-180°C.

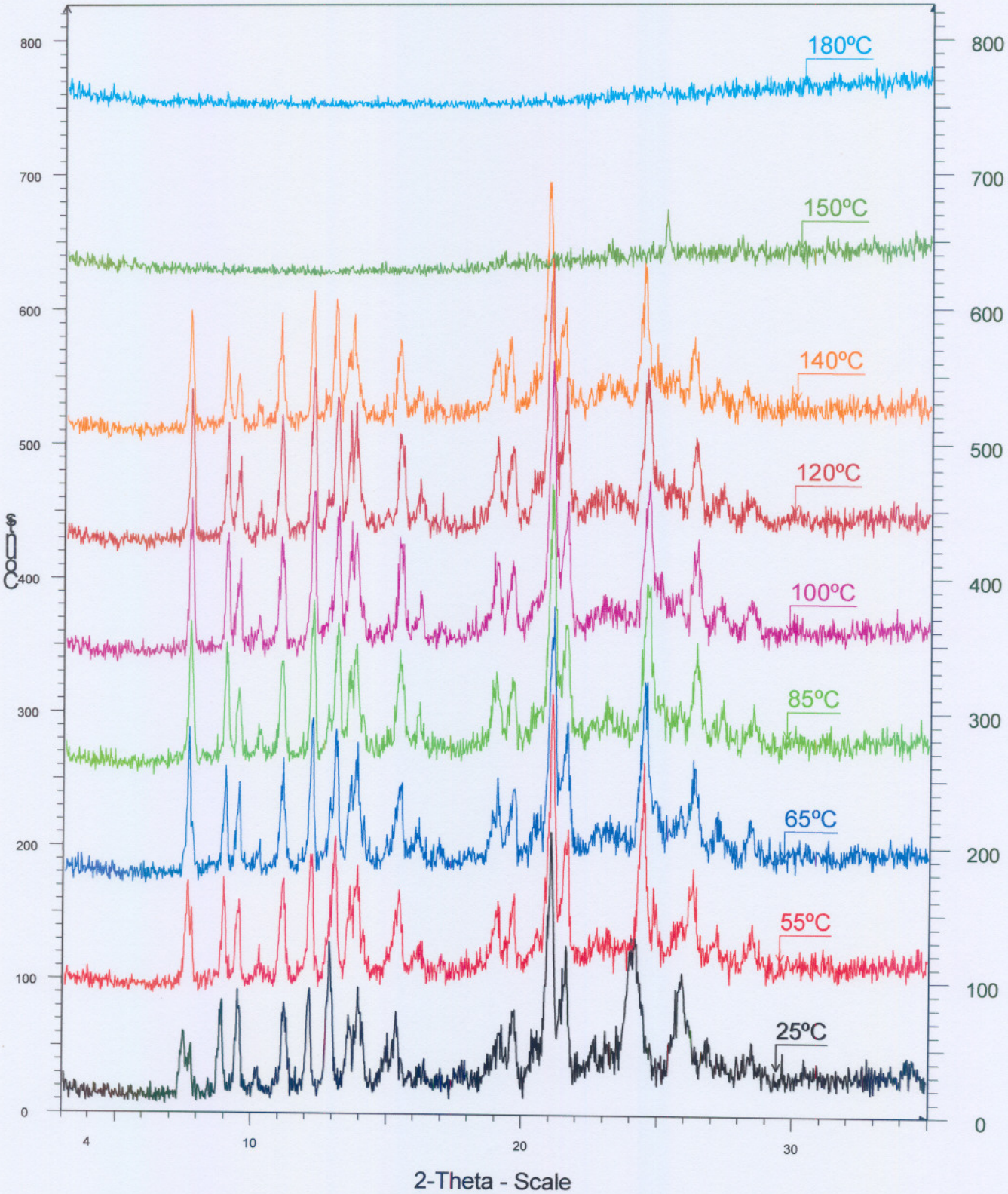

Figure 5.30 Overlay of the VT-XRPD patterns of ZP4 at temperatures ranging from 25-180°C.

TGA and KF did not indicate the presence of a significant amount of solvent in ZP4. ZP4 was classified as an anhydrous form of gatifloxacin. The DSC thermogram revealed a broad endotherm at 153.64°C, an exotherm at 162.88°C followed by another endotherm with a peak maximum at 174.64°C. The superimposed TGA and DSC thermograms are illustrated in figure 5.31.

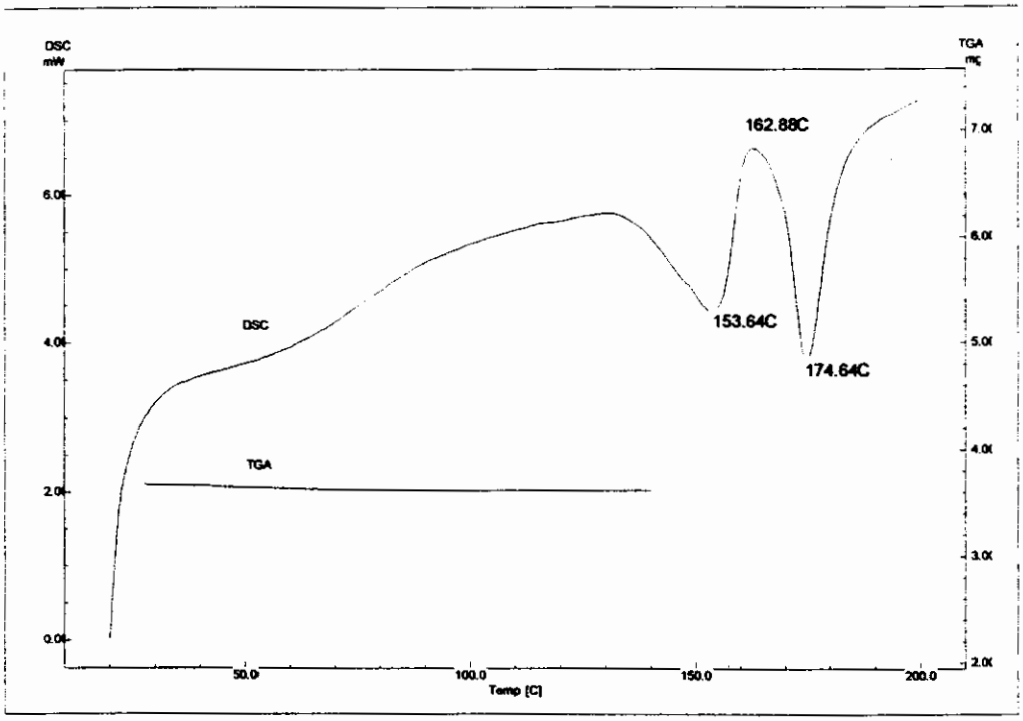

Figure 5.31 Superimposed DSC and TGA thermograms of ZP4.

Observations from HSM confirmed the thermal events observed in the DSC thermogram. The crystals started to melt at 153°C and seemed to solidify at 169°C. The solidified form melted at 172°C-176°C. These observations enabled the elucidation of the events of the DSC thermogram. HSM events are tabulated in table 5.24.

Table 5.24 Photomicrographs of the HSM events observed for ZP4

Photomicrograph	Observation	Temperature (°C)
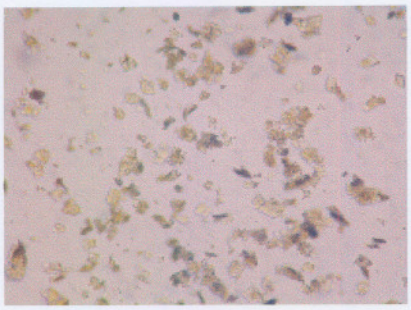	Initial.	25
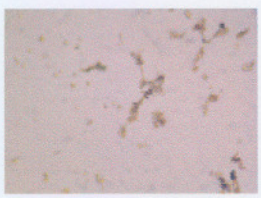 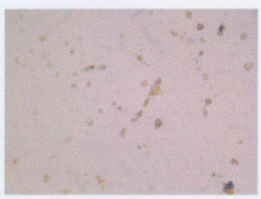	Melting of the sample.	153 159
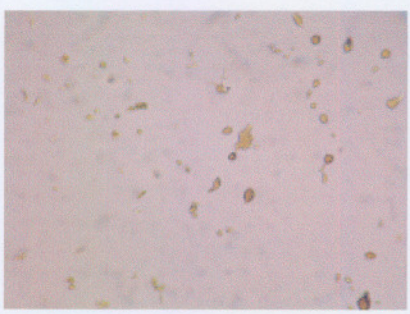	Solidification of the melt.	164

Table 5.24 continued…

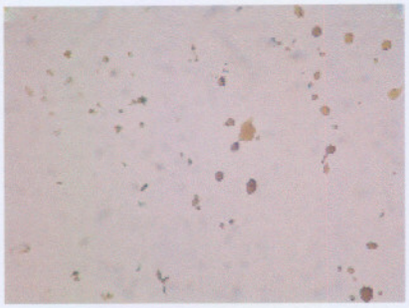		169
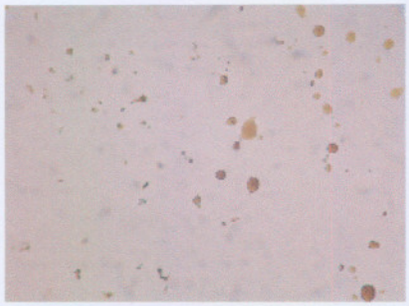 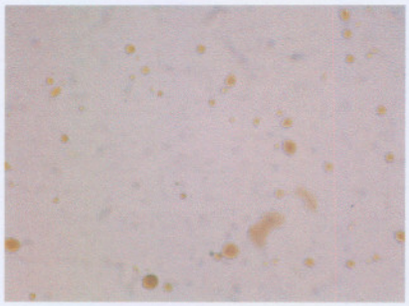	Melting of the solidified product.	172 176

To distinguish between ZP3 and ZP4 the following identification tools can be utilised: XRPD (table 5.25), thermal behaviour (table 5.26) and IR spectrometry (table 5.27 and figure 5.32).

Table 5.25 XRPD peak position (°2θ) and relative peak intensities of ZP3 and ZP4

ZP3		ZP4	
Position (°2θ)	**Intensity (I/I_0)**	**Position (°2θ)**	**Intensity (I/I_0)**
5.54	4.2	-------	-------
6.69	6.5	-------	-------
7.37	11.2	7.416	28.6
-------	-------	7.70	23.8
8.33	9.0	-------	-------
8.77	12.7	8.815	39.5
9.26	13.9	-------	-------
9.58	18.7	9.46	37.1
-------	-------	10.14	14.8
10.67	17.2	-------	-------
11.27	22.1	11.16	38.6
12.08	18.9	12.07	43.8
12.81	35.6	12.84	60.5
-------	-------	13.58	34.3
14.08	20.9	13.93	44.3
14.28	20.9	-------	-------
15.31	16.4	15.31	35.7
16.01	10.7	-------	-------
18.40	8.0	-------	-------
19.34	18.9	------	-------
-------	-------	19.66	36.2
19.95	22.4	-------	-------
20.44	25.1	20.43	27.1
21.06	100.0	21.04	100.0
21.58	44.0	21.59	59.5
-------	-------	22.64	26.7
23.15	23.6	-------	-------
23.96	56.0	24.13	62.4
24.65	25.6	-------	-------
25.80	30.1	25.86	47.1
-------	-------	26.87	27.6
-------	-------	28.52	25.7

Table 5.26 Thermal behaviour of ZP3 and ZP4

Event	ZP3	ZP4
Dehydration endotherm	65.86°C	Absent
Total weight loss (TGA)	6.74%	Insignificant (0.83%)
Final melting point of solidified product	187.71°C	174.64°C

Table 5.27 The main absorptions in the IR spectra of ZP3 and ZP4

ZP3	ZP4
Wavenumber (cm^{-1})	Wavenumber (cm^{-1})
-------	3485
3412	-------
-------	3329
2984	2991
2840	2835
2463	-------
-------	1728
1647	1647
1544	1545
1448	1445
1396	1397
1319	1318
1279	1278
1214	1215
-------	1188
1177	-------
1144	1145
1114	1110
1095	1095
1055	1056
1037	1037
1001	1000
941	940
913	914
886	887
845	845
821	821
-------	806
786	785
734	735
687	686
660	660
647	648
595	595
571	573
549	549
517	518
485	485
451	450

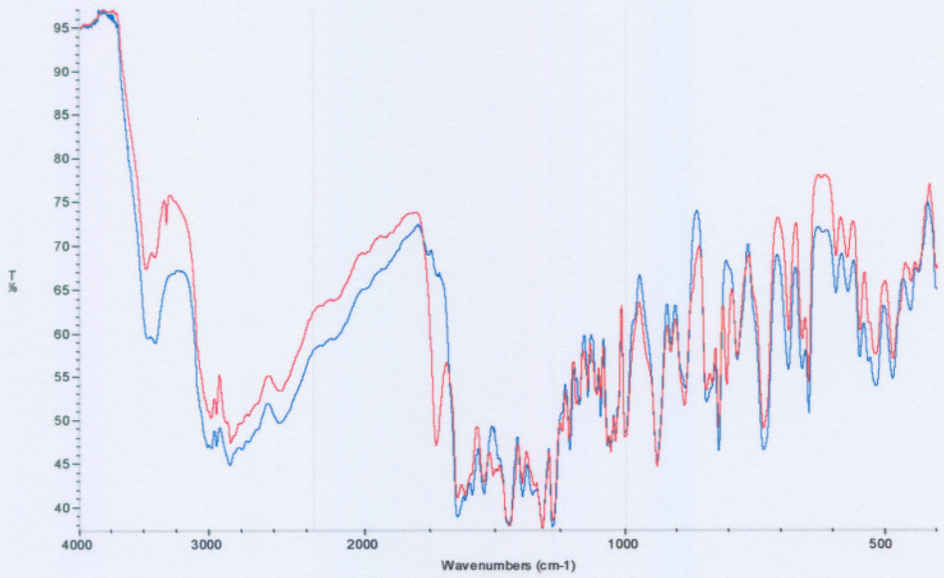

Figure 5.32 Superimposed IR spectra of ZP3 and ZP4.

5.3 Scanning electron microscopy (SEM)

SEM photomicrographs were taken of ZP0 (ethanol solvate), ZP0 (isomorphic desolvate), ZP1, Ω (from ZP1), J (as sesquihydrate), I (anhydrous), ZP2, Ω (from ZP2), ZP3 and ZP4. These photomicrographs are tabulated and discussed in tables 5.28-5.32.

Table 5.28 SEM photomicrographs of ZP0 and its isomorphic desolvate

Form	SEM photomicrograph	Brief description
ZP0 (ethanol solvate)	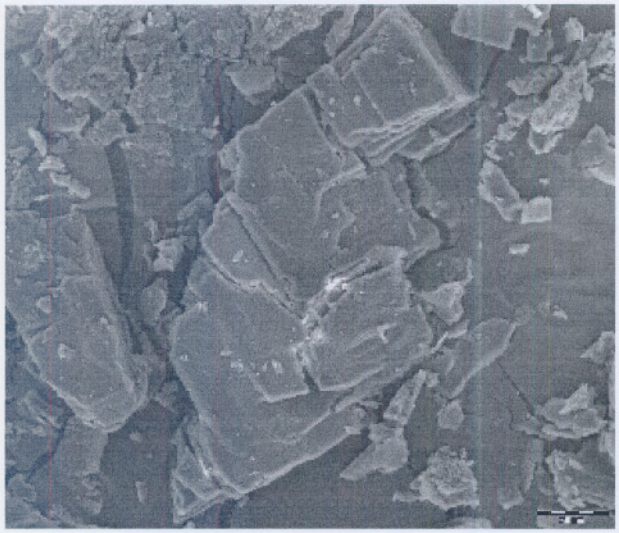	Shapeless crystals that seemed to agglomerate.
ZP0 (isomorphic desolvate)	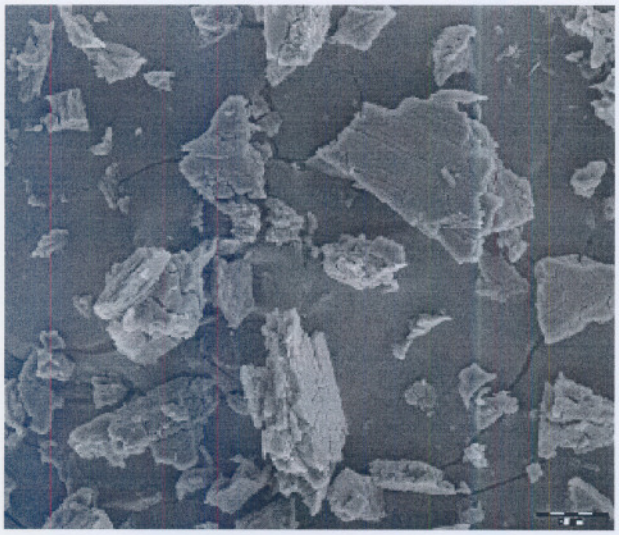	Shapeless agglomerates of crystals that vary in size.

Table 5.29 SEM photomicrographs of form ZP1 and form Ω(from ZP1 and ZP2)

Form	SEM photomicrograph	Brief description
ZP1	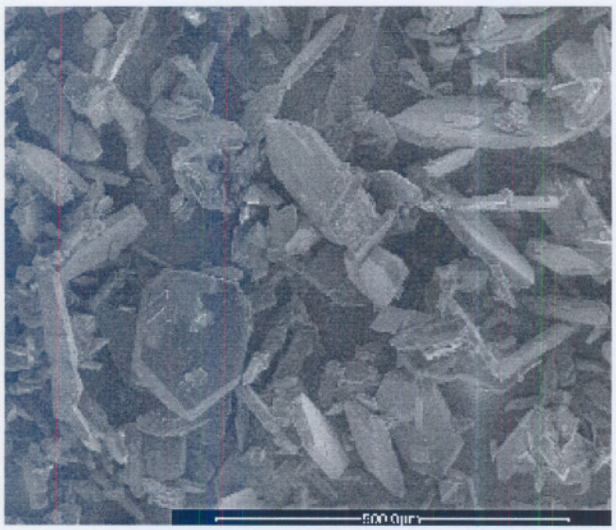	Sharp-edged, plate-like crystals with no distinct shape, were observed.
Form Ω	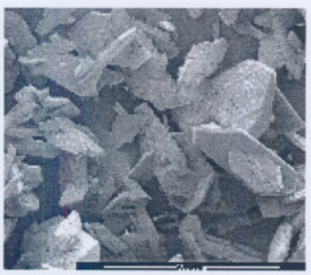 (a) from ZP1 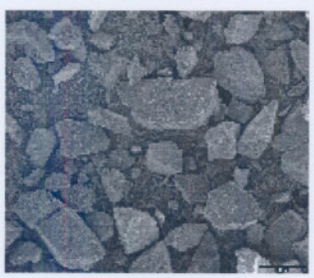 (b) from ZP2	Form Ω from ZP1 and ZP2 revealed different crystal morphologies, indicative that that it is possible for this form to have different crystal habits.

Table 5.30 SEM photomicrographs of form J and its dehydrated product, form I

Form	SEM photomicrograph	Brief description
Form J (sesquihydrate)	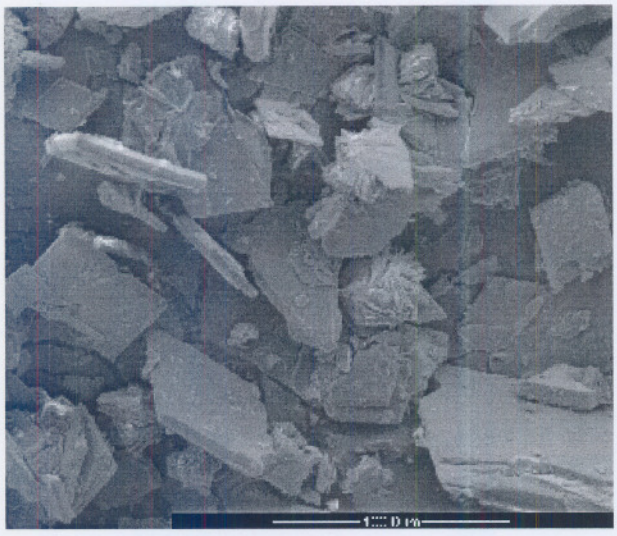	No specific particle shape was observed for this sample.
Form I (anhydrous)	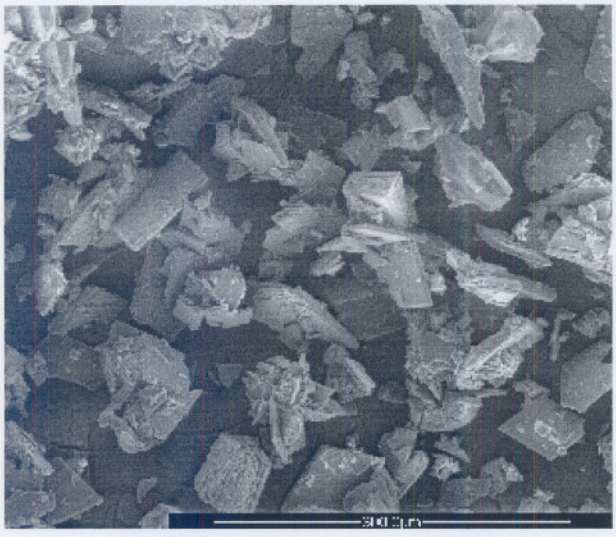	This sample revealed sharp-edged, shapeless agglomerates.

Table 5.31 SEM photomicrographs of form ZP2 and ZP3

Form	SEM photomicrograph	Brief description
ZP2	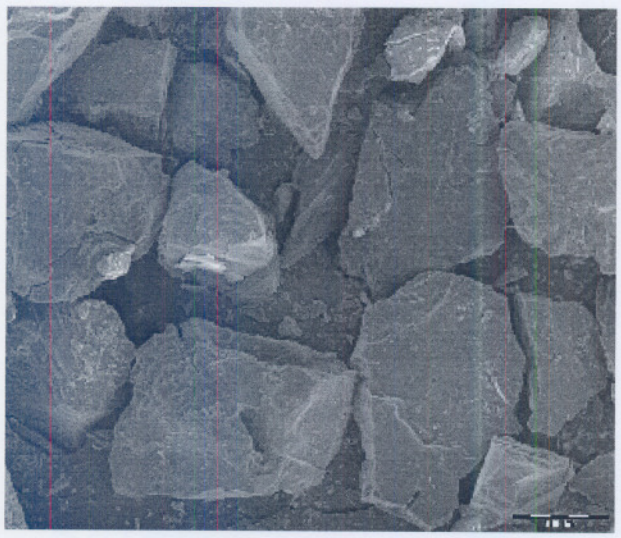	Bulky, shapeless crystals were observed.
ZP3	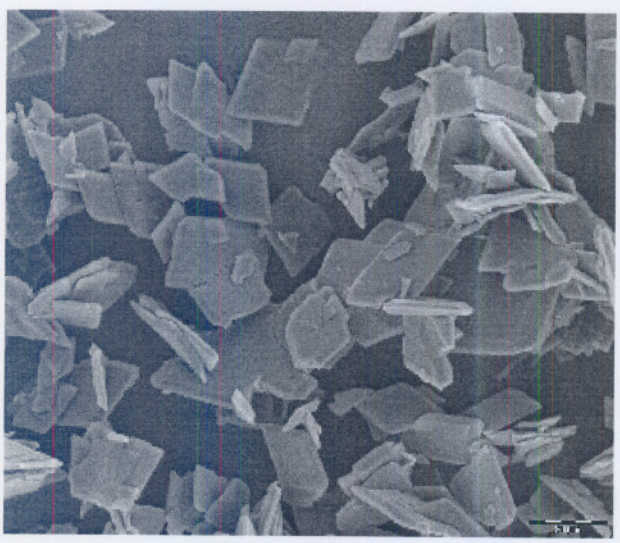	ZP3 revealed plate-like, sharp-edged crystals that seemed to agglomerate.

Table 5.32 SEM photomicrographs of form ZP4

Form	SEM photomicrograph	Brief description
ZP4	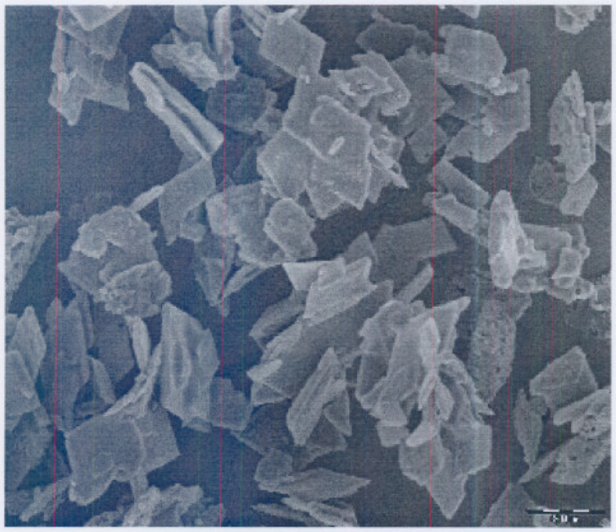	Shapeless agglomerates were observed.

5.4 Flowability

To provide some insight into the flow behaviour of the various crystal forms the Carrs index (CI) and Haussner ratio (HR) of the samples were calculated. The analysis of each sample was performed in three fold as discussed in chapter 3. The averages of the results are given in table 5.33. Flow properties are classified as follows (according to Staniforth, 2002:208):

- excellent (5<CI<15)
- good (12<CI<16)
- poor (23<CI<35)
- extremely poor (CI>40)

Table 5.33 Flow properties of the various crystal forms of gatifloxacin

Crystal form	Average CI	Average HR	Flow properties
ZP0	23.43	1.31	Poor
Isomorphic desolvate of ZP0	27.91	1.39	Poor
ZP1	28.37	1.40	Poor
Form Ω (from ZP1)	28.04	1.39	Poor
Form J	20.42	1.26	Fair
Form I (anhydrous)	28.40	1.41	Poor
ZP2	23.90	1.32	Poor
Form Ω (from ZP2)	26.41	1.36	Poor
ZP3	36.08	1.57	Very poor
ZP4	34.65	1.53	Very poor
H4 (sesquihydrate)	44.33	1.80	Extremely poor
Anhydrous gatifloxacin	42.96	1.75	Extremely poor

Overall a poor powder flow was observed for all the samples. Possible reasons include the following:

1. the crystals did not possess very favourable shapes (favourable being ideally spherical) as illustrated by the SEM photomicrographs of the samples and
2. the samples tended to agglomerate.

These results suggest that powder flow will be problematic and might have a negative impact on the manufacturing process of solid dosage forms.

5.5 Relative stability

Due to differences in the physico-chemical properties of polymorphs it is understandable that polymorphs may reveal different water sorption capabilities that may influence the polymorphic/chemical stability of the crystal form (chapter 1).

Stability testing is a crucial step during pre-formulation studies in order to select the most desired crystal form for manufacturing.

This section reveals results obtained during a one month accelerated stability testing of form Ω at different storage conditions (temperature and relative humidity).

The XRPD patterns of the samples obtained after one month at 30°C & 65 %RH and 40°C & 75 %RH are respectively illustrated in figure 5.33.

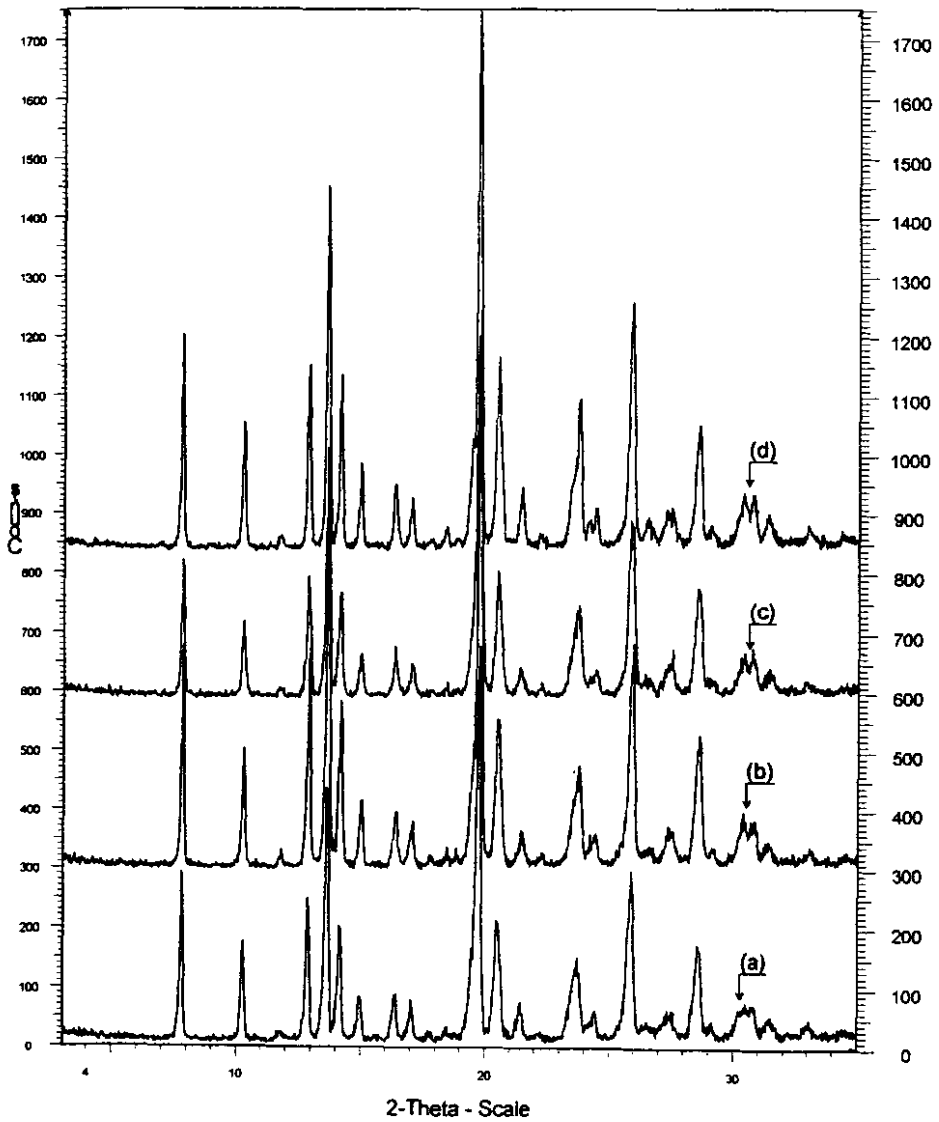

Figure 5.33 Overlay of the XRPD patterns of form Ω: after 1 month at (a) 30°C & 65 %RH, (b) 40°C & 75 %RH (c) ambient conditions and (d) XRPD pattern of form Ω initially.

No significant changes in the XRPD pattern were observed at the mentioned conditions after one month at the 3 storage conditions. Thus it can be suggested that the crystal lattice remained unaffected when exposed to accelerated stability testing conditions for one month.

The samples did show a small increase in water content (determined by TGA) as seen in table 5.34.

Table 5.34 Initial water content of form Ω and water content after one month at accelerated stability conditions

Initial	Ambient	30°C 65 %RH	40°C 75 %RH
0.11%	0.12%	0.17%	0.75%

The slight increase in the water content may be regarded as insignificant, however it revealed the possibility that form Ω (although stable for 1 month) may undergo moisture sorption at higher temperatures and humidities when exposed for longer periods of time that could influence the stability of the crystal form.

DSC analysis revealed a single melting point at 187.70°C and 187.59°C for the 30°C & 65 %RH and the 40°C & 75 %RH exposed samples respectively. These melting points were slightly lower than the initial sample and the sample exposed to ambient conditions (189.95°C and 190.14°C respectively). Dehydration endotherms were not observed, indicating that no water was incorporated into the crystal lattice, supporting the observation that an insignificant amount of water was present in the samples.

IR spectroscopy revealed no significant changes between the exposed samples and the initial sample of form Ω. The IR spectra of form Ω exposed to ambient conditions, 30°C & 65 %RH and 40°C & 75 %RH and the initial form Ω are illustrated in figure 5.34.

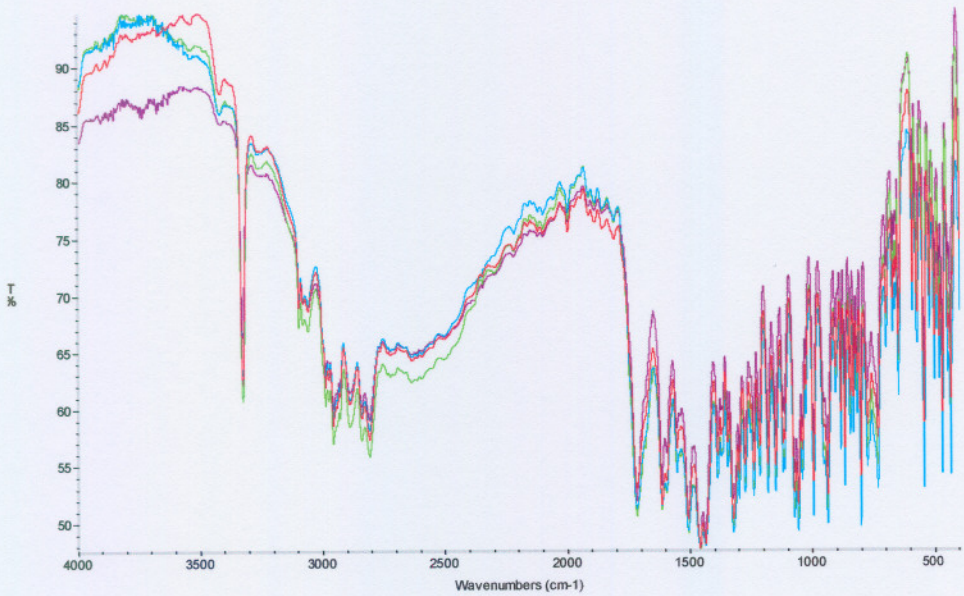

Figure 5.34 IR spectra of form Ω (initial) after 1 month of exposure to ambient conditions, 30°C 65 %RH and 40°C 75 %RH.

Conclusion

Results from this chapter are summarised in table 5.35.

Table 5.35 Summary of results

Recrystallisation solvent	Form	Classification		Form	Classification
99-100% Ethanol	ZP0	Mono-ethanol solvate	DRYING	Isomorphic desolvate of ZP0	Anhydrous
n-Butanol	ZP1	Sesqui-butanol solvate		Form Ω	Anhydrous
THF	J	Sesquihydrate		Form I	Anhydrous
Ethyl acetate	ZP2	Hemi-ethyl acetate solvate		Form Ω	Anhydrous
Dichloromethane	ZP3	Sesquihydrate		ZP4	Anhydrous

The recrystallisation studies identified four possibly new pseudopolymorphic forms ZP0, ZP1, ZP2, ZP3 and ZP4 that were found to be: an ethanol solvate, sesqui-butanol solvate, hemi-ethyl acetate solvate, sesquihydrate and an anhydrous form of gatifloxacin respectively.

As ZP1 and ZP2 are new forms, the drying of these two forms to produce form Ω can be suggested to be novel methods for the preparation of form Ω.

The isomorphic behaviour and classification of ZP0 was not documented at the time of this study. This study therefore provided a significant contribution to the available literature, as it was able to classify ZP0 as a mono-ethanol solvate and describe the isomorphic behaviour of ZP0.

The recrystallisation product from THF in this study was found not to be a THF solvate as stated by the innovators (for form J), but rather a sesquihydrated form of gatifloxacin. According to the literature Niddam-Hildesheim *et al.* (2004a:1-55) the drying of form J should produce form Ω. The results for the dried form J obtained in this study did have similarities to that of form Ω, but shared greater resemblances to form I (anhydrous).

From the literature study it was found that there are numerous sesquihydrated forms of gatifloxacin. Gatifloxacin sesquihydrate therefore exhibits polymorphic pseudopolymorphism. Form J and ZP3 (being sesquihydrated forms) can therefore be added to the list of polymorphic pseudopolymorphs of gatifloxacin sesquihydrate.

The powder flow properties of new and previously described crystal forms were evaluated. The results obtained for previously described crystal forms contributed to the available literature, as powder flow was not discussed in available literature (at the time of this study). The obtained powder flow results added supplementary information to the available data on these crystal forms.

Form Ω did not undergo any phase changes when exposed to ambient conditions nor during the exposure to the accelerated stability testing conditions (for the duration of one month). TGA analysis indicated a slight increase in water content of the samples exposed to the accelerated stability testing conditions. However small this increase was (0.01-0.64%), it revealed that form Ω may be susceptible to moisture sorption.

This study proved to be significant as it:

- Identified four possible new pseudopolymorphs and one true polymorph of gatifloxacin.
- Provided two novel preparation methods for form Ω.
- Contributed valuable information regarding previously described crystal forms.
- Contributed valuable information regarding the powder flow properties of the forms obtained herein this study.
- Revealed that form Ω remained stable over a month period when exposed to accelerated stability testing conditions.

Chapter 6

Solubility and dissolution behaviour of gatifloxacin crystal modifications

Introduction

As mentioned in chapter 1, different polymorphs may exhibit differences in solubility (and dissolution) due to the differences in bonding strength (lattice strength) and packing arrangement. It is therefore of importance to study the differences in solubility and dissolution behaviour, as these factors may influence the bioavailability of the API that can lead to toxicity or ineffective dosages.

In this chapter the solubility and dissolution behaviour of the various recrystallisation products will be discussed and compared.

6.1 Solubility testing

Solubility testing was done in 5 fold per medium in test tubes that were rotated at 65 rpm in a water bath maintained at 37±2°C (chapter 3). The solubility and dissolution behaviour of the solvated/hydrated crystal forms and their desolvated products will be discussed in section 6.1.1 and 6.1.2 respectively.

6.1.1 Solvated/Hydrated forms of gatifloxacin

The solubility behaviour of the following crystal forms (as discussed in chapter 5) will be discussed in this section: Form H4 (sesquihydrate), ZP0 (mono-ethanol solvate), ZP1 (sesqui-butanol solvate), form J (sesquihydrate), ZP2 (hemi-ethyl acetate solvate) and ZP3 (sesquihydrate).

6.1.1.1 Gatifloxacin sesquihydrate (H4)

In table 6.1 the average solubility of gatifloxacin sesquihydrate (form H4) is given.

Table 6.1 Solubility of gatifloxacin sesquihydrate (H4) in various media

Medium	pH	Average solubility (mg/ml)	%CV
0.01 M HCl	2.13	4.798	3.72
Acetate buffer (pH 4.5)	4.50	4.502	3.67
Milli-Q water	5.50	1.977	3.27
Phosphate buffer (pH 6.8)	6.80	2.639	0.47

From this data it was observed that form H4 was slightly more soluble in 0.01 M HCl than in acetate buffer and poorly soluble in water and phosphate buffer. The solubility of form H4 was in the following order 0.01 M HCl > acetate buffer > phosphate buffer > milli-Q water. It seemed as if the solubility of this form was pH dependant, being more soluble in acidic media (figure 6.1).

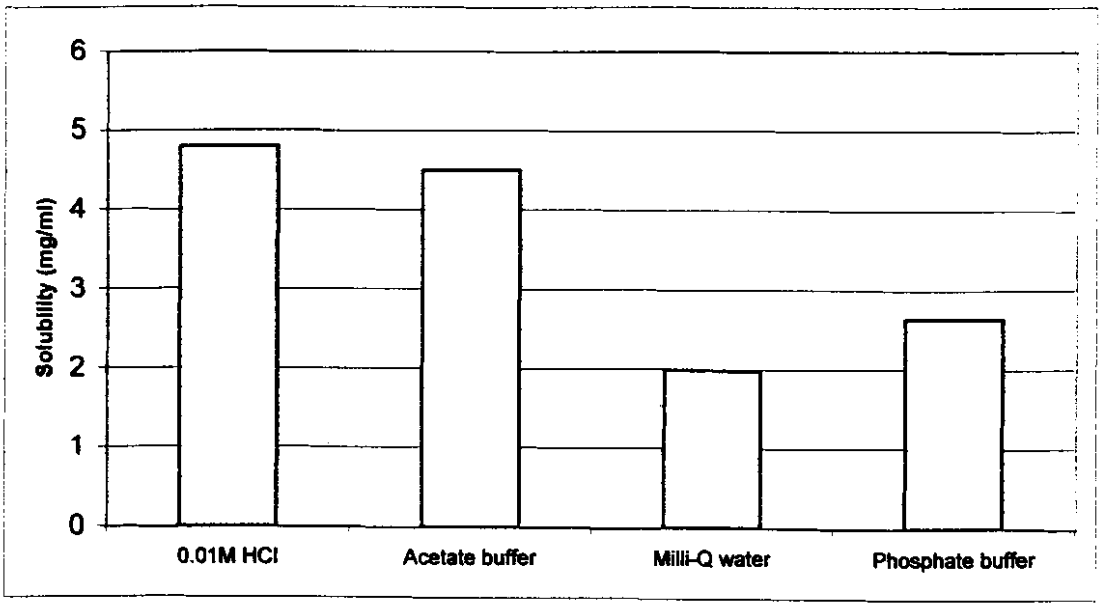

Figure 6.1 Solubility of form H4 in various media at 37±2°C.

6.1.1.2 ZP0

As discussed in chapter 5, ZP0 was found to be a mono-ethanol solvate. Table 6.2 provides a summary of the solubility testing results for ZP0.

Table 6.2 Solubility of ZP0 in various media

Medium	pH	Average solubility (mg/ml)	%CV
0.01 M HCl	2.15	3.833	4.99
Acetate buffer (pH 4.5)	4.51	4.116	3.40
Milli-Q water	5.90	2.134	6.51
Phosphate buffer (pH 6.8)	6.81	2.378	1.99

From this data it was observed that ZP0 was slightly more soluble in acetate buffer than in 0.01 M HCl. A great decrease in solubility of ZP0 was observed in milli-Q water and phosphate buffer. It seemed as if the solubility of ZP0 was pH dependant, being more soluble in acidic media (figure 6.2).

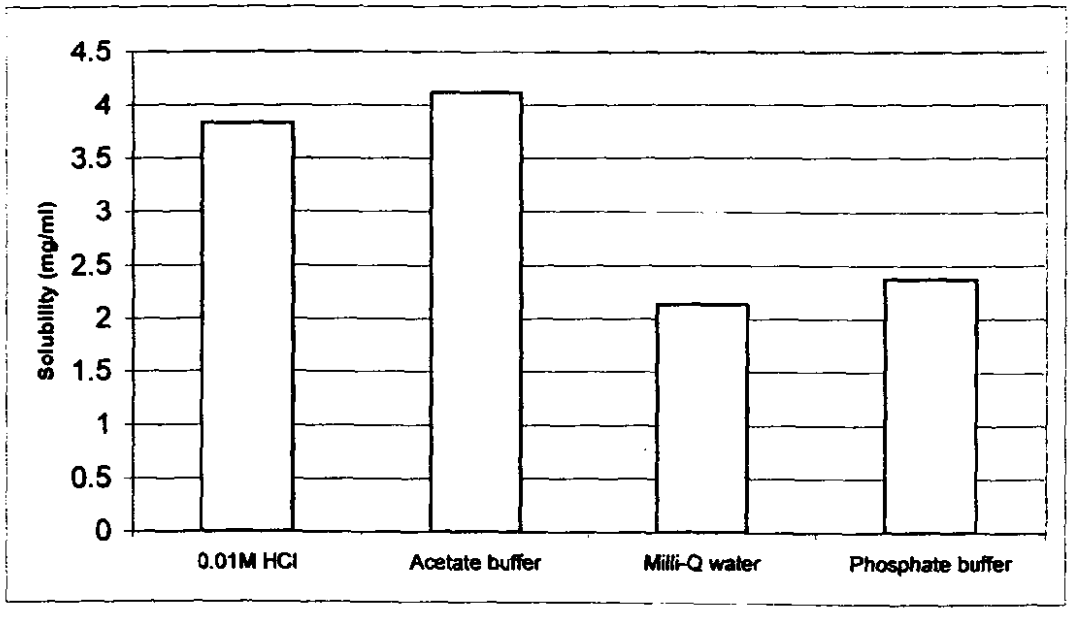

Figure 6.2 Solubility of ZP0 in various media at 37±2°C.

The solubility of ZP0 was in the following order: acetate buffer > 0.01 M HCl > phosphate buffer > milli-Q water.

6.1.1.3 Form ZP1

Form ZP1 was found to be a new pseudopolymorph of gatifloxacin. As mentioned in chapter 5, it was classified as a sesqui-butanol solvate.

The solubility testing results revealed that this form was slightly more soluble in 0.01 M HCl compared to the solubility in acetate buffer. The solubility in phosphate buffer was also slightly higher compared to the solubility in water. Solubility test results are reported in table 6.3 and figure 6.3.

Table 6.3 Solubility of ZP1 in various media

Medium	pH	Average solubility (mg/ml)	%CV
0.01 M HCl	2.11	3.950	2.64
Acetate buffer (pH 4.5)	4.54	3.743	0.62
Milli-Q water	5.91	2.142	2.36
Phosphate buffer (pH 6.8)	6.80	2.261	1.63

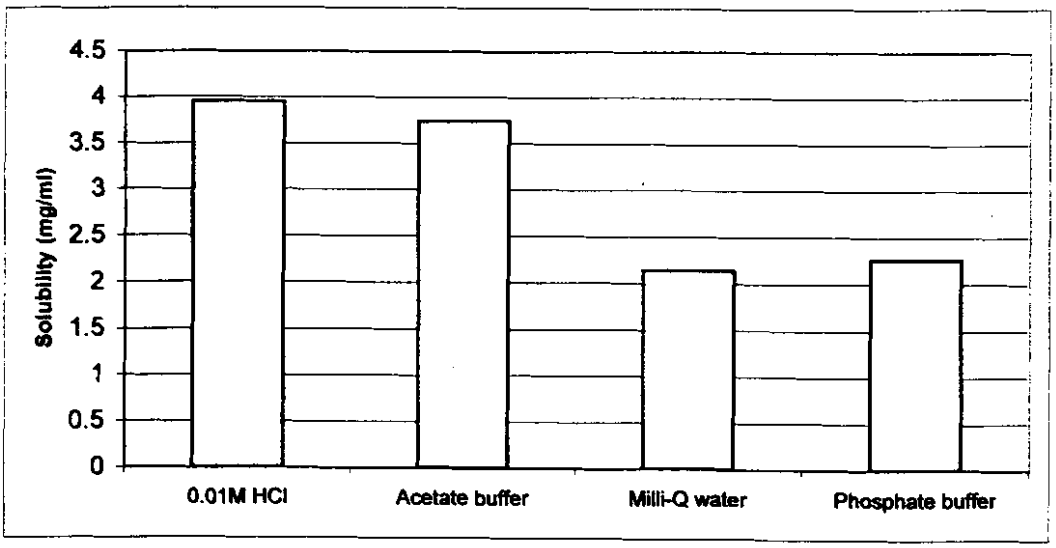

Figure 6.3 Solubility of ZP1 in various media at 37±2°C.

6.1.1.4 Form J

Form J was the product obtained using THF as recrystallisation solvent (as discussed in chapter 5). Form J was found to be a sesquihydrate.

The solubility of form J was in the following order: 0.01 M HCl > acetate buffer > phosphate buffer > milli-Q water (table 6.4).

Table 6.4 Solubility of form J in various media

Medium	pH	Average solubility (mg/ml)	%CV
0.01M HCl	2.14	4.402	1.87
Acetate buffer (pH 4.5)	4.52	4.038	5.00
Milli-Q water	5.86	2.386	2.46
Phosphate buffer (pH 6.8)	6.83	2.504	3.16

The solubility results of form J (sesquihydrate) are displayed in figure 6.4.

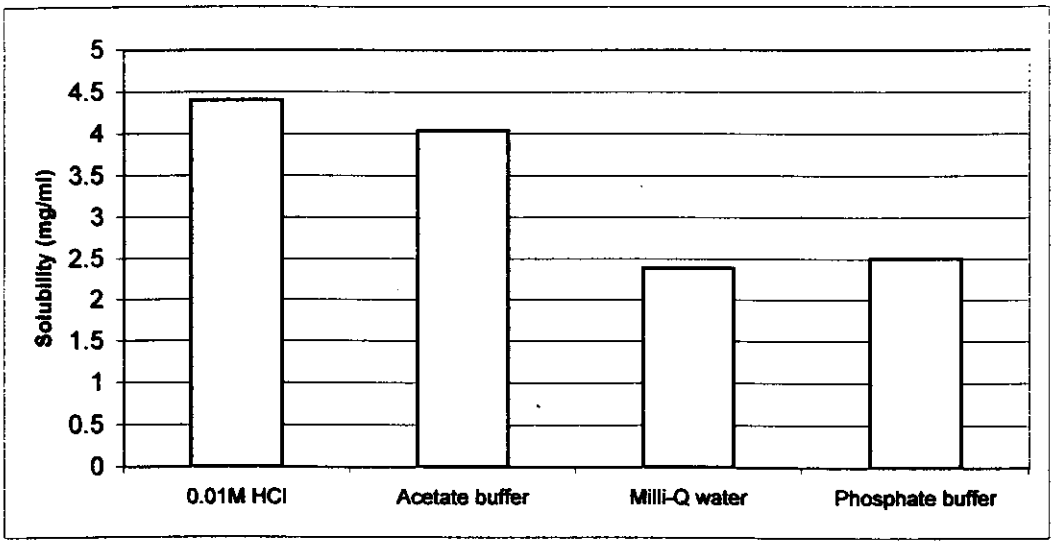

Figure 6.4 Solubility of form J in various media at 37±2°C.

6.1.1.5 Form ZP2

Form ZP2 was classified as a hemi-ethyl acetate pseudopolymorph (as discussed in chapter 5).

The solubility testing results for ZP2 are tabulated in table 6.5 and displayed in figure 6.5.

Table 6.5 Solubility of ZP2 in various media

Medium	pH	Average solubility (mg/ml)	%CV
0.01 M HCl	2.14	4.576	2.88
Acetate buffer (pH 4.5)	4.52	4.188	1.07
Milli-Q water	5.86	2.589	0.77
Phosphate buffer (pH 6.8)	6.83	2.507	5.53

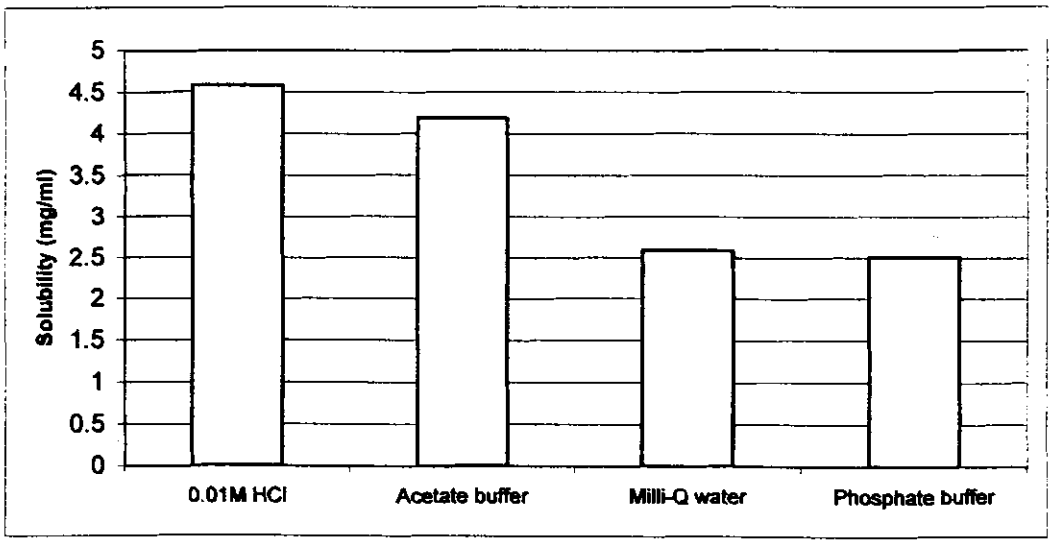

Figure 6.5 Solubility of ZP2 in various media at 37±2°C.

6.1.1.6 Form ZP3

ZP3 was found to be a new polymorph that was obtained from a dichloromethane recrystallisation. ZP3 was classified as a sesquihydrate (as discussed in chapter 5).

The solubility of ZP3 in various media is tabulated in table 6.6. Figure 6.6 displays the differences in solubility observed for form ZP3 in the various media.

Table 6.6 Solubility behaviour of ZP3 in various media

Medium	pH	Average solubility (mg/ml)	%CV
0.01 M HCl	2.12	4.741	1.24
Acetate buffer (pH 4.5)	4.50	4.600	1.25
Milli-Q water	5.95	1.985	5.46
Phosphate buffer (pH 6.8)	6.80	2.610	4.27

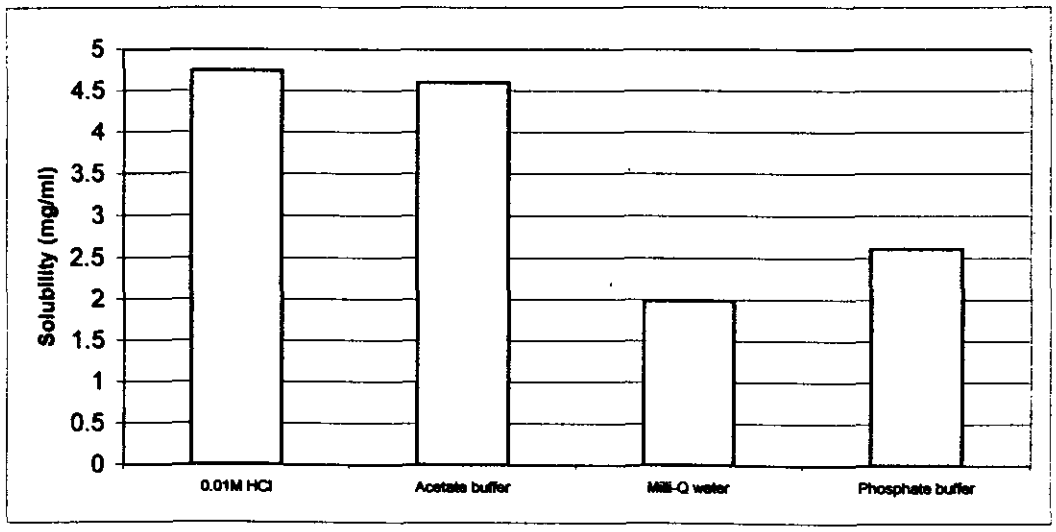

Figure 6.6 Solubility of ZP3 in various solvents at 37±2°C.

From these results it was observed that the solubility of ZP3 was pH dependant being more soluble in 0.01 M HCl, compared to its solubility in water and phosphate buffer (higher pH). No significant differences in solubility were observed between 0.01 M HCl and acetate buffer, however a significant difference in solubility was observed in milli-Q water and phosphate buffer.

6.1.2 Desolvated/Dehydrated forms of gatifloxacin

The solubility of the following crystal forms (as discussed in chapter 5) will be discussed in this section: anhydrous gatifloxacin, isomorphic desolvate of ZP0, form Ω, form I anhydrous and ZP4. All these forms were prepared by drying of the corresponding parent solvate, as discussed in chapter 4 and 5.

6.1.2.1 Anhydrous form from the sesquihydrate (H4)

Significant differences were observed in the solubility of this anhydrous form in the various media. The solubility of the anhydrous form was found to be in the following order: 0.01 M HCl > acetate buffer > phosphate buffer > milli-Q water. The solubility results are displayed in table 6.7 and figure 6.7.

Table 6.7 Solubility of anhydrous gatifloxacin in various media

Medium	pH	Average solubility (mg/ml)	%CV
0.01 M HCl	2.12	5.022	0.97
Acetate buffer (pH 4.5)	4.50	4.906	2.33
Milli-Q water	5.50	2.684	3.64
Phosphate buffer (pH 6.8)	6.80	2.870	2.14

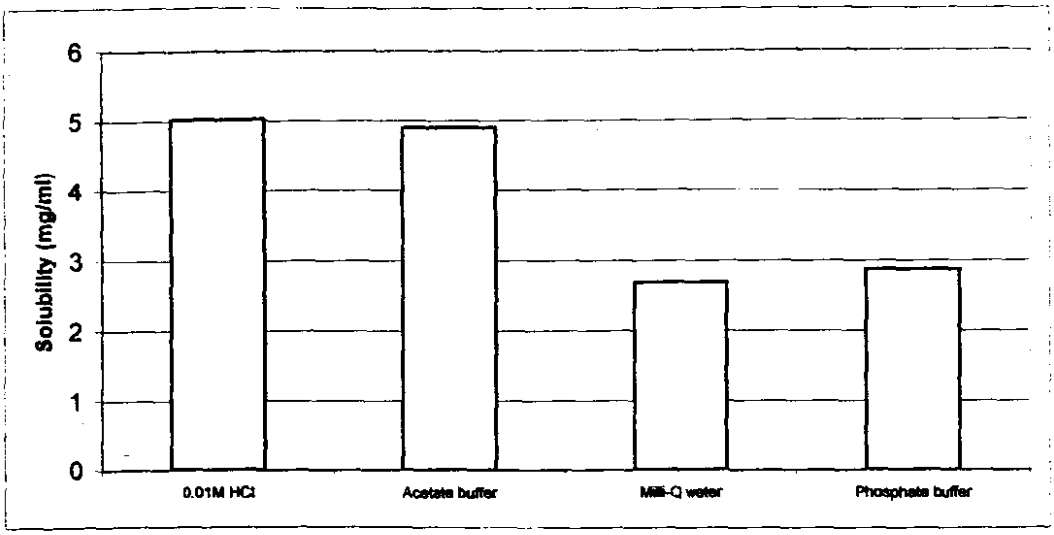

Figure 6.7 Solubility of anhydrous gatifloxacin in various media at 37±2°C.

6.1.2.2 Isomorphic desolvate of ZP0

Drying of the mono-ethanol solvate (ZP0) produced an isomorphic desolvate thereof (as discussed in chapter 5). As explained in chapter 1, the crystal lattice of an isomorphic desolvate and its parent solvate may be considered to be similar, due to the fact that the XRPD patterns are similar. It was therefore appropriate to determine the solubility to establish whether the incorporated solvent (ethanol) influenced the solubility of this crystal lattice.

The results obtained from the solubility study of the isomorphic desolvate of ZP0 are summarised in table 6.8.

Table 6.8 Solubility of the isomorphic desolvate of ZP0 in various media

Medium	pH	Average solubility (mg/ml)	%CV
0.01 M HCl	2.15	4.600	6.01
Acetate buffer (pH 4.5)	4.51	2.699	3.41
Milli-Q water	5.84	2.751	4.06
Phosphate buffer (pH 6.8)	6.82	2.416	10.66

The isomorphic desolvate was more soluble in all media except in the acetate buffer, compared to its parent solvent. As explained in chapter 1, stronger crystal lattices are harder to dissolve. The presence of the solvent molecules in ZP0 (incorporated solvent) appeared to stabilise the crystal lattice and decrease the solubility of the solvated form in 0.01 M HCl, milli-Q water and phosphate buffer.

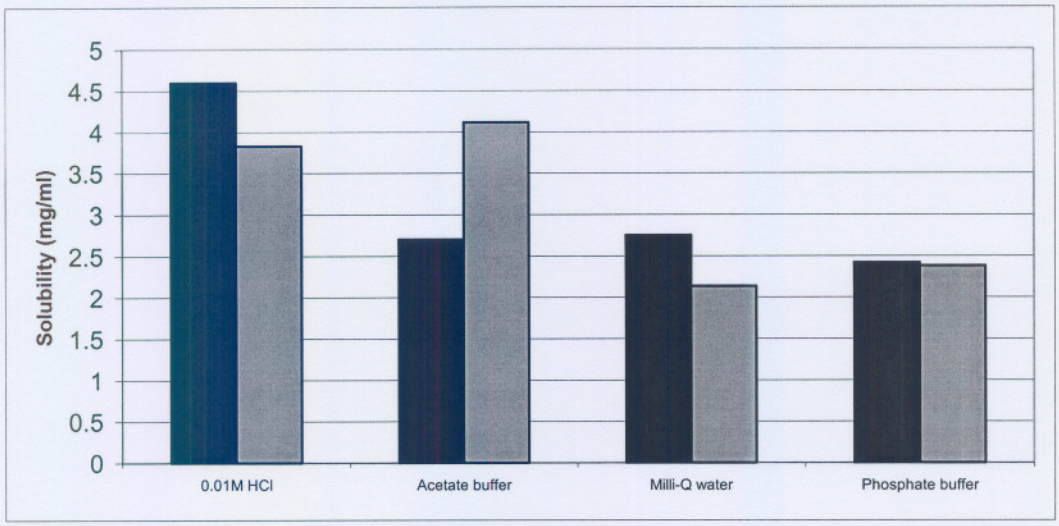

Figure 6.8 Solubility of the **isomorphic desolvated ZP0** and its parent solvate (ZP0) in various media at 37±2°C.

The solubility of the isomorphic desolvate of ZP0 was in the following order: 0.01 M HCl > acetate buffer > milli-Q water > phosphate buffer.

6.1.2.3 Form Ω

As discussed in chapter 5, form Ω was obtained by the drying of ZP1 and ZP2. This section discusses and compares the solubility results obtained for form Ω from the different parent solvates to determine whether the formation of these products from different parent solvates influenced the solubility.

Form Ω (from ZP1) revealed a significant difference in solubility between the acidic media compared to the solubility of the media with higher pH values. No significant differences were observed between the solubility obtained in 0.01 M HCl and the acetate buffer. The solubility of form Ω (from ZP1) in milli-Q water and the

phosphate buffer were comparable. Table 6.9 summarises the solubility results of form Ω (from ZP1).

Table 6.9 Solubility behaviour of form Ω (from ZP1) in various media

Medium	pH	Average solubility (mg/ml)	%CV
0.01 M HCl	2.12	5.171	2.61
Acetate buffer (pH 4.5)	4.50	4.970	1.09
Milli-Q water	5.94	3.092	3.09
Phosphate buffer (pH 6.8)	6.81	3.031	0.84

The solubility results of form Ω (from ZP2) are given in table 6.10.

Table 6.10 Solubility behaviour of form Ω (from ZP2) in various media

Medium	pH	Average solubility (mg/ml)	%CV
0.01 M HCl	2.13	4.818	0.83
Acetate buffer (pH 4.5)	4.50	4.669	5.06
Milli-Q water	5.91	3.180	1.88
Phosphate buffer (pH 6.8)	6.81	2.893	3.36

These results (table 6.9 and 6.10) are illustrated in figure 6.11 to indicate possible differences in solubility.

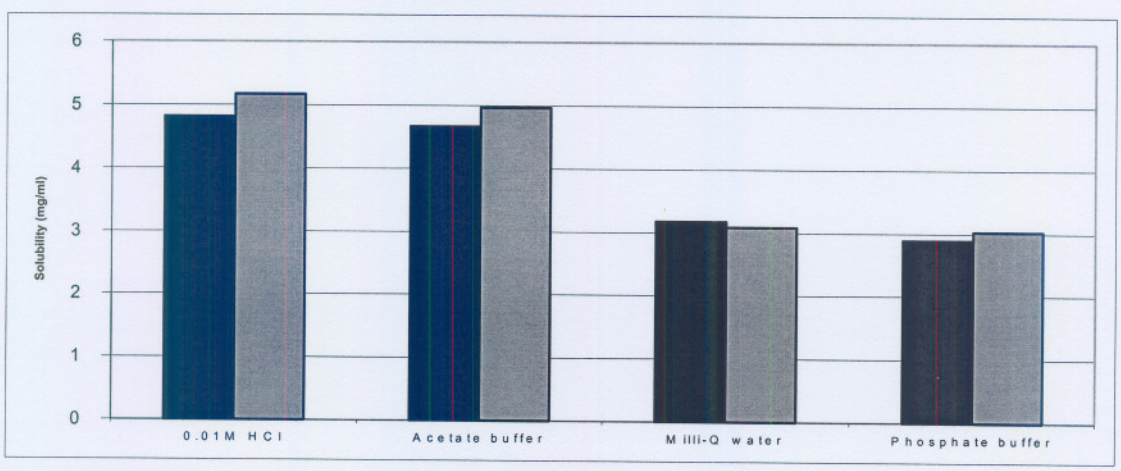

Figure 6.9 Solubility of the form Ω from ZP1 and **ZP2** in various media at 37±2°C.

No significant differences in solubility between the two dried forms from different parent solvates were observed. It can therefore be suggested that either method can be used to prepare form Ω.

6.1.2.4 Form I anhydrous

The results obtained from the solubility testing for the anhydrous form I are given in table 6.11.

Table 6.11 Solubility behaviour of anhydrous form I in various media

Medium	pH	Average solubility (mg/ml)	%CV
0.01 M HCl	2.11	5.100	1.70
Acetate buffer (pH 4.5)	4.53	4.745	4.90
Milli-Q water	5.87	2.861	4.05
Phosphate buffer (pH 6.8)	6.81	3.034	2.06

The solubility of form I (anhydrous) was found to be in the following order: 0.01 M HCl > acetate buffer > phosphate buffer > milli-Q water. The results of table 6.11 are displayed in figure 6.10.

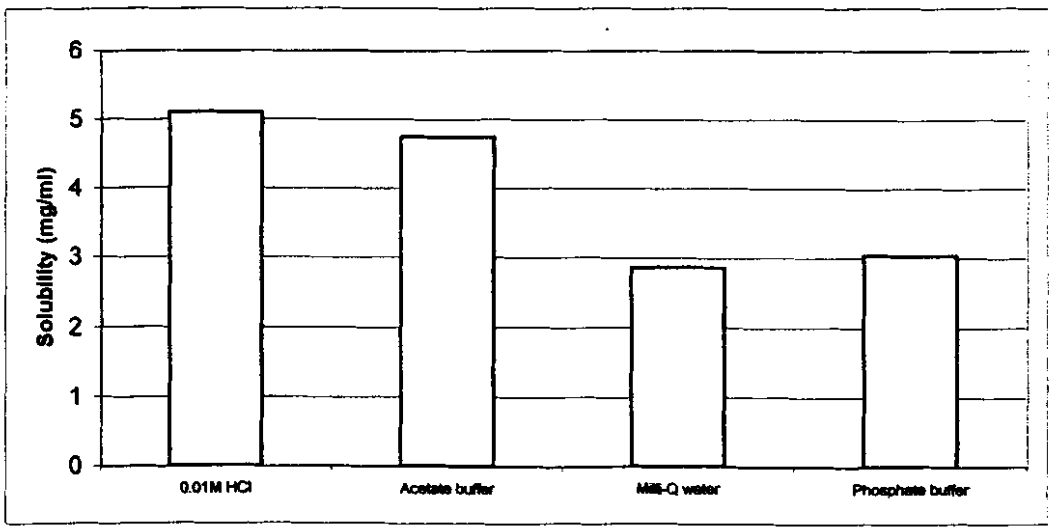

Figure 6.10 Solubility behaviour of form I (anhydrous) in various media at 37±2°C.

6.1.2.5 Form ZP4

ZP4 was found to be a new true polymorph of gatifloxacin (as discussed in chapter 5) ZP4 revealed a significant difference in solubility in the acidic media compared to the solubility thereof in water and phosphate buffer (suggesting a pH dependant solubility). A slight difference in solubility was observed in the 0.01 M HCl and acetate buffer. No significant difference was observed for the solubility in water and phosphate buffer. The solubility results are displayed in table 6.12.

Table 6.12 Solubility behaviour of ZP4 in various media

Medium	pH	Average solubility (mg/ml)	%CV
0.01 M HCl	2.12	4.359	0.98
Acetate buffer (pH 4.5)	4.51	4.609	5.30
Milli-Q water	5.91	2.731	2.46
Phosphate buffer (pH 6.8)	6.82	2.632	1.04

These results are graphically illustrated in figure 6.11.

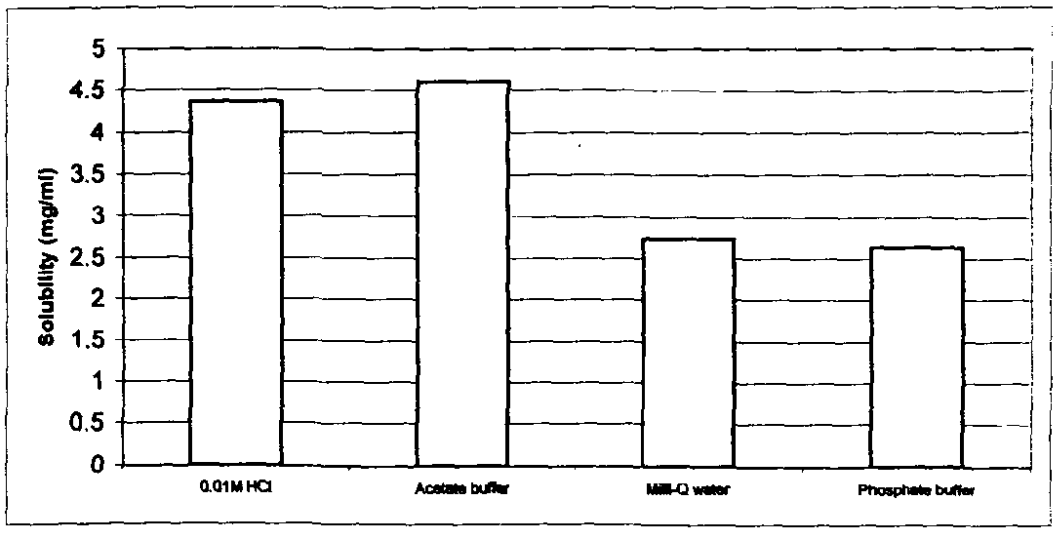

Figure 6.11 Solubility of ZP4 in various media at 37±2°C.

From table 6.12 and figure 6.11 it was observed that the solubility of ZP4 was in the following order: Acetate buffer ≥ 0.01 M HCl > milli-Q water ≥ phosphate buffer.

A general discussion and overview of the solubility results obtained will be discussed in the conclusion.

6.2 Dissolution testing

As discussed in chapter 3, multiple point dissolution testing was performed at predetermined time intervals: 7.5, 15 and 30 minutes in 0.01 M HCl medium at 37±0.2°C. The powder dissolution study was performed according to the method described by Lotter *et al.* (1983:56) using apparatus 2 (paddles) of the USP 28 (2005:2413). The dissolution profiles of the percentage powder dissolved at the various time intervals were plotted and compared. Dissolution profiles were compared utilising the similarity factor (*f2* value) described by Moore & Flanner (1996:64-67). The calculation of the *f2* value is described by the following equation:

$$f2 = 50\log\left\{\left[1+\frac{1}{n}\sum_{t=1}^{n}(Rt-Tt)^2\right]^{-0.5}\times 100\right\}$$

Whereas:

n is the number of withdrawals

R_t is the % reference sample dissolved at time t

T_t is the % sample dissolved at time t

6.2.1 Solvated/Hydrated forms of gatifloxacin

The dissolution behaviour of the following crystal forms will be discussed in this section: Form H4 (sesquihydrate), ZP0 (mono ethanol solvate), ZP1 (sesqui-butanol solvate), form J (sesquihydrate), ZP2 (hemi-ethyl acetate solvate) and ZP3 (sesquihydrate).

6.2.1.1 Gatifloxacin sesquihydrate (form H4)

Powder dissolution testing results for gatifloxacin sesquihydrate (Form H4) are given in table 6.13.

Table 6.13 Dissolution testing results for gatifloxacin sesquihydrate (form H4)

Vessel number	% Dissolved at time interval		
	7½ minutes	15 minutes	30 minutes
1	99.8	100.6	100.6
2	100.7	101.0	101.1
3	101.1	100.5	101.8
4	100.5	100.6	101.0
5	101.1	100.5	100.8
Average	101.0 ±0.5	101.0 ±0.2	101.0 ±0.5

The dissolution profile that was derived from this data is illustrated in figure 6.12.

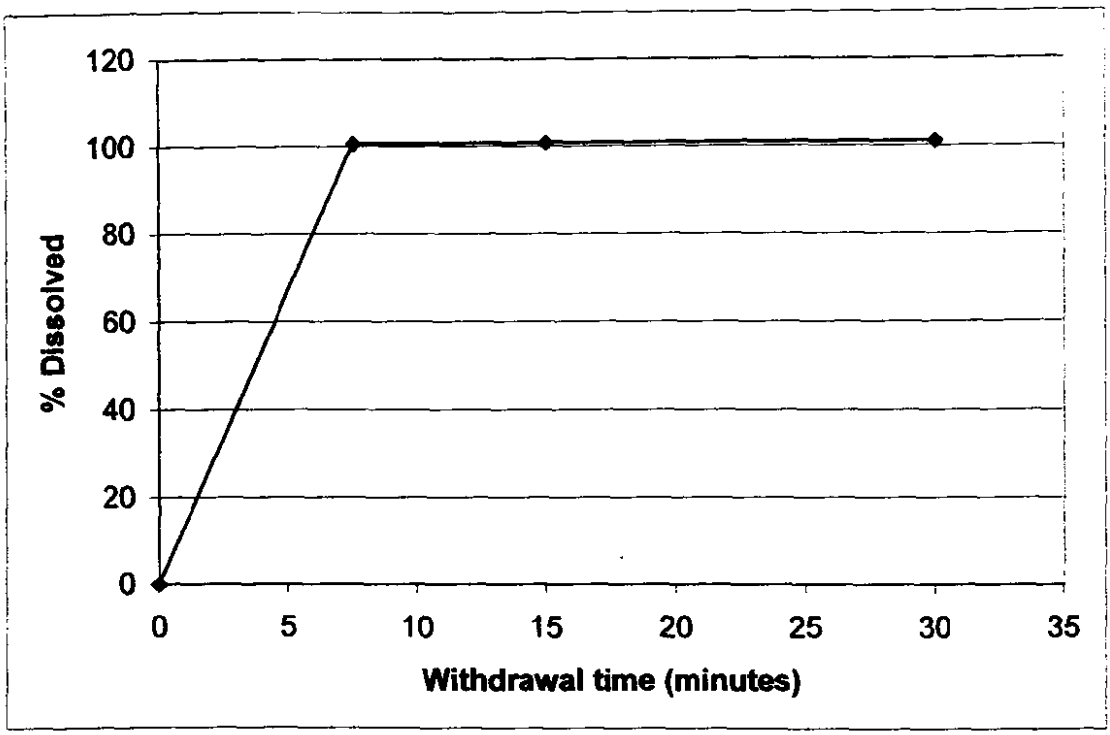

Figure 6.12 Dissolution profile of gatifloxacin sesquihydrate (form H4) in 0.01 M HCl.

From the dissolution profile it was clear that form H4 dissolved completely in the dissolution medium within 7½ minutes. This result conformed to an in-house tolerance that not less than 75% of the sample should be dissolved within 30 minutes.

It should be noted that gatifloxacin sesquihydrate dissolution test results served as the reference profile for the comparison between the different crystal forms.

The similarity factor (*f2*-value) was calculated for each crystal form tested when compared to the gatifloxacin sesquihydrate dissolution profile to determine whether significant differences in dissolution profiles existed between the various crystal modifications.

6.2.1.2 ZP0

The dissolution profile of ZP0 differed from that of the reference dissolution profile. The results can be seen in table 6.14 and figure 6.13.

Table 6.14 Dissolution testing results for ZP0

Vessel number	% Dissolved at time interval		
	7½ minutes	15 minutes	30 minutes
1	72.6	77.7	84.7
2	72.8	80.4	89.3
3	72.9	80.5	89.2
4	78.3	83.0	89.9
5	78.4	83.0	90.0
Average	75.0 ±3.1	81.0 ±2.2	89.0 ±2.2

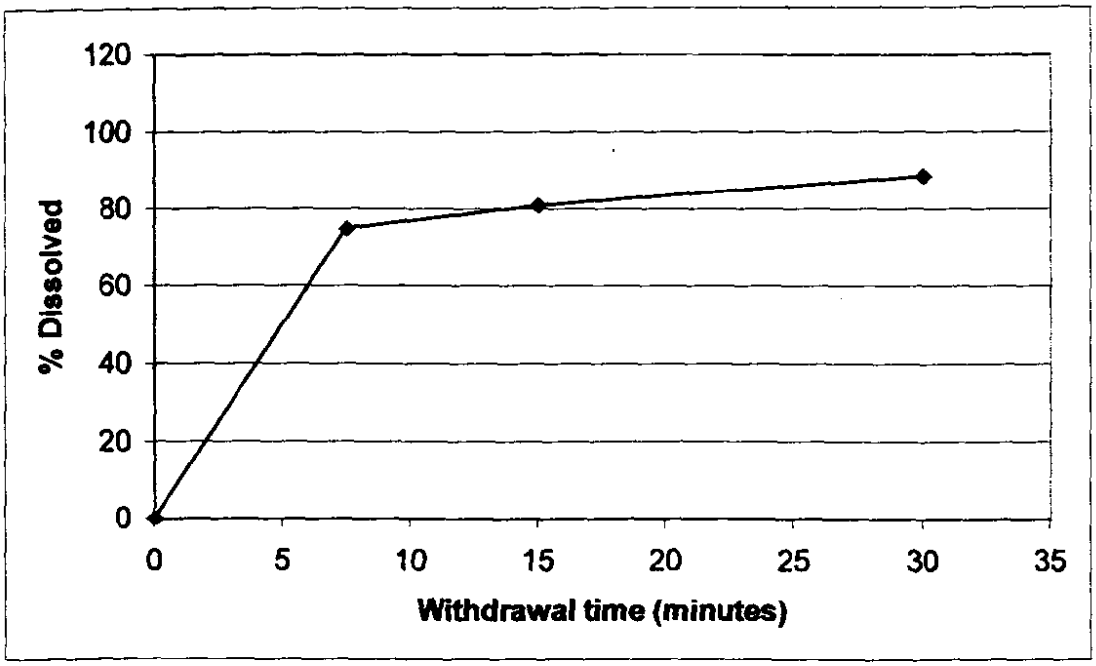

Figure 6.13 Dissolution profile for ZP0 in 0.01 M HCl.

From the results obtained, it was clear that only 75.0±3.1% of the sample dissolved after 7½ minutes and only 89.0±2.2% of the sample dissolved after 30 minutes.

The $f2$ value calculated for ZP0 was 42.24, which signified that the dissolution profile of ZP0 differed significantly from that of the reference profile (form H4).

6.2.1.3 Form ZP1

The dissolution testing results of ZP1 revealed that the sample dissolved completely within 7½ minutes. The results of the dissolution testing of form ZP1 are given in table 6.15 and figure 6.14.

Table 6.15 Dissolution testing results for ZP1

Vessel number	% Dissolved at time interval		
	7½ minutes	15 minutes	30 minutes
1	103.6	102.4	102.3
2	101.7	101.4	102.0
3	100.2	99.8	100.8
4	102.8	102.2	101.7
5	100.3	99.9	101.0
Average	102.0 ±1.5	101.0 ±1.2	102.0 ±0.6

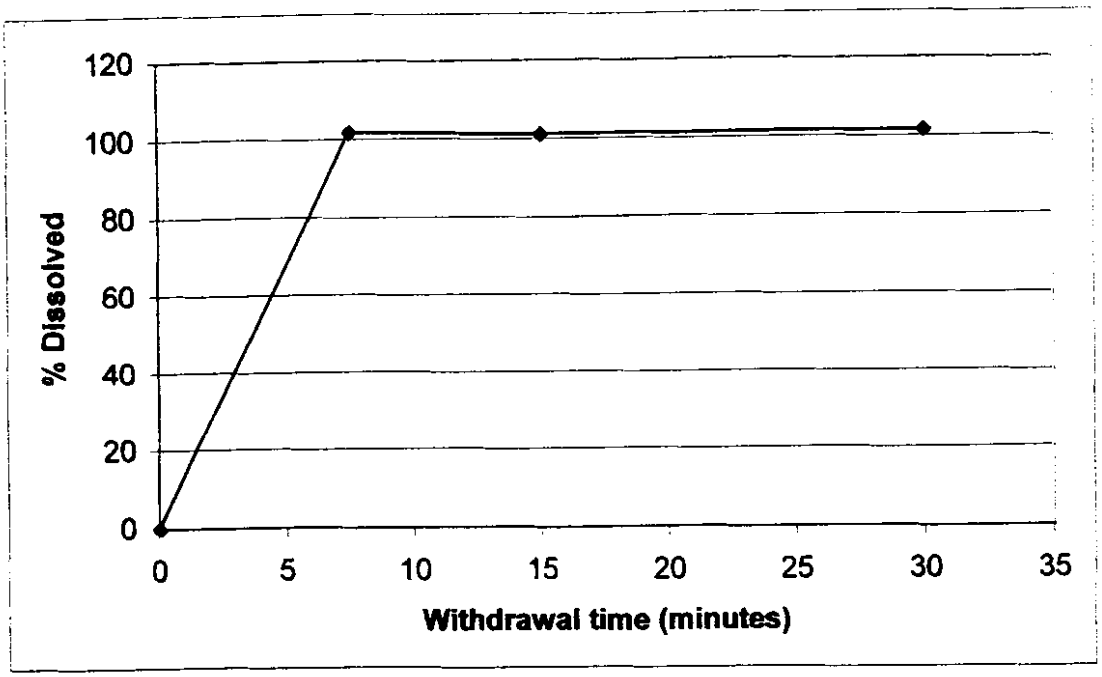

Figure 6.14 Dissolution profile for ZP1 in 0.01 M HCl.

The calculated *f2* value (96.88) indicated that the dissolution profile of ZP1 was comparable to that of the reference profile (H4).

6.2.1.4 Form J

The dissolution testing results of form J (sesquihydrate) seemed to differ from that of the dissolution profile of the reference (form H4 sesquihydrate). The results that were obtained are given in table 6.16 and figure 6.15.

Table 6.16 Dissolution testing results of form J

Vessel number	% Dissolved at time interval		
	7½ minutes	15 minutes	30 minutes
1	61.9	71.9	81.5
2	68.0	76.9	82.6
3	61.4	74.0	84.0
4	70.1	78.5	85.5
5	62.6	73.2	82.6
Average	65.0 ±4.0	75.0 ±2.7	83.0 ±1.5

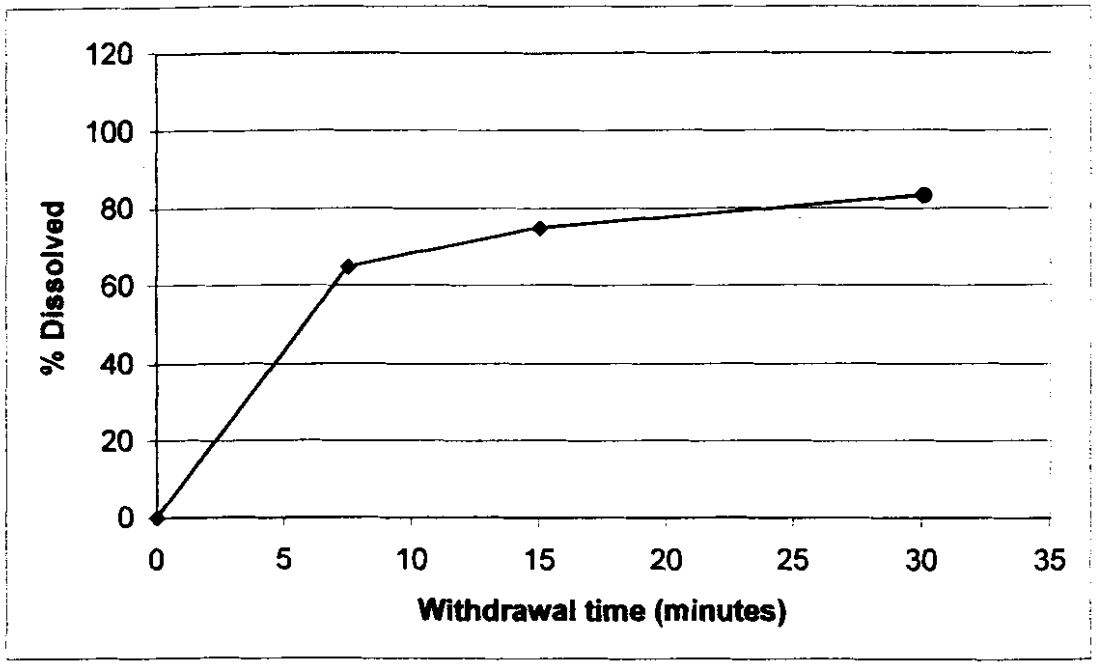

Figure 6.15 Dissolution profile of form J in 0.01 M HCl.

The *f*2 value for form J was found to be 27.89 and therefore it was indicated that the dissolution profile of this crystal form differed significantly from the sesquihydrate (form H4).

6.2.1.5 Form ZP2

The dissolution profile of ZP2 conformed to the in-house tolerance that of not less than 75% of the sample should be dissolved within 30 minutes. The results for the dissolution testing of ZP2 are given in table 6.17 and illustrated in figure 6.16. It should be noted that only four dissolution vessels were used because of a shortage of sample due to the weak yield of recrystallisation product.

Table 6.17 Dissolution testing results of ZP2

Vessel number	% Dissolved at time interval		
	7½ minutes	15 minutes	30 minutes
1	78.9	84.4	95.4
2	74.2	81.7	95.2
3	74.1	93.3	99.5
4	80.1	92.9	98.7
Average	77.0 ±3.1	88.0 ±5.9	97.0 ±2.2

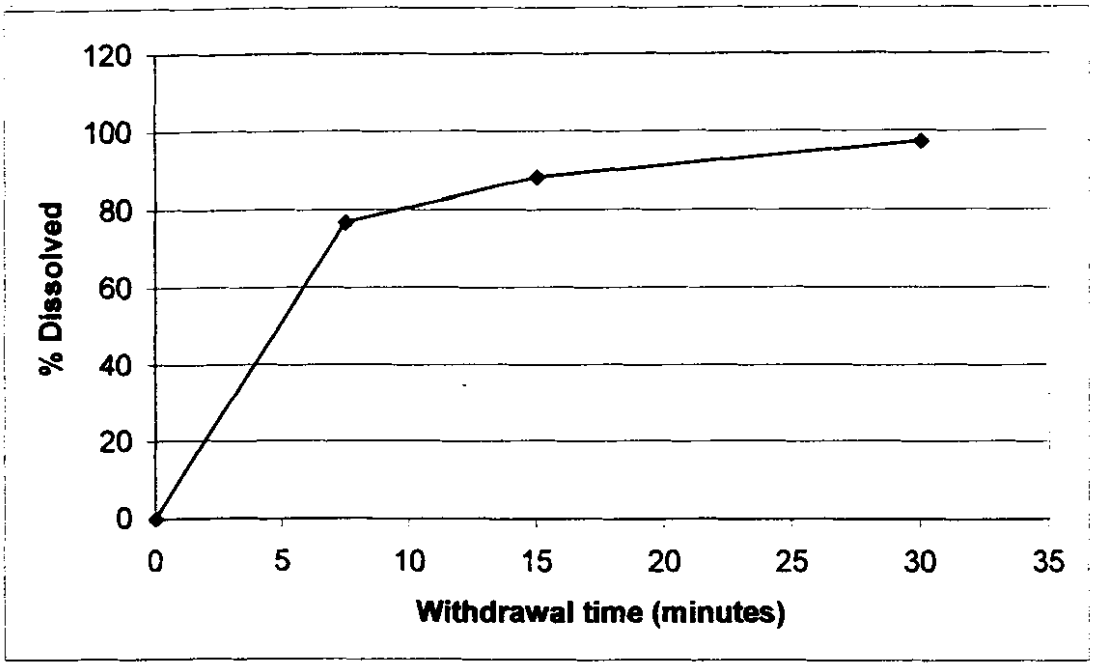

Figure 6.16 Dissolution profile of ZP2.

The calculated similarity factor ($f2$) value was found to be 39.85. The $f2$ value indicated that the dissolution profile of ZP2 differed significantly from form H4.

6.2.1.6 Form ZP3

The dissolution testing results obtained for ZP3 seemed to correspond well with the reference. The results are given in table 6.18 and figure 6.17.

Table 6.18 Dissolution testing results of ZP3

Vessel number	% Dissolved at time interval		
	7½ minutes	15 minutes	30 minutes
1	100.6	101.4	101.0
2	102.8	103.7	102.9
3	101.1	102.8	102.3
4	100.5	100.4	105.6
5	99.6	101.7	103.6
Average	101.0 ±1.2	102.0 ±1.3	103.0 ±1.7

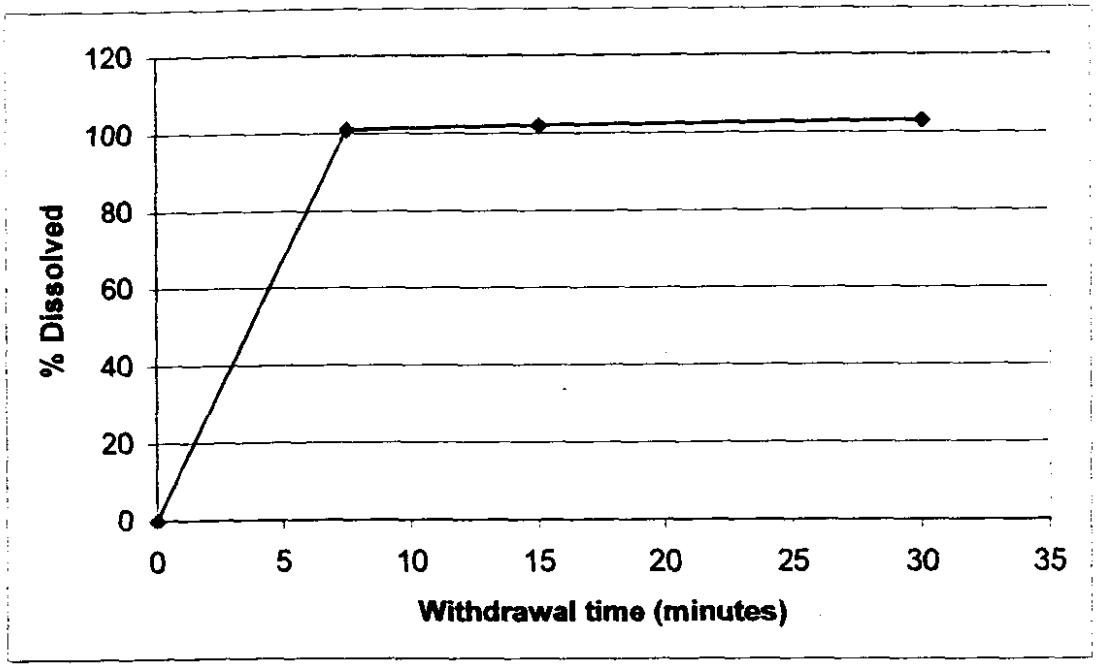

Figure 6.17 Dissolution profile of ZP3 in 0.01 M HCl.

From the dissolution profile of ZP3 it was clear that the sample was fully dissolved within 7½ minutes. The *f2* value (89.35) and confirmed that the dissolution profiles of ZP3 and the reference (H4 sesquihydrate) to be similar.

6.2.2 Desolvated/Dehydrated forms of gatifloxacin

The dissolution behaviour of the dried samples (desolvation/dehydration products) was evaluated. The dissolution behaviour of the following crystal forms will be discussed in this section: anhydrous gatifloxacin, isomorphic desolvate of ZP0, form Ω, form I (anhydrous) and ZP4.

6.2.2.1 Anhydrous gatifloxacin from the sesquihydrate (H4)

The dissolution behaviour of the dried product from the sesquihydrate (form H4) was tested. The results obtained from this study are summarised in table 6.19 and illustrated in figure 6.18.

Table 6.19 Dissolution testing results of anhydrous gatifloxacin

Vessel number	% Dissolved at time interval		
	7½ minutes	15 minutes	30 minutes
1	72.2	84.0	95.7
2	75.0	89.0	99.6
3	67.9	82.1	92.8
4	67.0	83.6	98.7
Average	71.0 ±3.7	85.0 ±3.0	97.0 ±3.1

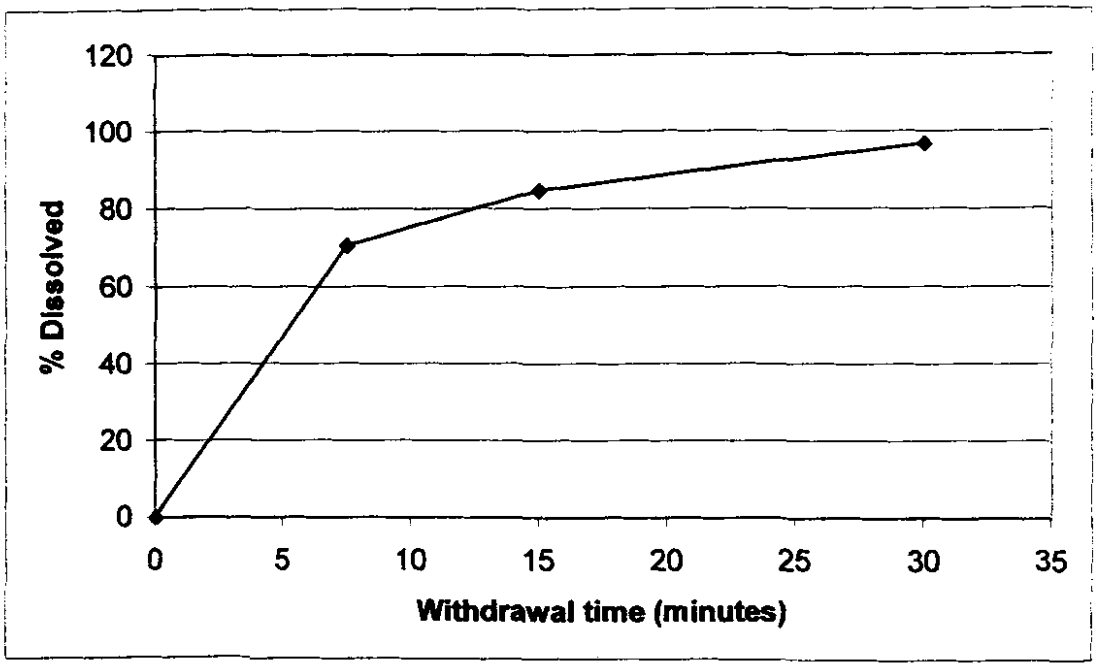

Figure 6.18 Dissolution profile of anhydrous gatifloxacin in 0.01 M HCl.

The dissolution profile was found to differ significantly from the reference dissolution profile, verified by the *f2* value of 35.18.

6.2.2.2 Isomorphic desolvate of ZP0

As discussed in chapter 5, the desolvation of ZP0 produced an isomorphic desolvate (similar XRPD pattern to that of its parent solvated form). Although the XRPD patterns were mostly concordant, it was deemed appropriate to determine whether the presence of the solvent (ethanol) influenced the dissolution behaviour. The dissolution testing results of the isomorphic desolvate are summarised in table 6.20 and illustrated in figure 6.19.

Table 6.20 Dissolution testing results of the isomorphic desolvate ZP0

Vessel number	% Dissolved at time interval		
	7½ minutes	15 minutes	30 minutes
1	83.9	84.9	95.2
2	77.9	87.5	95.6
3	79.5	90.7	97.3
4	84.0	91.8	97.2
5	84.1	90.9	97.5
Average	82.0 ±3.0	89.0 ±2.9	97.0 ±1.1

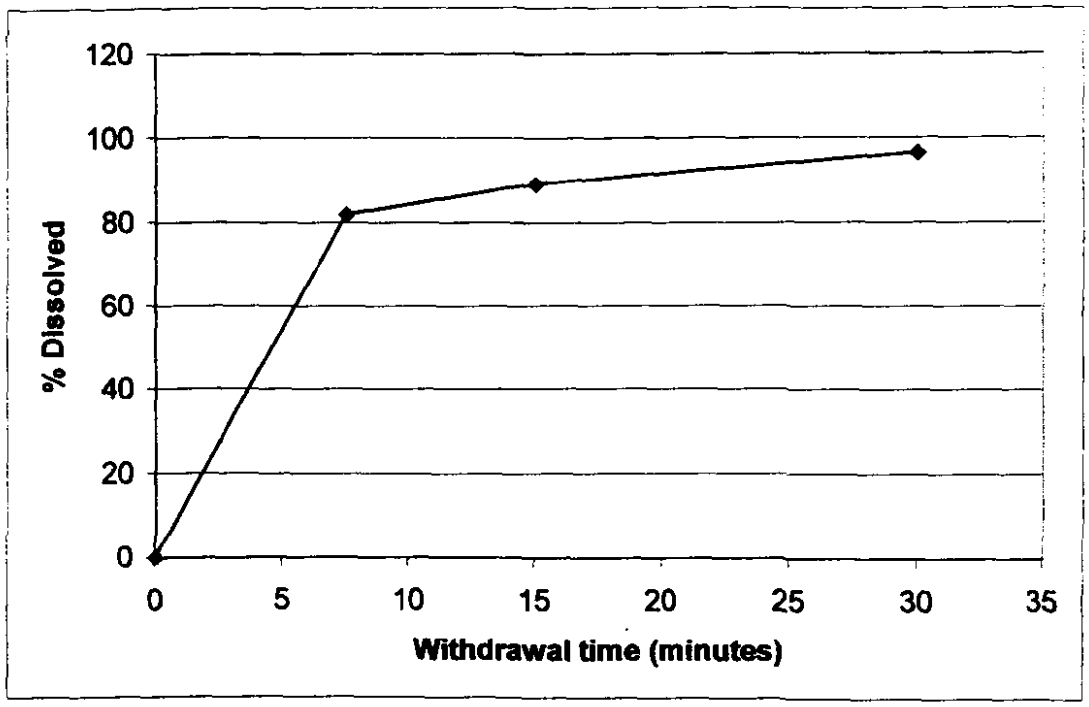

Figure 6.19 Dissolution profile of the isomorphic desolvate of ZP0 in 0.01 M HCl.

To determine whether the dissolution profiles of the solvated form (ZP0) and the isomorphic desolvate were similar, the *f2* value was calculated, using the dissolution profile of the solvated form (ZP0) as the reference. The *f2* value was found to be 55.87, which indicated that the profiles of the parent solvate (ZP0) and its isomorphic desolvate were comparable. It can thus be assumed that the presence of the solvent (ethanol) did not influence the dissolution behaviour of this crystal lattice significantly.

When the dissolution profile of the isomorphic desolvate was compared to the raw material dissolution profile (by means of $f2$) the profiles differed significantly as the $f2$ value was found to be 43.88.

6.2.2.3 Form Ω

Form Ω was found to be the desolvation product of ZP1 and ZP2 (chapter 5). The dissolution testing of both these forms were performed to investigate possible differences in dissolution behaviour between these two desolvated products (both form Ω) obtained from different parent solvates.

The dissolution testing results of form Ω (from ZP1) revealed results as tabulated in table 6.21.

Table 6.21 Dissolution testing results of form Ω (from ZP1)

Vessel number	% Dissolved at time interval		
	7½ minutes	15 minutes	30 minutes
1	100.8	100.6	100.9
2	97.4	98.6	100.7
3	100.8	101.9	102.5
4	97.7	99.1	101.9
5	98.9	100.6	101.4
Average	99.0 ±1.6	100.0 ±1.3	101.0 ±0.7

The calculated $f2$ value for form Ω (from ZP1) equaled 89.35, thereby indicating that the dissolution profiles of form Ω (from ZP1) were similar to the H4 sesquihydrate reference profile.

The results obtained from the dissolution testing of form Ω (from ZP2) revealed the results as tabulated in table 6.22.

Table 6.22 *Dissolution testing results of form Ω (from ZP2)*

Vessel number	% Dissolved at time interval		
	7½ minutes	15 minutes	30 minutes
1	86.9	91.9	96.7
2	86.7	92.7	96.9
3	91.0	92.8	97.0
4	89.2	92.7	96.9
5	89.2	95.1	100.8
Average	89.0 ±1.8	93.0 ±1.2	98.0 ±1.8

To compare the dissolution profiles of form Ω from ZP1 and ZP2, a superimposed dissolution profile (figure 6.20) was plotted.

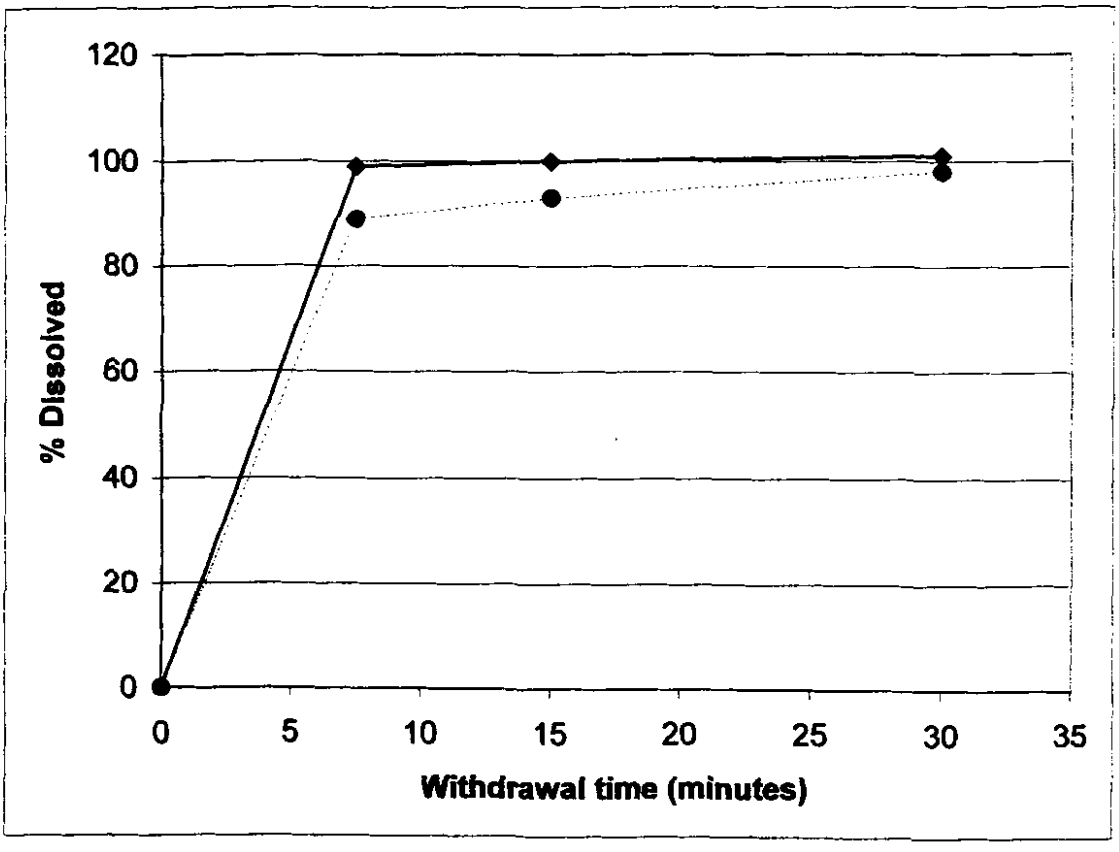

Figure 6.20 Dissolution profile of form Ω from ZP1 (♦) and ZP2 (•) in 0.01 M HCl.

To determine the similarity between the profile of form Ω obtained form ZP1 and ZP2, the *f2* value was determined using the profile of form Ω (from ZP1) as reference. The f2 value was found to be 56.76 which suggested that these two profiles are

comparable. When comparing the dissolution profile of form Ω (from ZP2) to that of the reference, the *f2* value (53.37) verified that the dissolution profile of form Ω (from ZP2) was comparable to that of form H4.

6.2.2.4 Form I anhydrous

Dissolution testing of the anhydrous form I revealed the results displayed in table 6.23 and figure 6.21.

Table 6.23 Dissolution testing results of anhydrous form I

Vessel number	% Dissolved at time interval		
	7½ minutes	15 minutes	30 minutes
1	87.8	93.4	98.5
2	81.5	90.6	97.9
3	73.2	93.9	93.7
4	73.3	94.0	93.6
Average	79.0 ±7.1	93.0 ±1.6	96.0 ±2.6

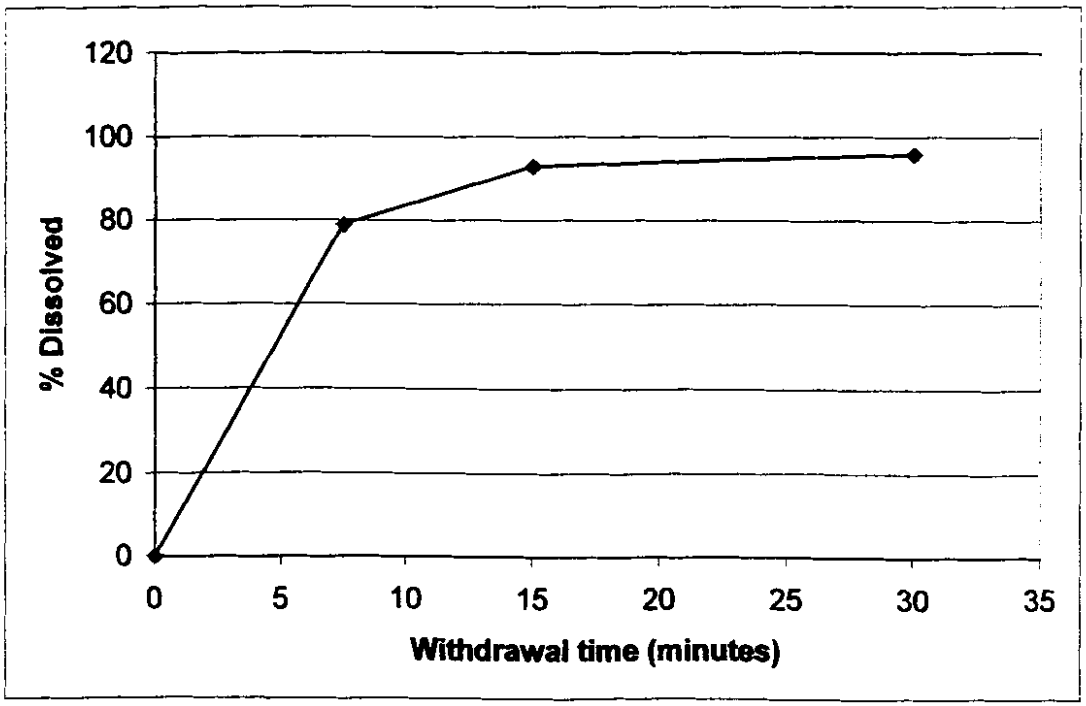

Figure 6.21 Dissolution profile of anhydrous form I in 0.01 M HCl.

The similarity factor ($f2$) for ZP4 indicated that there were significant differences between the profiles of form I anhydrous and the sesquihydrated gatifloxacin ($f2$ value = 42.92).

6.2.2.5 Form ZP4

The powder dissolution results of ZP4 are tabulated and illustrated in table 6.24 and figure 6.22 respectively.

Table 6.24 Dissolution testing results of ZP4

Vessel number	% Dissolved at time interval		
	7½ minutes	15 minutes	30 minutes
1	101.7	102.9	101.2
2	99.7	100.4	100.6
3	98.1	98.5	102.0
4	101.3	101.1	101.1
5	101.5	100.9	102.3
Average	100.0 ±1.5	101.0 ±1.6	101.0 ±0.7

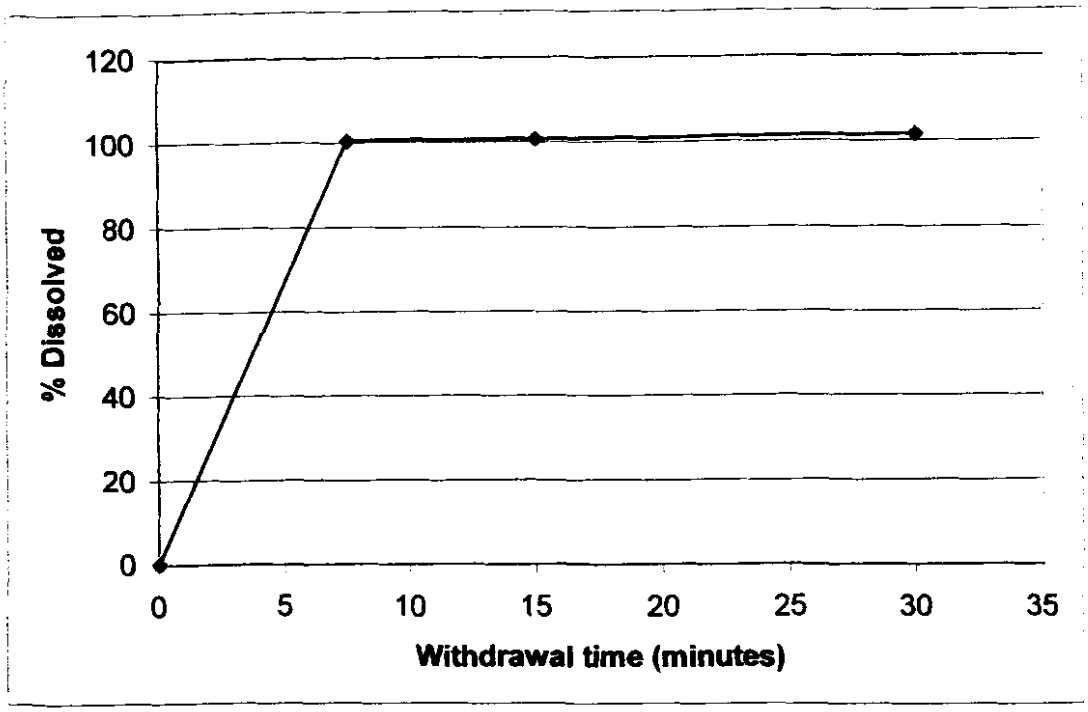

Figure 6.22 Dissolution profile of ZP4 in 0.01 M HCl.

From the dissolution profile of ZP4 it was clear that the sample was fully dissolved within 7½ minutes.

The *f2* value (96.88) indicated that the dissolution profile of ZP4 to be similar to the dissolution profile of form H4 sesquihydrate (reference profile).

Conclusion

To conclude this chapter a summarised overview of the solubility and dissolution behaviour of all the crystal modifications described in this chapter will be discussed.

The differences in solubility behaviour for the various forms are illustrated in figure 6.23.

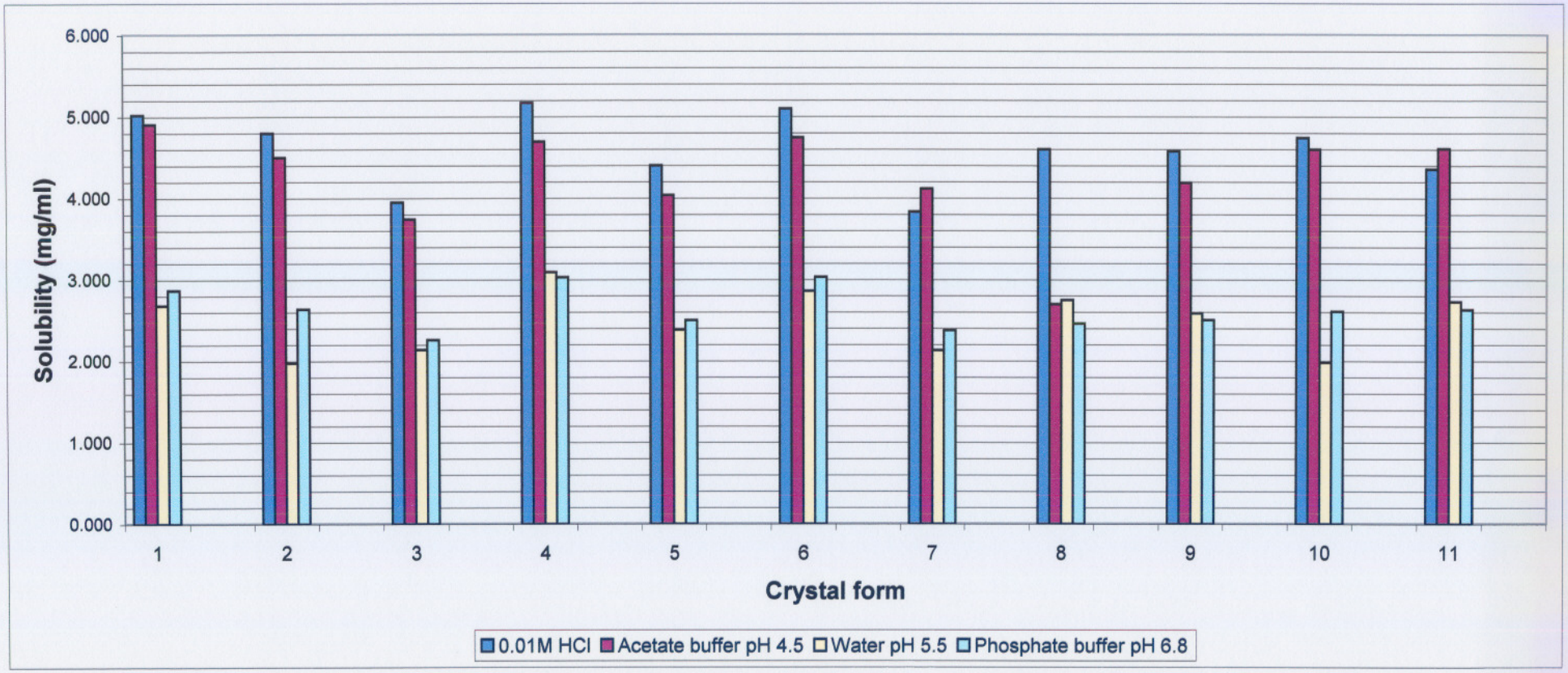

Figure 6.23 Solubility differences for various crystal forms of gatifloxacin. Whereas 1 = anhydrous form from H4, 2 = H4 sesquihydrate, 3 = ZP1 (sesqui-butanol solvate), 4 = Ω, 5 = J (sesquihydrate), 6 = I (anhydrous), 7 = ZP0, 8 = isomorphic desolvate of ZP0, 9 = ZP2 (mono-ethyl acetate solvate), 10 = ZP3 (sesquihydrate) and 11 = ZP4 (anhydrous).

From figure 6.23 it is clear that all the crystal forms were more soluble in 0.01 M HCl than in acetate buffer, except for ZP0. The overall solubility for all forms were in the following order: 0.01 M HCl > acetate buffer > phosphate buffer > milli-Q water except for form Ω, isomorphic desolvate of ZP0, ZP2 and ZP4 (figure 6.23). These forms revealed solubility in the following order: 0.01 M HCl > acetate buffer > milli-Q water > phosphate buffer. Form Ω and form I (figure 6.23) revealed the greatest results of all the forms while ZP0 and ZP1 revealed the poorest solubility results.

Anhydrous gatifloxacin from H4, form Ω and form I revealed solubility results greater than the commercially available sesquihydrate form (number 2, figure 6.23).

ZP2 and ZP4 (figure 6.23) revealed similar solubility behaviour in the various media.

From the three sesquihydrated forms (numbers 2, 5 and 10) it was observed that H4 and ZP3 revealed similar solubility results that differed from form J. Form J was more soluble in milli-Q water and phosphate buffer compared to the solubility of forms H4 and ZP3 in milli-Q water and phosphate buffer.

As discussed in chapter 1, an extremely high solubility may result in an increased bioavailability, whereas poor solubility may result in insufficient drug delivery.

From this study it was clear that the different gatifloxacin crystal modifications (polymorphs and pseudopolymorphs) exhibited significant differences in solubility in the different media, thus care should be taken to select the most appropriate crystal form for pharmaceutical manufacturing.

An overlay of all the dissolution profiles of the different forms is given in figure 6.24.

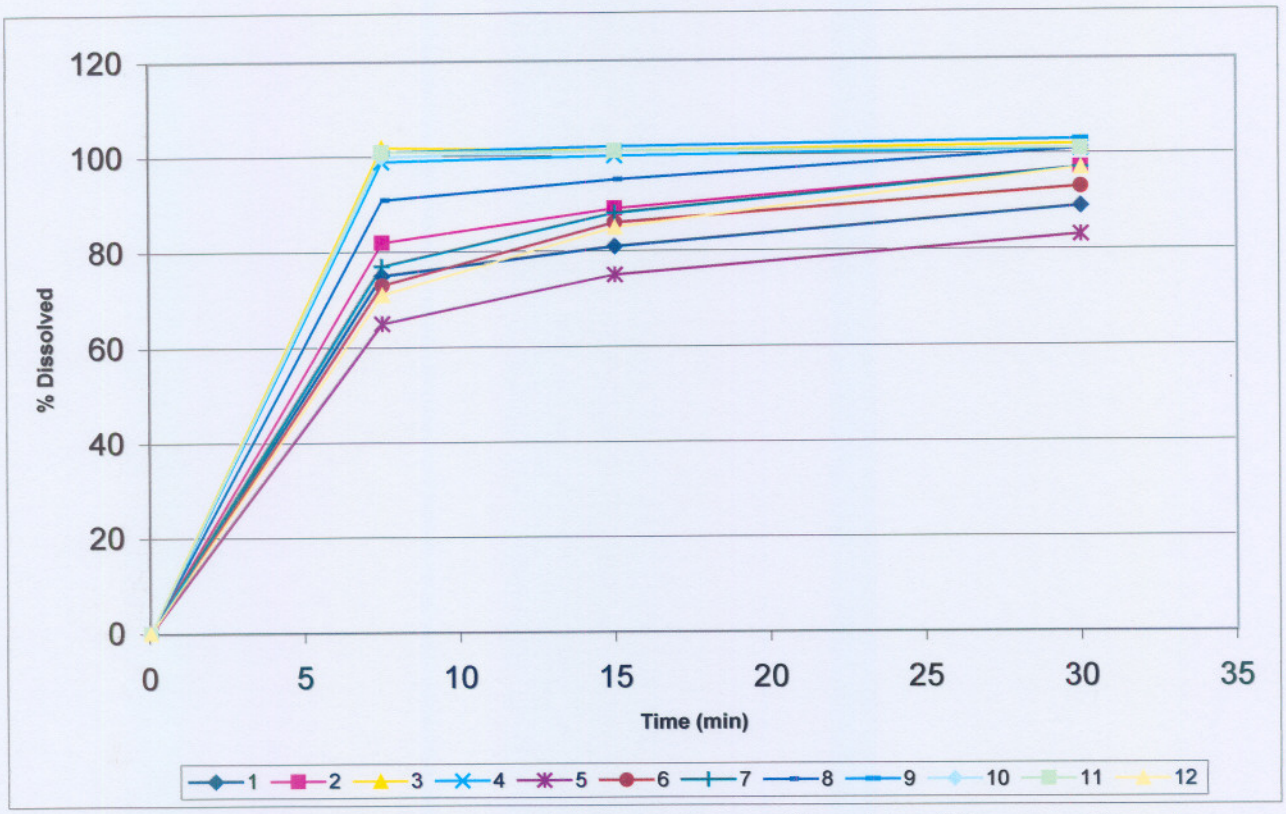

Figure 6.24 Comparison between the dissolution profiles of the different gatifloxacin crystal modifications. Whereas 1 = ZP0, 2 = isomorphic desolvate of ZP0, 3 = ZP1, 4 = Ω (from ZP1), 5 = Form J (sesquihydrate), 6 = I anhydrous, 7 = ZP2, 8 = Ω (from ZP2), 9 = ZP3, 10 = ZP4, 11 = Sesquihydrate (H4), 12 = Anhydrous gatifloxacin.

Table 6.25 Comparison between the dissolution behaviour of the different gatifloxacin crystal modifications

Form	*f*2 value	Similarity to reference dissolution profile	75% ≥ dissolved in 30 minutes
ZP0	34.74	No	Yes
Isomorphic desolvate of ZP0	43.88	No	Yes
ZP1	96.88	Yes	Yes
Form Ω (from ZP1/2)	89.35	Yes	Yes
Form J (sesquihydrate)	27.89	No	Yes
Form I anhydrous	42.92	No	Yes
ZP2	39.85	No	Yes
ZP3	89.35	Yes	Yes
ZP4	96.88	Yes	Yes
Anhydrous	35.18	No	Yes

It was observed that the dissolution profiles of ZP1, form Ω (from ZP1 and ZP2), ZP3 and ZP4 were similar to that of the current commercially favoured crystal form (H4-sesquihydrate). This observation stimulated the idea that these forms may be therapeutically equivalent. With further study on these crystal forms, a proposal for the incorporation of these crystal forms (desolvated forms – form Ω or ZP4) into appropriate dosage forms might arise.

Chapter 7

Polymorphic behaviour of gatifloxacin crystal modifications

Introduction

This chapter takes an in depth look into the behaviour of one gatifloxacin crystal modification (ethanol solvate). Preliminary studies revealed great inconsistency in the data obtained from recrystallisation products using different batches of ethanol as recrystallisation solvent.

A previously described crystal form, form E, an ethanol solvate (patent number US 6,413,969), was obtained by a recrystallisation process using 90-95% ethanol. Form E has been described as a six-sided platelet ethanol solvate with gigantic solvent channels, causing it to be extremely unstable in the absence of the mother liquor. However no physico-chemical data were available to characterise and describe this crystal form. The thermodynamic instability of form E is summarised in figure 7.1. Drying of form E produced a hemi-hydrate (form TE), which probably contained traces of form T2RP. The exposure of form E and TE to an aqueous environment produced a hexa-hydrate (form H6) and a sesqui-dihydrate (form RP) respectively.

As discussed in chapter 5, section 5.1.1, an ethanol solvate (ZP0) was prepared by a recrystallisation method using absolute ethanol as recrystallisation solvent. This pseudo-polymorph was however found to be fairly stable as VT-XRPD studies did not show a significant change in the crystal lattice during desolvation (section 5.1.1- figure 5.1).

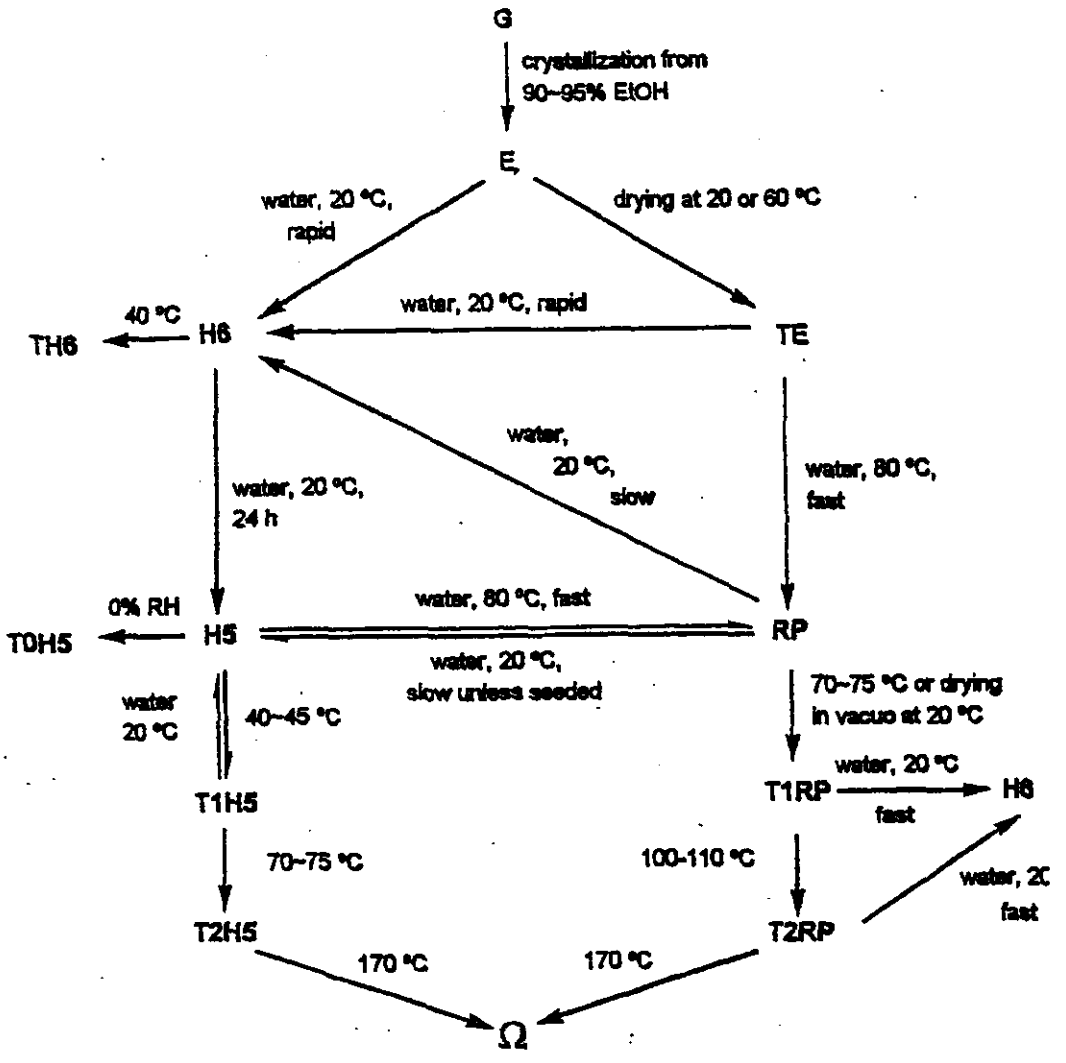

Figure 7.1 Summary of gatifloxacin ethanol solvate and the behaviour thereof (Raghavan *et al.*, 2002:1-18).

This chapter focuses on the different recrystallisation products obtained from various grades of ethanol and binary mixtures of ethanol and water. The aim of this chapter was to establish whether the presence of water in the organic recrystallisation solvent influenced the crystal form obtained.

7.1 Methods and materials

Byrn *et al.* (1999:244) reported that it is common practice to use mixtures of solvents in the crystallisation process of API's. The addition of an *anti-solvent* is often employed to speed-up the crystallisation process as the anti-solvent decreases the solubility of the solute in the solvent. By adding an anti-solvent to the solvent it often happens that crystals with different solvate composition and stoichiometry are formed due to the presence of two solvents (the solvent and the anti-solvent) in different ratios. The crystal form that will eventually form from the solution is at that ratio where it is the most favourable for that crystal form to grow (Byrn *et al.*, 1999:244).

A similar approach was used to evaluate the influence of water present in a recrystallisation solvent by preparing various ethanol recrystallisation solvents:

A – Absolute ethanol (99-100%)
B –Ethanol (95%)
C –Ethanol:water (75:25)
D –Ethanol:water (50:50)
E –Ethanol:water (25:75)

Solvents A-E were used as recrystallisation solvents using the recrystallisation method described in chapter 3. The various recrystallised products obtained from these solvents were then analysed by means of XRPD, TGA, KF, DSC and DRIFT-IR spectrometry. The XRPD patterns of the various products from solvents A-E are illustrated in figure 7.2.

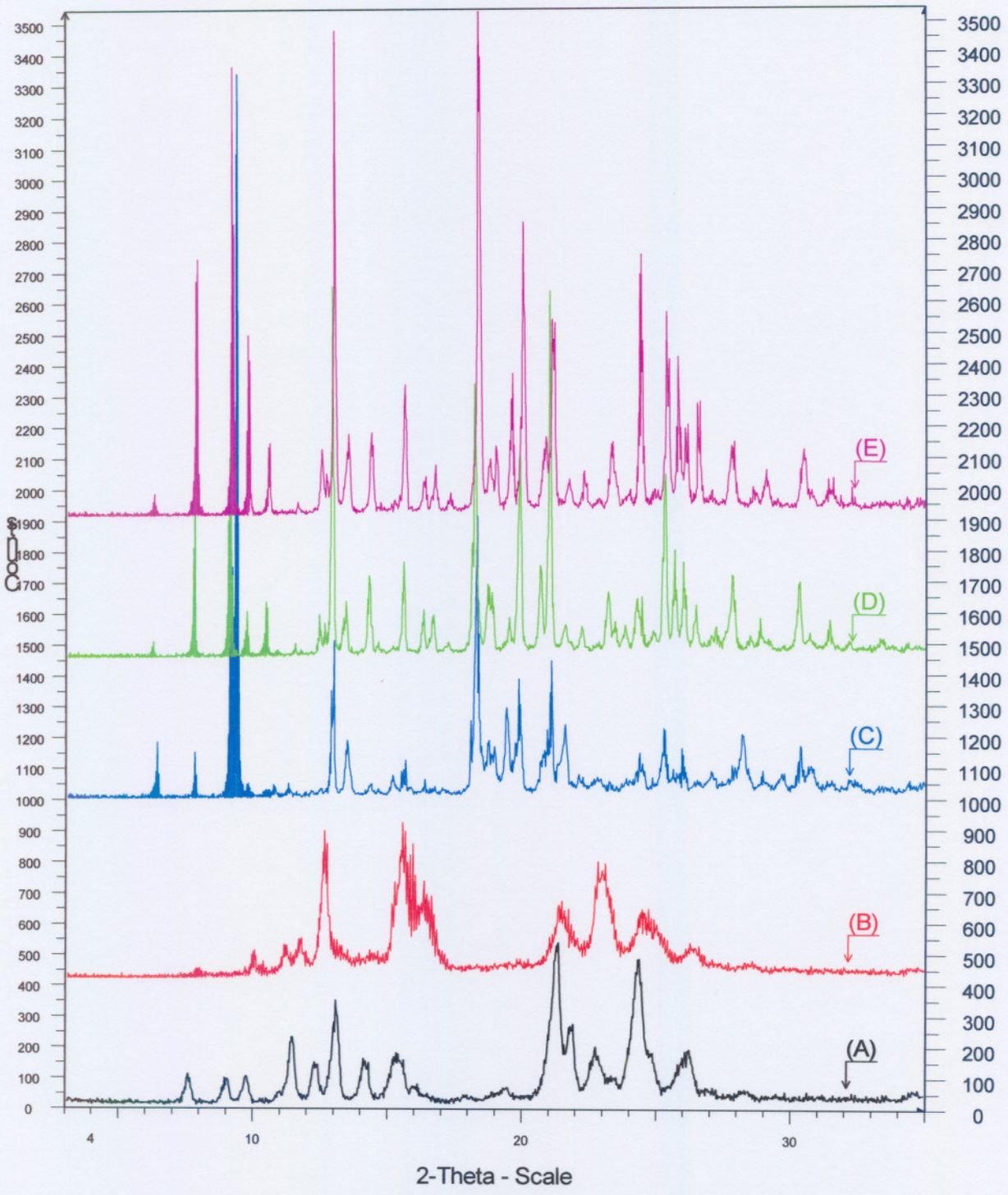

Figure 7.2 XRPD patterns of the samples obtained from recrystallisation solvents A-E, whereas (A) is absolute ethanol (99-100%), (B) is ethanol (95%), (C) is ethanol:water (75:25), (D) is ethanol:water (50:50) and (E) is ethanol:water (25:75).

From the XRPD patterns of the various recrystallisation products (from solvents A-E) it was clear that different crystal forms were obtained from the different solvents. The physico-chemical properties of each crystal product will be discussed in sections 7.2 to 7.6.

7.2 Recrystallisation study using absolute ethanol (99-100%) as solvent

The physico-chemical properties of the recrystallisation product obtained using 99-100% ethanol as recrystallisation solvent are discussed in chapter 5, section 5.1.1. These results revealed a mono-ethanol solvated crystal form (ZP0) of gatifloxacin, which produced an isomorphic desolvate upon drying.

7.3 Recrystallisation study using ethanol (95%) as solvent

Recrystallisation of gatifloxacin using 95% ethanol produced an unstable crystal form. The XRPD pattern of this form differed significantly from that of the recrystallised product obtained when using absolute ethanol (99-100%). TGA (figure 7.7) and KF analysis of this sample revealed a percentage weight loss of 15.0% and a water content of 3.0% respectively. The theoretical % ethanol present in a mono-ethanol solvate of gatifloxacin is 10.9%, and the theoretical water content for a monohydrated form should be 4.6%. Thus, this crystal form was classified as a mono-ethanol-hemihydrated form (i.e. solvated-hydrate).

The mono-ethanol hemihydrated sample was exposed to ambient conditions for 45 minutes. TGA and KF titration of the exposed sample revealed a total percentage weight loss of 2.7% and a water content of 3.1%, which indicated that this form transformed into a hemi-hydrated form. The XRPD patterns of these two forms were compared to the XRPD patterns of previously described crystal forms. It was found that the XRPD pattern of the mono-ethanol-hemi-hydrate showed resemblances to the XRPD pattern of form P, while the hemi-hydrate resembled the XRPD pattern of form T1 (figure 7.3 and 7.4).

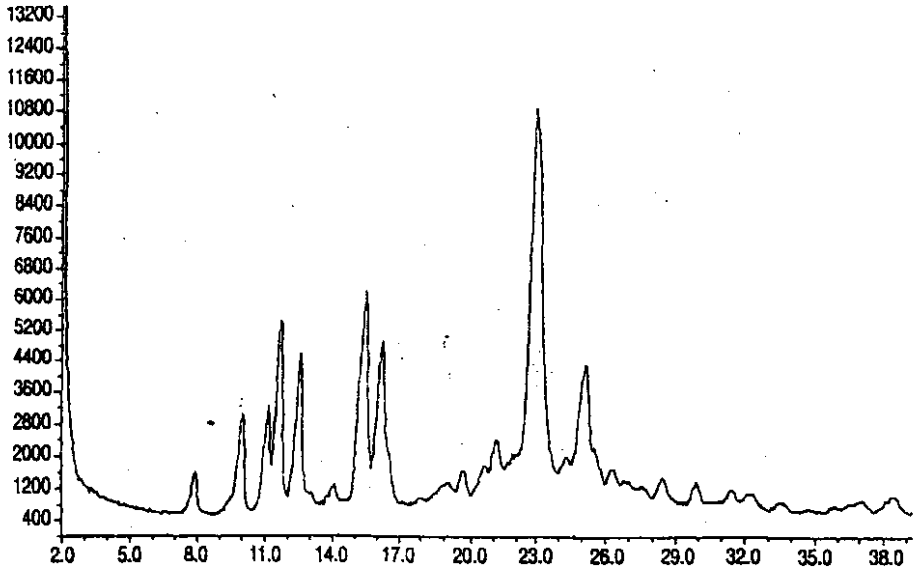

Figure 7.3 XRPD pattern of form P (Niddam-Hildesheim *et al.*, 2004c:6).

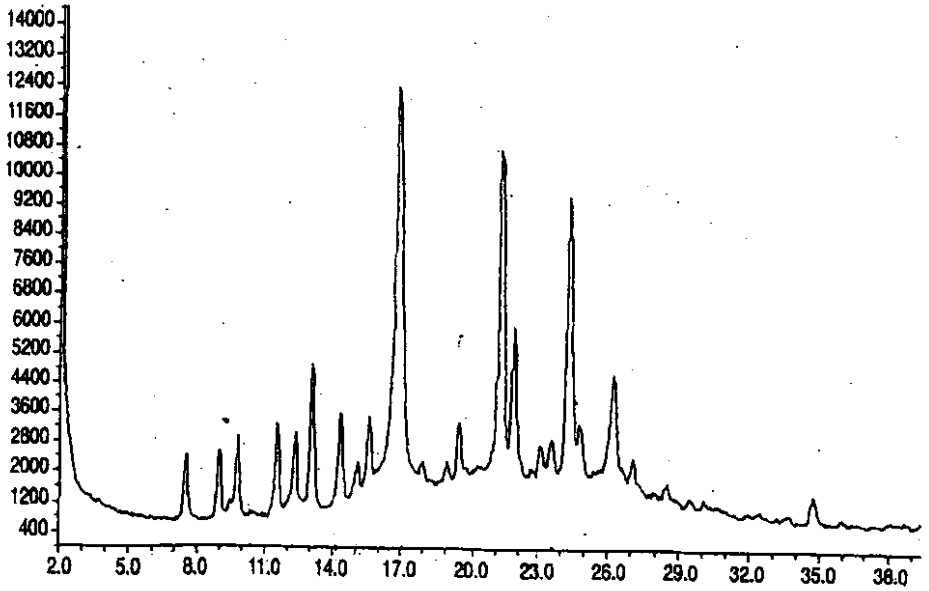

Figure 7.4 XRPD pattern of form T1 (Niddam-Hildesheim *et al.*, 2004c:7).

The available literature on both these forms (P and T1) did not clearly indicate whether these forms were polymorphs or pseudo-polymorphic forms (no available physico-chemical data were presented except for XRPD patterns). This study made it possible to classify form P as a mono-ethanol-hemi-hydrate and form T1 as a hemi-hydrate. The literature stated that form T1 is the dried product of form P (Niddam-Hildesheim *et al.*,

2004c:2), however in this study it was found that form P spontaneously transformed into form T1 at ambient conditions within 45 minutes.

According to Niddam-Hildesheim *et al.* (2004c:1-8) it was also stated that form P converts into a sesquihydrated form when exposed to ambient conditions. This statement (with the understanding that form P converts first into form T1) was investigated. Form P was exposed to ambient conditions. Samples were withdrawn at two weeks, four weeks and three months intervals, and analysed. The XRPD patterns confirmed the transformation into form H4 (sesquihydrate). A schematic representation of the polymorphic conversion is illustrated in figure 7.5.

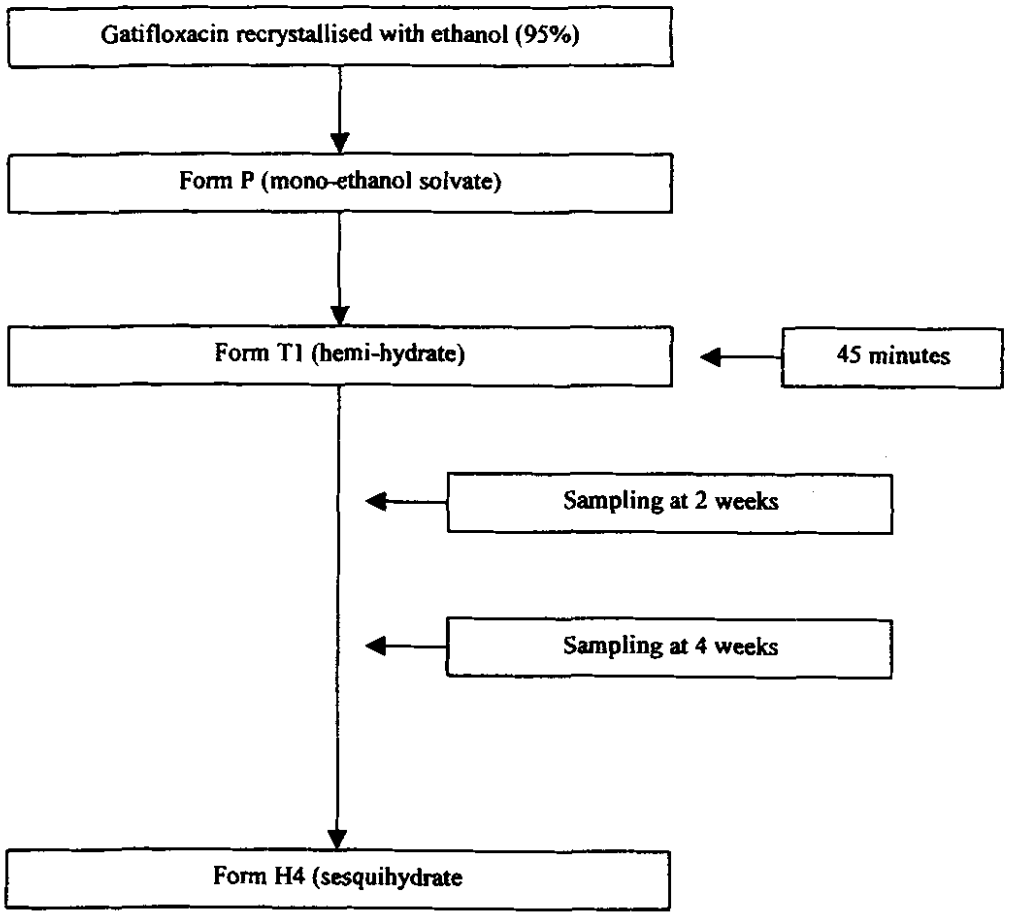

Figure 7.5 Schematic representation of the polymorphic conversion of the recrystallisation product from ethanol (95%).

As illustrated in figure 7.1, form E displayed a similar polymorphic transition tendency. Form E was the recrystallised product from 90-95% ethanol that was found to be unstable when removed from the mother liquor. From figure 7.1 it was observed that form E converted into form TE (hemi-hydrate) upon drying. It can thus be suggested that form E might be related to form P, and also that form T1 may be related to form TE.

The XRPD patterns of form P, T1 and the conversion thereof to form H4 are illustrated in figure 7.6.

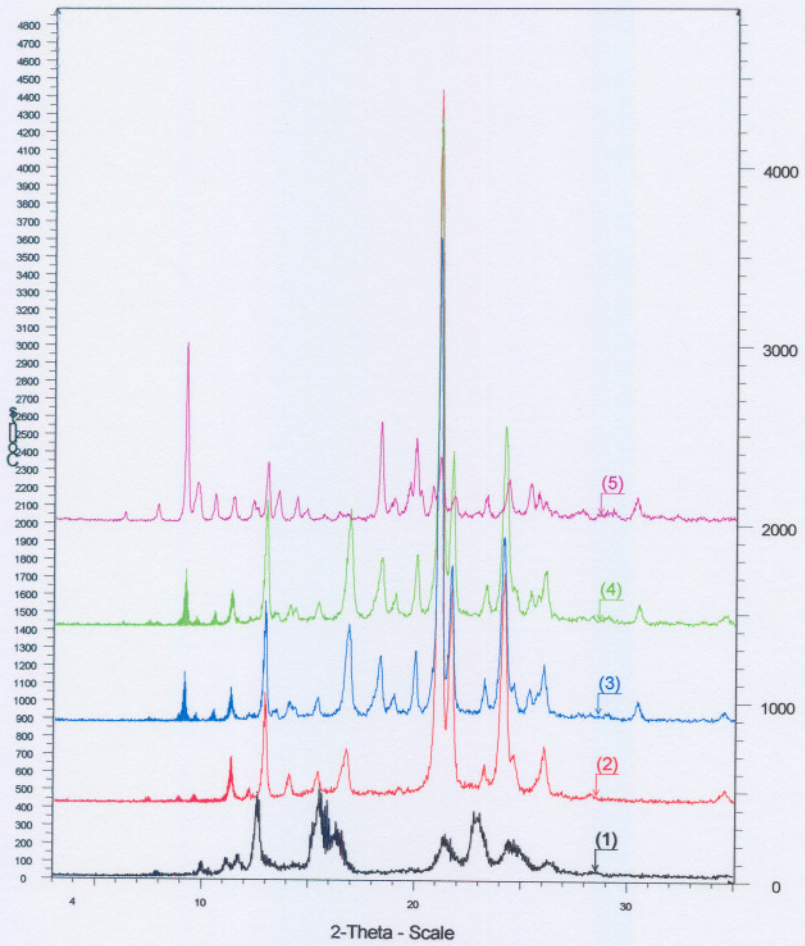

Figure 7.6 Superimposed XRPD patterns of form P, T1 and the conversion thereof to form H4, whereas (1) is form P, (2) is Form T1, (3) is sample after 2 weeks of exposure to ambient conditions, (4) is the sample after 4 weeks exposure to ambient conditions and (5) is the sample after 3 months of exposure to ambient conditions.

The thermal behaviour of form P is illustrated in figure 7.7.

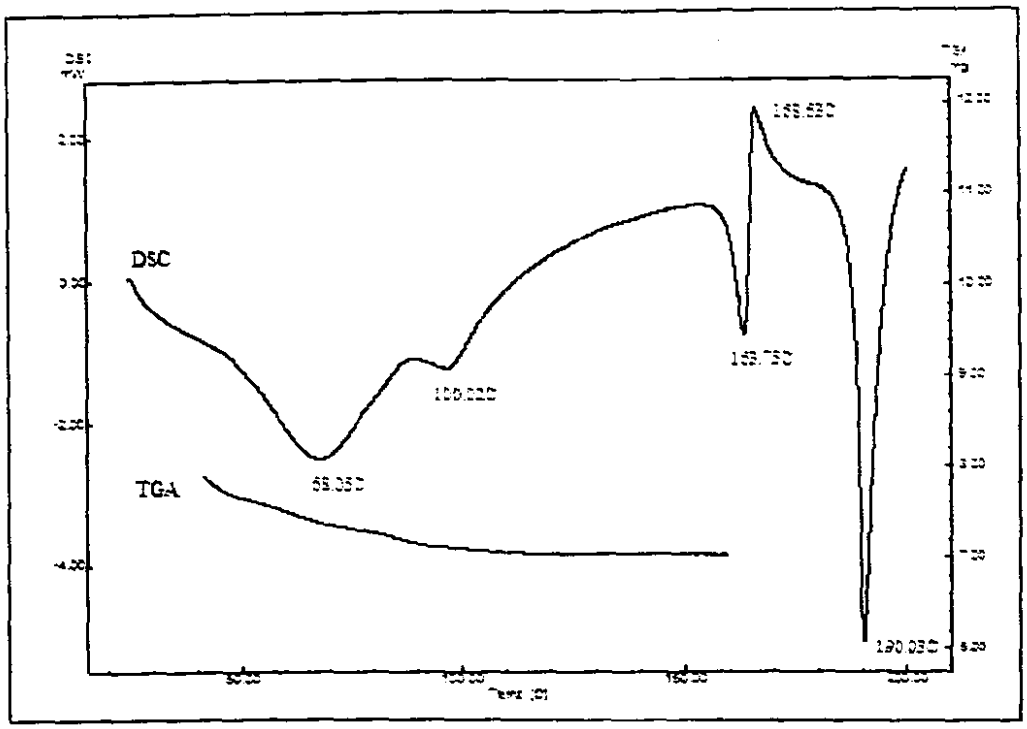

Figure 7.7 Superimposed DSC and TGA thermograms of form P.

From the DSC thermogram (figure 7.7) the desolvation of ethanol was observed at 68.05°C and the dehydration process was recorded at a peak maximum of 100.02°C. The TGA thermogram revealed a weight loss that occurred from 40-106°C supporting the observation of the loss of ethanol and water. A melting endotherm was observed at 163.75°C followed by a recrystallisation exotherm at 168.63°C. The melting point at 190.03°C indicated the melting of the recrystallised product. HSM observations confirmed the thermal events observed in DSC thermogram. These events are discussed in table 7.1.

7.4 Recrystallisation study using a mixture of 75% ethanol and 25% water as solvent

The recrystallisation product from this mixture was found to differ from the forms described in section 7.2 and 7.3. The recrystallisation product obtained revealed a total % weight loss (TGA) of 15.5% (figure 7.9) and a total water content of 8.6% (KF). Theoretical ethanol content for a hemi-ethanol solvate is 5.5%, while the theoretical water content for a sesquihydrate is 6.9%. Thus the recrystallisation product from this mixture was classified as a hemi-ethanol-sesquihydrated form of gatifloxacin. The XRPD pattern of this crystal form is illustrated in figure 7.8.

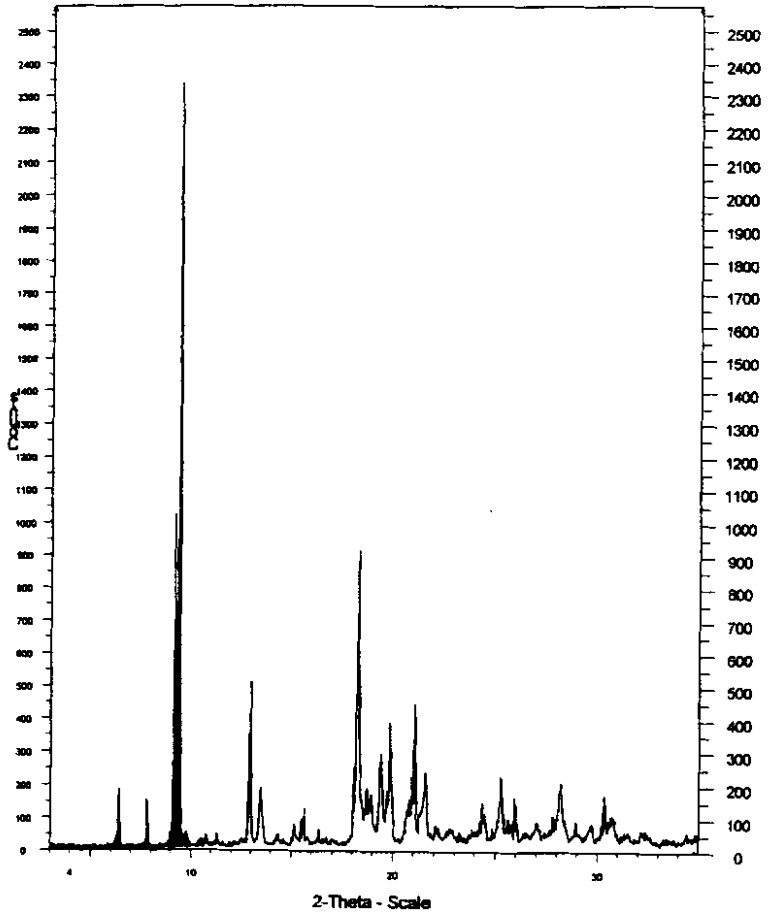

Figure 7.8 XRPD pattern of the recrystallisation product using ethanol: water (75:25) as solvent.

The DSC thermogram revealed a desolvation peak at 82.25°C (ethanol) and the dehydration at 105.29°C. A melting endotherm was observed at 166.22°C, followed by a recrystallisation exotherm at 172.25°C. The recrystallised product melted at 191.03°C. The TGA supported the desolvation and dehydration observations from the DSC thermogram. The DSC and TGA thermograms of the sample are illustrated in figure 7.9.

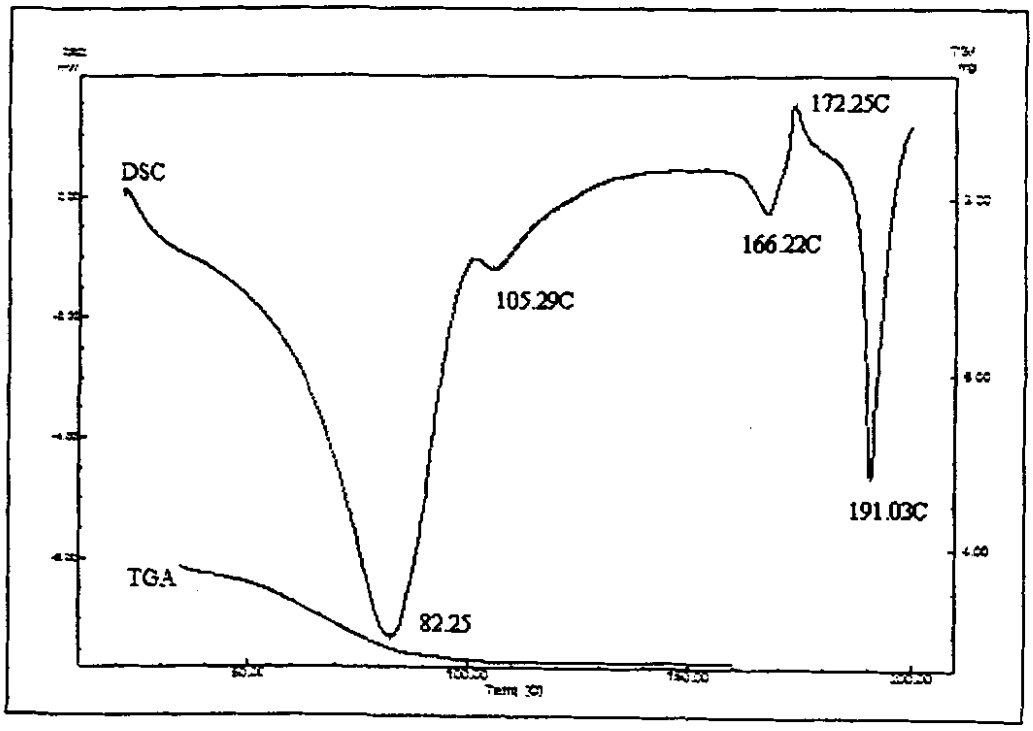

Figure 7.9 Superimposed DSC and TGA thermograms of the sample obtained using ethanol:water (75:25) as solvent.

HSM microscopy confirmed the observations as discussed. HSM observations are discussed in table 7.1.

7.5 Recrystallisation study using a mixture of 50% ethanol and 50% water

The resulting product from this recrystallisation revealed a total % weight loss (TGA) of 7.2% (figure 7.11) and a total water content of 8.1% (KF). These results suggested that this crystal form mainly contained water and may therefore be classified as a sesquihydrate (theoretical water content for a sesquihydrate is 6.9%). The XRPD pattern of this crystal form is illustrated in figure 7.10. It was found that the XRPD pattern obtained for this sample resembled that of the commercially favoured sesquihydrate (H4).

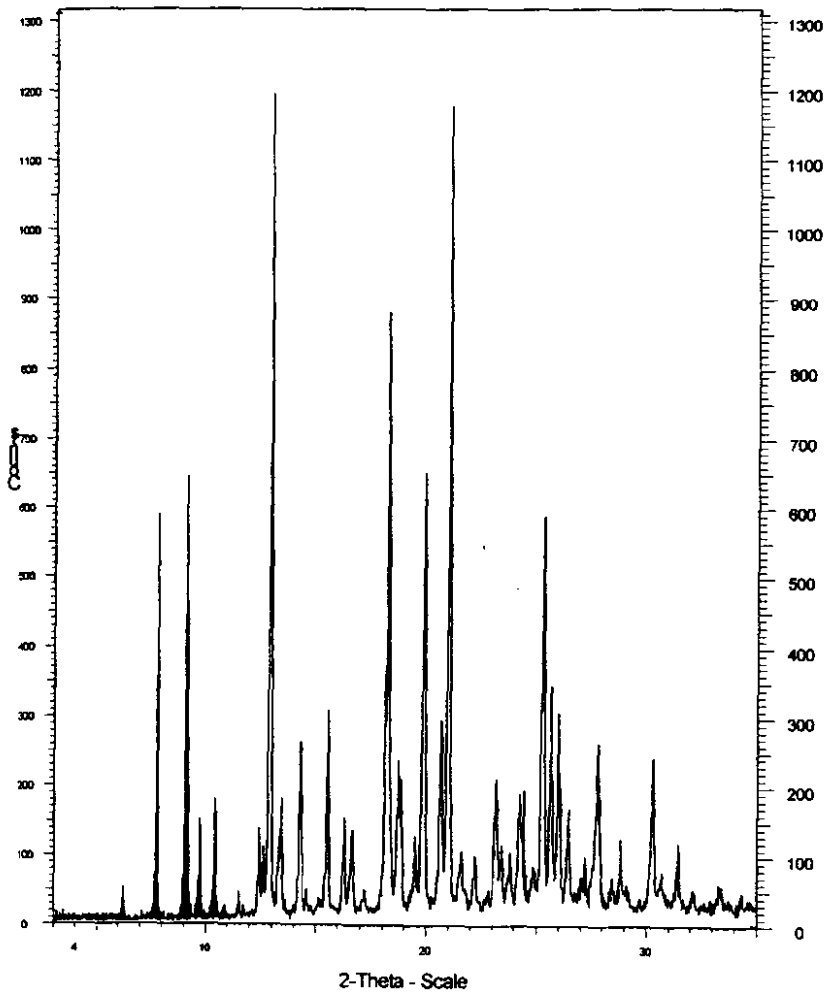

Figure 7.10 XRPD pattern of the recrystallisation product from ethanol:water (50:50) as solvent.

Since the recrystallised product was found to be a sesquihydrated form, it was anticipated that the DSC thermogram should reveal only one dehydration peak at 100°C (boiling point of water) and that the desolvation peak should be absent. The superimposed DSC and TGA thermograms are illustrated in figure 7.11.

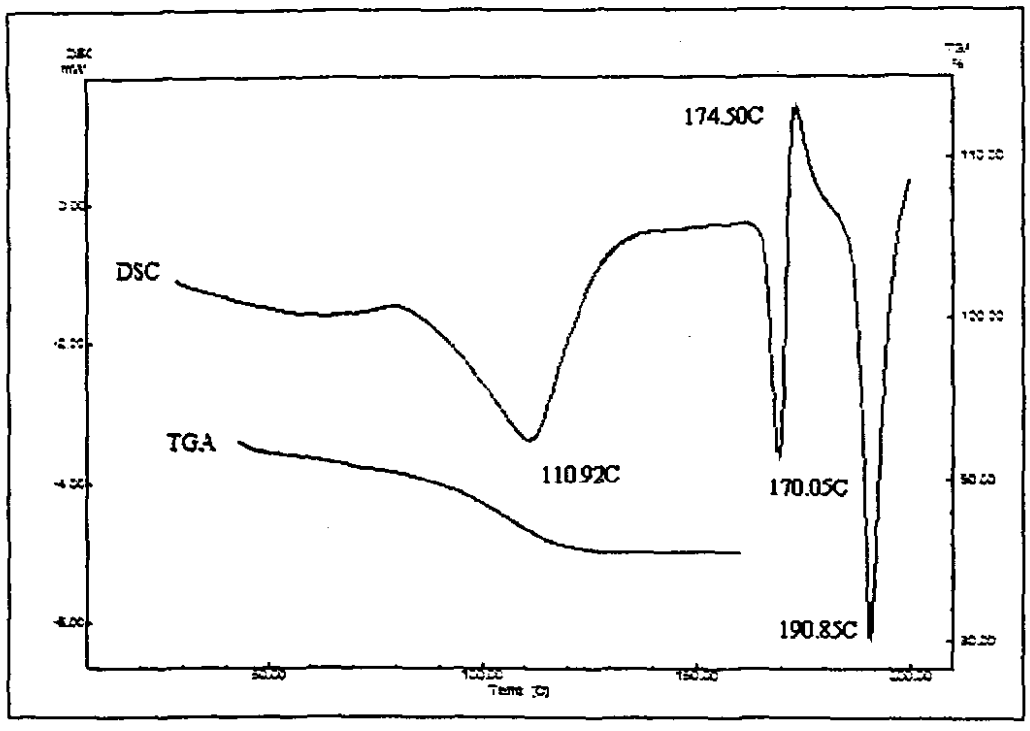

Figure 7.11 Superimposed DSC and TGA thermograms of the sample obtained from the ethanol:water (50:50) mixture as solvent.

The DSC thermogram did indeed reveal only one endothermic peak at 110.92°C that indicated the dehydration of the sample. The TGA supported this observation as the maximum weight loss occurred between 95-110°C. As with the recrystallised products from solvents A-C, a melting endotherm, followed by a recrystallisation exotherm and a final melting point were observed form this sample. The HSM observations (as discussed in table 7.1) confirmed these thermal events.

7.6 Recrystallisation study using a mixture of 25% ethanol and 75% water as solvent

The XRPD pattern obtained from this study was similar to that of the sample obtained from the 50:50 mixture (section 7.5). The total weight loss (TGA) was found to be 8.1% whilst the KF analysis revealed a total water content of 8.2%, therefore this crystal form was also classified as a sesquihydrate. The superimposed XRPD patterns of the recrystallisation products of the ethanol:water (50:50) mixture and the ethanol:water (25:75) mixture are illustrated in figure 7.12. The XRPD pattern revealed that the two forms obtained from the ethanol:water (50:50) and (25:75) mixtures were comparable (slight differences present in the 18-20 °2θ region). As mentioned in section 7.5, the XRPD pattern of the sample obtained from the ethanol:water (50:50) mixture was found to resemble the XRPD pattern of the commercially favoured H4 sesquihydrated form, therefore the sample from the ethanol:water (25:75) mixture was also identified as form H4 (sesquihydrate).

The DSC thermogram of this sample was comparable to the DSC thermogram of the sesquihydrate as discussed in section 7.5 (figure 7.11).

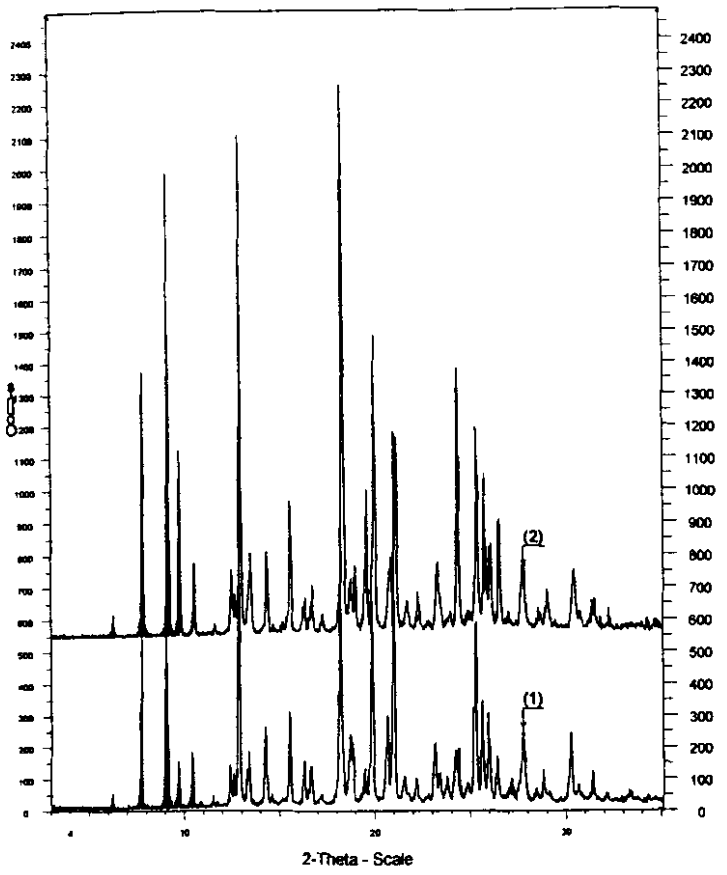

Figure 7.12 Superimposed XRPD patterns of the recrystallisation products obtained using a ethanol:water (50:50) mixture (1) and ethanol:water (25:75) mixture (2) as recrystallisation solvents respectively.

7.7 Discussion

From sections 7.1-7.6 it is clear that different crystal forms with varying amounts of solvent (water and ethanol) incorporated into the crystal lattices, were produced from the recrystallisation solvents A-E. To investigate the differences between these forms, the DSC and TGA thermograms of these forms were superimposed to provide an overall perspective of the influence of water present in a recrystallisation solvent on the thermal behaviour of the various crystal forms produced. It should be noted that the DSC and TGA thermograms of the sample from solvent E were not included as the samples from solvent D and E were both the same sesquihydrated form.

The superimposed TGA thermograms of the samples from the recrystallisation solvents (A-D) are illustrated in figure 7.13. The desolvation step and dehydration step correlated well with the boiling point of ethanol and water respectively.

Figure 7.13 and KF titrations indicated that the % ethanol incorporated in the crystal forms decreased as the % ethanol in the recrystallisation solvent decreased (from A-E), while the % water incorporated in the crystal forms increased as the water in the recrystallisation solvent increased (from A-E).

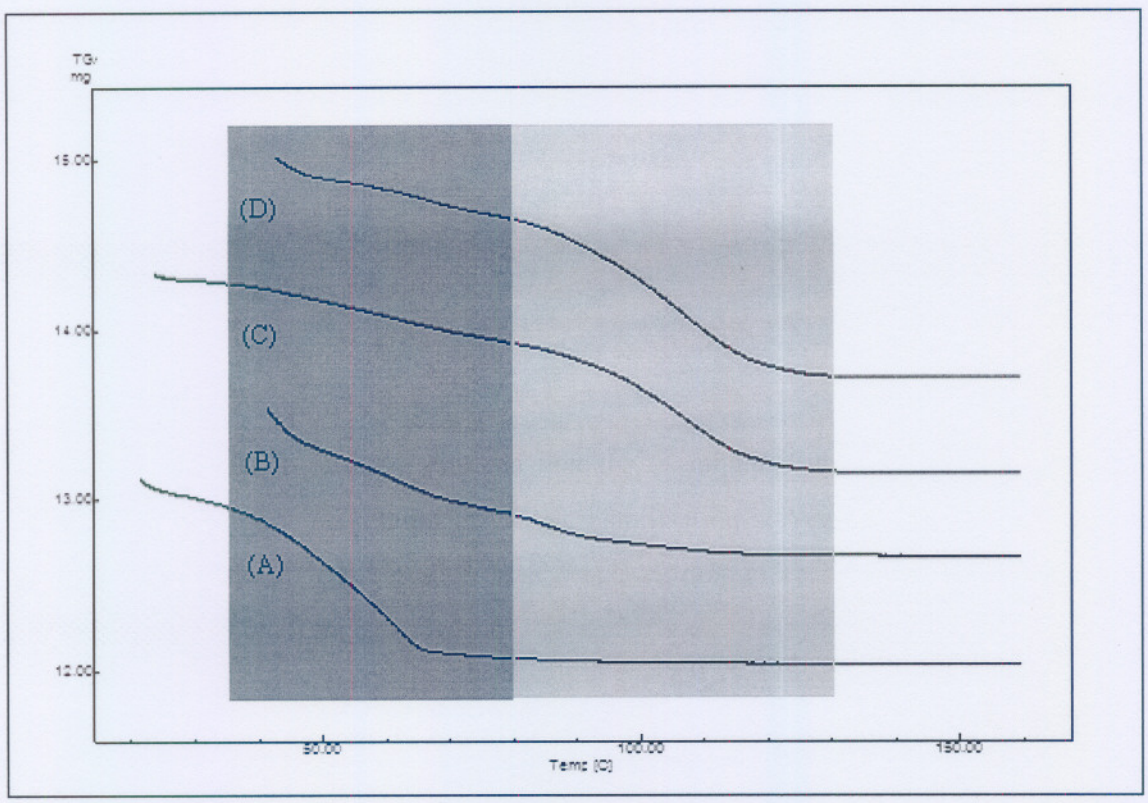

Figure 7.13 Superimposed TGA thermograms of samples obtained from solvents A-E, whereas (A) is absolute ethanol, (B) is ethanol (95%), (C) is ethanol:water (75:25), (D) is ethanol:water (50:50). The lighter shade of gray indicates temperature regions associated with dehydration and the darker shade indicates temperature regions associated with desolvation.

From figure 7.13 it was observed that the desolvation onset and endset temperatures were influenced by the presence of water in the recrystallisation solvent. Figure 7.13 clearly indicated that the weight loss step associated with dehydration (80-120°C) became more prominent with an increase in the water content of the recrystallisation solvent.

The superimposed DSC thermograms of the samples obtained from solvents A-D are illustrated in figure 7.14.

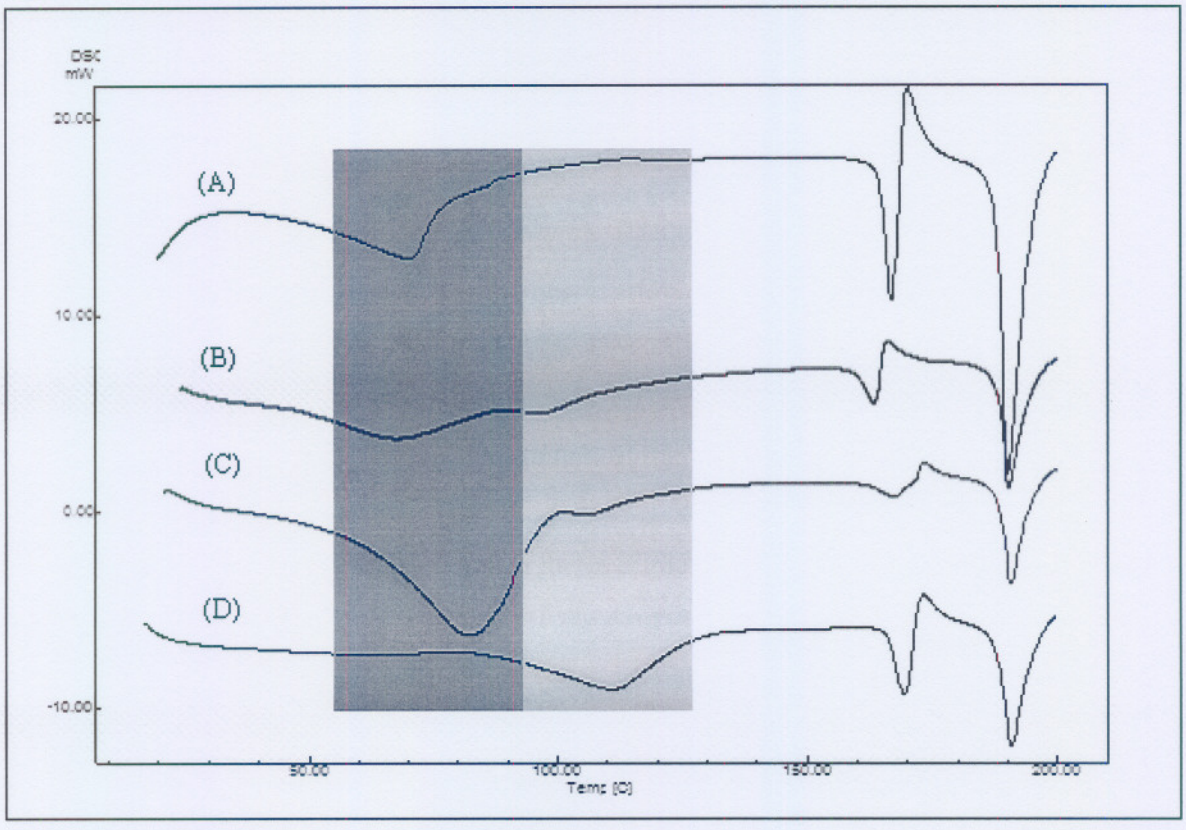

Figure 7.14 Superimposed DSC thermograms of samples obtained from solvents A-E, whereas (A) is absolute ethanol, (B) is ethanol (95%), (C) is ethanol:water (75:25), (D) is ethanol:water (50:50). The lighter shade of gray indicates temperature regions associated with dehydration and the darker shade indicates temperature regions associated with desolvation.

From figure 7.14 it was observed that the dehydration endotherm (at 90-120°C) became more prominent with increased water content of the recrystallisation solvent, while the desolvation endotherm (ethanol desolvation) was decreased into inexistence. The TGA thermograms revealed a shift in the desolvation onset and endset temperatures as the water content of the crystal increased, confirming the DSC observations.

HSM observations correlated well with the DSC thermogram events. The HSM observations are discussed in table 7.1.

Table 7.1 Photomicrographs of the HSM events observed for the forms from different ethanol:water mixtures (without silicon oil) Whereas: 1 is the initial, 2 is indicative of desolvation/dehydration (darkened crystals), 3 is melting, 4 is recrystallisation from the melt, 5 is the melting of recrystallised product.

#	**Mono-ethanol solvate (Solvent A)**	**Mono-ethanol hemihydrate (Solvent B)**	**Hemi-ethanol sesquihydrate (Solvent C)**	**Sesquihydrate (Solvent D)**
1	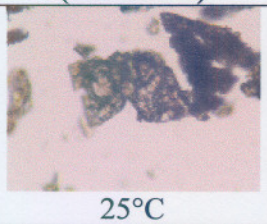 25°C	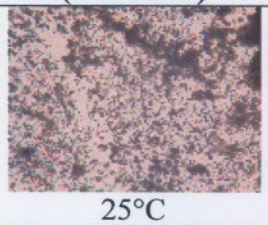 25°C	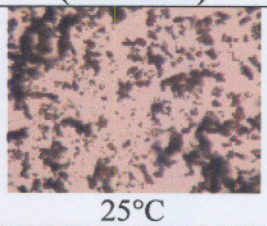 25°C	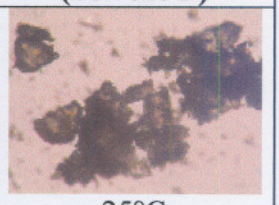 25°C
2	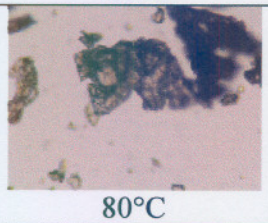 80°C	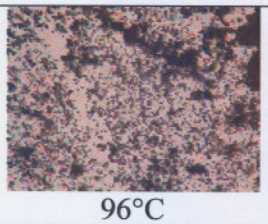 96°C	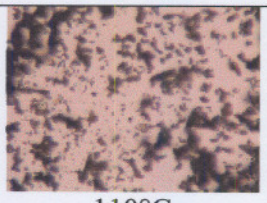 110°C	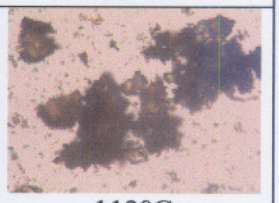 113°C
3	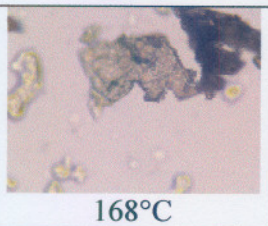 168°C	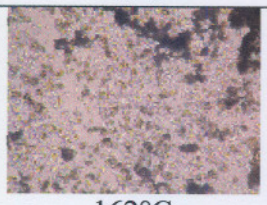 162°C	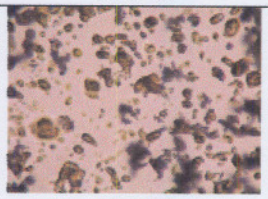 171°C	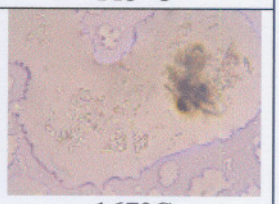 167°C

Table 7.1 continued...

#	Mono-ethanol solvate (Solvent A)	Mono-ethanol hemihydrate (Solvent B)	Hemi-ethanol sesquihydrate (Solvent C)	Sesquihydrate (Solvent D)
4	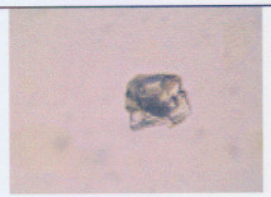 175°C	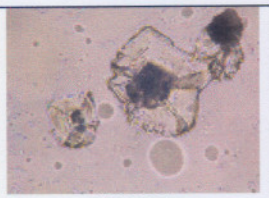 170°C	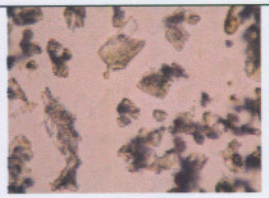 176°C	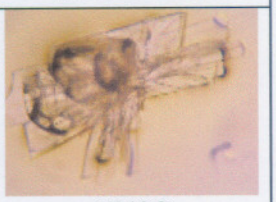 174°C
5	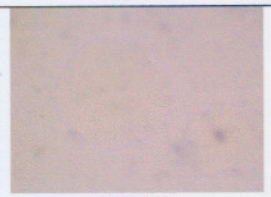 190°C	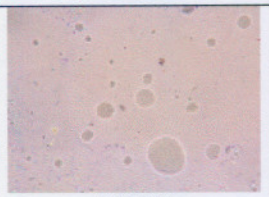 190°C	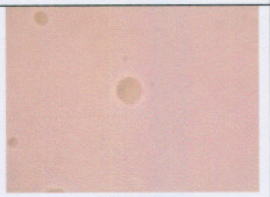 190°C	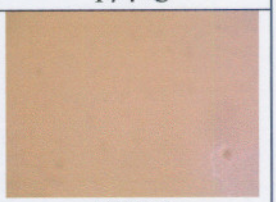 190°C

These samples were also studied submerged in silicon oil. The photomicrographs that were taken revealed no bubble evolution (i.e. desolvation) for the mono-ethanol solvate, however bubble evolution became progressively more visible as the hydration status of the crystal forms increased. These HSM events are illustrated in table 7.2.

Table 7.2 Photomicrographs of the HSM events observed for the forms from different ethanol:water mixtures (submerged in silicon oil)

Mono-ethanol solvate (Solvent A)	Mono-ethanol hemihydrate (Solvent B)	Hemi-ethanol sesquihydrate (Solvent C)	Sesquihydrate (Solvent D)
96°C	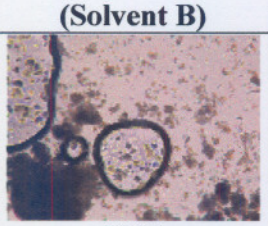 99°C	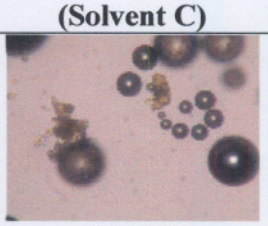 113°C	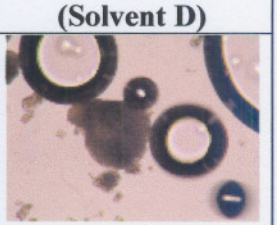 115°C

DRIFT-IR spectrometry was used to further investigate the different crystal forms. The most significant differences in the IR spectra of these forms were observed in the range of 4000- 2000 cm^{-1}. The mono-ethanol solvate revealed a broad band around 3400 cm^{-1}

that was absent in the DRIFT-IR spectrum of the sesquihydrated form and the sesquihydrate form revealed a band at 3650 cm^{-1} which was not present in the DRIFT-IR spectrum of the mono-ethanol solvate. Thus it can be suggested that the band at 3400 cm^{-1} indicates the presence of ethanol in the lattice, whilst a band present at 3650 cm-1 indicates the presence of water in the crystal lattice. This statement is illustrated in figure 7.15. In figure 7.15 it can be seen that the samples containing water and ethanol possessed both the ethanol and water bands, while the pure ethanol solvate and the pure hydrate only revealed the presence of the band at 3400 cm^{-1} and 3650 cm^{-1} respectively.

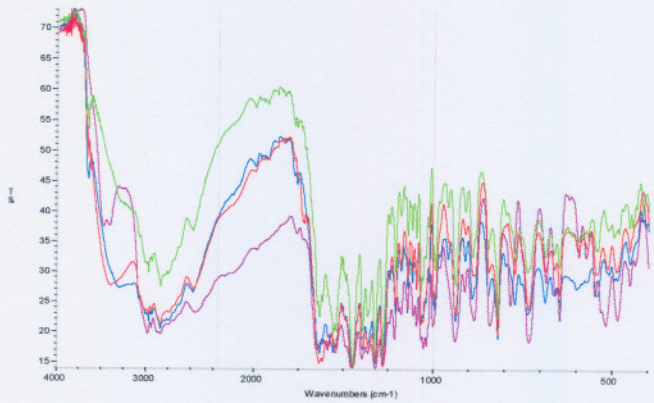

(a)

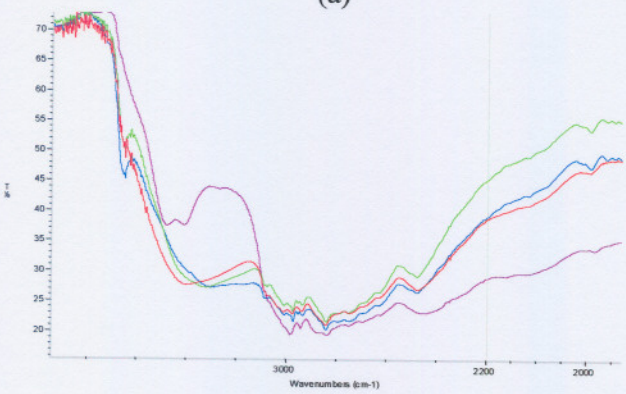

(b)

Figure 7.15 (a) IR spectra of the mono-ethanol solvate, mono-ethanol-hemihydrate, hemi-ethanol sesquihydrate and sesquihydrate and (b) enlargement of the area ranging from 4000-2000 cm^{-1}.

An increase in the water content of the recrystallisation solvent (ethanol) lead to an increased incorporation of water into the crystal lattice. The ethanol band was found to diminish (from A to E), while the water band became more prominent as the water content in the recrystallisation solvent used, increased.

Conclusion

A summary of the results obtained in this study is given in table 7.3 and figure 7.16.

Table 7.3 Summary of results obtained from the different crystal forms obtained using various mixtures of ethanol and water as recrystallisation solvents

Recrystallisation solvent	% weight loss (TGA)	% water *1	% Ethanol *2	Classification
A	12.8	0.2 (0)	12.6	Mono-ethanol solvate
B	15.0	3.0	12.0	Mono-ethanol-hemihydrate
C	15.5	8.6	6.9	Hemi-ethanol-sesquihydrate
D	7.2	8.1	-0.9 (≈ 0)	Sesquihydrate
E	8.1	8.2	-0.1 (≈ 0)	Sesquihydrate

*1 is the water content determined by KF titrations.

*2 is the ethanol content determined: total weight loss % (TGA) - water content (KF).

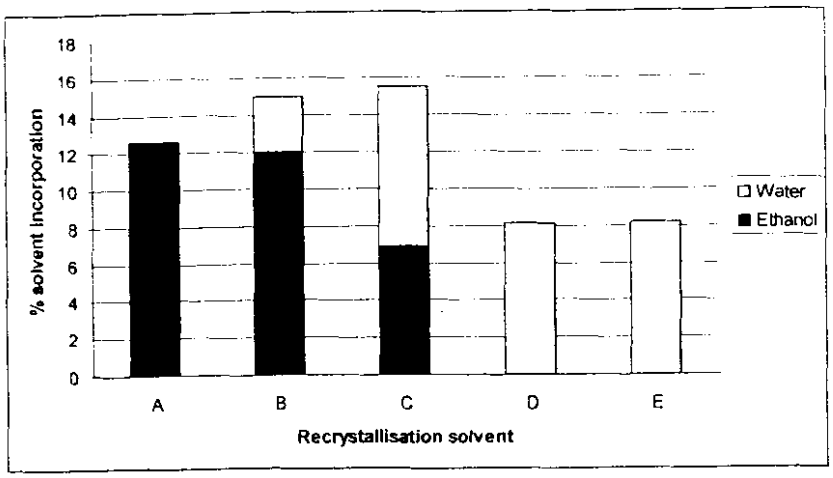

Figure 7.16 Percentage solvent incorporated into the crystal lattice using various ethanol: water mixtures as recrystallisation solvents respectively. Whereas (A) is absolute ethanol, (B) is ethanol (95%), (C) is ethanol:water (75:25), (D) is ethanol:water (50:50) and (E) is ethanol:water (25:75).

This study revealed that small traces of water in the recrystallisation solvent (ethanol) resulted in different crystal forms. This observation is of great importance for the pharmaceutical industry as a fairly stable crystal form was obtained using 99-100% ethanol (see section 5.1.1) as recrystallisation solvent, whilst a very unstable form (form P) was obtained when 95% ethanol was used as recrystallisation solvent.

This study also revealed that water in concentrations of 5-50% v/v greatly influenced the solvate/hydrate incorporation stoichiometry. It was found that gatifloxacin showed a greater affinity for the incorporation of water into the crystal lattice. In ethanol:water mixtures with a water content greater (or equaled) than 50% v/v only hydrated crystal forms were produced and no ethanol was incorporated into the lattice.

The behaviour described in this chapter may substantiate the varying results of the crystal forms described in the literature (variations between batches from the same solvent and method). The water content of the solvents used in these literature studies might have varied, producing new crystal forms/mixtures of forms from the same recrystallisation method. This phenomenon may also explain why some forms are irreproducible using the

same method/solvent, giving rise to disappearing polymorphs (as explained in chapter 1, section 1.3.4)

Bearing this behaviour in mind, good recrystallisation techniques should include the proper sealing of recrystallisation containers to prevent moisture from the atmosphere to influence the recrystallisation solvent composition. It is advisable to perform moisture content determinations on recrystallisation solvents to ensure reproducibility of recrystallisation procedures, and prevent the occurrence of possible disappearing polymorphs. These results suggest that relative humidity should be strictly controlled during recrystallisation/manufacturing of the raw material.

Chapter 8

Summary and conclusion

Due to gatifloxacin's efficacy in the treatment of bacterial infections, it is of utmost importance to ensure that the pharmaceutical dosage form that is to be used by the patient is of outstanding quality. As mentioned in the literature overview (chapter 1), polymorphism may influence the performance of the product (i.e. bio-availability and dissolution properties etc.). An extensive literature search proved that gatifloxacin exhibits polymorphism. Thus a thorough understanding of the behaviour and properties on each available polymorph/pseudopolymorph will assist in the selection of the most desired crystal form, to prevent possible formulation problems and to ensure that the final product is safe and effective.

In chapter 2 the pharmaceutical, pharmacologic and physico-chemical properties of gatifloxacin were investigated and discussed. From the literature it was proved that gatifloxacin is an excellent antibiotic as it: has minimal bacterial resistance (of susceptible bacteria), is relatively safe and has few contra-indications, has very few drug interactions and is a highly effective (broad spectrum) in the treatment of several bacterial infections.

A well-balanced set of analytical techniques was used to attain the following aims and objectives.

1. Characterise and investigate the solid-state properties of the gatifloxacin sesquihydrate raw material obtained from XIAMEN MCHEM PHARMA (GROUP) LTD (chapter 4).
2. Characterise the anhydrous form produced by the drying of gatifloxacin sesquihydrate (form H4) (chapter 4).
3. Compare the physico-chemical properties of gatifloxacin sesquihydrate (H4) and its dehydrated product (chapter 4).

4. To investigate the dehydration process of gatifloxacin sesquihydrate (H4) and determine the dehydration activation energy (chapter 4).
5. Identify and characterise possible new crystal forms of gatifloxacin produced by recrystallisation with absolute ethanol (99-100%), *n*-butanol, THF, ethyl acetate and dichloromethane (chapter 5).
6. Provide supplementary data on previously discussed crystal forms of gatifloxacin (chapter 5).
7. Evaluate the influence of drying (desolvation) on the recrystallised products (chapter 5).
8. Investigate the relative stability of an anhydrous form of gatifloxacin when exposed to increased temperature and relative humidity conditions (chapter 5).
9. Determine possible differences in solubility and dissolution behaviour (chapter 6) of solvated and desolvated crystal forms of gatifloxacin prepared.
10. Establish the influence of water content present in a recrystallisation solvent (using ethanol as an example) (chapter 7).

To ensure that the aims from this study would be achieved, it was necessary to gain knowledge on the principal and applications of the apparatus to be used and the interpretation of the results obtained. The methods compiled for this study were evaluated and the apparatus were calibrated and maintained according to GLP procedures to ensure accurate and trustworthy results (chapter 3).

A schematic representation of the layout of this study is illustrated in figure 8.1.

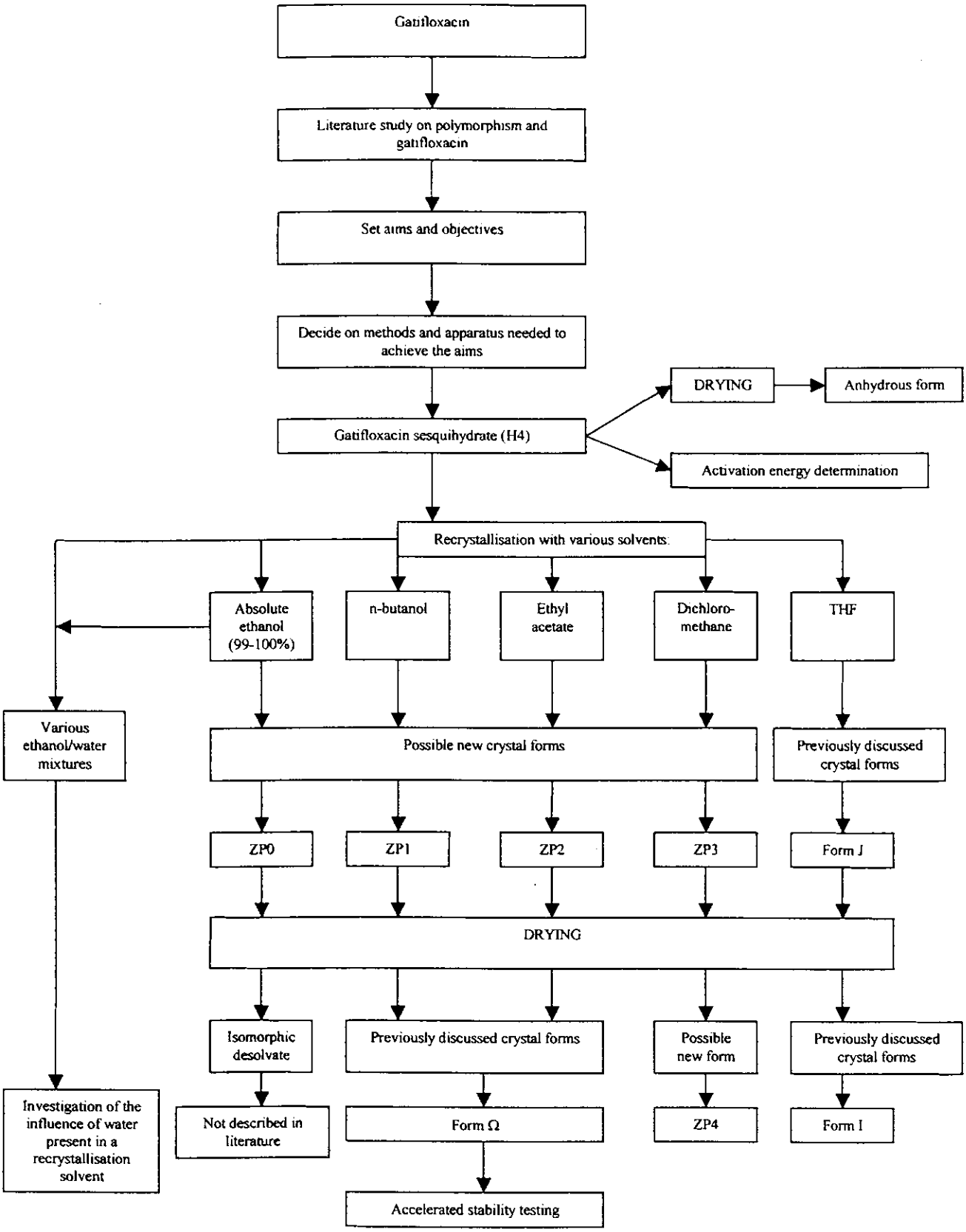

Figure 8.1 Schematic representation of the layout of this study.

The raw material obtained from XIAMEN MCHEM PHARMA (GROUP) LTD revealed a XRPD closely related to that of form H4 sesquihydrate, which produced an anhydrous form upon drying.

Gatifloxacin sesquihydrate (form H4) revealed complex dehydration behaviour as its dehydration activation energy (E_a) did not remain constant during the dehydration process.

Recrystallisation using absolute ethanol, *n*-butanol, ethyl acetate and dichloromethane produced 4 possible new pseudopolymorphic forms (ZP0, ZP1, ZP2 and ZP3 respectively). Drying of ZP3 produced a possible new anhydrous form, ZP4, drying of ZP1 and ZP2 produced previously discussed form Ω. Recrystallisation using absolute ethanol (99-100%) produced ZP0 which converted to an isomorphic desolvate upon drying. The phenomenon of isomorphism that was found for ZP0 proved to be a supplementary addition to the available literature of ethanol solvates. The recrystallisation product obtained from THF recrystallisation produced form J. As stated in the literature, form J can be prepared from recrystallisation with THF (and other solvents such as acetone and *n*-propanol). According to the literature form J (from THF) should be a THF solvate, however in this study it was found that form J exhibited properties characteristic to a sesquihydrate. The possibility that form J (from THF) can exist as a sesquihydrate was found to be a supplementary addition to the available literature on form J.

Accelerated stability testing of form Ω at 30°C & 65% RH and at 40°C & 75% RH was performed and compared to a reference sample of form Ω stored at ambient conditions. The results revealed that form Ω does not convert to another form after 1 month of exposure to these conditions, although a slight increase in water content was noticed (<1%).

The classification of the prepared crystal forms are summarised in figure 8.2.

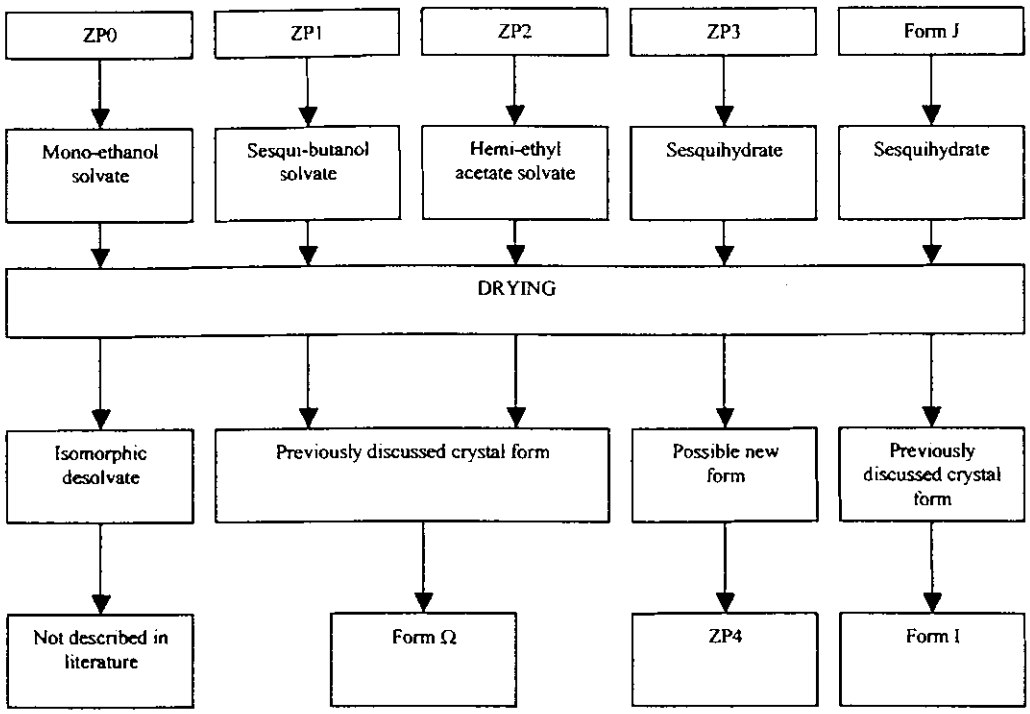

Figure 8.2 Summary of the classification of the prepared crystal modifications.

Solubility testing was performed over a period of 24 hours. It was clear that the different crystal forms did exhibit differences in solubility in the various media. The influence of the solvent in the solvated forms resulted in weaker solubility than their dried counterparts, except with ZP3. Seeing that the crystal lattice was minimally affected by drying of ZP0 (drying of ZP0 produced an isomorphic desolvate), it seemed that the solvent (ethanol) played a distinct role in the solubility behaviour of this form, as its crystal lattice remained comparable.

The dissolution profiles of the crystal forms prepared in this study (figure 8.3) were compared to that of the commercially obtained form H4 (sesquihydrate) using the *f*2 similarity indicator as described by Moore & Flanner (1996:64-67).

From the summary of the dissolution results (figure 8.3) it was observed that the dissolution profiles of ZP1, ZP3, ZP4 and Ω were similar (by *f*2 calculation) to that of the

commercially favoured sesquihydrated form, whereas the dissolution profiles of all other crystal forms were dissimilar.

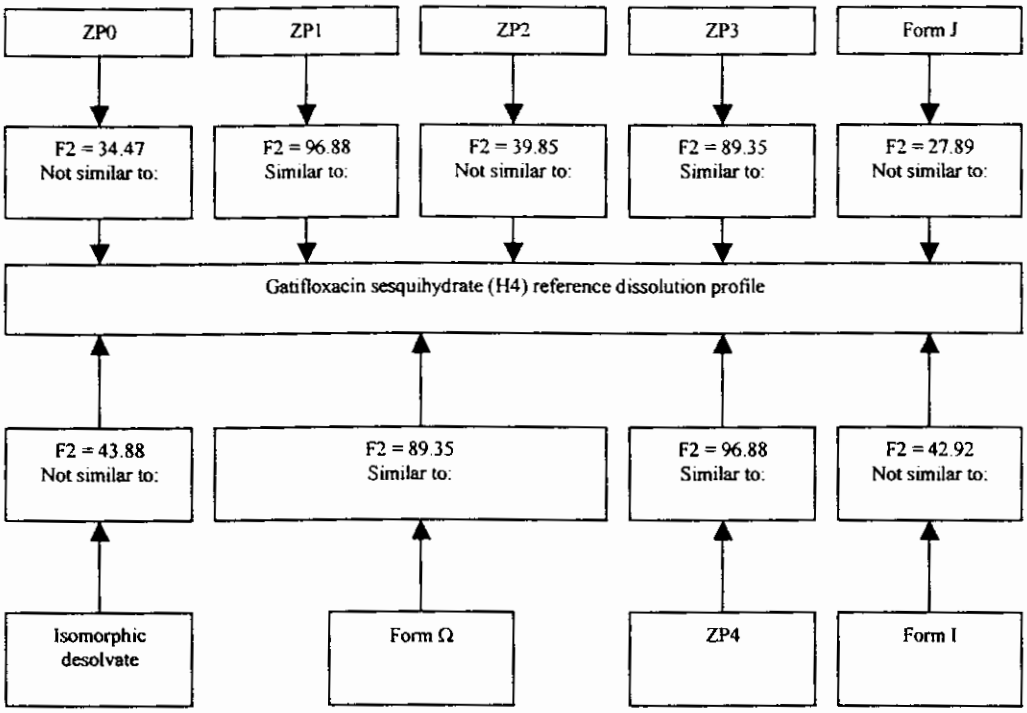

Figure 8.3 Summary of dissolution profile comparison.

The flow properties of the different crystal modifications are listed in table 8.1.

Table 8.1 Flow properties of the various recrystallised products of gatifloxacin

Crystal form	Average CI	Average HR	Flow properties
ZP0	23.43	1.31	Poor
Isomorphic desolvate of ZP0	27.91	1.39	Poor
ZP1	28.37	1.40	Poor
Form Ω (from ZP1)	28.04	1.39	Poor
Form J	20.42	1.26	Fair
Form I (anhydrous)	28.40	1.41	Poor
ZP2	23.90	1.32	Poor
Form Ω (from ZP2)	26.41	1.36	Poor
ZP3	36.08	1.57	Very poor
ZP4	34.65	1.53	Very poor
H4 (sesquihydrate)	44.33	1.80	Extremely poor
Anhydrous gatifloxacin	42.96	1.75	Extremely poor

From table 8.1 it was observed that form J was the only crystal form that had fair powder flow, whilst the other forms exhibited poor flow. The reason for these poor results might be attributed to the crystals' nature to agglomerate and the non-spherical particles shapes (see tables 5.28-5.32).

To evaluate the influence of water present in a solvent during recrystallisation, various mixtures of ethanol and water were prepared and used as recrystallisation solvent. The results obtained are illustrated in figure 8.4. The results proved that even the slightest traces of water influenced the outcome of the recrystallisation. This study revealed that water in concentrations of 5-50 % v/v greatly influenced the solvate/hydrate incorporation stoichiometry. It was found that gatifloxacin showed a greater affinity for the incorporation of water into the crystal lattice. In ethanol:water mixtures with a water content greater (or equaled) than 50 % v/v only hydrated crystal forms were produced and no ethanol was incorporated into the lattice.

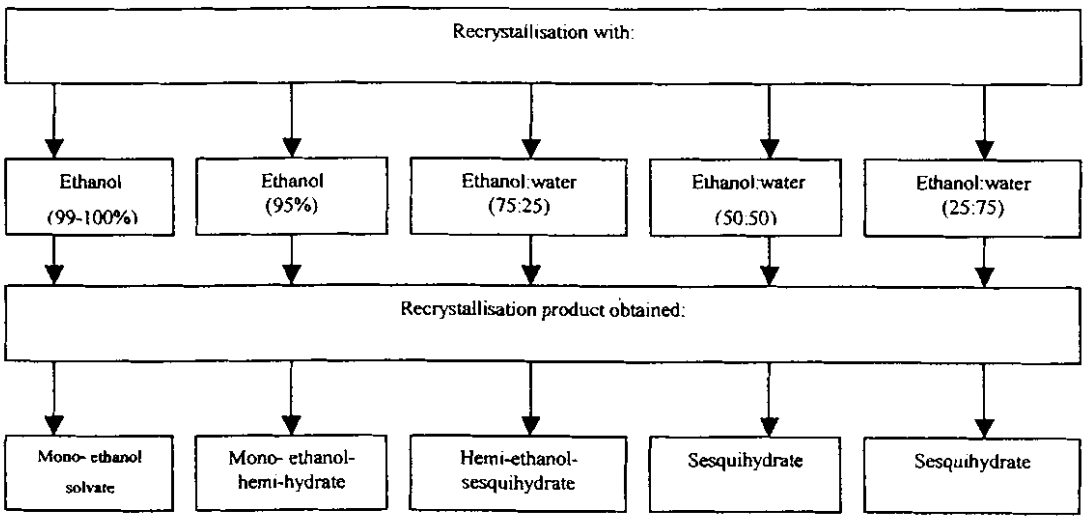

Figure 8.4 Recrystallisation products obtained using various grades of ethanol and binary mixtures of ethanol and water.

From the results obtained it is clear that this study made a valuable contribution towards the knowledge of polymorphic and pseudopolymorphic behaviour of gatifloxacin crystal modifications as it:

1. Illustrated that the dehydration behaviour of the commercially favoured gatifloxacin sesquihydrate varies in activation energy throughout the dehydration process.
2. Identified and characterised 5 new forms.
3. Provided supplementary information on previously discussed crystal forms regarding behavioral aspects that was lacking from literature.
4. Revealed that form Ω remained unaffected when exposed to accelerated stability testing conditions for a period of 1 month.
5. Discussed the dissolution, solubility and powder flow behaviour of the solvated and desolvated/dehydrated forms.
6. Identified and extensively characterised the desolvated/dehydrated products of these forms.
7. Can be reported to the pharmaceutical industry that gatifloxacin is extremely sensitive to moisture content during recrystallisation.

The best way to describe research is to take a shot into the dark. Take the following parable for example: Three friends where going on a night-time hunting trip. With the use of their spotlight on the jeep they saw a small deer about 80 meters away. One man got ready to fire at the deer. Just before taking the shot, the spotlight went out. The man however was determined to take the shot, as his aim was spot on just before the light went out. The hunter took the shot, not knowing that he slightly lowered the gun from his original aim. The men decided to return to their camp and agreed to search for their small deer the following day seeing that they can no longer continue in the darkness. The next day they drove out to where they thought the deer would have been. The deer however was not in sight, but continuing with the search they found a big lion, of trophy worth, 30 meters from the spot.

More often than not, research taught me that you get unexpected answers to your questions, but eventually when all the answers are available, one can pair up the answers to the appropriate question to formulate an explanation. And even if something remains unanswered, **you still have to be willing to take a shot in the dark**...and maybe even come up with a better result than expected.

Bibliography

AIRAKSINEN, S., KARJALAINEN, M., RASANEN, E., RANTANEN, J., & YLIRUUSI, J. 2004. Comparison of the effects of two drying methods on polymorphism of theophylline. *International Journal of Pharmaceutics*, 276: 129-141.

ALLERGAN®. 2005. Consumer products: Zymar. [Web:] http://www.allergan.com/site/products/consumers/home.asp?id=zymar [Date of access: 23 April 2005].

AMIR, E., NIDDAM-HILDESHEIM, V., STERINBAUM, G. & WIZEL, S. Novel crystalline forms of gatifloxacin and processes for preparation. Patent: US 2004/0171621. 26p.

BARTOLOMEI, M., BERTOCCHI, P., RAMUSINO, M.C., SANTUCCI, N. & VALVO, L. 1999. Physico-chemical characterisation of the modifications I and II of (R,S) Propranolol hydrochloride: solubility and dissolution studies. *Journal of Pharmaceutical and Biomedical Analysis*, 21: 299-309.

BEHTA, M., KHAN, K.M. & HARTMAN, B.J. 2005. The new fluoroquinolones: A review of their properties. [Web:] http://www.emedmag.com/html/pre/fea/features/011501.asp [Date of access: 29 September 2005].

BLADGEN, N., DAVEY, R.J., ROWE, R. & ROBERTS, R. 1998. Disappearing polymorphs and the role of reaction by-products: the case of sulphathiazole. *International Journal of Pharmaceutics*, 172: 169-177.

BRISTOL-MEYERS SQUIBB. 2004. Tequin. [Web:] http://www.tequin.com [Date of access: 23 April 2005].

BRITS, M. 2003. Crystal polymorphism and pseudopolymorphism of Venlafaxine hydrochloride. Potchefstroom: Potchefstroom University for Christian Higher Education (PU for CHE). (Dissertation – M.Sc.) 212p.

BUCKTON, G. 2002. Solid-state properties. (*In* AULTON, M.E. *ed.* Pharmaceutics: The science of dosage form design. New York, NY: Churchill Livingstone p. 141-152).

BUGAY, D.E. & FINDLAY, W.P. 2002: Vibrational spectroscopy. (*In* Ohannesian, L. & Streeter A.J., *ed.* Handbook of pharmaceutical analysis. New York: Marcel Dekker, INC. 585p.).

BYRN, S., PFEIFFER, R., GANEY, M., HOIBERG, C. & POOCHCIKIAN, G. 1995. Pharmaceutical solids: A strategic approach to regulatory considerations. *Pharmaceutical Research*, 12(7): 945-954.

BYRN, S.R. 1982. Solid-state chemistry of drugs. New York: Academic press, INC. 346p.

BYRN, S.R., PFEIFFER, R.R. & STOWELL, J.G. 1999. Solid-state chemistry of drugs. West Lafayette, Indiana: SSCI, Inc. 575p.

BYRN, S.R., XU, W. & NEWMAN, A.W. 2001. Chemical reactivity in solid-state pharmaceuticals: formulation implications. *Advanced Drug Delivery Reviews*, 48:115-136.

CARSTENSEN, J.T. 1990. Drug stability: Principles and practices. New York: Marcel Dekker, INC. 520p.

CHAMBERS, H.F. 2001. Sulfonamides, Trimethoprim, & Quinolones. (*In* Katzung, B.G., *ed.* Basic and clinical pharmacology 8th edition. New York: McGraw-Hill. 793-802p.).

CHAWLA, G., GUPTA, P., THILAGAVATHI, R., CHAKRABORTI, A.K. & BANSAL, A.K. 2003. Characterization of solid-state forms of celecoxib. *European Journal of Pharmaceutical Sciences*, 20: 305-317.

CHEMICALLAND21. 2005. Gatifloxacin. [Web:] http://www.chemicalland21.com/arokorhi/lifescience/phar/GATIFLOXACIN.htm [Date of access: 23 April 2005].

CHEMINDUSTRY.COM. 2005. Gatifloxacin. [Web:] http://www.chemindustry.com/chemicals/17513.html [Date of access: 29 September 2005].

CHONGPRASERT, S., GRIESSER, U.J., BOTTORFF, A.T., WILLIAMS, N.A., BYRN, S.R. & NAIL, S.L. 1998. Effects of freeze-dry processing conditions on the crystallization of pentamidine isethionate. *Journal of Pharmaceutical Sciences,* 87(9): 1155-1160.

DAHL, O., ZIEDRICH, K.H., MAREK, G.J. & PARADIES, H.H. 1989. Physico-chemical and structural studies of triamterene. *Journal of Pharmaceutical Sciences,* 78(7):598-606.

DE SMIDT, J.H., FOKKENS, J.G., GRIJSEELS, H. & CROMMELIN, D.J.A. 1986. Dissolution of theophylline monohydrate and anhydrous theophylline in buffer solutions. *Journal of Pharmaceutical Sciences*, 75(5): 497- 501.

DE VILLIERS, M.M., TERBLANCHE, R.J., LIEBENBERG, W., SWANEPOEL, E., DEKKER, T.G. & SONG, M. 2005. Variable temperature X-ray powder diffraction analysis of the crystal transformation of the pharmaceutically preferred polymorph C of Mebendazole. *Journal of pharmaceutical and biomedical analysis*, 38: 435-441.

DOTZEL, M.M. 2000. Federal register notices. Volume 65, No. 251: ICH guidelines. [Web:] http://www.fda.gov/cber/gdlns/frich122900.pdf [Date of access: 19 July 2005].

EMD CHEMICALS INC. 2000. Aquastar® - Karl Fisher titration basics. [Web:] http://www.emdchemicals.com/analytics/literature/KF_titration_basics.pdf [Date of access: 19 August 2005].

ENGEL, G.L., FARID, N.A., FAUL, M.M., RICHARDSON, L.A. & WINNEROSKI, L.L. 2000. Salt form selection and characterization of LY333531 mesylate monohydrate. *International Journal of Pharmaceutics*, 198: 239-247.

FLYNN, J.H. & WALL, L.A. 1966. *Polymer letters*, 4:323-328.

FUKUOKA, E., MAKITA, M. & YAMAMURA, S. 1989. Glassy state of pharmaceuticals III. Thermal properties and stability of glassy pharmaceuticals and their binary glass systems. *Chemical Pharmaceutical Bulletin*, 37(4): 1047-1050.

GARCIA, E., VEESLER, S., BIOSTELLE, R. & HOFF, H. 1999. Crystallization and dissolution of pharmaceutical compounds: An experimental approach. *Journal of crystal growth*, 198/199: 1360-1364.

GIBBON, C.J. *ed.* 2003. South African medicine formulary. 6th ed. Pinelands. South African medical association, Health and Medical Publication Group. 569p.

HAKANEN, A. & LAINE, E. 1995. Characterisation of two terfenadine polymorphs and a methanol solvate: kinetic study of the thermal rearrangement of terfenadine from the methanol solvate to the lower melting polymorph. *Thermochemica Acta*, 248:217-227.

HAN, J., GUPTE, S. & SURYANARAYANAN, R. 1998. Application of pressure differential scanning colorimetry in the study of pharmaceutical hydrates. II. Ampicillin trihydrate. *International Journal of Pharmaceutics*, 170: 63-72.

HANCOCK, B.C., SHALAEV, E.Y. & SHAMBLIN, S.L. 2002. Polyamorphism: a pharmaceutical science perspective. *Journal of Pharmacy and Pharmacology*, 54:1152-1153.

HE, X., GRIESSER, U.J., STOWELL, J.G., BORCHARDT, T.B. & BYRN, S.R. 2000. Conformational color polymorphism and control of crystallization of 5-methyl-2-[(4-methyl-2-nitrophenyl)amino]-3-thiophenecarbonitrile. *Journal of Pharmaceutical Sciences*. 90: 371-388.

KIEFFER, J. 2002. Structural transitions and polyamorphism in glass-forming oxides. *Journal of Non-Crystalline Solids*, 307-310: 644-653.

KIVELSON, D. & TARJUS, G. 2002. Apparent polyamorphism and frustration. *Journal of Non-Crystalline Solids*, 307-310: 630-636.

KUHNERT-BRANDSTATTER, M. 1971. Thermomicroscopy in the analysis of pharmaceuticals. New York: Pergamon press. 409p.

LÖTTER, A.P., FLANAGAN, D.R., PALEPU, N.R. & GUILLORY, J.K. 1983. A simple reproducible method for determining dissolution rates of hydrophobic powders. *Pharmaceutical Technology*. April. 59-66.

LUND. W. *ed.* 1994. The pharmaceutical codex. 12th edition. London: The pharmaceutical press. 1117p.

MAGGI, L., CONTE, U. & BETTINETTI, G.P. 1998. Technological properties of crystalline and amorphous α-cyclodextrine hydrates. *International Journal of Pharmaceutics*, 172: 211-217.

MARTINO, P.D., SCOPPA, M., JOIRIS, E., PALMIERI, G.F., ANDRES, C., POURCELOT, Y. & MARTELLI, S. 2001. The spray drying of acetazolamide as method to modify crystal properties and to improve compression behaviour. *International Journal of Pharmaceutics*, 213: 209- 221.

MICHEL, A., DROUIN, M. & GLASER, R. 1994.
Solid-state stereochemistry of (-)-scopolamine hydrobromide sesquihydrate, a new polymorph of the anticholinergic drug. *Journal of Pharmaceutical Sciences*, 83(4): 508-513.

MIYAWA, J.H. & SCHULMAN, S.G. 2002. Ultra-violet-visible spectroscopy. (*In* Ohannesian, L. & Streeter A.J., *ed.* Handbook of pharmaceutical analysis. New York: Marcel Dekker, INC. 585p.).

MOORE, J.W. & FLANNER, H.H. 1996. Mathematical comparison of dissolution profiles. *Pharmaceutical Technology*, June: 64-68.

MORRIS, K.R., GRIESSER, U.G., ECKHARDT, C.J. & STOWELL, J.G. 2001. Theoretical approaches to physical transformations of active pharmaceutical ingredients during manufacturing processes. *Advanced Drug Delivery Reviews*, 48: 91-114.

MURPHY, D., CINTRON, F.R., LANGEVIN, B., KELLY, R.C. & RODRIGUEZ-HORNEDO, N. 2002. Solution mediated phase transformation of anhydrous to dihydrate carbamazepine and the effect of lattice disorder. *International Journal of Pharmaceutics*, 246: 121-134.

NEWMAN, A.W. & STAHLY, G.P. 2002. Form selection of pharmaceutical compounds. (*In* Ohannesian, L. & Streeter A.J., *ed.* Handbook of pharmaceutical analysis. New York: Marcel Dekker, INC. 585p.).

NIDDAM-HILDESHEIM, V., DOLITZKY, B-Z., PILARSKI, G. & STERIMBAUM, G. 2005. Novel synthesis of gatifloxacin. Patent: US 2005/0080264. 8p.

NIDDAM-HILDESHEIM, V., WIZEL, S. & STERINBAUM, G. 2004c. Novel crystalline forms of gatifloxacin. Patent: US 2004/0192700. 8p.

NIDDAM-HILDESHEIM, V., WIZEL, S., STERIMBAUM, G. & AMIR, E. 2004a. Novel crystalline forms of gatifloxacin. Patent: US 2004/0009989. 55p.

NIDDAM-HILDESHEIM, V., WIZEL, S., STERIMBAUM, G. & AMIR, E. 2004b. Novel crystalline forms of gatifloxacin. Patent: US 2004/0038988. 6p.

PARK, J., KANG, H.W., PARK, S.J & KIM, C. 2005. Use of CP/MAS solid-state NMR for the characterisation of solvate molecules within estradiol crystal forms. *European Journal of Pharmaceutics and Biopharmaceutics*, 60: 407-412.

RAGHAVAN, K.S., RANADIVE, S.A., GOUGOUTAS, J.Z., DIMARCO, J.D., PARKER, W.L., DAVIDOVICH, M. & NEWMAN, A. 2002. Gatifloxacin pentahydrate. Patent: US 6,413,969. 18p.

REDDY, B.P., REDDY, K.R., REDDY, R.R. & REDDY, M.M. 2004(b). Novel crystalline forms of gatifloxacin. Patent: WO 2004/087688. 26p.

REDDY, B.P., REDDY, K.R., REDDY, R.R., REDDY, M.M, REDDY, J.S. 2004(a). Purifications methods of gatifloxacin and a novel form of gatifloxacin. Patent: WO 2004/101547. 13p.

REDDY, M.S., RAJU, C.N., RAJU, V.V.N.K.V.P., REDDY, N.S. & KUMAR, R.R. 2003. Anhydrous crystalline forms I and II of 1- cyclopropyl-6-fluoro-8methoxy-7-(3-methyl-1-piperazinyl) 4-oxo-1,4-dihydroquinoline-3-carboxylic acid (gatifloxacin). Patent: WO 03/086402. 25p.

SHEIKH SALEM, M., PILLAI, G.K., NABULSI, L., AL-KAYSI, H.N., ARAFAT, T.A., MALOOH, A.A., SALEH, M. & BADWAN, A.A. 1996. Preparation, characterisation and transformation of terfenadine polymorphic forms. *International Journal of Pharmaceutics*, 141: 257-259.

STANIFORTH, J. 2002. Powder flow. (*In* AULTON, M.E. *ed.* Pharmaceutics: The science of dosage form design. New York, NY: Churchill Livingstone 197-210p.).

STEPHENSON, G.A., GROLEAU, E.G., KLEEMAN, R.L., XU, W. & RIGSBEE, D.R. 1998. Formation of isomorphic desolvates: creating a molecular vacuum. *Journal of Pharmaceutical Sciences*, 87(5): 536-542.

SWANEPOEL, E., LIEBENBERG, W. & DE VILLIERS, M.M. 2003. Quality evaluation of generic drugs by dissolution test: changing the USP dissolution medium to distinguish between active and non-active Mebendazole polymorphs. *European Journal of Pharmaceutics and Biopharmaceutics*, 55: 345-349.

UNITED STATES PHARMACOPOEIAL CONVENTION. 2005. USP 25:NF 23. Rockville, Md. 3187p.

VAKIL, M.H., PATEL, S.G., LAKKAD, M.G., NAIK, A.P., AGARWAL, V.K, PANDITA, K. & PATEL, P.R. 2004. Patent: WO 2004/101527. 18p.

VAN TONDER, E.C., MALEKA, T.S.P., LIEBENBERG, W., SONG, M. WURSTER, D.E. & DE VILLIERS, M.M. 2004. Preparation and physiochemical properties of niclosamide anhydrate and two monohydrates. *International Journal of Pharmaceutics*, 269: 417- 432.

WELLS, J. 2002. Pharmaceutical preformulation: the physicochemical properties of substances. (*In* AULTON, M.E. *ed.* Pharmaceutics: The science of dosage form design. New York, NY: Churchill Livingstone 114-139p.).

YORK, P. 2002. The design of dosage forms. (*In* AULTON, M.E. *ed.* Pharmaceutics: The science of dosage form design. New York, NY: Churchill Livingstone 1-12p.).

YU, L., REUTZEL, S.M. & STEPHENSON, G.A. 1998. Physical characterisation of polymorphic drugs: an integrated characterization strategy. *PSTT*, 1(3): 118-127.

ZHANG, G.G.Z., LAW, D., SCHMITT, E.A. & QUI, Y. 2004. Phase transformation considerations during process development and manufacture of solid oral dosage forms. *Advanced Drug Delivery Reviews*, 56: 371-390.

ZHOU, D., SCHMITT, E.A., ZHANG, G.G.Z., LAW, D., WIGHT, C.A., VYAZOVKIN, S. & GRANT, D.J.W. 2003a. Model-free treatment of the dehydration kinetics of nedocromil sodium trihydrate. *Journal of Pharmaceutical Sciences*, 92(7). 1367-1376.

ZHU, H., YOUNG, V.G. & GRANT, D.J.W. 2002. Crystal structure and thermal behaviour of nedocromil nickel octahydrate. *International Journal of Pharmaceutics*. Vol. 232: 23-33.

ZUPANCIC, V., OGRAJSEK, N., KOTAR-JORDAN, B. & VRECER, F. 2005. Physical characterization of pantoprazole sodium hydrates. *International Journal of Pharmaceutics*, 291: 59-68.

Acknowledgements

I would like to make use of this opportunity to express my thanks.

To God all the glory for providing me the opportunity to be a MSc. Pharmaceutics student at the Research Institute for Industrial pharmacy (RIIP) and blessing me with courage, perseverance and will power that enabled me to finish this project.

- Mr. Marius Brits and Prof. Wilna Liebenberg, who inspired, supported and guided me in this study. Thanks for all the hard work, late nights and early mornings.
- The RIIP for the use of their excellent equipment and providing me with experience in the field of industrial pharmacy.
- All the personnel at the RIIP for their support and friendship. In particular Dr. (tannie) Elsa van Tonder, Prof. Theo Dekker, Ntobeko Dladla and Suzan May.
- My fellow students and friends at the RIIP, in particular Marius Brits, Mari-Alet (Mia) de Jager, Marique Aucamp, Danie Otto and Joseph Labuschagne.
- All my predecessor students from the RIIP, in particular Handre Rossouw.
- Mr. Jaco van Biljon (Boehringer Ingelheim, Germany) for all his interest and support.
- The NWU library and its personnel.
- Dr. Louwrens Tiedt for his time and experience on SEM microscopy.
- Prof. A.P. Lotter fulfilling his duties as my tutor during my internship.
- My parents Brahm and Annie, my brother Jaco and my sisters Nelia and Marlise.
- All the musicians that I support, in particular The Goo Goo Dolls, Collective Soul and The Dave Matthews Band.
- The NRF for financial support.
- Emtia Paxton for her love, support and understanding.

Poster presented at the 26th Annual conference of the Academy of Pharmaceutical Sciences, Port Elizabeth, 2005

Physico-chemical Properties of Gatifloxacin Crystals from Ethanol recrystallisations

Zak Perold[1], Emtia Paxton[1], Marius Brits[1], Wilna Liebenberg[1]

1 Research Institute for Industrial Pharmacy, School for Pharmacy, North-West University, Potchefstroom Campus, Potchefstroom, 2520, South Africa.

Purpose:

To identify and characterise the physico-chemical properties and polymorphic behaviour of gatifloxacin crystals recrystallised using ethanol as solvent.

Background:

Gatifloxacin can be classified as a flouroquinolone anti-microbial agent, which is part of the DNA gyrase inhibitor family along with ciprofloxacin for example. Gatifloxacin is a synthetically derived analogue of nalidixic acid and is active against various gram positive and – negative bacteria. This flouroquinolone anti-biotic is excellent in the treatment of acute sinusitis, lower respiratory tract-, urinary tract- and various soft tissue infections (Chambers, 2001:797).

Methods:

Gatifloxacin sesquihydrate (commercially favoured crystal form) was used as raw material in this recrystallisation study, using various organic solvents. This presentation will focus on the physico-chemical properties and lattice-dynamic behaviour of crystals produced using ethanol as recrystallisation solvent. Various analytical techniques were used to characterise and investigate the polymorphic behaviour including: DSC, TGA, FT-IR, KF, XRPD and HSM.

Results:

Various crystal forms of gatifloxacin have been described in scientific literature. Very little information regarding these forms and their interrelationship are available. Such is the case with form P. According to literature form P is the product of an ethanol recrystallisation. The literature also states that form P transforms spontaneously to a polymorphic sesquihydrate at ambient conditions or when exposed to heat, to form T1. The only available physico-chemical data describing form P and T1 were XRPD patterns, and neither of these forms were classified.

The ethanol recrystallisation product of this study was analysed by means of XRPD, TGA, KF, HSM, DSC and FT-IR.

The recrystallisation product was placed in two different containers; one left uncovered and the other one sealed. The crystals from these different containers were analysed by means of XRPD, TGA, KF, HSM, DSC and FT-IR.

The results obtained can be seen in figures 1-3 and table 1.

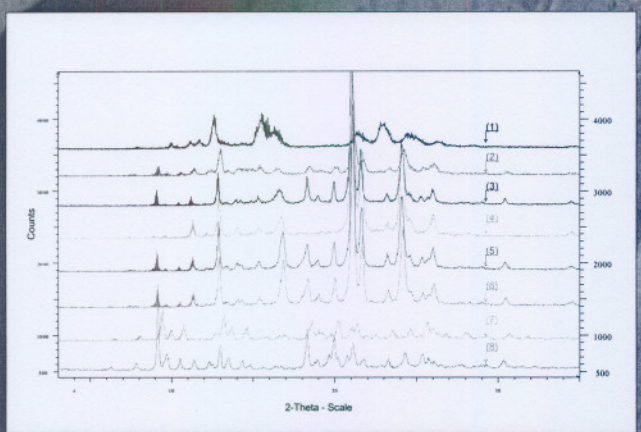

Figure 1: XRPD overlay whereas:

- - Ethanol recrystallisation product
- - Sample (1) that was stored in a sealed container
- - Sample (2) at ambient conditions for 45 minutes (open)
- - Sample (1) at ambient conditions for 45 minutes (open)
- - Sample (4) at ambient conditions after 2 weeks (open)
- - Sample (4) at ambient conditions after 4 weeks (open)
- - Sample (4) after 3 months (open)
- - Gatifloxacin sesquihydrate raw material (form H4)

Table 1: % Water content and % weight loss of samples

Sample	Analysis			Experimental % Ethanol (TGA-KF)	Classification
	XRPD	TGA	KF		
(1)	Resembling form P	15%	3%	12%	Mono-Ethanol-hemihydrate
(2)	Slow transformation to T1	8%	3%	5%	Transformation intermediate
(4)	Rapid transformation to T1	3%	3%	0%	Hemihydrate
(7)	Resembling the H4 sesquihydrate	6%	6%	0%	H4 sesquihydrate

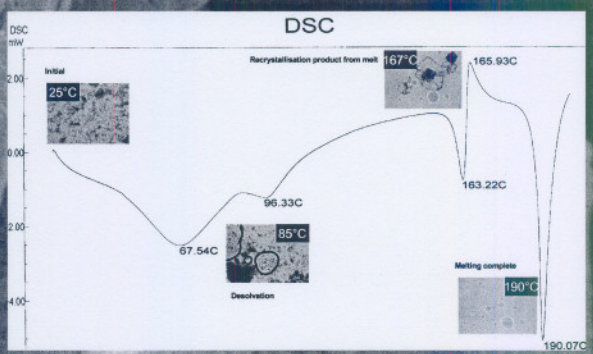

Figure 2: DSC and corresponding HSM photos of sample (1) form P.

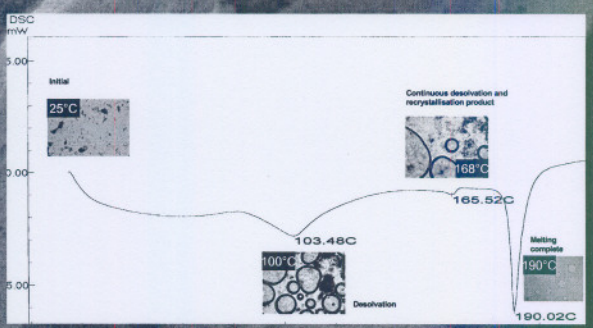

Figure 3: DSC and corresponding HSM photos of the H4 sesquihydrate crystal form.

Conclusion

- From this data it was possible to classify form P as a mono-ethanol-hemihydrated form of gatifloxacin.
- It was also possible to classify form T1 as a hemihydrated form of gatifloxacin, and that the conversion rate between form P and T1 may be manipulated.
- T1 converts to form H4 sesquihydrate.
- This study also revealed that the conversion of P to T1 does not necesarily require heat exposure, as this conversion was observed at ambient conditions.
- This study also clarified that form P does not convert directly to the sesquihydrate form upon standing, but first into the metastable T1 form that converts to H4.

References:

CHAMBERS, H.F. 2001. Sulfonamides, Trimethoprim, & Quinolones. (*In* Katzung, B.G., *ed.* Basic and clinical pharmacology 8th edition. New York : McGraw-Hill. p. 793-802).

YUNIBESITI YA BOKONE-BOPHIRIMA
NORTH-WEST UNIVERSITY
NOORDWES-UNIVERSITEIT

Potchefstroom Campus

Article in the process of submission

Polymorphic behaviour of gatifloxacin crystal modifications

Zak Perold[a], Marius Brits[a], Wilna Liebenberg[a]

[a]Research Institute for Industrial Pharmacy, North-West University, Potchefstroom Campus, Potchefstroom, 2531.

Abstract

Gatifloxacin can be classified as a flouroquinolone anti-bacterial agent, which belongs to the DNA gyrase inhibitor family along with ciprofloxacin for example.

When organic solvents are to be used during polymorphic screening, the water content of these solvents should be taken into account. It has been reported that when a drug substance is known to form multiple hydrated pseudopolymorphs, a small difference of water content can easily produce different hydrated crystals from the recrystallisation [1].

This study proved that even the slightest traces of water influenced the outcome of the recrystallisation. It was found that gatifloxacin showed a greater affinity for the incorporation of water into the crystal lattice when using various grades and binary mixtures of ethanol and water as recrystallisation solvents. In ethanol:water mixtures with a water content greater (or equaled) than 50 % v/v only hydrated crystal forms were produced and no ethanol was incorporated into the lattice.

Keywords: Polymorphism; Gatifloxacin; solvate; incorporation stoichiometry; sesquihydrate.

1. Introduction

Polymorphism is the phenomenon where a compound can exist in different solid forms due to the difference in crystal packing arrangement. Polymorphism and pseudopolymorphism are commonly exhibited in pharmaceuticals, particular in steroids and barbiturates. Different polymorphs of the same chemical entity may have different properties (such as solubility and stability) that might result in costly manufacturing/production problems. Extensive research of all possible polymorphic/pseudopolymorphic behaviour of solids can thus prevent formulation problems and ensure stable, active and adequately bio-available drug products [1].

Gatifloxacin (figure 1) is a synthetically derived analogue of nalidixic acid and is active against various gram-positive and gram-negative bacteria. This flouroquinolone antibiotic is a drug of choice for the treatment of acute sinusitis, lower respiratory tract-, urinary tract- and various soft tissue infections [2].

Various companies and individuals have already patented many different crystal forms of gatifloxacin (table 1). The aim of this article was to establish the influence of water content present in a recrystallisation solvent (using ethanol as an example) on the crystal modification and behaviour thereof, produced.

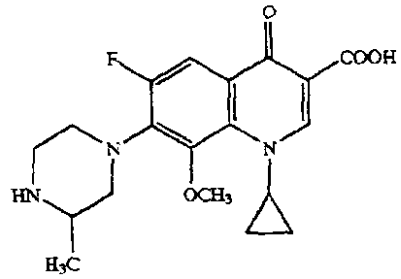

Figure 1
Gatifloxacin

Table 1
Various gatifloxacin crystal forms described in the literature

Patent number
US 2004/0038988 or WO 03/105851.
US 6,413,969 or WO 02/22126.
US 2004/0171621 or WO 2004/054583.
US 2004/0009989 or WO 03/094919.
WO 2004/087688.
WO 2004/101547.
WO 2004/101527.
WO 03/086402. US 2004/0192700 or WO 2004/012739.

2. Materials and methods

2.1 Materials

Gatifloxacin sesquihydrate raw material (batch number 20031110) was obtained from XIAMEN MCHEM PHARMA (GROUP) LTD situated in China. The raw material was manufactured in November 2003 (expiration date: November 2006).

2.2 Preparation of crystal forms

It is common practice to use mixtures of solvents in the crystallisation process of API's [1]. The addition of an *anti-solvent* is often employed to speed-up the

crystallisation process as the anti-solvent decreases the solubility of the solute in the solvent. By adding an anti-solvent to the solvent it often happens that crystals with different solvate composition and stoichiometry are formed due to the presence of two solvents (the solvent and the anti-solvent) in different ratios. The crystal form that will eventually form from the solution is at that ratio where it is the most favourable for that crystal form to grow [1].

A similar approach was used to evaluate the influence of water present in a recrystallisation solvent by preparing various ethanol recrystallisation solvents:

A – Absolute ethanol (99-100%)

B –Ethanol (95%)

C –Ethanol:water (75:25)

D –Ethanol:water (50:50)

E –Ethanol:water (25:75)

Supersaturated solutions of gatifloxacin were prepared using various solvents (A-E). Weighed gatifloxacin sesquihydrate raw material was transferred into an appropriate recrystallisation container. Supersaturated solutions were prepared by dissolving the gatifloxacin sesquihydrate raw material in the appropriate solvent, whilst the heat of the solution was kept at the boiling point of the solvent. These solutions were prepared under constant magnetic stirring. The containers were then covered with either a cap or in the case of beakers, with laboratory parafilm. The solutions were then left at ambient conditions until the crystal yield was sufficient for analysis.

2.3 Characterisation of crystal forms prepared

A well-balanced set of analytical techniques was used for the characterisation of the crystal forms prepared, which included: XRPD, DSC, DRIFT-IR, TGA, HSM and KF.

2.3.1 X-ray powder diffraction (XRPD)

A Bruker D8 Advanced diffractometer (Bruker, Germany) was used to obtain XRPD and Variable Temperature X-ray Powder Diffraction (VT-XRPD) patterns. A sufficient amount of sample was lightly ground to decrease preferred orientation using a pestle and mortar. The ground sample was transferred into an aluminium sample holder.

The sample was then exposed to the following measurement conditions: target, Cu; voltage, 40 kV; current, 30 mA; divergence slit, 2 mm; anti-scatter slit, 0.6 mm, detector slit, 0.2 mm; monochromator; scanning speed, 2°/min with a step size of 0.025° and a step time of 1.0 sec.

2.3.2 Diffuse reflectance infra-red spectroscopy (DRIFT-IR)

For the recording of DRIFT-IR spectra a Nicolet Nexus 470-DRIFT-IR spectrometer (Nicolet instrument corporation, USA) was used at wave numbers ranging from 400-4000 cm^{-1}. Diffuse Reflectance Infrared Fourier Transform spectroscopy (DRIFTS) was used to record the IR spectrum of the sample. The samples were dispersed in powdered KBr (background) and transferred into the reflectance cell prior to analysis.

2.3.3 Differential Scanning Calorimetry (DSC)

An appropriate amount of sample (ranging from 2-3 mg) was weighed into an aluminium sample pan. The sample pan was fitted with a lid and lightly crimped. The lids were pierced to ensure that solvent vapours would be able to escape readily from the crimped pans as pressure build-up in a crimped sample pan may alter the course of desolvation and may produce inaccurate DSC thermograms. DSC samples pans were analysed by a Shimadzu DSC-50 (Shimadzu, Kyoto, Japan). The apparatus heated the samples at a heating rate of 10°C/minute to a maximum of 200°C. The nitrogen flow rate of the Shimadzu DSC-50 (Shimadzu, Kyoto, Japan) was set to 35 ml/min.

2.3.4 Thermogravimetric Analysis (TGA)

Samples ranging between 5-15 mg were weighed into an open platinum sample pan. TGA analysis was performed using a Shimadzu TGA-50 (Shimadzu, Kyoto, Japan).

Samples were heated at a heating rate of 10°C/min, under a nitrogen purge of 35 ml/min to a maximum temperature of 160°C.

2.3.5 Hot-stage microscopy (HSM)

A small amount of sample was placed on an object plate either in a drop of silicon oil or as is, and covered with a cover plate. A Nikon Eclipse E400 (Nikon, Japan) thermo-microscope was used in conjunction with a Metratherm 1200d-heating unit. Events were captured with a Nikon Coolpix 5400 digital camera (Nikon, Japan) that was affixed to the microscope.

2.3.6 Karl-Fischer analysis

A Metro-ohm (Metro-Ω) KF Titrino (Metro-Ω, Switzerland) was used in the determination of water content in samples. The apparatus was calibrated using distilled water and sodium tartrate dihydrate.

3. Results and discussion

Preliminary studies revealed great inconsistency in the data obtained from recrystallisation products using different batches of ethanol as recrystallisation solvent.

3.1 Recrystallisation of gatifloxacin using absolute ethanol (99-100%)

A previously described crystal form, form E, an ethanol solvate (patent number US 6,413,969), was obtained by a recrystallisation process using 90-95% ethanol. Form E has been described as a six-sided platelet ethanol solvate with gigantic solvent channels, causing it to be extremely unstable in the absence of the mother liquor. However, no physico-chemical data were available to characterise and describe this crystal form. The thermodynamic instability of form E is summarised in figure 2. Drying of form E produced a hemi-hydrate (form TE), which probably contained traces of form T2RP. The exposure of form E and TE to an aqueous environment produced a hexa-hydrate (form H6) and a sesqui-dihydrate (form RP) respectively.

VT-XRPD revealed an initial XRPD pattern (25°C) that is characteristic of a crystalline powder (i.e. relatively strong diffraction peaks), as seen in figure 3. During the analysis there were no significant changes in the XRPD pattern between 25°C and 160°C. No significant changes in the crystal lattice were observed during desolvation, thus implying isomorphism (isomorphism is a phenomenon where the desolvated crystal form reveals a similar XRPD pattern to it parent solvated form).

A slight shifting in the °2θ peak positions was observed for the XRPD patterns from 25-160°C. These slight changes can be attributed to a possible change in powder bed height due to the prolonged exposure to increased temperatures (crystal expansion and relaxation).

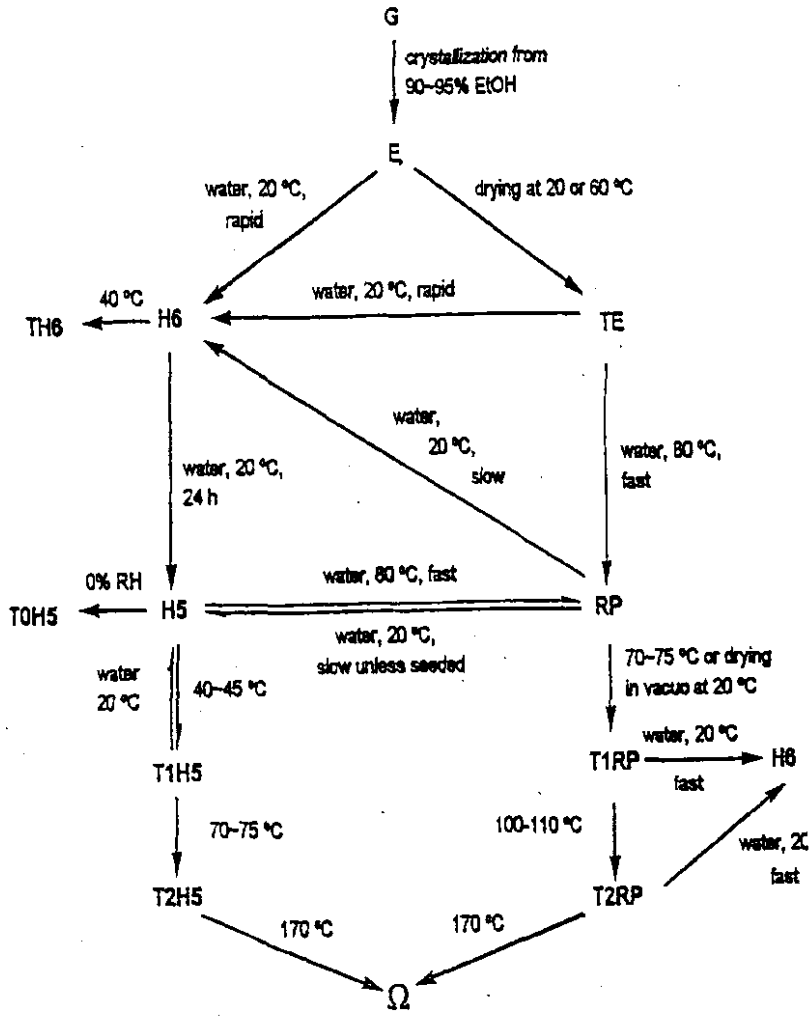

Figure 2

Summary of gatifloxacin ethanol solvate and the behaviour thereof [3].

Significant changes in the XRPD patterns were observed between 160°C and 180°C. The pattern at 170°C revealed few peaks in the range of 5-15°2θ with low intensities. At 180°C the XRPD pattern revealed amorphic behaviour due to the melting of the sample.

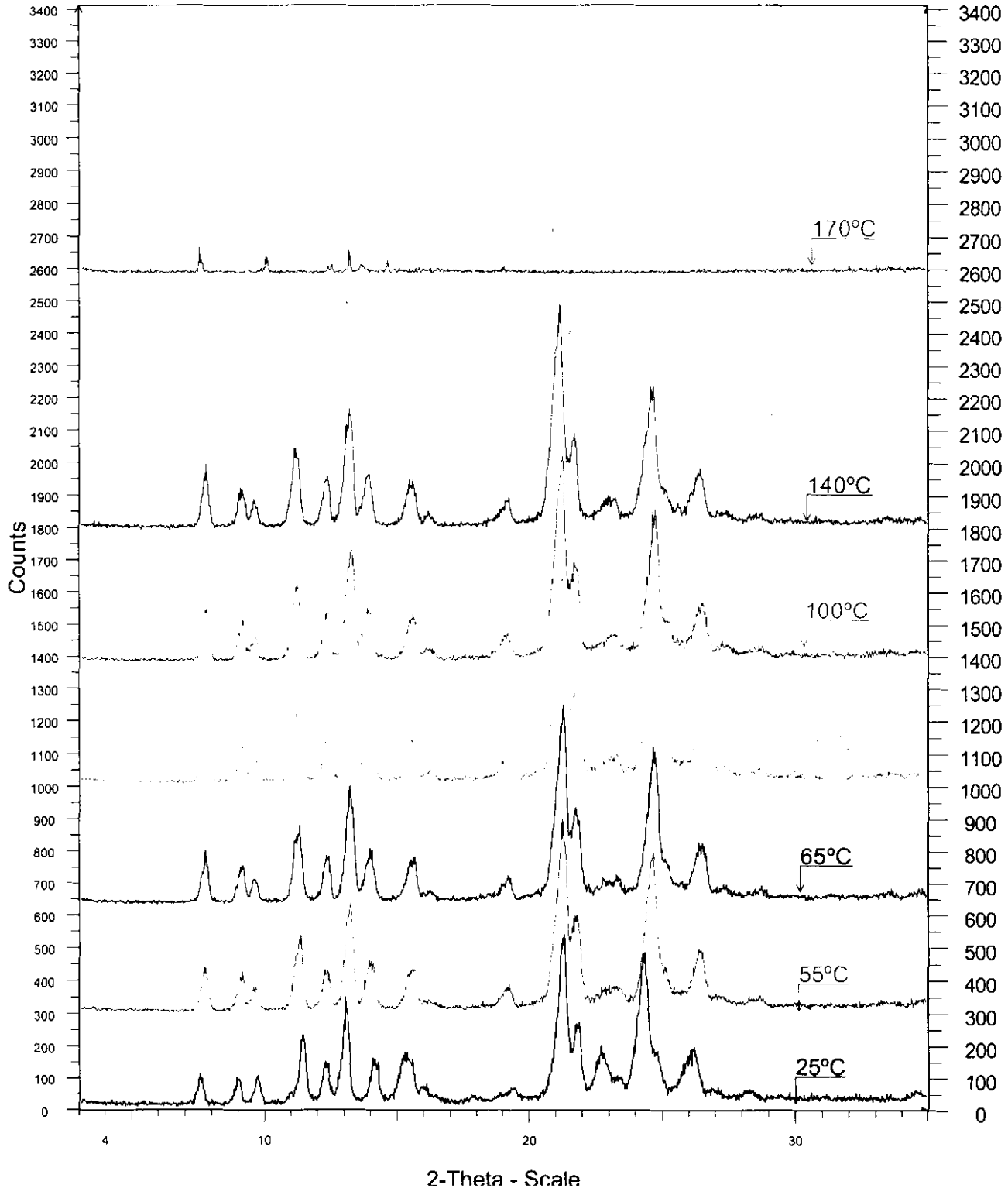

Figure 3

Overlay of the VT-XRPD patterns of ZP0 at temperatures ranging from 25-180°C.

XRPD, TGA, KF and DSC results were used to compare this crystal form to previously described crystal forms (table 1). Form E, produced from recrystallisation using 90-95% ethanol, was described as a six-sided platelet ethanol solvate that has gigantic solvent channels (figure 2). The mono-ethanol solvate (as prepared in this study) was found to be fairly stable at ambient conditions (i.e. desolvation did not occur) and the VT-XRPD studies indicated that desolvation did not cause significant changes in the crystal lattice. The ethanol solvate prepared in this study can thus be considered to be a novel pseudopolymorph of gatifloxacin and was dubbed ZP0.

3.2 Recrystallisation of gatifloxacin using ethanol (95%)

Recrystallisation of gatifloxacin using 95% ethanol produced an unstable crystal form. The XRPD pattern of this form differed significantly from that of the recrystallised product obtained when using absolute ethanol (99-100%). TGA and KF analysis of this sample revealed a percentage weight loss of 15.0% and a water content of 3.0% respectively. The theoretical % ethanol present in a mono-ethanol solvate of gatifloxacin is 10.9%, and the theoretical water content for a monohydrated form should be 4.6%. Thus, this crystal form was classified as a mono-ethanol-hemihydrated form (i.e. solvated-hydrate).

The mono-ethanol hemihydrated sample was exposed to ambient conditions for 45 minutes. TGA and KF titration of the exposed sample revealed a total percentage weight loss of 2.7% and a water content of 3.1%, which indicated that this form transformed into a hemi-hydrated form. The XRPD patterns of these two forms were compared to the XRPD patterns of previously described crystal forms. It was found that the XRPD pattern of the mono-ethanol-hemi-hydrate showed resemblances to the XRPD pattern of form P, while the hemi-hydrate resembled the XRPD pattern of form T1.

The available literature on both these forms (P and T1) did not clearly indicate whether these forms were polymorphs or pseudo-polymorphic forms (no available physico-chemical data were presented except for XRPD patterns). This study made it possible to classify form P as a mono-ethanol-hemi-hydrate and form T1 as a hemi-hydrate. The literature stated that form T1 is the dried product of form P [4], however

in this study it was found that form P spontaneously transformed into form T1 at ambient conditions within 45 minutes.

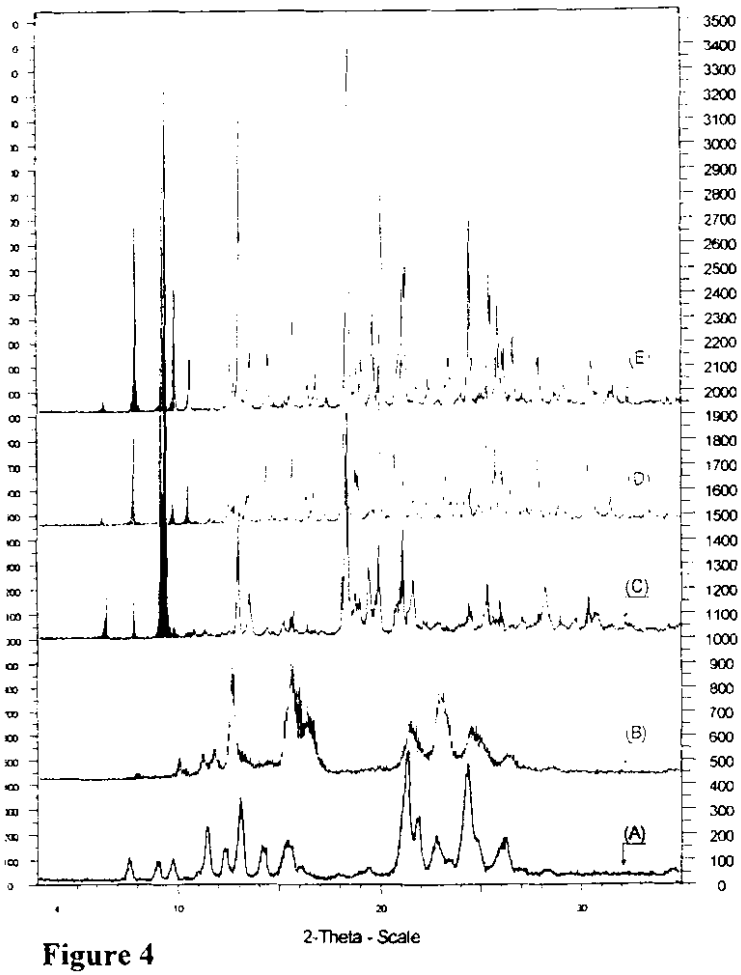

Figure 4

XRPD patterns of the samples obtained from recrystallisation solvents A-E, whereas (A) is absolute ethanol (99-100%), (B) is ethanol (95%), (C) is ethanol:water (75:25), (D) is ethanol:water (50:50) and (E) is ethanol:water (25:75).

According to Niddam-Hildesheim *et al.* [4] it was also stated that form P converts into a sesquihydrated form when exposed to ambient conditions. This statement (with the understanding that form P converts first into form T1) was investigated. Form P was exposed to ambient conditions. Samples were withdrawn at two weeks, four weeks and three months intervals, and analysed. The XRPD patterns confirmed the transformation into form H4 (sesquihydrate).

As illustrated in figure 2, form E displayed a similar polymorphic transition tendency. Form E was the recrystallised product from 90-95% ethanol that was found to be unstable when removed from the mother liquor. From figure 2 it was observed that form E converted into form TE (hemi-hydrate) upon drying. It can thus be suggested that form E might be related to form P, and also that form T1 may be related to form TE.

From the DSC thermogram the desolvation of ethanol was observed at 68.05°C and the dehydration process was recorded at a peak maximum of 100.02°C. The TGA thermogram revealed a weight loss that occurred from 40-106°C supporting the observation of the loss of ethanol and water. A melting endotherm was observed at 163.75°C followed by a recrystallisation exotherm at 168.63°C.

The melting point at 190.03°C indicated the melting of the recrystallised product. HSM observations confirmed the thermal events observed in DSC thermogram.

3.3 Recrystallisation of gatifloxacin using a mixture of ethanol and water as solvent (75:25)

The recrystallisation product from this mixture was found to differ from the forms described in section 3.1 and 3.2. The recrystallisation product obtained revealed a total % weight loss (TGA) of 15.5% and a total water content of 8.6% (KF). Theoretical ethanol content for a hemi-ethanol solvate is 5.5%, while the theoretical water content for a sesquihydrate is 6.9%. Thus, the recrystallisation product from this mixture was classified as a hemi-ethanol-sesquihydrated form of gatifloxacin. The XRPD pattern of this crystal form is illustrated in figure 4.

The DSC thermogram revealed a desolvation peak at 82.25°C (ethanol) and the dehydration at 105.29°C. A melting endotherm was observed at 166.22°C, followed by a recrystallisation exotherm at 172.25°C. The recrystallised product melted at 191.03°C. The TGA supported the desolvation and dehydration observations from the DSC thermogram.

3.4 Recrystallisation of gatifloxacin using a mixture of ethanol and water as solvent (50:50)

The resulting product from this recrystallisation revealed a total % weight loss (TGA) of 7.2% and a total water content of 8.1% (KF). These results suggested that this crystal form mainly contained water and may therefore be classified as a sesquihydrate (theoretical water content for a sesquihydrate is 6.9%). The XRPD pattern of this crystal form is illustrated in figure 4. It was found that the XRPD pattern obtained for this sample resembled that of the commercially favoured sesquihydrate (H4).

Since the recrystallised product was found to be a sesquihydrated form, it was anticipated that the DSC thermogram should reveal only one dehydration peak at 100°C (boiling point of water) and that the desolvation peak should be absent.

The DSC thermogram did indeed reveal only one endothermic peak at 110.92°C that indicated the dehydration of the sample. The TGA supported this observation as the maximum weight loss occurred between 95-110°C. As with the recrystallised products from solvents A-C, a melting endotherm, followed by a recrystallisation exotherm and a final melting point were observed form this sample.

3.5 Recrystallisation of gatifloxacin using a mixture of ethanol and water as solvent (25:75)

The XRPD pattern obtained from this study was similar to that of the sample obtained from the 50:50 mixture (section 3.4). The total weight loss (TGA) was found to be 8.1% whilst the KF analysis revealed a total water content of 8.2%, therefore this crystal form was also classified as a sesquihydrate. The XRPD pattern revealed that the two forms obtained from the ethanol:water (50:50) and (25:75) mixtures were comparable (slight differences present in the 18-20 °2θ region). As mentioned in section 3.4, the XRPD pattern of the sample obtained from the ethanol:water (50:50) mixture was found to resemble the XRPD pattern of the commercially favoured H4 sesquihydrated form, therefore the sample from the ethanol:water (25:75) mixture was also identified as form H4 (sesquihydrate).

3.6 Comparative discussion

From sections 3.1-3.5 it is clear that different crystal forms with varying amounts of solvent (water and ethanol) incorporated into the crystal lattices, were produced from the recrystallisation solvents A-E. To investigate the differences between these forms, the DSC and TGA thermograms of these forms were superimposed to provide an overall perspective of the influence of water present in a recrystallisation solvent on the thermal behaviour of the various crystal forms produced. It should be noted that the DSC and TGA thermograms of the sample from solvent E were not included as the samples from solvent D and E were both the same sesquihydrated form.

The superimposed TGA thermograms of the samples from the recrystallisation solvents (A-D) are illustrated in figure 5. The desolvation step and dehydration step correlated well with the boiling point of ethanol and water respectively.

Figure 5 and KF titrations indicated that the % ethanol incorporated in the crystal forms decreased as the % ethanol in the recrystallisation solvent decreased (from A-E), while the % water incorporated in the crystal forms increased as the water in the recrystallisation solvent increased (from A-E).

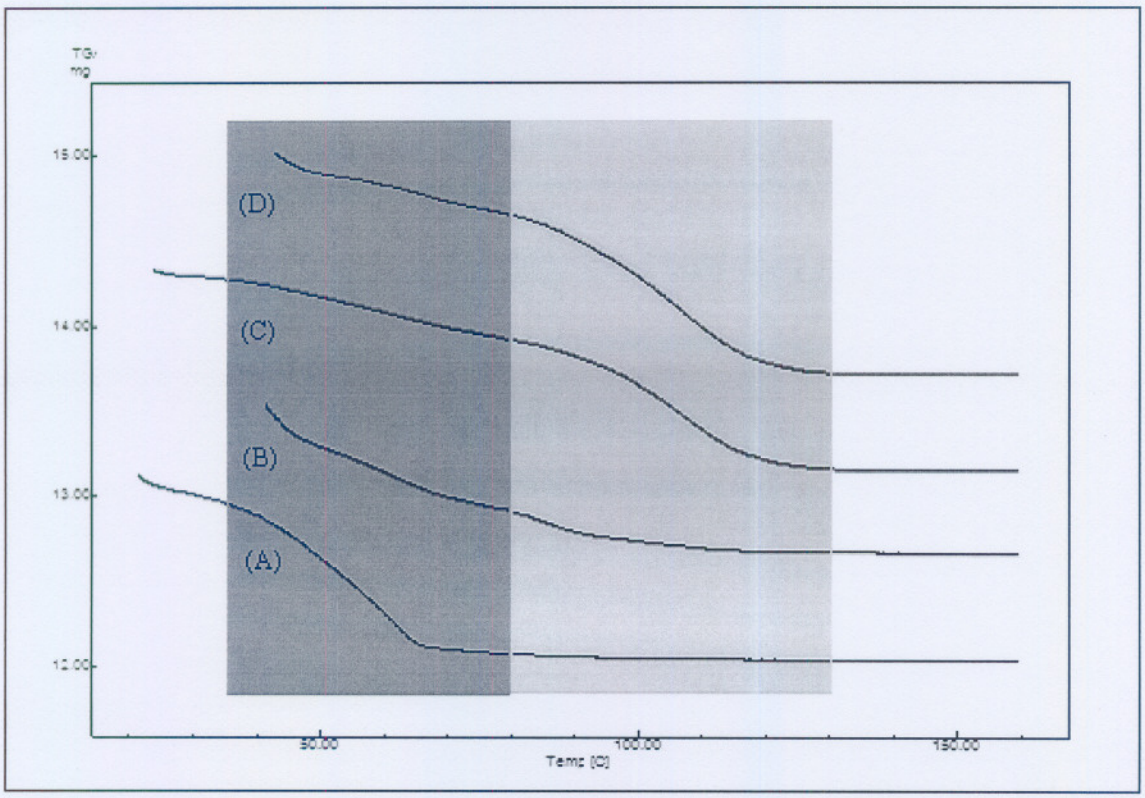

Figure 5

Superimposed TGA thermograms of samples obtained from solvents A-E, whereas (A) is absolute ethanol, (B) is ethanol (95%), (C) is ethanol:water (75:25), (D) is ethanol:water (50:50). The lighter shade of gray indicates temperature regions associated with dehydration and the darker shade indicates temperature regions associated with desolvation.

From figure 5 it was observed that the desolvation onset and endset temperatures were influenced by the presence of water in the recrystallisation solvent. Figure 5 clearly indicated that the weight loss step associated with dehydration (80-120°C) became more prominent with an increase in the water content of the recrystallisation solvent.

The superimposed DSC thermograms of the samples obtained from solvents A-D are illustrated in figure 6.

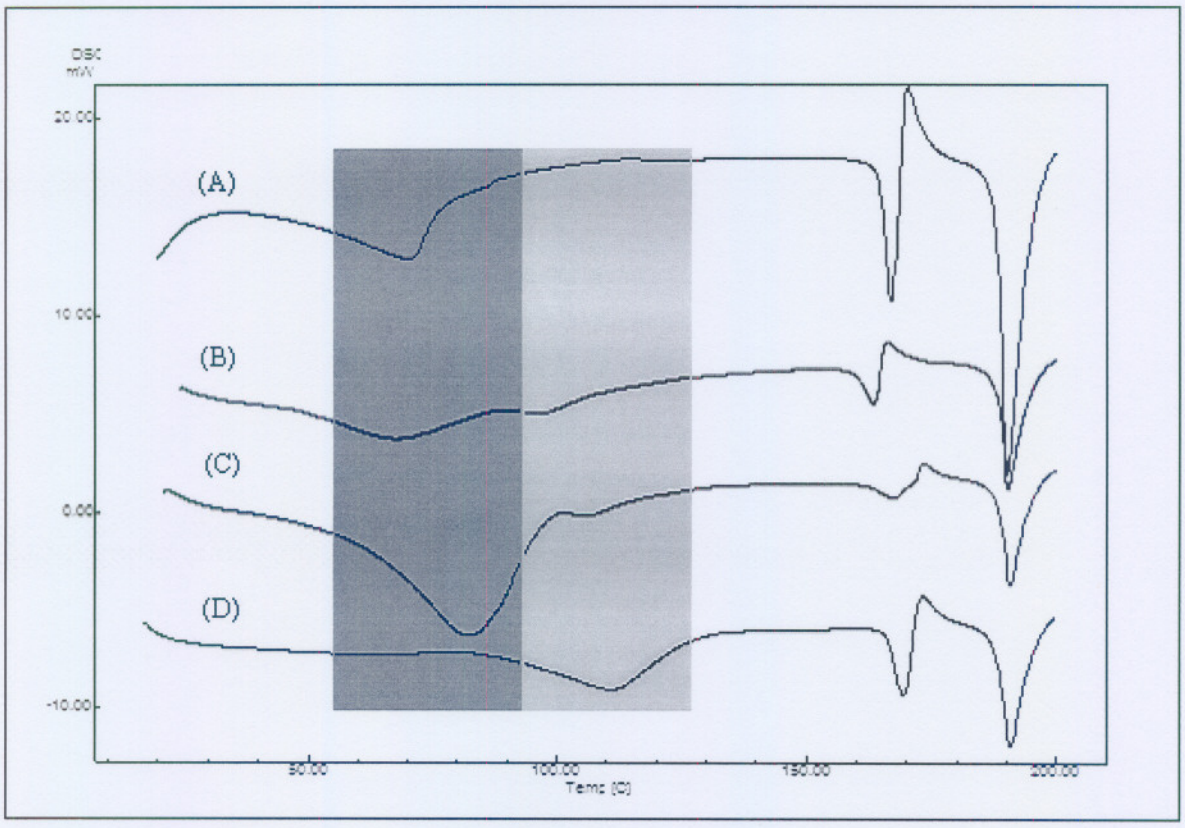

Figure 6

Superimposed DSC thermograms of samples obtained from solvents A-E, whereas (A) is absolute ethanol, (B) is ethanol (95%), (C) is ethanol:water (75:25), (D) is ethanol:water (50:50). The lighter shade of gray indicates temperature regions associated with dehydration and the darker shade indicates temperature regions associated with desolvation.

From figure 6 it was observed that the dehydration endotherm (at 90-120°C) became more prominent with increased water content of the recrystallisation solvent, while the desolvation endotherm (ethanol desolvation) was decreased into inexistence. The TGA thermograms revealed a shift in the desolvation onset and endset temperatures as the water content of the crystal increased, confirming the DSC observations.

HSM observations correlated well with the DSC thermogram events. The HSM observations are discussed in table 2.

Table 2

Photomicrographs of the HSM events observed for the forms from different ethanol:water mixtures (without silicon oil) Whereas: 1 is the initial, 2 is indicative of desolvation/dehydration (darkened crystals), 3 is melting, 4 is recrystallisation from the melt, 5 is the melting of recrystallised product.

#	**Mono-ethanol solvate** **(Solvent A)**	**Mono-ethanol hemihydrate** **(Solvent B)**	**Hemi-ethanol sesquihydrate** **(Solvent C)**	**Sesquihydrate** **(Solvent D)**
1	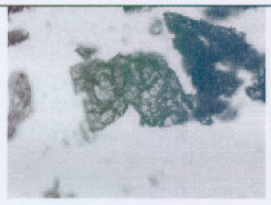 25°C	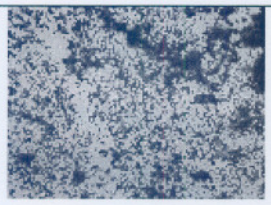 25°C	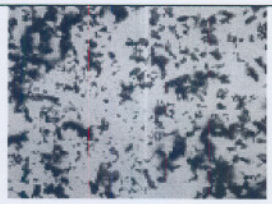 25°C	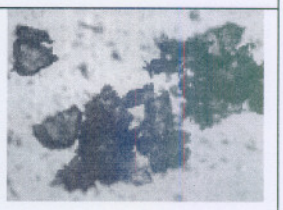 25°C
2	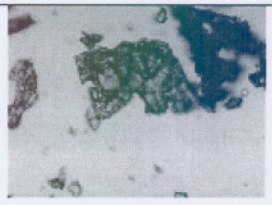 80°C	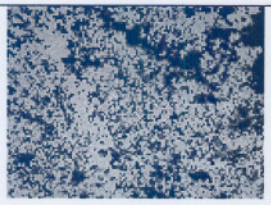 96°C	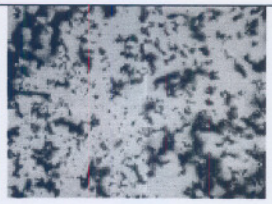 110°C	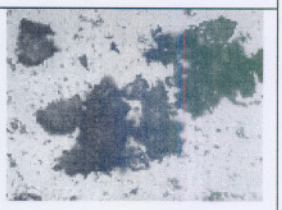 113°C
3	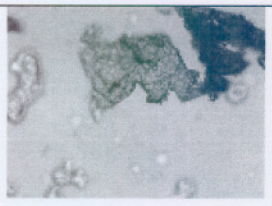 168°C	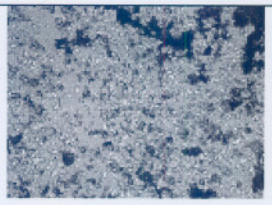 162°C	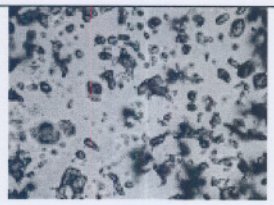 171°C	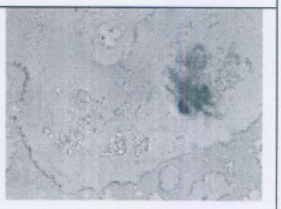 167°C

Table 2 continued…

#	Mono-ethanol solvate (Solvent A)	Mono-ethanol hemihydrate (Solvent B)	Hemi-ethanol sesquihydrate (Solvent C)	Sesquihydrate (Solvent D)
4	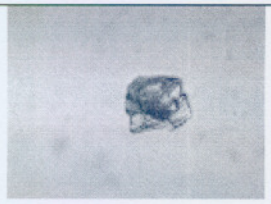 175°C	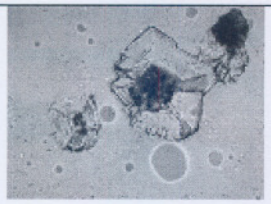 170°C	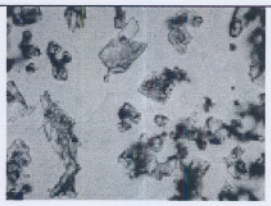 176°C	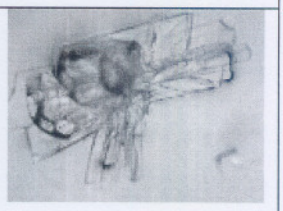 174°C
5	190°C	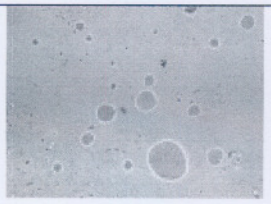 190°C	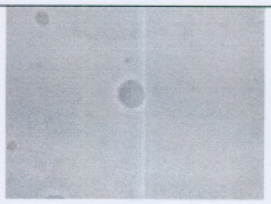 190°C	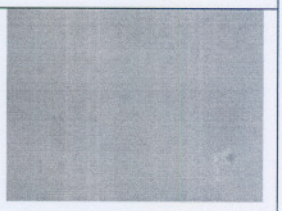 190°C

These samples were also studied submerged in silicon oil. The photomicrographs that were taken revealed no bubble evolution (i.e. desolvation) for the mono-ethanol solvate, however bubble evolution became progressively more visible as the hydration status of the crystal forms increased. These HSM events are illustrated in table 3.

Table 3 Photomicrographs of the HSM events observed for the forms from different ethanol:water mixtures (submerged in silicon oil)

Mono-ethanol solvate (Solvent A)	Mono-ethanol hemihydrate (Solvent B)	Hemi-ethanol sesquihydrate (Solvent C)	Sesquihydrate (Solvent D)
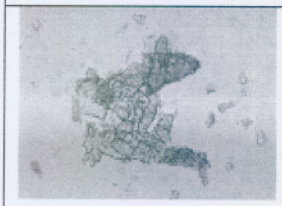 96°C	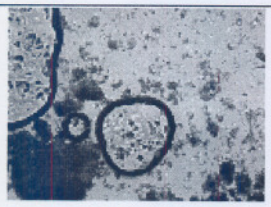 99°C	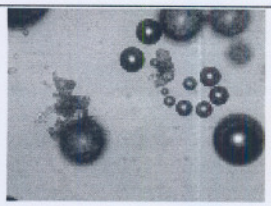 113°C	115°C

DRIFT-IR spectrometry was used to further investigate the different crystal forms. The most significant differences in the IR spectra of these forms were observed in the range of 4000- 2000 cm^{-1}. The mono-ethanol solvate revealed a broad band around 3400 cm^{-1} that was absent in the DRIFT-IR spectrum of the sesquihydrated form and the sesquihydrate form revealed a band at 3650 cm^{-1} which was not present in the DRIFT-IR spectrum of the mono-ethanol solvate. Thus it can be suggested that the band at 3400 cm^{-1} indicates the presence of ethanol in the lattice, whilst a band present at 3650 cm-1 indicates the presence of water in the crystal lattice. This statement is illustrated in figure 7. In figure 7 it can be seen that the samples containing water and ethanol possessed both the ethanol and water bands, while the pure ethanol solvate and the pure hydrate only revealed the presence of the band at 3400 cm^{-1} and 3650 cm^{-1} respectively.

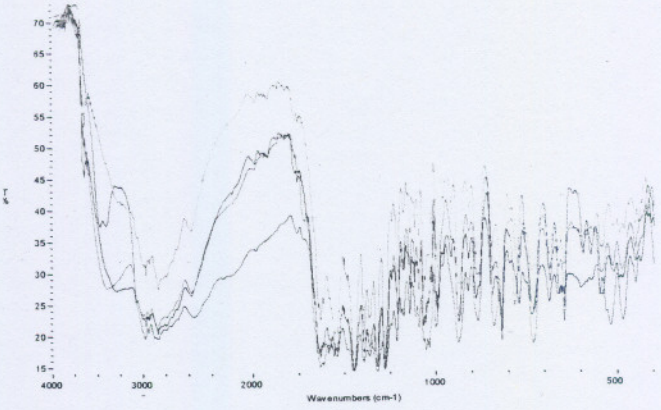

(a)

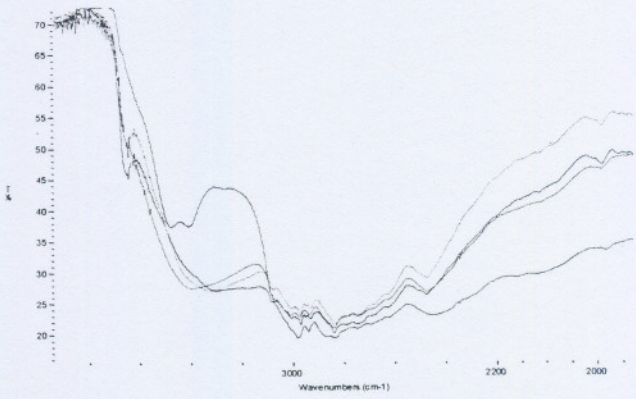

(b)

Figure 7

(a) IR spectra of the mono-ethanol solvate, mono-ethanol-hemihydrate, hemi-ethanol sesquihydrate and sesquihydrate and (b) enlargement of the area ranging from 4000-2000 cm^{-1}.

An increase in the water content of the recrystallisation solvent (ethanol) lead to an increased incorporation of water into the crystal lattice. The ethanol band was found to diminish (from A to E), while the water band became more prominent as the water content in the recrystallisation solvent used, increased.

4. Conclusion

This study revealed that small traces of water in the recrystallisation solvent (ethanol) resulted in different crystal forms (see figure 8). This observation is of great importance for the pharmaceutical industry as a fairly stable crystal form was obtained using 99-100% ethanol (see section 3.1) as recrystallisation solvent, whilst a very unstable form (form P) was obtained when 95% ethanol was used as recrystallisation solvent.

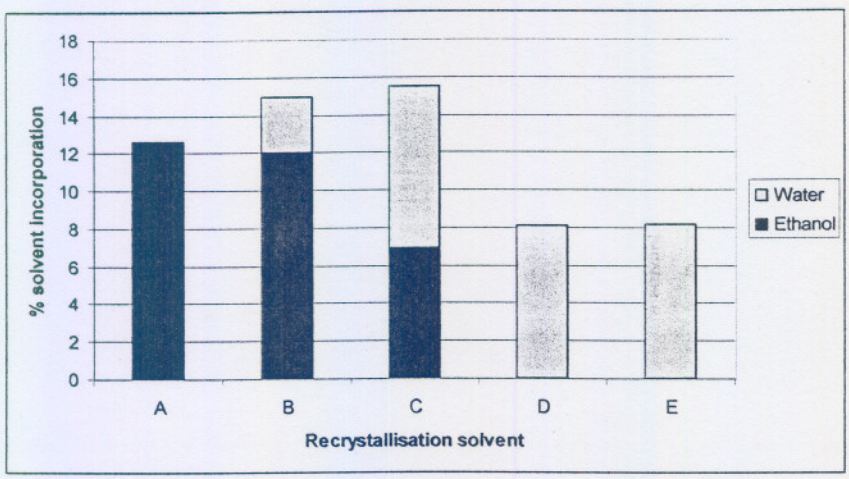

Figure 8

Percentage solvent incorporated into the crystal lattice using various ethanol: water mixtures as recrystallisation solvents respectively. Whereas (A) is absolute ethanol, (B) is ethanol (95%), (C) is ethanol:water (75:25), (D) is ethanol:water (50:50) and (E) is ethanol:water (25:75).

This study also revealed that water in concentrations of 5-50% v/v greatly influenced the solvate/hydrate incorporation stoichiometry. It was found that gatifloxacin showed a greater affinity for the incorporation of water into the crystal lattice. In ethanol:water mixtures with a water content greater (or equaled) than 50% v/v only hydrated crystal forms were produced and no ethanol was incorporated into the lattice.

The behaviour described in this article may substantiate the varying results of the crystal forms described in the literature (variations between batches from the same solvent and method). The water content of the solvents used in these literature studies might have varied, producing new crystal forms/mixtures of forms from the same recrystallisation method. This phenomenon may also explain why some forms are irreproducible using the same method/solvent, giving rise to disappearing polymorphs.

Bearing this behaviour in mind, good recrystallisation techniques should include the proper sealing of recrystallisation containers to prevent moisture from the atmosphere to influence the recrystallisation solvent composition. It is advisable to perform moisture content determinations on recrystallisation solvents to ensure reproducibility of recrystallisation procedures, and prevent the occurrence of possible disappearing polymorphs. These results suggest that relative humidity should be strictly controlled during recrystallisation/manufacturing of the raw material.

References

1. **BYRN, S.R., PFEIFFER, R.R. & STOWELL, J.G.** 1999. Solid-state chemistry of drugs. West Lafayette, Indiana: SSCI, Inc. 575p.
2. **CHAMBERS, H.F.** 2001. Sulfonamides, Trimethoprim, & Quinolones. (*In* Katzung, B.G., *ed.* Basic and clinical pharmacology 8th edition. New York: McGraw-Hill. 793-802p.).
3. **RAGHAVAN, K.S., RANADIVE, S.A., GOUGOUTAS, J.Z., DIMARCO, J.D., PARKER, W.L., DAVIDOVICH, M. & NEWMAN, A.** 2002. Gatifloxacin pentahydrate. Patent: US 6,413,969. 18p.
4. **NIDDAM-HILDESHEIM, V., WIZEL, S. & STERINBAUM, G.** 2004. Novel crystalline forms of gatifloxacin. Patent: US 2004/0192700. 8p.